Using EEG-based BCI settings and brain-state dependent stimulation as research tools for hypothesis-testing in cognitive neuroscience

A test-bench for brain-behavioural α-theories in visual perception and spatial attention

Irene Vigué-Guix

TESI DOCTORAL UPF / 2022

Thesis supervisor:

Dr. Salvador Soto-Faraco

Department of Information and Communication Technologies

Universitat Pompeu Fabra Barcelona

To life itself

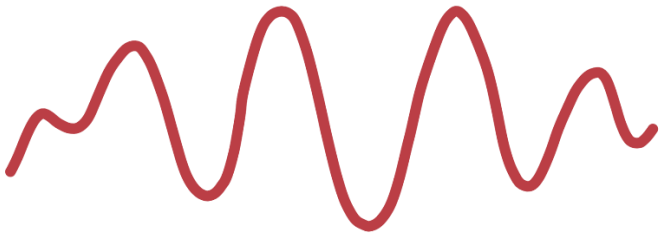

ACKNOWLEDGEMENTS

"Science and everyday life
cannot and should not be separated".

ROSALIND FRANKLIN

After this long journey to pursue my PhD, I would like to start this dissertation by sharing some words with the people I shared the path with over the past years and felt deeply connected with.

First, I would like to say thanks to my supervisor Salva. He has been the kind of supervisor I needed to write my thesis. His way of thinking, sensibility and unique sense of seeing and dealing with people has helped me commit to our relationship for all these years and finish my thesis. He has seen my growth as a person and become a better scientist. After I made a big mistake in my first PhD study, I still remember he told me: "*I don't care that you make a mistake, but I do care about your attitude when you make it and how you react to it*". I will never forget these words, and I applied that mantra to the errors I made afterwards. We did not have time to fly toy-helicopters with the modulation of α-activity, but let us give it time.

Second, this would not have been possible without my group's help, support, and collaboration: the multisensory research group (MRG). For many years I have been in charge of organizing the group seminars, and I enjoyed it until I had to focus on the last step of my PhD. I want to thank all the research group colleagues that have been on and off, especially Mireia, Luís, Manu, Alice(s), Lena, and Daria. I have learned so many things by your side, and I will always be grateful for your unconditional support, both at the lab and at the bar. I want to give a special thanks to Martín for his appearance in the right place and at the right moment to help me in the last steps of my PhD journey.

Moreover, I would like to thank all the people from the Center for Brain and Cognition (CBC). It's been an enormous pleasure to be part of the CBC family and share my experience with you. In particular, Xavi and Silvia have been there whenever I needed them and for the

mindfulness sessions of watching Xavi welding at the technical lab workshop.

Also, I would like to leave some room to thank the funding institution that has paid me to make this dissertation possible and the participants who have come to the lab to participate in my experiments.

Given that before scientists, we are people, I would like to give a big hug to my favourite people in this world who have given me support, hugged me, and told me nice words when I most needed them. Thanks to my family, friends, life companions, and therapists who have accompanied me along this journey.

Lastly, I would like to thank my mother especially. Although you are not physically here with me, I felt your support and strength from where you are right now. This dissertation is also for you.

Finally, I would like to thank all the versions of myself that contributed to this dissertation, going from the version who said 'yes' at the beginning of this adventure to the version who wrote and defended all the work done here. I have learned so much, and I will always be grateful for what this thesis represents in my life.

ABSTRACT

Spontaneous oscillations in the alpha band (α, 8–12 Hz) reflect ongoing fluctuations in cortical excitability. Several theoretical frameworks and empirical studies have supported the notion that distinct features of α-oscillations (e.g., power, phase, phase-coupling) influence sensory processing and subsequent behavioural performance in visual perception and spatial attention. While the evidence for the role of α-power in perception seems well-established, the roles of the α-phase in perception and the long-range α-phase coupling in spatial attention are still not clearly settled. This dissertation presents EEG-based brain-computer interface systems as a test bench for the predictions of brain-behavioural theories and to understand the connection between brain oscillations and behaviour. Our findings garner mixed support for the roles of features of α-oscillations in visual perception and spatial attention and shed additional light on the use of BCI systems as a promising research tool in cognitive neuroscience.

Key words: brain-computer interface, brain oscillations, brain-state dependent stimulation, behaviour, reaction time, alpha rhythm, visual perception, spatial attention, human cognition augmentation.

RESUMEN

Las oscilaciones espontáneas en la banda alfa (α, 8 a 12 Hz) reflejan fluctuaciones continuas en la excitabilidad cortical. Varios marcos teóricos y estudios empíricos han respaldado la noción de que las distintas características de las oscilaciones α (p. ej., potencia, fase, acoplamiento de fase) influyen en el procesamiento sensorial y el desempeño conductual posterior en la percepción visual y la atención espacial. Si bien la evidencia del papel del poder α en la percepción parece estar bien establecida, los roles de la fase α en la percepción y el acoplamiento de la fase α de largo alcance en la atención espacial aún no están claramente establecidos. Esta disertación presenta sistemas de interfaz cerebro-computadora basados en EEG como un banco de pruebas para las predicciones de las teorías del comportamiento del cerebro y para comprender la conexión entre las oscilaciones cerebrales y el comportamiento. Nuestros hallazgos obtienen un apoyo mixto para los roles de las características de las oscilaciones α en la percepción visual y la atención espacial y arrojan luz adicional sobre el uso de los sistemas BCI como una herramienta de investigación prometedora en neurociencia cognitiva.

Palabras clave: interfaz cerebro-ordenador, oscilaciones cerebrales, estimulación dependiente del estado cerebral, comportamiento, tiempo de reacción, ritmo alfa, percepción visual, atención espacial, aumento de la cognición humana.

RESUM

Les oscil·lacions espontànies a la banda d'alfa (α, 8–12 Hz) reflecteixen les fluctuacions en curs en l'excitabilitat cortical. Diversos marcs teòrics i estudis empírics han donat suport a la idea que les característiques diferents de les oscil·lacions α (per exemple, potència, fase, acoblament de fases) influeixen en el processament sensorial i el comportament comportamental posterior en la percepció visual i l'atenció espacial. Tot i que l'evidència del paper del poder α en la percepció sembla ben establerta, els papers de la fase α en la percepció i l'acoblament de la fase α de llarg abast en l'atenció espacial encara no estan clarament resolts. Aquesta tesi presenta sistemes d'interfície cervell-ordinador basats en EEG com a banc de proves per a les prediccions de teories del comportament cerebral i per entendre la connexió entre les oscil·lacions cerebrals i el comportament. Els nostres resultats obtenen un suport mixt pels rols de les característiques de les oscil·lacions α en la percepció visual i l'atenció espacial i aporten llum addicional sobre l'ús de sistemes BCI com a eina de recerca prometedora en neurociència cognitiva.

Paraules clau: interfície cervell-ordinador, oscil·lacions cerebrals, estimulació dependent de l'estat cerebral, comportament, temps de reacció, ritme alfa, percepció visual, atenció espacial, augment de la cognició humana.

TABLE OF CONTENTS

CHAPTER 1

General Introduction

"Our tendency to examine a problem from one point of view tends to reduce the likelihood of viewing an issue from another viewpoint."

MICHEAL I. POSNER

Psychology is a discipline that can be approached from many points of view: self-awareness (introspection), neural activity (brain processes), and behaviour (performance) (Posner 1986). Although each point of view is characterised by its unique techniques, a key aspect of this thesis is to combine behavioural and neural activity measurement techniques to study how they relate to each other in particular cognitive processes.

Almost half a century ago, Mountcastle (1976) wrote:

"... It has been clear or a long time – at least since the time of Lashley- that the quantitative study of behavior, traditionally the domain of the Psychologist, and the neural events in the brain, called 'Neurophysiology,' are conceptually different approaches to what are generically the same set of problems, and identity long emphasised by Jung (1972). What is new is that it is now possible to combine in one experiment the methods and concepts of each to yield a deeper insight into the brain mechanisms that govern behaviour than is possible with either alone. In this 'combined experiment,' one controls and measures behaviour and records simultaneously the signs of cerebral events thought relevant [p.1]."

Many researchers have followed this research line and have built the current framework of modern cognitive neuroscience. **Cognitive neuroscience** is a scientific field concerned with studying the physiological processes underlying cognition (Gazzaniga et al. 2002), focusing on the neural activity and connections across the brain

involved in cognitive processes (e.g., perception, attention, behaviour monitoring/control).

This dissertation aims to combine measurements of neural activity and behavioural outcomes to understand the cognitive components of behaviour better and address whether behaviour can be modulated using real-time estimations of "brain states' to augment human cognition and boost performance. The standard procedure of research in cognitive neuroscience studies is to relate different outcomes of behavioural response to distinct features of the brain activity (e.g., power, phase, frequency). Here, we will apply this logic in reverse to address the brain-behaviour relationship: we try to modulate the behavioural outcome by monitoring the brain activity and sending stimuli when a particular brain activity pattern previously related to the given outcome is detected in real-time.

In order to achieve this, we designed a brain-computer interface (BCI) system based on electroencephalography (EEG) to capture the electrical activity produced by populations of neurons from the human scalp in real-time. The EEG-based BCI system is a closed-loop that allows the presentation of stimuli in real-time depending on an individual's **brain-state** (i.e., for brain-state dependent stimulation; BSDS) while performing a cognitive task that requires a behavioural response. The target brain state will capitalise on different features of the ongoing oscillatory activity (e.g., amplitude or power, phase) in the alpha-band (α, 8 – 12 Hz), with a hypothesis-driven approach based on the insights of brain-behavioural theories on the functional role of α-oscillations in visual perception and attention.

In the first section of this introduction, I will explain how oscillations are present in our daily lives and how our brain's spontaneous neural activity takes the form of brain oscillations when captured at the human scalp by EEG sensors. Then, I will focus on the specific role of α- oscillations in visual perceptual and attentional processes and their relation to behavioural performance, according to the current brain-behavioural theories. I will then explain the approach of using EEG-based BCI systems as a tool for BSDS and cognitive augmentation in humans, together with the importance of using robust control signals for BCI based on insights from brain-behavioural theories. Further, I will account for single-trial dynamics and individualisation in BCI studies. Finally, I will explain the main aims, the hypotheses, and the scope of this thesis with a brief overview of the studies presented in later chapters.

How oscillations shape the world around us, including our brains

Oscillations in our daily lives

Cyclic changes unfold everywhere around us. We live surrounded by oscillations even if we do not know what they are or where we should look for them. The Earth spins on its axis every day, turning day into night and night into day, and it rotates around the sun once per year. The position of the hands of the clock indicates the pass of time, and it changes every second, minute, and hour. The moon waxes and wines around the Earth, and we can observe the different moon phases completing an entire cycle of changes approximately every month. These are all examples of oscillations (**Figure 1**). However, oscillations not only surround us but are also within us. The well-known **circadian rhythms** are part of our body's internal clock (Glass 2001) and exemplify how different physical, mental, and behavioural changes follow a day cycle (Czeisler et al. 1999), such as the sleep-wake cycle. Since our sleep-wake cycle is tied to the day-night cycle of where we live, a change in the environment (e.g., the light) can influence our internal clock (Blume et al. 2019). Thus, if we travel to another time zone for a brief time (e.g., taking an international flight), we might probably deal with jet lag until our circadian rhythms re-adapt to the new environment (Sack 2009).

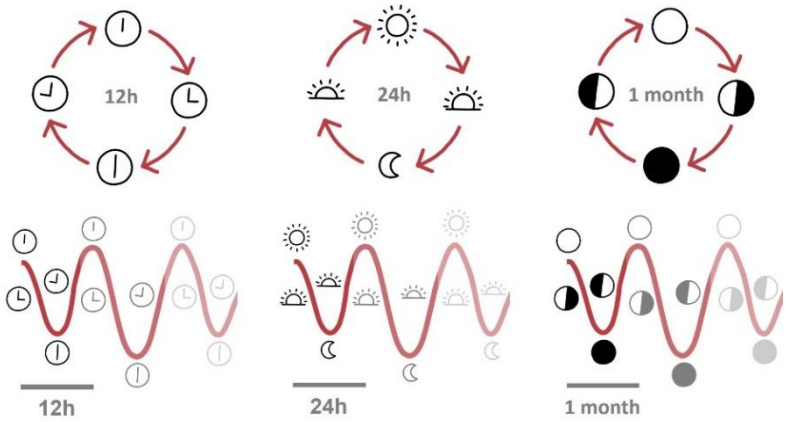

FIGURE 1. An illustrative example of how cycles become oscillations in the world around us. The positions of the hands of an analogic clock (left; 12h), day-night cycles (middle; 24h), and the moon phases (right; almost a month) can be perceived as cycles (top), but they can also be seen as oscillatory cycles that generate oscillations over time (bottom).

Although we can perceive, for example, the day-night changes as a repetitive cycle that goes over and over, there is also another way to see the cycle if we add the variable of 'time': a cycle represented by a circle can turn into a fluctuation of states that evolve generating a repetitive signal called oscillation (**Figure 1 bottom**).

What is an oscillation?

An **oscillation** is a rhythmic fluctuation between states of a system that can be characterised using three features: frequency, amplitude (or power), and phase (**Figure 2**). The **frequency** refers to the oscillation speed and reflects how long a cycle takes to complete per unit of time. For example, our body holds a broad range of oscillations at different frequencies: our lungs take a breath about every four seconds, our heart beats around once per second, and groups of neurons can oscillate together between high and how excitability states of tens or even hundreds of times per second (Cohen 2014). The **amplitude** (directly related to power) denotes the difference between the peak and the valley of the oscillation and refers to the amount of energy in the oscillation, which varies and fluctuates over time. For example, when we breathe, we go through rhythmic sequences of inhalations and exhalations, and we can either in/exhale unforced or let the air in/out with much intensity. In an oscillation, the **phase** refers to a moment in time (i.e., when) and reflects the position (i.e., where) of the oscillation along its cycle (e.g., the peak); it measures the 'state' of the oscillation at a given instant. For example, we can know at which point of the breathing cycle we are in each moment: inhaling, holding our breath, exhaling, or between these moments. These features of oscillations can either change over time or remain stable, in which case they can be used to predict when a specific state will reoccur in the future (Cohen 2014).

Brain oscillations captured by EEG from the human scalp

Oscillations shape not only our world and our bodies but also our brains. Neuroscientists use the terms **brain rhythms, brain oscillations,** or **neural oscillations** when referring to patterns of brain electrical activity that reflect rhythmic fluctuations. Oscillatory brain rhythms occur in various frequency bands (e.g., theta, alpha, beta, or gamma bands), at different temporal scales (e.g., from seconds to milliseconds), and at multiple spatial scales, from the single-cell to whole-brain areas, as measured with neuroimaging techniques (e.g., magneto- or electroencephalography (M/EEG). In this dissertation,

the primary focus will be on human brain oscillatory activity measured with the non-invasive neuroimaging method of EEG.

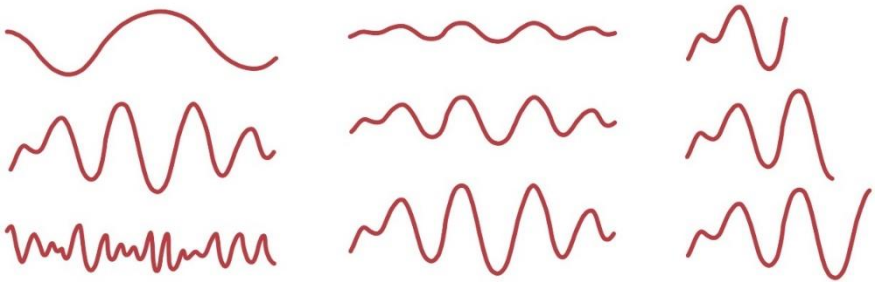

FIGURE 2. An illustrative example of the characterising features of oscillations: frequency, amplitude (or power), and phase are illustrated in each column, respectively. **Frequency (left column).** Oscillations are arranged from slow frequency (top) to fast frequency (bottom). **Amplitude (middle column).** Oscillations go from low amplitude (top) to high amplitude (bottom). **Phase (right column).** Oscillations are arranged accordingly to the moment (phase) at which the drawing ends. The top oscillation ends almost at the peak of a cycle, the middle oscillation ends at the through of the same cycle, and the bottom oscillation ends at the peak of the next oscillation cycle.

The EEG signal is recorded non-invasively by electrodes placed on the human scalp and primarily samples electrical fluctuations produced by post-synaptic activity in the superficial layers of the cortex (i.e., **cortical excitability**; Buzsáki and Draguhn 2004). The captured fluctuations receive the name of **cortical oscillations,** and the ones picked up with EEG are generated mainly by changes in the membrane potential of several thousands of (pyramidal) neurons that create an extracellular current that can be measured from the brain or scalp (Lopes da Silva et al. 1980; Buzsáki 2006). The amplitude of cortical oscillations denotes the strength of the signal, which depends on the number of firing neurons, how often they fire, and to what extent they fire together. When behaving synchronously, the overall activity of thousands of neurons captured by EEG follows a quasi-sinusoidal pattern, alternating with high- and low-level brain activity. The phase of cortical oscillations is where the signal finds itself on this activity cycle at a specific point in time, and the signal frequency denotes how often the sinusoidal activity goes up and down in a certain amount of time (Gallotto et al. 2017).

Brain activity can be detected and recorded throughout the brain's cortical regions and is reflected in cortical oscillations. It is important to notice that the human brain exhibits neural activity that includes

both **spontaneous activity** (also called endogenous, intrinsic, pre-stimulus, ongoing, or resting-state activity) and stimulus-induced activity (exogenous, event-based, or task-evoked activity; Northoff 2018; Raichle 2015). Although the brain's stimulus-induced or task-evoked activity has been considered and related to sensory and cognitive functions since early EEG research, the functional role of the brain's spontaneous activity has been more disputed and has recently gained momentum (Buzsáki 2006).

The intrinsic view of the spontaneous brain

The existence of the brain's spontaneous activity has been known since Hans Berger observed for the first-time spontaneous activity in the brain independently of an explicit task (Berger 1929). By that time, the brain's ongoing activity was considered noise. Only recent advances in neuroscience have been able to clarify the nature of such activity (Braeutigam et al. 2019) and accept that the brain's ongoing activity is not merely noise but instead reflects specific patterns of neuronal processing in the local and global neuroanatomy (Arieli et al. 1996; Damoiseaux et al. 2006; Fox et al. 2006).

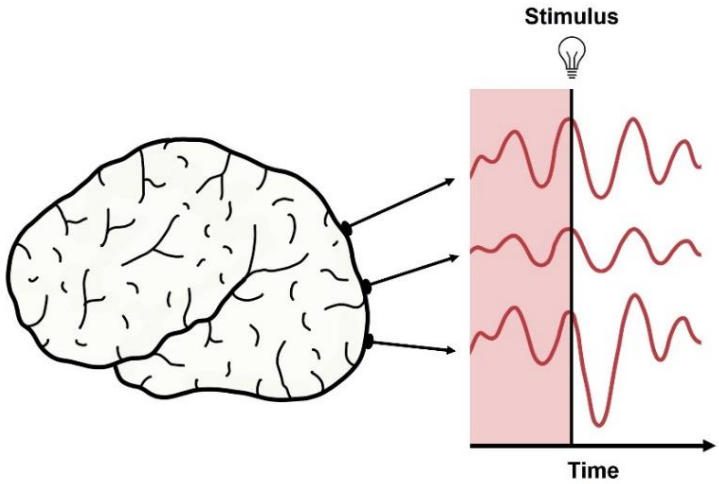

FIGURE 3. An illustrative example of the intrinsic view of the brain. Idealised EEG traces from three electrodes in posterior brain regions, with pre- and post-stimulus periods indicated by different shading. The stimulus-evoked signal interacts with the brain's spontaneous activity (shaded area) and generates a neural response that functions in the brain's activity.

Early work by Sherrington (1906) investigated the link between sensory-motor (input-output) functions, relating it to behaviourism. This input-output view of the brain sees behaviour as a conditioned

reaction of the brain. Sherrington's research, for which he was awarded a Nobel prize, underpinned most of the current neuroscientific work that has led to considerable advances in our understanding of the brain's structure, processes, and functional organisation (Braeutigam et al. 2019). Many studies with stimulus- or event-based approaches, including neuroimaging techniques, have dominated the field of cognitive neuroscience under the assumption of seeing the brain as a **reactive system**. According to this view, sensory input would cause some brain activity, resulting in significant motor activity responses or higher-level cognitive processes (Bechtel and Abrahamsen 2010; Raichle and Snyder 2007). Thus, the brain would be mainly driven by the environment, and activity generated not associated with a response of some input would be regarded as noise.

However, this reactive view has been challenged by empirical research demonstrating that behavioural responses can exhibit high intra-individual variability given a constant set of stimuli, even controlling for other factors (e.g., trial history and fatigue). This variability is often considered noise, and it is smoothed out by averaging the data or other kinds of statistical treatment. It has been assumed that this variability is critical to unlocking the system from predictable behavioural patterns and better adapting to environmental changes. This idea is reflected in models of sensorimotor processes linking reaction time variability to choice/decision variability (see Bompas et al. 2015 for further details). In addition, the reactive view of the brain ignores the possibility that fluctuations in behaviour are related to (and can be predicted by) the ongoing activity in the brain. This possibility is known as the **intrinsic (endogenous) view** (Braeutigam et al. 2019), and it is based on Hebbian reasoning: *"It is, therefore, impossible that the consequence of a sensory event should often be uninfluenced by the existing activity"* (Hebb 1949; Sporns 2011, p. 149).

It is generally agreed that the brain's ongoing activity accounts for the inter-trial variability of event-related or stimuli-induced neuronal responses at the individual level in a given task with constant conditions (Squires et al. 1976; Truccolo et al. 2002; Eichele et al. 2010; Ratcliff et al. 2009). The interaction between spontaneous and stimulus-related activity is a complex and non-linear process showing particular reproducible patterns (Huang et al. 2017). Indeed, it has been suggested that neither the brain's spontaneous activity alone nor the external stimuli themselves determine event-related activity in the brain (Northoff 2018). Instead, the event-related activity determines how they stand to each other and their dynamic interaction. Since

there is a vast continuum of possible relations between spontaneous activity and external stimuli, Northoff has proposed a 'spectrum model of the brain' (Northoff 2018). Such a spectrum model entails a continuum between different degrees of activity and passivity in the brain's neural activity. Some EEG studies have accumulated evidence towards a wide range of possible interrelated mechanisms. For instance, Chaumon and Busch (2014) found that the brain's ongoing activity may reflect rhythmic variations in cortical excitability, allowing for control of incoming brain responses. Alternatively, Lou et al. (2011) reasoned that stimulation spontaneously improves the pre-existing causal interaction between brain regions at stimulus onset. However, from a neuroscience perspective, the nature of the interaction between spontaneous and stimulus-related activity is yet unresolved (Uddin and Menon 2010; Braeutigam et al. 2019).

Understanding how spontaneous brain activity might impact cognitive processes has gained momentum (Northoff 2018). The idea behind this research line is to relate pre-stimulus brain activity with the subsequent behavioural performance in response to a stimulus and quantify the correlation between them (Linkenkaer-Hansen et al. 2004; van Dijk et al. 2008; Hanslmayr et al. 2005a; Ergenoglu et al. 2004; Romei et al. 2012; Samaha and Postle 2015). In particular, ongoing cortical oscillations have been hypothesised to play a role in perception (van Dijk et al. 2008; Samaha and Postle 2015), attention (Worden et al. 2000; Thut et al. 2006), and memory (Bonnefond and Jensen 2012; Cruzat et al. 2021), among other cognitive processes. This thesis will focus exclusively on how brain oscillations in the alpha-band (α, 8–14 Hz), recorded over posterior brain regions, play a role in visual perception and spatial attention. From this point onwards, the term **'α-oscillations'** will refer to this cortical rhythm in the posterior visual areas, and the **'α-theories'** will generalise the theoretical proposals covering this rhythm.

The brain-behaviour α-theories: the role of oscillatory α-activity in visual perception and spatial attention

α-amplitude and the inhibition hypotheses

The α-rhythm was first described by Hans Berger in the late 1920s (Berger 1929) when he found that high amplitude oscillations around 10 Hz dominated human EEG recording. The α-rhythm is the strongest electrophysiological signal with a high signal-to-noise ratio

that can be recorded from the human scalp, and it is usually prominent in the occipito-parietal regions. During relaxed wakefulness, the amplitude of α-activity increases (i.e., α-synchronization), especially with eyes closed (Grandy et al. 2013). The α-amplitude decreases when the eyes are opened and/or while performing tasks under mental effort (i.e., α-desynchronization; see Klimesch et al. 2007 for a detailed review). In the early days of EEG research, this finding inspired the idea that the α-rhythm might be an idling rhythm (Pfurtscheller et al. 1996) that reflected a brain state of reduced information processing.

Recent evidence, however, has challenged the **idling hypothesis** and has suggested instead that α-activity increases do not reflect simple idling of cortical regions but possibly active inhibition of task-irrelevant regions during mental operations (Palva and Palva 2007; Klimesch et al. 2007; Thut and Miniussi 2009; Jensen and Mazaheri 2010). Some studies have directly manipulated the engagement and disengagement of some brain areas during cognitive tasks (Rihs et al. 2007; Haegens et al. 2010; Sauseng et al. 2009; Romei et al. 2010; van Gerven and Jensen 2009). For instance, in the case of spatial attention, it is well-established that posterior α-activity decreases when covert attention is directed toward visual stimuli, for instance, when using the classical Posner cueing paradigm (Posner 1980). Illustrating this, studies in which attention is covertly directed toward the left or right visual field have found α-activity decreases in the hemisphere contralateral to the attended location and, in some cases, increases ipsilaterally (Sauseng et al. 2005; Worden et al. 2000; van Gerven and Jensen 2009; Yamagishi et al. 2003; Rihs et al. 2007; Kelly et al. 2006; Gould et al. 2011; Thut et al. 2006; Foster and Awh 2019). Importantly, at the behavioural level, it is usually expected that visual targets appearing at the attended location led to higher detection rates, quicker reaction times, and higher performance compared to those appearing in unattended locations (Posner 1980; Posner et al. 1980; Petersen and Posner 2012). Together, these findings support the view that α-activity reflects the inhibition of irrelevant brain areas that must be suppressed to optimize the performance of a given task (Klimesch et al. 2007). This inhibition acts as a selective tool to narrow the relevant information and allocate brain resources to the relevant areas for processing (Carrasco 2018). Indeed, it has been proposed that oscillatory brain activity supports a gating function reflected in the α-activity fluctuations (Lopes da Silva 1991). This view is the foundation

of the **gating-by-inhibition hypothesis** (Jensen and Mazaheri 2010), according to which the α-activity reflects an inhibitory, top-down mechanism that suppresses information in task-irrelevant areas while actively gating it to task-relevant areas. Under this framework, in spatial attention, decreases in α-activity could be interpreted to reflect higher cortical excitability to facilitate visual processing at the attended, likely target position. In contrast, α-increases potentially could reflect an active inhibitory process protecting against distraction input from task-irrelevant positions. By this principle, performance is poor when α-activity is low in the task-irrelevant areas (**Figure 4**; Jensen et al. 2011). Indeed, Klimesch proposed the **inhibition-timing hypothesis** (Klimesch et al. 2007), in which oscillatory α-activity plays a key role in the brain's ability to process information and represents a mechanism of top-down inhibitory control. They postulated that low α-amplitudes in the EEG signal reflect a state of comparatively high excitability, whereas high α-amplitudes reflect a state of inhibition (i.e., low excitability). Both hypotheses (Klimesch et al. 2007; Jensen and Mazaheri 2010) suggest that parieto-occipital α-amplitude reflects the excitatory/inhibitory state of visual processing, thereby enhancing or diminishing, respectively, the likelihood of stimulus perception. Several findings have provided evidence that strong pre-stimulus occipital α-activity leads to a negative impact on visual perception (Ergenoglu et al. 2004; Hanslmayr et al. 2005b; Hanslmayr et al. 2007; van Dijk et al. 2008; Mazaheri et al. 2009; Mathewson et al. 2009). For instance, Mathewson et al. (2009) found that errors in button-press responses were preceded by higher pre-stimulus α-activity in a go/no-go task. In the case of visual perception, Hanslmayr et al. (2005b) showed that lower performance in a visual perception task was linked to higher α-amplitudes in parieto-occipital regions. Also, the higher the pre-stimulus α-power activity within participants, the less likely the stimulus's detection was. For example, Ergenoglu et al. (2004) found that the probability of detection can be predicted by the amount of pre-stimulus α-power (in the ~ 10 Hz range) on a trial-by-trial b from α-activity originating in the parieto-occipital regions. This link between trial-by-trial variability in the posterior α-power and visual performance has been replicated by other studies using other experimental paradigms (van Dijk et al. 2008; Busch et al. 2009; Mathewson et al. 2011). Comparable results at the between-subjects level showed that participants exhibiting poor performance were characterised by high α-amplitudes (Hanslmayr et al. 2005b; Klimesch et al. 2007). One potential interpretation of these results is that α-

power can index an inverse state of cortical excitability (Klimesch et al. 2007), and another would be that a reduction of α-power may increase visual excitability (Lange et al. 2013).

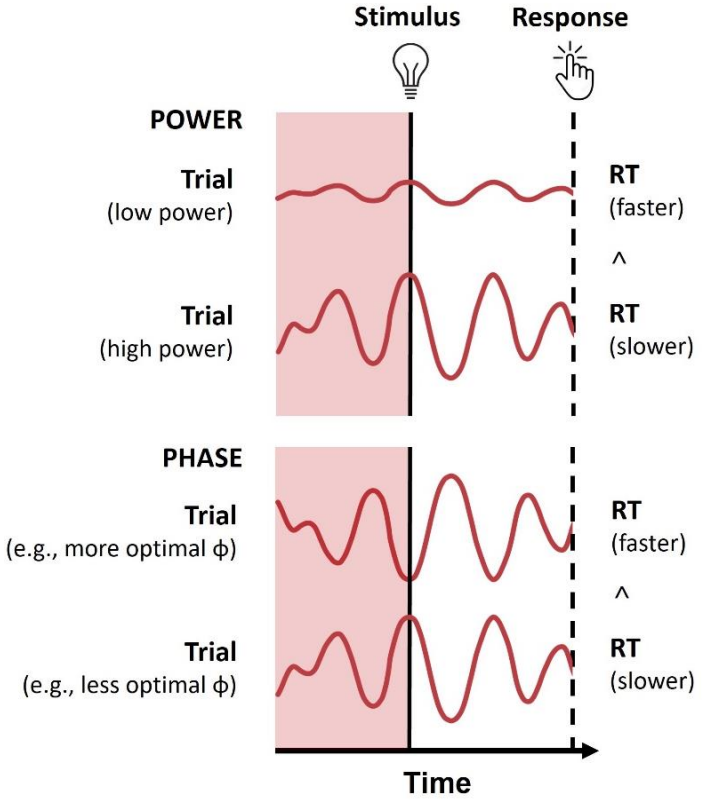

FIGURE 4. According to α-theories, an illustrative schema of the brain-behavioural relationship between oscillatory α-power and α-phase and reaction time (RT) in visual perception. Power (top). Higher α-amplitudes (power) in parieto-occipital regions during stimuli presentation would lower the probability of stimulus detection and, thus, slower reaction times (RTs). On the other side, low α-power at stimulus onset would increase the probability of detection and, thus, lead to faster RTs. **Phase (bottom).** Stimuli delivered at the more optimal phase of the α-cycle (e.g., peak) of the α-oscillation would lead to faster RTs (better performance) compared to stimuli presented at the less optimal phase of the α-cycle (e.g., through), which would lead to slower RTs (poorer performance). Here, the relationship between the selected parts of the α-cycle (peak/through) and the most/less optimal phases is arbitrary and only meant for illustrative purposes.

α-phase and the pulsed inhibition hypotheses

Inherently, the **phase** of low-frequency oscillations fluctuates more quickly than power, and some authors have proposed that inhibition

by α-oscillations, at the finer grain, acts as a pulsed inhibitory mechanism. This phasic inhibition has been proposed to control incoming information from sensation to perception in a pulsed manner under the **pulsed inhibition hypothesis** by Mathewson et al. (2011). In particular, the peak and the trough of a fluctuation would correspond to moments of low and high levels of cortical excitability, respectively. When it comes to the visual system, oscillations would therefore lead to a cyclic alternation between favourable and unfavourable states of information processing, or **perceptual cycles**, effectively chunking the inflow of sensory information into perceptual events depending on the phase of the α-cycle (**Figure 4**; Klimesch et al. 2007; VanRullen 2016b; Jensen et al. 2014). Consistent with this view, the **rhythmic pulsing hypothesis** (Mazaheri and Jensen 2010) proposed that spontaneous α-activity along with asymmetric amplitude properties can be viewed as rhythmic pulses producing bouts of inhibition every 100 ms. Stimulus processing can only occur between α-pulses (i.e., discrete processing; VanRullen 2016b), and importantly, this rhythmic inhibition only occurs when the pulses of α-activity are at a sufficiently high amplitude. Evidence of such a precise phase-dependent mechanism, through which sensory information is organized into perceptual moments depending on cycles of cortical excitability (Lindsley 1952), could be correlated with fluctuations in behaviour. Indeed, the phase of α-oscillations at the moment of target presentation has been related, among others, to trial-by-trial fluctuations in threshold-level visual detection (Nunn and Osselton 1974; van Dijk et al. 2008; Mathewson et al. 2009; Busch et al. 2009; Busch and VanRullen 2010; Hanslmayr et al. 2007; Hanslmayr et al. 2013); to supra-threshold visual perception as measured by reaction times (Lansing 1957; Dustman and Beck 1965; Callaway and Yeager 1960); to attention sampling and visual search (Busch and VanRullen 2010; Fiebelkorn et al. 2013; Buschman and Miller 2009; Dugué et al. 2015), among others. In particular, Busch et al. (2009) found that the threshold to detect visual flashes covaries over time with pre-stimulus α-phase measured with EEG. Similarly, Mathewson et al. (2009) showed that the detection rate of visual targets differed between opposite phases of α-oscillations, and the prediction of detection performance by means of α-phase was only possible with high α-power. These findings suggest that oscillations of α-activity (described by phase) directly relate to oscillations in cortical excitability (Lindsley 1952). Although these studies provide evidence of a link between the phase of α-oscillations and behavioural

performance in various cognitive domains, these findings have been primarily based on exploratory approaches and inferential group statistics.

α-phase coupling and the 'communication trough coherence' hypothesis

Beyond investigating the role of the oscillatory α-power and α-phase, which relate to neural dynamics at the local level, some studies have gone one step further and employed different methods to explore **phase-coupling** between distant brain areas (Friston 2002; Hanslmayr et al. 2013). Some oscillatory interaction mechanisms have been highlighted in brain function using phase-amplitude coupling (PAC), in which, typically, the amplitude of fast frequencies is nested into the phase of slow oscillations (Lakatos et al. 2005). Other oscillatory mechanisms involve phase-phase or cross-frequency coupling (CFS), which reflects the synchrony between the phase of distinct frequencies (Palva et al. 2005; Palva and Palva 2018). However, this thesis will focus on the phase coupling method to assess the functional connectivity between two distinct brain regions over time and at the same frequency (α) at the single-trial level.

In visual perception, Hanslmayr et al. (2013) suggested that a low-frequency oscillatory signal at ~7 Hz dynamically gates time windows for sensory information transfer between occipital and parietal regions. Remarkably, the frequency in which they found these effects matches the behavioural time constant of visual sampling (VanRullen et al. 2007; Landau and Fries 2012), suggesting that the propagation of oscillatory activity between cortical regions underlies the rhythmic nature of our visual system. This finding supports the notion that oscillations route cortical information flow (Bressler 1996; Varela et al. 2001; Saalmann et al. 2012; Baldauf and Desimone 2014) and aligns with the **communication-through-coherence (CTC) hypothesis** (Fries 2005, 2015). The idea behind the CTC hypothesis is that oscillations could facilitate the communication of information (i.e., propagation of activity) by synchronising cycles of excitability between a distant population of neurons, thereby increasing the likelihood that spikes from neurons in one brain region will discharge post-synaptic potentials during the excitable phase of neurons in the other (Fries 2005). Crucially, however, Hanslmayr et al. (2013) demonstrated that even if two task-relevant brain regions are synchronised, they will only transmit information during the optimal, not the non-optimal phase. Long-range phase-connectivity between distant neural populations

(Varela et al. 2001; Fries 2005, 2015) and phase at the local level are essential for transmitting information within cortical oscillations across different brain regions.

Various complex cognitive functions, such as attention orienting, are dependent on synchrony between neural populations over a network of distant neural populations, often called the **frontoparietal network (FPN)** (Petersen and Posner 2012; Buschman and Miller 2009). Although the increases in ipsilateral α-power have been attributed to local α-synchronisation reflecting inhibitory processing, other studies have also related this ipsilateral power increase to long-range synchronisation of α-oscillations between cortical regions (Sauseng et al. 2005; Freunberger et al. 2009; Freunberger et al. 2008; Doesburg et al. 2009; Palva and Palva 2011). Indeed, Palva and Palva (2007) proposed the **active-processing hypothesis**, in which the oscillatory long-range α-phase dynamics play a role in coordinating neural processing in active task-relevant cortical structures. Such long-range α-synchronisation is a potential mechanism to increase the fidelity and effectiveness of communication throughout the brain (Clayton et al. 2018), especially among front-posterior regions (Sadaghiani and Kleinschmidt 2016). This long-range α-synchronisation co-occurs with local α-synchronisation in the ipsilateral visual cortex, suggesting the involvement of α sensory inhibition and integration of top-down control networks dedicated to the deployment of visual attention (Doesburg et al. 2009; Clayton et al. 2015, 2018). These findings align with the **premotor theory of attention** (Rizzolatti et al. 1987), which postulates that the same neural circuits in frontoparietal areas control attention orientation.

Overall, the idea that EEG captures significant fluctuations in neural excitability is at the core of evidence for various hypotheses about the neural mechanisms of cognitive processes and their relation to behaviour (e.g., perceptual cycles, see VanRullen 2016b). This putative brain-behaviour connection raises the possibility of measuring, anticipating, and even manipulating cognitive processing by using measurements of brain activity online to parse sensory, electrical, or magnetic stimulation to the user (e.g., to boost the effectiveness of brain stimulation, see Zrenner et al. 2018). One way to explore this possibility is by using brain-computer interfaces (BCIs) as a research tool for providing new knowledge of cognitive neuroscience and augmenting human behaviour.

Using EEG-based BCI systems as a research tool for brain-state dependent stimulation (BSDS)

Why brain-computer interfaces (BCIs)?

In recent years there has been a substantial increase in the interest in characterising online brain activity using non-invasive brain imaging techniques (e.g., EEG) to address cognitive questions, particularly in the context of **brain-computer interfaces (BCIs)** (Jensen et al. 2011). A BCI is a hardware and software communication system designed to recognise specific patterns in the ongoing brain oscillations and allow interaction between the brain and the outside world (Nicolas-Alonso and Gomez-Gil 2012). Although BCI has its roots in applications for communication and control by patients who suffer from severe motor impairments (Wolpaw et al. 2002), diverse applications have emerged trough out the years as new forms of human-computer interaction (Abiri et al. 2019) and augmenting human performance and novel methods of data analysis in cognitive neuroscience (van Gerven and Jensen 2009). Indeed, a review paper by Jensen et al. (2011) has shown the utility of and the need for BCIs in brain research. For instance, BCIs represent a new, potentially powerful tool for studying the brain at work (Bahramisharif 2012).

Moreover, it can also be used for assessing brain states in real-time, such as intentions, attention, and accuracy capabilities (Blankertz et al. 2010; Zander and Kothe 2011; Martel et al. 2014). From a pure engineering perspective, the objective of a BCI system is to decode signatures of brain activity associated with an individual's brain state as reliably and as fast as possible to determine an outcome. Many studies have demonstrated the feasibility of monitoring brain states in real-time and adapting BCI accordingly (Chavarriaga and Del Millan 2010; Freeman et al. 2004; Papadelis et al. 2007; Gangadhar et al. 2009; Aricò et al. 2018; Kuc et al. 2021; Mora-Sánchez et al. 2020).

Challenges of EEG-based BCIs systems

Most non-invasive BCI research relies on recordings of MEG or EEG, which are optimal for real-time measures of brain processes (Enriquez-Geppert et al. 2017; Saha et al. 2021). The significant advantage of MEG over EEG is the high spatial resolution and the opportunity of recording data beyond the surface of brain regions. However, MEG devices are extremely costly and unfeasible to move about (Bahramisharif 2012), making them less suited for practical BCI

applications outside research. Indeed, EEG represents the most dominant measurement modality and holds the most potential to enable true wearable BCIs promptly. EEG offers high temporal precision and directly measures human population-level neural activity. The downsides of EEG are the limitation to capturing brain activity mainly from cortical structures, the low signal-to-noise ratio, and the high susceptibility to artefacts generated by eye or muscle movements (Muthukumaraswamy 2013). Overall, the EEG equipment is low-cost, easy to use, and accessible (Cohen 2017b), making it an efficient acquisition method for real-time BCI.

To build a robust EEG-based BCI, it is essential to use signatures of the ongoing brain activity that can be analysed using short chunks of data (e.g., data buffer). These data segments should be continuously updated and detected with a reasonable signal-to-noise ratio (SNR). Nonetheless, performing EEG-based BCI studies is highly challenging, given that data needs to be streamed and processed online and that BCI researchers need to be able to suppress environmental noise in real-time to perform online artefact removal (mostly muscular activity unrelated to brain signals) to prevent confounding the signals of interest (Jensen et al. 2011). A real-time framework holds advantages over the more conventional offline analysis approach in theoretical advance despite the caveats. Proof of functioning real-time tools based on current cognitive neuroscience knowledge could further consolidate the theoretical frameworks and pave the way to further research and applications. Thus, BCI could be a research tool using hypothesis-driven approaches as a test bench for brain-behavioural theories. In finding a solid link between prestimulus α-oscillations and behaviour, the hypothesis-driven framework could be further used in BCI applications to augment human cognition (Horschig et al. 2014).

Using EEG-BCI for brain-state dependent stimulation (BSDS)

One of the potential uses of BCI as a research tool for cognitive neuroscience and as a practical tool for augmenting human behaviour is the **brain-state dependent stimulation (BSDS)**. The principle behind BSDS is the following: If brain-state fluctuations are reflected in ongoing oscillatory activity, and these fluctuations impact cognitive processing, then delivering stimuli in real-time to subjects contingent on certain identified brain states makes it possible to investigate the functional role of the brain state (Sergeeva et al. 2014). A substantial amount of empirical knowledge and theoretical basis about the

relationship between brain states and behaviour must exist to use this approach.

For example, it would be interesting to investigate whether behavioural performance can be modulated online on a single-trial basis using α-activity from posterior brain regions (**Figure 5**). Current theoretical and empirical knowledge indicates that visual perception is reduced when the amplitude of posterior α-activity is high (e.g., van Dijk et al. 2008), and therefore ground an online BCI setup where difficult-to-detect visual stimuli are only presented when the α-activity is low. According to the brain-behavioural α-theories, we should expect an increase in visual performance (i.e., detection rate) compared to when stimuli are presented at high α-activity, for example. Hence, a potential BCI application could use this strategy to send information only when detecting low α-activity in a given individual's brain to enhance cognitive and behavioural performance. The possibility of augmenting performance using BCI for BSDS could have many practical applications. Note that a valuable side product might be new insight gained in cognitive neuroscience when developing these BCI applications.

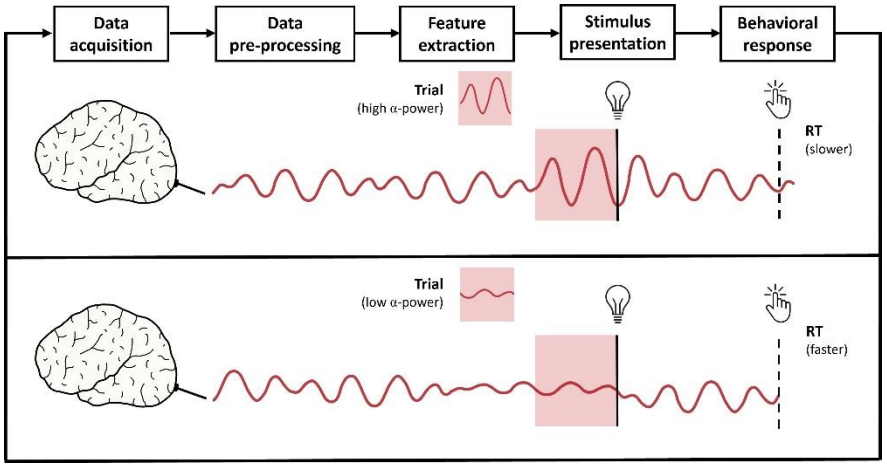

FIGURE 5. An illustrative example of the design of an EEG-based BCI for brain-state-dependent stimulation (BSDS). The BCI system recognises particular patterns of ongoing brain oscillations following the serialised stages of data acquisition, data pre-processing, feature extraction, stimulus presentation, and behavioural response. For instance, according to the α-theories, when looking for high α-power patterns in the ongoing brain activity and triggering stimuli, we should expect slower reaction times (RTs) than when stimuli are delivered when α-power is low.

The design of an EEG-based BCI using a BSDS approach consists of a processing analysis pipeline with serialised stages (**Figure 5**). In short, the **data acquisition (1)** stage captures the brain activity from the human scalp using EEG, either from one or many channels. Then, in the **data pre-processing (2)** stage, the data is processed to detect and reject eye and muscle artefacts. The **feature-extraction (3)** stage concerns selecting and extracting features computed from the EEG and using them for later stimulus presentation. This stage mainly selects the features of brain oscillations relevant to the study's intended purpose and applies filtering and time-frequency (TF) analysis to the data (e.g., low- and high-power). Note that this stage is a critical part of the BCI implementation and design (Shahid and Prasad 2011), and noise from the brain recording can be reduced by adequately selecting the features representing a brain function of interest. When the patterns of the feature of interest match the patterns detected in the ongoing brain activity, the BCI uses this match as the **control signal** to trigger the stimulus to the user in the **stimulus presentation (4)** stage. Finally, the **behavioural response (5)** stage registers the individual's behavioural response (e.g., response time). The BCI goes back to the beginning of the pipeline, ready to start another loop iteration. Depending on the study's design, the feature-extraction pattern in the subsequent trial can be the same as the initial trial (e.g.., low/low power) or different from another study condition (e.g.., low/high power).

Innovative approaches such as BSDS, based on the online characterisation of the ongoing brain activity (Hartmann et al. 2011), are currently in rapid development and hold the promise of providing new ways for investigating the working brain and complementing new insights gained from offline M/EEG studies in cognitive neuroscience (Jensen et al. 2011). For instance, the core idea of studying sensory perception using online stimulus triggering based on the phase of ongoing brain oscillations has attracted interest since the 1950s (e.g., Callaway and Yeager 1960; Gho and Varela 1988). Similar approaches are currently used in research (e.g., BSDS using auditory attentional modulation: Andermann et al. 2012; BSDS-TMS: Zrenner et al. 2018). Nonetheless, the number of studies that have previously used online stimulus triggering contingent on the ongoing brain activity is low.

Manifold potentiality of analysis in hypothesis-driven studies

Given that studies using BSDS use real-time monitoring of ongoing brain activity to trigger the stimulus to specific features of oscillations,

it is essential to determine a priori some parameter choices of the BCI analytical pipeline. Those choices can be based on previous literature showing the brain-behavioural effect of interest (see **Chapters 2 & 3**) and/or on previous offline analyses addressing the brain-behavioural effect as a putative control signal for the BCI before enrolling on the real-time experiment (see **Chapter 4**). Usually, the BSDS approach relies on limiting the parameters of the oscillatory frequency of interest (e.g., the α-band), the time point of interest (e.g., stimulus onset), and the brain regions of interest (e.g., posterior visual areas). Importantly, selecting the parameters and coding the analysis pipeline of the BCI before the study facilitates the **pre-registration of such studies** (as we did in both real-time studies; **Chapters 2 & 3**). We need replications in cognitive neuroscience so results can be observed repeatedly in different situations, especially in the context of BSDS research. We need brain-behavioural effects that can be replicated many times and constitute a robust control signal for the BCI setting.

Note that the potentialities of BSDS studies not only rely on the real-time analysis but also on the wide range of potential reality checks and exploratory analyses that can be performed afterwards. On the one hand, real-time analysis can optimise the number of trials recorded at each of the selected features of oscillations (in comparison to offline studies presenting stimuli at random times). Also, obtaining the expected results would implicitly corroborate and ground the brain-behaviour theory behind the decisions for the BCI. In this sense, real-time BSDS can be considered a test bench for brain-behaviour theories. On the other hand, after data collection from the real-time study, the dataset can be further explored by performing offline analysis. Depending on whether the results of the real-time study were positive or negative, the analysis can be performed with different aims. For example, in the case of null results (as in **Chapter 2**), the post-hoc analysis can be focused on performing some reality checks to ensure that the choices in the real-time setting were appropriately chosen and did not influence the findings. In case of positive results (as in **Chapter 3**), offline analysis can further explore the possibility that the brain-behavioural effect can also be found beyond the selected parameters (time windows, frequencies, electrodes). To this end, offline analysis can complement the real-time analysis and allow for finding possible effects that would have gone missing using only the real-time approach.

One of the significant challenges is that BCI must work at the single-trial level. Therefore, previous knowledge of the group and multi-trial

offline approaches is valid but insufficient. A vital aspect of a successful BCI using BSDS, thus, is to rely on the most robust task-dependent modulations of brain activity on a trial-by-trial basis as a control signal, ensuring a hypothesis-driven approach based on research evidence relating to brain oscillations and cognition or behaviour (Jensen et al. 2011; Horschig et al. 2014).

Modulations of α-oscillations in visual attention and perception as control signals for BSDS

Studies using α-modulations in visuospatial attention

Previous attempts at finding BCI control signals for applications have gained insight into which signals are potentially robust given a specific task. For example, it is becoming clear that the amplitude of oscillatory brain activity in the low frequencies is modulated in various cognitive tasks (Hari 1997; Klimesch et al. 2007; Jensen and Mazaheri 2010; Jensen et al. 2011). In the case of **covert visuospatial attention (CVSA)**, it has been found that the direction of attention is reflected in the inter-hemispheric distribution of α-activity in parieto-occipital regions (Rihs et al. 2007; Bahramisharif 2012; van Gerven and Jensen 2009). The differential changes of α-activity across hemispheres, and ideally the direction of visuospatial attention, can be indexed by an **α-power imbalance** over posterior regions. This imbalance can be computed using different methods, such as the logarithm of the left hemisphere α-power divided by the right hemisphere α-power used by Kelly et al. (2005a) or the lateralisation index by Thut et al. (2006). Indeed, several offline studies showed that modulations of posterior α-power due to the direction of covert attention had the potential to be used as a control signal for continuous control in an online BCI setting (Kelly et al. 2005a; Kelly et al. 2005b; Kelly et al. 2005c; Rihs et al. 2007; van Gerven and Jensen 2009; Treder et al. 2011; Tonin et al. 2012). In addition, Belyusar et al. (2013) showed that it was possible to decode α-power lateralisation in a few hundred milliseconds in EEG. Shortly after, Tonin et al. (2013) developed the first online BCIs using the modulation of α-power in CVSA, and other studies came afterwards (Tonin et al. 2017; Trachel et al. 2018).

Importantly, this collection of offline and online studies demonstrates that these attention-related modulations of α-power are robust enough to be used in a BCI setup and decoded on a single trial basis (van

Gerven and Jensen 2009; Treder et al. 2011; Bahramisharif 2012) with up to 90% accuracy for protocols in which targets are presented to a left/right location (Treder et al. 2011; Tonin et al. 2013). A detailed review covering visual attention based BCIs can be found in Astrand et al. (2014b). Note that the spatial distribution of α-power is linked to behavioural performance (Posner 1980). To this end, α-power modulations should allow for fast and reliable classification of the locus of attention and, thus, it should be possible to manipulate subsequent behaviour (e.g., reaction time or visual discrimination performance). Hence, α-power modulations by CVSA as control signals for BCI seem to be a good fit for BSDS.

Moreover, despite the evidence from offline group-based studies that local α-modulations coincide with long-range α-modulations in the ipsilateral visual cortex in the deployment of visual attention (Sauseng et al. 2005; Doesburg et al. 2009), online EEG-based **phase synchronisation** between brain regions has not yet been systematically addressed in the context of CVSA. Thus, it would be interesting to go one step further in the current use of BCI systems for CVSA and transform the concept of using α-power modulations in real-time as a local phenomenon to framing it as a network of task-relevant connected brain regions through α-phase synchronisation, corroborating the proposed communication-through-coherence hypothesis (Fries 2005, 2015) in a visual attention task. This step is undertaken and addressed in **Chapter 4** of this dissertation.

Studies using spontaneous α-modulations in visual perception

Regarding visual perception, as discussed earlier, high prestimulus **α-power** in task-relevant regions has negatively impacted stimuli processingHanslmayr et al. 2005b; van Dijk et al. 2008; Mazaheri et al. 2009; Ergenoglu et al. 2004; Hanslmayr et al. 2007). With this brain-behaviour link in mind, in a BCI-BSDS design, the stimulus could be triggered only when α-power is low, optimizing the stimulus processing. On the contrary, if the purpose is to inhibit the stimulus information, then the reverse rationale applies, and the stimulus presentation can be triggered during high α-power. Despite the insight gained from the various offline studies pointing in this direction (e.g., Jensen et al. 2011; Horschig et al. 2014), to the best of our knowledge, an online study following this strategy using EEG-based BCI-BSDS has not yet been attempted. I address this in this dissertation in **Chapter 3**.

Even when using lateralized α during attention as a control signal, most studies have resorted to the power of brain oscillations for BCI. These applications have advantages concerning phase (e.g., more robust estimate, higher signal-to-noise ratio) but clear limitations (e.g., lower temporal precision, blind to neural communication). Therefore, an attempt to use temporal-precise, phase-related BCI would provide a definite advance in the field. Considering a BCI based on the **phase** of neural oscillations, for example, forces the developer to use a clear hypothesis-based distinction between optimal and non-optimal phases that facilitate a better difference between brain states and their associated impact on behavioural performance (e.g., a particular phase latency will yield faster detection reaction times). Because of the phasic component of α-theories (in modern times, the gating-by-inhibition hypothesis), this core idea has attracted interest since the 1950s (Lansing 1957; Callaway and Yeager 1960; Dustman and Beck 1965; Varela et al. 2001; Gho and Varela 1988) and has received renewed support from human neuroimaging studies using M/EEG recordings at low frequencies roughly covering from 5 to 15 Hz (Landau and Fries 2012; VanRullen 2016a, 2016b), as well as at higher frequencies in the gamma range (30 - 90 Hz; Fries 2005, 2015; Fries et al. 2008). A typical experimental approach to relating the ongoing oscillatory phase with the outcome of a particular cognitive process consists of repeating the same trial multiple times, leading to various behavioural responses. For example, in a supra-threshold visual perception task, successive trials with presentations of the same stimulus would eventually fall at different phases over the critical oscillatory frequency of interest. By analysing offline, the phase at which the stimulus was presented may reveal consistent behavioural results (e.g., reaction times) over different phases (VanRullen 2016b).

However, such an offline procedure can reveal these relationships after the fact since there is no precise a priori control about which phase will be stimulated at each trial. In order to do so, one would have to anticipate in real-time, from the EEG, the distinct phase in the relevant frequency with sufficient time and precision to trigger a stimulus. Callaway and Yeager (1960) performed this procedure. They showed that faster responses to visual stimuli occurred if the stimulus was presented at the positive phase of an α-cycle (see Dustman and Beck 1965; for similar results). Similarly, Varela et al. (1981) presented two stimuli successively, with a very short interval, and showed that the subjects perceived the two stimuli as one if they were presented at the positive peak of the α-cycle. In addition, Gho and Varela (1988)

used a similar protocol to deliver rapid pairs of visual stimuli depending on the phase of the ongoing α-activity. They found that perception (two flashes versus one) could be somewhat manipulated depending on α-phase at stimulus onset. These studies were promising but only partially successful. Hence, we argue that given the current state of the art, the confidence in the theory and the reliability of the measurements make it possible to validate the proposed framework and explore the role of phase in cognitive processes. Interestingly, it is remarkable that this research line has not been followed up by new research after all this time until recently (see **Chapter 2** of this dissertation for further details).

Recent studies using α-modulations in cognitive neuroscience

Some recent studies have continued exploring in real-time the relationship between the phase of the pre-stimulus oscillatory activity (going beyond the α-band) and the upcoming perceptual performance in other cognitive and motor processes (Ngo et al. 2013; Zrenner et al. 2018; Helfrich et al. 2014). For example, Ngo et al. (2013) performed auditory stimulation in phase with the ongoing rhythmic occurrence of up states of slow-wave oscillations during sleep (SO) to enhance memory consolidation. Moreover, Mansouri et al. (2017) developed a novel approach for delivering electrical stimulation (transcranial alternating current stimulation; tACS) phase-locked to the activity of the underlying brain region in real-time. Similarly, Zrenner et al. (2018) used, for the first time, real-time EEG-triggered BSDS for magnetic stimulation (transcranial magnetic stimulation; TMS) in the human motor cortex to demonstrate that the phase of the ongoing μ-oscillations modulates corticospinal excitability in the α-band from the sensorimotor cortex. Note that most of this modern research uses EEG-based BSDS for electrical or magnetic stimulation (e.g., TMS, tACS; see Bergmann 2018 for a review), which is beyond the scope of the sensory stimulation approach presented in this thesis.

Note that the goal of a BSDS system based on the insight gained in brain-behavioural theories is to extract information from the EEG signal without the possibility of averaging over trials and identify the brain state of interest for the controlled delivery of a given event or stimulus. Brain activity modifications should be present on a trial-by-trial basis for a given individual to identify the brain state successfully. Therefore, it is essential when doing research with BCI for BSDS to capitalise on single-trial dynamics and account for the individualisation

of the brain activity features of interest. This single-trial approach brings challenges and opportunities, which we discuss below.

Practical considerations for EEG-based BCI in cognitive neuroscience

Within-subject vs group-level analysis

Most cognitive neuroscience studies looking at pre-stimulus activity have used neuroimaging techniques to address differences in brain activity by estimating means from many trials calculated across conditions and/or groups of individuals (**Figure 6** illustrates this offline approach at the group-level in a visual perception task based on the level of α-power; Pernet et al. 2011). In these studies, stimuli that demand a fast behavioural response are presented at random (or pseudo-random) intervals while EEG is recorded. There is a brain-behaviour pair of data points in each trial: an EEG signal (e.g., level of α-power within a pre-stimulus window the stimuli happened to fall) and behavioural response (e.g., RT). Trials are sorted post-hoc for each individual based on the behavioural outcome (e.g., fast vs slow reaction times; RTs), and averaged responses across conditions are then statistically compared (e.g., t-test) across fast and slow RTs to conclude a power-behavioural relationship. A significant relationship between α-power and behaviour (here, RT), when found at group-level, provides support for the α-theories (VanRullen et al. 2011). However, finding a brain-behaviour effect in a trial-averaged study across individuals does not imply that the same effect can be found for each individual and not even on a trial-by-trial basis (Horschig et al. 2014).

Statistical analysis can be done at two levels: at the individual level (i.e., within-subject analysis), in which the trial is the unit for analysis, and at the group level, in which the averaged data of each individual is the unit for analysis (Cohen 2017a). These analyses have different purposes, and they complement each other to see a bigger picture of the data (see Cohen 2017a for further explanation). **Group-level analyses** provide the consistency of the effect direction across individuals and deeper insights into how likely the findings will generalise to individuals. However, they do not provide information about the variability across trials within an individual.

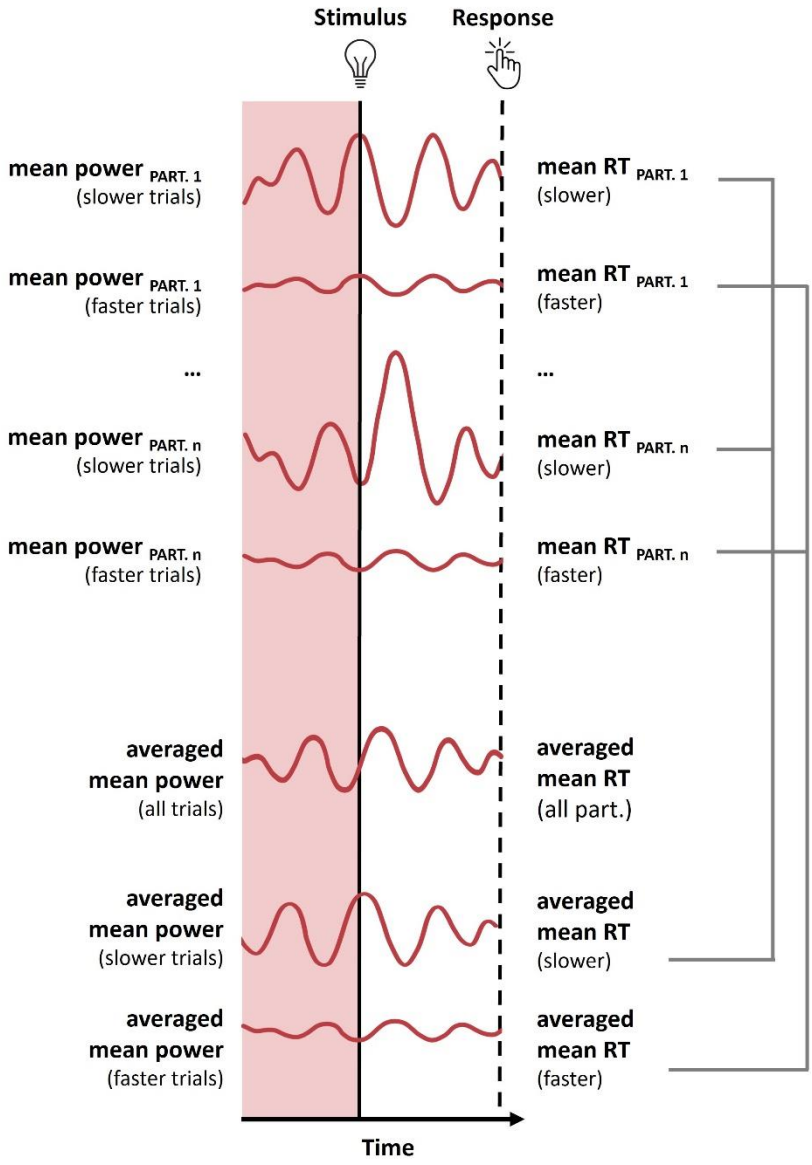

FIGURE 6. An illustrative example of the average offline approach to study changes in visual perception as a function of the level of α-power (e.g., low vs high power) at group-level. Stimuli demanding a behavioural response are presented at random intervals while EEG is recorded (here, the trials are aligned to the moment of stimulus presentation for convenience). Trials are then separated based on behavioural outcomes (e.g., fast vs slow RTs). Average responses are then statistically compared across fast and slow RTs to conclude a power-behavioural relationship at group-level than can provide support for the theory if it turns out to be significant. Figure inspired by VanRullen et al. (2011).

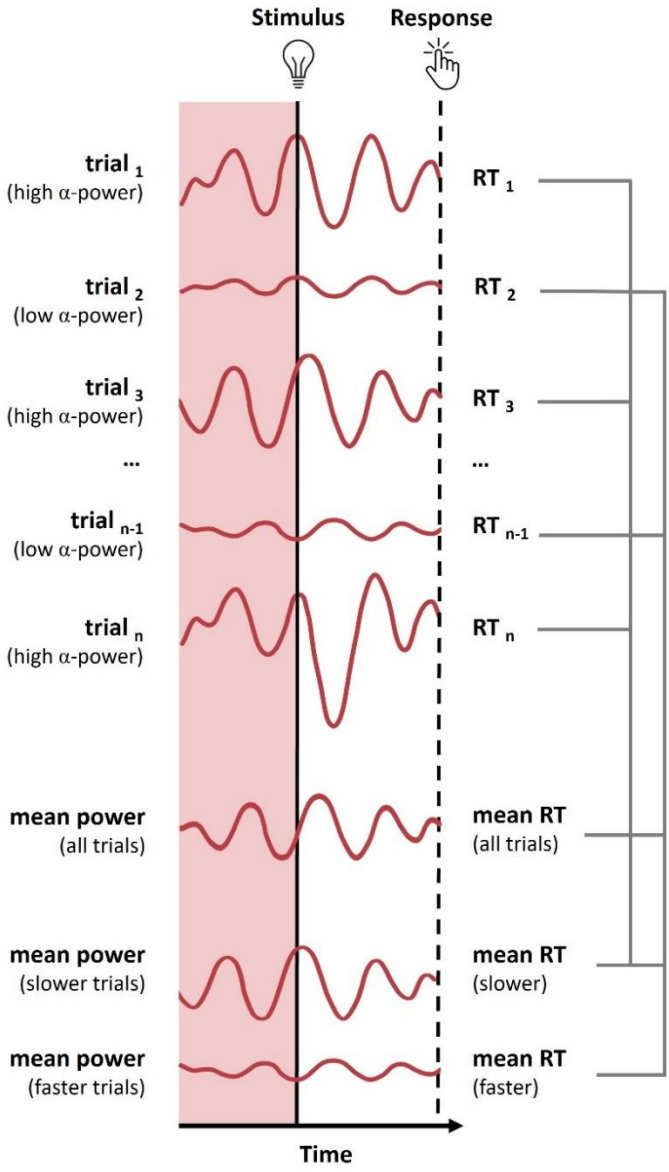

FIGURE 7. An illustrative example of the online approach to study changes in visual perception as a function of the level of α-power (e.g., low vs high power) at the individual level. Stimuli demanding a behavioural response are presented at specific moments (e.g., low vs high power) contingent upon the ongoing EEG (here, the trials are aligned to the moment of stimulus presentation for convenience). Trials are then post-hoc separated based on behavioural outcomes (e.g., fast vs slow RTs). Responses are then statistically compared across fast and slow RTs conditions within an individual. Figure inspired by VanRullen et al. (2011).

On the other hand, **within-subject analyses** provide information on the variability across trials of an effect relative to the magnitude of the effect within the same individual. This information cannot be generalised to other individuals, but they provide insight into the robustness of the effects and a brain-behaviour link for each individual. This dissertation includes both types of analysis.

For BCI-BSDS research, one should gather offline brain-behavioural evidence at the group level to be found at the individual level and, finally, at the single-trial level. It is essential to realise that the brain does not operate according to the 'average response' (Stokes and Spaak 2016). Real-world interaction requires real-time perception, encoding, and decision making on a single-trial level. To understand the neural basis of behaviour, we need to understand the neural dynamics as they unfold on a single trial.

Tackling brain-behaviour relationships on a trial-by-trial basis

Single-trial analyses allow us to provide, in some situations, additional information that is unnoticeable if we average over repeated observations (Cohen and Cavanagh 2011; Pernet et al. 2011). For example, analyses at the single-trial trial can help us systematically map brain activity with the subject's behavioural variability (Ratcliff et al. 2009). However, exploring these dynamics is not trivial, and any measure of brain activity at a single trial (especially with EEG) is subject to much more noise than when dealing with averages (Stokes and Spaak 2016). Although averaging information over trials tends to cancel noise and increase the signal-to-noise ratio, capturing highly consistent patterns and increasing statistical power in the analysis, in many cases, it can also smooth important behaviorally relevant information embedded in the signal (Stokes and Spaak 2016).

Taking back the offline approach at group-level in a visual perception task based on the level of α-power (**Figure 6**), one could use BCI-BSDS to capitalise on the real-time brain-behavioural relationship trial-by-trial basis for a given individual (**Figure 7**). The BCI pipeline could trigger visual stimuli contingent upon the level of α-power (e.g., low vs high power) of ongoing α-oscillations in order to predict and modulate behaviour (e.g., fast vs slow RTs) in real-time. The EEG recording and the behavioural outcomes could then be used offline to perform within-subject and group-level analysis. Trials could be sorted post-hoc based on the behavioural outcome (e.g., fast vs slow RTs). Responses and averaged responses across conditions could be

statistically compared (e.g., t-test) to conclude a power-behavioural relationship at individual and group levels. The α-power and RT relationship could provide (or not) support for the α-theories (VanRullen et al. 2011; Drewes and VanRullen 2011).

A key aspect favouring single-trial analysis is that trial averaging can misrepresent neural dynamics in many ways. For example, studies have shown that stimulus-evoked activity in the gamma-band (γ, 25-80 Hz) comprises intermittent γ-bursts in single trials, despite the robust, sustained profile apparent in the trial-average representation (Lundqvist et al. 2016; Lowet et al. 2016). Thus, a step forward in cognitive neuroscience would be to harness **real-time single-trial dynamics** since this approach can allow increasingly detailed characterisation of fine-grained information, not only for our understanding of cognition but also for the potential development of BCIs (Stokes and Spaak 2016). Indeed, relying on offline studies relating to brain-behavioural effects at the single-trial level can be the most-suited option when selecting task and feature extraction as the control signal of a potential BCI. One way to better harness the α-theories on a single-trial basis and develop robust BCI systems is to adapt the processing pipeline to each individual and better fit the brain-behaviour modulation.

Accounting for individualisation of feature extraction

If the goal of a BCI-BSDS is to detect specific patterns in the brain activity reflecting a 'brain-state', then the BCI processing pipeline would be more effective when relying on individualised features rather than generalized features for a group of individuals (Dias et al. 2009). Thus, the BCI system should accommodate specific features that may vary among individuals, such as age, neurological diseases, brain volume, task demands, and memory capacity (Klimesch 1999; Uhlhaas and Singer 2006; Klimesch et al. 2007). One illustrative example is using frequency intervals optimal for each individual (e.g., a band centred around the **individual alpha frequency; IAF**) instead of using a fixed one-fits-all frequency band (e.g., standard α-band range of 8 – 12 Hz). Indeed, some studies have used the IAF as an anchor point to adjust the frequency bands individually (Klimesch et al. 1998; Klimesch 1999; Thut et al. 2006; Horschig et al. 2014; Limbach and Corballis 2016; Ruzzoli et al. 2019; Kosciessa et al. 2020) to prevent interaction from other frequency bands (Klimesch 1999). The IAF can be obtained from few-minute resting-state EEG recordings and is defined as the frequency corresponding to the strongest peak

observed by EEG within the alpha range of 8-12 Hz (Klimesch et al. 1998). As shown in **Figure 8**, the peak can often be easily discerned by visualising the power spectral density (Corcoran et al. 2018), and a basic approach is to look for the local maxima within the background spectral activity (e.g., 1 – 40 Hz). The IAF has been proved to vary interpersonally (Haegens et al. 2014), although it has high stability within each person (Grandy et al. 2013). It has also been correlated with performance in perceptual-cognitive tasks (Klimesch et al. 1998; Samaha et al. 2015; Cecere et al. 2015; Samaha and Postle 2015; Mierau et al. 2017; Torralba Cuello et al. 2022) and has been used as a stable individual biomarker for BCI applications (Horschig et al. 2014). Thus, the IAF can be used as an anchor point to adjust frequency bands individually, predict BCI performance, and pre-screen participants in a practical setting.

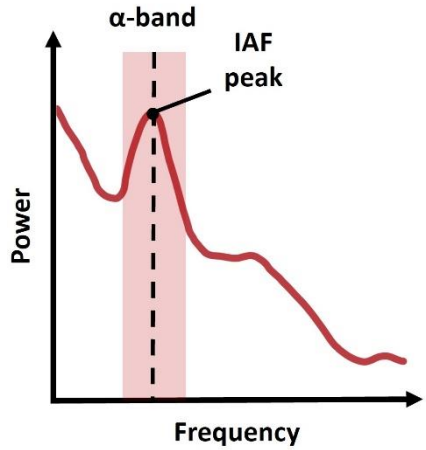

FIGURE 8. An illustrative example of the power spectrum. The shaded area denotes the standard α-band (8 - 12 Hz), and the dashed line denotes the IAF as the strongest peak (e.g., 10 Hz) within the α-band.

A balance between replications and novel findings

We need replications in cognitive neuroscience so results can be regarded in a positive light and repeatedly observed in different situations (e.g., from different research groups, using different datasets or analysis techniques). Particularly in the light of BCI-BSDS research, we need brain-behavioural effects that can be replicated repeatedly and can constitute a robust control signal for the BCI setting. As previously pointed out by Cohen (2017a), whenever possible, we should try to combine replications of existing findings and novel

results into new experiments and in the same publications. Cognitive neuroscience needs to balance replicating existing findings and to produce new findings. This balance can be built naturally into research by ensuring that new experiments allow for replications and novel findings. Replications themselves can be one part of the results section, and additional analyses can then be performed to help contextualize the original findings and perform novel analyses not previously reported. If the original findings are not replicated, exploratory analyses can be performed to investigate why the original findings were not replicated. Note that it is inevitable that some evidence in the literature are statistical false alarms or are limited to a narrow population or specific experiment design. The progress in the field needs to determine which findings are overinterpreted and which are more stable.

Note that replication of experiments, analysis and results opens the door for sharing the data and the code used for the experiment and analysis. Many websites and repositories are currently available to share the data and the code, such as the Open Science Foundation (OSF; https://osf.io/), GitHub (https://github.com/), and personal or lab websites. Sharing code is much easier than sharing datasets code files since code files are smaller than datasets.

BCI pipeline with toolboxes vs custom-build code

Several initiatives working toward a standardised approach for data streaming and analysis have appeared in the last decade, including BCI2000, OpenVIBE, FieldTrip, EEGLAB, and more (Schalk et al. 2004; Renard et al. 2010; Hartmann et al. 2011; Oostenveld et al. 2011; Delorme et al. 2010 for a review of MATLAB-based tools for BCI research). Several toolboxes have been built over the past years under this line of research to analyse ongoing EEG/MEG in real-time. For example, the ConSole toolbox (Hartmann et al. 2011) can be used to present auditory and visual stimuli contingent on the brain state. The BEST toolbox (Hassan et al. 2020) allows for magnetic stimulation using EEG-TMS, whereas the TORTE toolbox (Schatza et al. 2022) offers real-time detection of oscillatory phase and amplitude closed-loop studies. Indeed, real-time studies linking brain activity and behaviour based on ongoing oscillations are among the most active and trendy areas of development in cognitive neuroscience.

Using toolboxes for BCI research has the advantage that they are standardized, easy to use (usually include documentation and/or a

graphical user interface; GUI) and facilitate replications (different researchers can use the same functions). However, performing analysis only using toolboxes can be limiting, and some functions that one might need may not be available. Thus, depending on the research purpose and the coding abilities of the researchers involved in a given study, toolboxes can be substituted/combined with custom-built code.

In this dissertation, the preference was towards creating a custom-build BCI setting from scratch. In this way, it allows us to have all the degrees of freedom of the BCI setting to monitor the EEG data in real-time and full access to the entire analysis pipeline of the EEG data to tag the relevant feature of ongoing oscillatory activity. Also, it gives us complete control of the course of the user's visual environment dependent on specific oscillatory features defined in advance and a privileged position toward IPR claims for future transfer, given the potential BCI applications.

Aims and scope of the thesis

Supported by the literature in brain-behavioural α-theories, both the power (Foxe and Snyder 2011; Palva and Palva 2007; Klimesch et al. 2007; van Dijk et al. 2008) and the phase (Klimesch 2012; Palva and Palva 2007; Klimesch et al. 2007; Mathewson et al. 2009; Mathewson et al. 2011; Busch et al. 2009) of cortical α-oscillations appear to play a crucial role for visual perception and attention. Oscillatory power is taken as an index of local synchrony in neural populations, and its role in cognition has received reliable confirmation (see, for example, Jensen et al. 2011). Nevertheless, the role of oscillatory phase and long-range phase-synchrony in visual attention and perception is still under debate, at least when observing humans. The general hypothesis underlying this thesis project is: If our perception of the world depends on fluctuations in the ongoing activity of our brains, then by presenting stimuli time-locked to known brain states (through brain-state dependent stimulation), it should be possible to manipulate behavioural performance in cognitive processes (here, visual perception and attention).

Aims

The main aims of the present dissertation are: (i) to create a custom-built EEG-based BCI setting that allows brain-state dependent stimulation (BSDS), (ii) to provide evidence of the role of oscillations

in visual perception and visual-spatial attention according to the brain-behavioural α-theories, at the single-trial level and (iii) to seek for proof-of-concept cases of EEG-based BCI applications in real-time harnessing on α-fluctuations, adopting insights from a hypothesis-driven framework.

Scope

The first step in the present thesis was to create an EEG-based BCI for BSDS, which capitalises on distinctive features (e.g., amplitude, phase) of brain oscillations in real-time. This tool will help study the relevance of brain oscillations' dynamics in cognitive processes and create potential BCI applications. The ideal scenario would be that targeting stimulation at optimal brain states would lead to human cognitive augmentation. Such an approach should be complemented by exploratory studies to allow for more robust ex-post-facto inferences regarding the functional relevance of certain brain states.

The present thesis will provide evidence of the potential of oscillatory amplitude, phase, and phase coherence during spatial attention as a control signal using EEG-based BCI. The studies illustrate an approach to the potential role of these features for testing cognitive neuroscience theory and for augmented human behaviour. In **Chapter 2**, the closed-loop EEG-based BCI setting for BSDS will be used to deliver targets (i.e., visual stimuli) in real-time at distinct phases along the α-cycle in a visual detection task. The aim will be to harness the putative link between the α-phase and visual perception through reaction time. The experimental study adapted an approach used by Callaway and Yeager (1960) and was pre-registered in the Open Science Framework (OSF) with the design, the analysis pipeline, and the statistical analyses (https://osf.io/nfdsv/). In **Chapter 3**, visual targets will be presented contingent upon the occurrence (or the absence) of bursts of high α-power in the ongoing EEG in a visual go/no-go task. The oscillatory α-activity will be related to behaviour using reaction time measures. The study was also pre-registered in OSF (https://osf.io/z98ms/). Further, **Chapter 4** presents a proof-of-concept for an EEG-based BCI based on the phase-coherence across distant brain regions. This proof-of-concept is intended to estimate the direction of attention of a person in a visual cueing attentional task at the single-trial level. Moreover, **Chapter 5** summarises the findings of the thesis, highlighting their contribution to the research field, discussing the findings, and including

assumptions and limitations of the thesis. Finally, **Chapter 6** ends the thesis with some conclusions and ideas to expand the presented research in the future.

CHAPTER 2

Using α-phase to speed up visual detection

"Resilience to failure, humiliation, and rejection are the most important ingredients of a scientific career".

GYÖRG BUZSÁKI

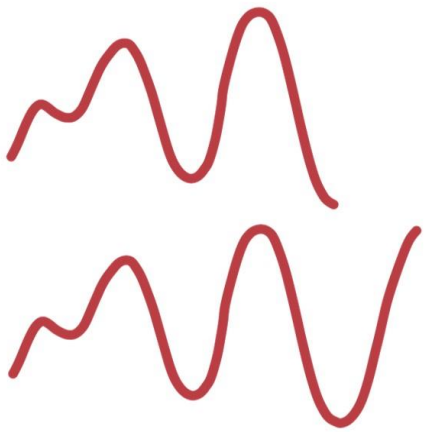

In this chapter I closely follow our study (Vigué-Guix et al. 2020): I. Vigué-Guix, L. Morís, M. Torralba & S. Soto-Faraco. *Can the occipital α-phase speed up visual detection through real-time EEG-based BCI? EJoN,* 2020.

Background

Alpha oscillations (α, 8-12 Hz) in the occipito-parietal cortex reflect ongoing fluctuations in cortical excitability (Bishop 1932; Adrian and Matthews 1934; Worden et al. 2000; Kelly et al. 2006). It follows that the perceptual fate of a visual stimulus would depend upon the instant it evokes neural activity within the ongoing α-cycle, leading to cyclic alternations between more and less favourable phases for perceptual processing (Klimesch et al. 2007; Jensen and Mazaheri 2010; Klimesch 2012; Jensen et al. 2014; VanRullen 2016b). This hypothesis has been entertained for nearly a hundred years (since Bishop 1932), and it has been revived recently (see VanRullen 2016b). The fact that α-fluctuations can be picked up extra-cranially via magnetic- or electrical encephalography (M/EEG) makes α an optimal candidate to study human perception non-invasively. Specifically, both the power (Worden et al. 2000; Ergenoglu et al. 2004; Babiloni et al. 2006; Thut et al. 2006; Klimesch et al. 2007; Palva and Palva 2007; Foxe and Snyder 2011) and the phase of the occipito-parietal α (Klimesch et al. 2007; Palva and Palva 2007; Mathewson et al. 2009; Klimesch 2012; Jensen et al. 2014; VanRullen 2016a) have been linked to performance in visual perception (van Dijk et al. 2008; Jensen and Mazaheri 2010; Jensen et al. 2011; Samaha and Postle 2015; VanRullen 2016b). However, while the evidence for the role of α-power in perceptual judgments seems well-established (Walsh 1952; Lansing et al. 1959; Jensen et al. 2011; Bompas et al. 2015; Benwell et al. 2017), the role of the α-phase is still not clearly settled (Walsh 1952; O'Hare 1954; Benwell et al. 2017; Ruzzoli et al. 2019).

So far, most studies have used an *offline* approach to study changes in perception based on the α-phase. In these studies, stimuli that demand a behavioural response are presented at random (or pseudo-random) intervals while EEG is recorded and, at a later time, trials are separated in terms of the behavioural outcome (hit vs miss; fast vs slow reaction times -RTs) and sorted post-hoc based on which phase within the pre-target α-cycle, the stimuli happened to fall. Average responses are then statistically compared across phase bins to conclude a phase-behavioural relationship (e.g., Busch et al. 2009). A significant correlation between phase and behaviour, when found, provides support for the theory.

However, the possibility of linking α-fluctuations to behaviour via non-invasive methods, such as EEG, is also attractive given the potential applications in Brain-Computer Interfaces (BCI) (Jensen et

al. 2011; Zrenner et al. 2016). For example, one could design closed-loop BCI systems that deliver information at favourable brain states for perceptual encoding to improve alerting, learning or memory (Brunner et al. 2015; Zrenner et al. 2016). To harness on the α-theories to develop BCI systems, one must use an *online* approach, which should be efficient even at the single-subject level. Real-time EEG analysis allows BCI settings to trigger stimuli at precise phase angles during the ongoing fluctuations in the individual α-rhythm that are thought to be associated with specific outcomes (hit/miss, fast/slow RTs). This approach exploits a specific brain-behaviour relationship (e.g., α-phase and perception) to augment information encoding with millisecond precision. The efficiency of closed-loop BCI must rely on predictable brain-behaviour relationships, in which the relevant parameters at play must be known beforehand. Hence, in turn, the attempt at using a closed-loop BCI approach is a test bench of neuro-cognitive theories such as the α-theories.

Interestingly, a good number of studies in the sixties already capitalized on the idea of time-locking stimulus presentation to the α-phase in real-time. Such attempts were popular enough by the middle of the decade to prompt Callaway and Layne to write: "*The idea of presenting photic stimuli at various phases of the spontaneous alpha rhythm to alter degrees of photic driving has occurred to many investigators*" (Callaway and Layne 1964, p. 421). In one preeminent study published in the journal *Science* in 1960, Callaway & Yeager (Callaway and Yeager 1960) endeavoured a closed-loop BCI addressing the relationship between the α-phase and RTs to visual events. They found that RTs were modulated as a function of the instant within the α-cycle the target flash was presented (see Lansing 1957; Dustman and Beck 1965 for similar results also in a real-time setting). Despite the substantial potential impact such closed-loop BCI on both theory and application, to the best of our knowledge, no modern study has implemented and reported a similar real-time protocol harnessing on occipital α-phase. The 60-year hiatus is remarkable, especially considering the α-theories are still entirely current up to this date.

Here, we capitalized on the putative relationship between the phase of ongoing α-oscillations and visual perception, adopting a closed-loop BCI approach to provide new evidence for the α-theories, which opened enduring questions a long time ago. At the same time, the present study aimed to provide a proof of concept for the use of the phase of ongoing α-oscillations as a control signal in a closed-loop BCI system for practical applications. This experiment is a modern

replication of Callaway & Yeager' study (1960). We employed a visual speeded detection task in which the visual target was triggered in real-time as a function of the phase of the participant's α-cycle. We expected that visual RTs would fluctuate along the α-cycle, or at least that it should be possible to find two distinct phases associated with fast and slow RTs, respectively. The hypothesis, procedure, and analysis pipeline were pre-registered before data collection (https://osf.io/nfdsv/). Deviations from the pre-registered procedure and exploratory analyses are clearly stated in this section.

Methods

Participants

Sample size. We planned a maximum sample of 16 participants with a stopping rule set after a minimum of 8 participants (see details below). Participants were selected without previous history of neurological or psychiatric diseases, with normal or corrected to normal vision, within 18-35 years old. The minimum/maximum sample size was decided a priori based on a Monte Carlo simulation on Callaway & Yeager' data (1960) (See **Supplementary Figure 1** in *Annex I*). We estimated that if less than 3 participants out of 8 showed a significant difference between fast and slow phase bins, then the size of the effect in this experiment would be null or negligible compared to the original study (Callaway & Yeager, 1960), assuming an error of 5%.

Exclusion criteria. A participant was excluded if any of the following criteria were met: *(i) No peak within the a-band:* This criterion applied to the screening stage and ensured that the individual's endogenous α-oscillation could be registered with a sufficiently high signal-to-noise ratio (SNR) to enable the BCI system to estimate instantaneous phases from the EEG signal reliably. This decision was based on two sub-criteria: strength and uniqueness (see *Screening and estimation of the Individual Frequency of Interest section* for more details). (*ii) Experiment duration:* Given that we had a block stopping rule based on the number of trials per phase bin, the length of the experiment could vary as a function of how frequently the EEG phase could be reliably estimated for stimulus presentation. Hence, we had to establish an experiment duration limit. We decided to stop the experiment if a participant spent more than 10 minutes in the training block or two consecutive blocks within the real-time experimental stages. This criterion was

added after we had run the first 2 participants, which required an update of the pre-registered protocol[1].

We recruited 27 participants, 6 of which were discarded for not satisfying the required α-peak criterion in the screening stage, and 13 because of the duration criterion. The remaining 8 participants (aged 19-30 years, average 24 years, three females; all right-handed) completed the experiment. Data from excluded participants were not analysed. All the participants took part in the study voluntarily after giving informed consent, and they were compensated for their time with 10€ per hour. The duration of the experiment varied between 70 and 120 min. The study was designed in accordance with the Declaration of Helsinki and approved by the local ethics committee CEIC Parc de Mar (University Pompeu Fabra, Barcelona, Spain) before starting the recruitment.

Experimental procedure

The experimental protocol started with a screening, followed by a training and two consecutive experimental stages (explained below). In the training and experimental stages, participants performed a speeded visual detection task in which stimuli were presented according to the phase of the spontaneous α-activity in real-time (see **Figure 9**).

Task. Participants sat on a comfortable chair wearing an EEG cap, and a pair of opaque sunglasses, with two LEDs, mounted on each lens. The LEDs were controlled through the parallel port (both LEDs switched on and off simultaneously; luminance 0.076 cd/m^2 at an approximate distance to participants' eye of 1 cm)[2]. Participants were asked to keep their eyes closed throughout the experiment to maintain α-activity high and to limit eye movements (a strategy first suggested

[1] We considered that a duration of > 10 min x block (leading to more than 160 minutes approximately of total experimental time + EEG cap montage + debriefing) was unacceptable due to fatigue effects (or sleepiness, easy to happen with eyes closed). These factors can have an impact on the α-activity and, therefore, on our phase estimation in the BCI setting.

[2] Please note that it is not possible to infer the proper stimulus intensity from Callaway & Yeager' (1960) experiment; therefore, we chose a fixed arbitrary value that was comfortable for the participants and ensure that response latencies were comparable to those in the original study.

by Callaway & Yeager, 1960). We instructed the participants to remain attentive and to respond to the visual flashes as fast as possible by pressing a button in a response box using their right index finger. After the response (or after 1 second time out), the LEDs were switched off. An inter-trial interval (ITI), randomly chosen between 1500 and 2500 ms, was introduced between the button response (or 1 s time out) and the beginning of the next trial. RTs were measured from the onset of the visual target until a button press was detected.

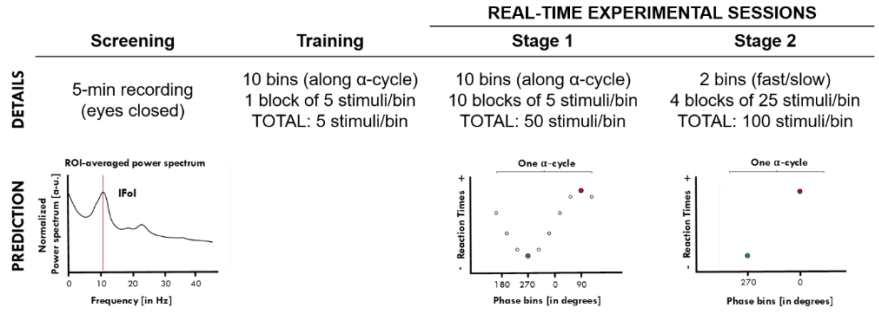

FIGURE 9. The protocol included four stages: Screening, Training, Stage 1 and Stage 2 of testing. During the Screening, we looked for the individual frequency of interest (IFoI) over the occipito-parietal area in a 5 min EEG recording at rest (eyes closed). Participants who did not display a single peak in the EEG within the range of interest (5-15 Hz) did not proceed to the following parts of the protocol. Included participants performed a Training and entered Stage 1 of the real-time experimental sessions. In Stage 1, visual stimuli were triggered phase-locked to 10 equally spaced phase bins along the IFoI-cycle. For illustration purposes of an ideal theoretical outcome, stimulus onset (circles) is represented as a function of the EEG alpha cycle through a cosine wave. From Stage 1, the specific phase bins associated with the faster (green dot) and slower (red dot) RTs were selected for each participant and used for Stage 2. In Stage 2, visual stimuli were triggered only at the two-phase bins (fast/slow) individually selected from Stage 1. As illustrated, we predicted that fast and slow phase bins would lead to fast and slow RTs, respectively.

*Training stage***.** Before the real-time experimental stages, participants were familiarised with the task in a training block (50 trials), identical to Stage 1 (see below).

Experimental stages. After training, participants went on to Stage 1, where visual targets were aimed at 10 equally-spaced phase bins covering the whole α-cycle (see *Real-time stimulus presentation*). This experimental stage was divided into 10 blocks, each ending after the acquisition of at least 5 valid RTs per phase bin, for a total of 50 RTs per phase bin across blocks. Once Stage 1 had been completed, the phase-bins corresponding to the fastest and slowest mean RTs were

selected and used for Stage 2 (at the individual level). No statistical test was performed at Stage 1. Stage 2 started right after Stage 1. In Stage 2, visual targets were aimed only at the "fast" and the "slow" phase bins, estimated from Stage 1. Participants ran 4 blocks, each block ended after the collection of at least 25 valid trials for each of the two-phase bins, for a minimum total of 100 trials per bin.

EEG recording. Continuous EEG data were recorded at 500 Hz using the ENOBIO 20 5G system (Neuroelectrics, Barcelona, Spain) from 14-channels (F3, Fz, F4, C3, Cz, C4, P7, P3, Pz, P4, P8, O1, Oz, O2) with Cl-Ag electrodes placed according to the 10-20 international system. Impedance was kept below 10 kΩ, according to the Enobio coded system. Additional external electrodes were used to record vertical and horizontal eye movements. Electrode AFz was used as online reference and the right mastoid as ground. Activity from the left mastoid was recorded for offline re-referencing.

Screening and estimation of the Individual Frequency of Interest (IFoI). We recorded 5 minutes of resting EEG with the eyes closed, which we used to determine the specific frequency of interest within the α-band for the real-time stages of the experiment. We estimated the power spectrum density (PSD) within the α-band (5-15 Hz) over occipito-parietal electrodes (OP-cluster: P7, P3, Pz, P4, P8, O1, Oz, O2) using the Welch method (window = 500 ms; overlap = 10%; resolution = 0.25 Hz). For each participant, the power spectrum was averaged across the electrodes of interest and normalized by the mean power spectrum from 1 to 40 Hz. We verified the strength of the peak - power at the local maximum within the 5-15 Hz window is greater than average power in the 1-40 Hz window - and its uniqueness - the peak is a single local maximum within a ± 5 Hz band. If a single frequency peak existed, it was considered as the IFoI[3] and used later as a parameter for real-time analyses (**Figure 9**). If a unique frequency peak could not be detected, the participant was excluded from the study (see *Exclusion Criterion 1*).

---

[3] We prefer to use the term Individual Frequency of Interest (IFoI), instead of Individual Alpha Frequency (IAF), often used in the literature, because we focused on a frequency range between 5-15 Hz, which spreads out a finer range in the conventional α-band (8-12 Hz).

Real-time stimulus presentation. We developed a BCI setting to trigger flashes (LEDs) at a specific α-phase based on real-time data from electrode O1 (as in Callaway & Yeager, 1960) through custom-built code in MATLAB (MathWorks, R2015.b). We used the Lab Streaming Layer (LSL) library (Swartz Center for Computational Neuroscience, UCSD, January 2018) to acquire EEG data with the ENOBIO acquisition software (NIC V2.0). Given that synchronization between the EEG time acquisition and local PC time is not supported for online streams by ENOBIO, we used an external signal (a parallel port pin connected to one of the ENOBIO electrodes) as time reference. In each iteration, we randomly pre-selected, among the bins available (10 bins in Stage 1, or 2 bins in Stage 2), a phase bin when to send the stimulus trigger. Ten-seconds of EEG data from the O1-electrode were continuously buffered, demeaned, and band-pass filtered (Butterworth forward filter, order 2, IFoI ± 5 Hz). Amplitude and phase were estimated at each time point using the Hilbert-transform. When the average amplitude in the last second of the buffer was above 30% of the median value of the buffered data, a reference time point was set at the peak (90°) of the last α-cycle. Then, the moment at which the phase of interest in a given trial would occur was forecasted by extending a sine wave (frequency = IFoI) from the reference point. We targeted one of the 10 phase bins (36º each) within the next α-cycle starting after a safety buffer of 72° (~20 ms) for computation time. The stimulus trigger switched on the LEDs at the latency corresponding to the centre of the targeted phase bin (error ≤ 2 ms).

Responses and trial selection. Responses were collected from a button press via a response box connected to the parallel port. There was a response time out of 1 second after the stimulus, following which the next trial iteration began. If a response was registered before time out, we stored the RT and checked the accuracy of the real-time phase estimation by calculating the difference between the empirical phase at which the stimulus was delivered (according to the recorded EEG) and the intended one, using the Circular Statistics Toolbox in MATLAB (Berens 2009). In Stage 1, if the stimulus had been triggered in an unintended phase, the trial was relocated to the actual (empirically measured) phase bin. In Stage 2, we only targeted two phases and set a tolerance of ± 1 phase bin to reduce the testing time, and we did not relocate trials. A trial was excluded if the empirical phase did not fall within the tolerance zone, or it fell in an overlapping

bin between the slow and the fast bin (this could happen if the fast/slow bins were less than 72º apart).

Only trials that satisfied all the following criteria were accepted as valid: *(1) Reaction time criterion:* RTs within 50 and 300 ms (as in Callaway & Yeager, 1960). *(2) Amplitude criterion*: the amplitude of the IFoI-cycle window centred at stimulus onset had to be above the 30% of the median amplitude in the last 10s (this threshold criterion facilitated reliable phase estimation at stimulus presentation).

A block stopped when the intended number of trials per phase bin was reached (N=5 in Stage 1 or N=25 in Stage 2). In between blocks, participants took a break before starting a new one. Excess trials (which could happen due to trial relocation) were discarded.

Statistical analyses

Stage 1 was designed to estimate the phase bins corresponding to faster and slower RTs throughout the α-phase, whereas Stage 2 provided data for the validation of the hypothesis. In Stage 1, we only ran descriptive statistics to calculate average RTs per phase bin, and to select the phase bins of interest. If the fast and slow phase bins selected in Stage 1 would indeed be representative of neural excitability states related to visual perception, then sending targets to these phase bins in Stage 2 should induce faster and slower responses, respectively. To test this prediction, in Stage 2, we performed individual and group-level analyses. For the individual analysis, we assessed the difference between the RTs collected in the predicted slow and predicted fast phase bins by a one-tailed t-test (independent samples) with α-level = 0.05. Note that in Stage 2, if slow/fast bins (± 1 phase bin) shared a common bin, then trials in that bin were post-hoc excluded and not used for the analysis. For the group analysis, we evaluated the difference between the mean RTs collected in the slow vs fast phase bins across participants by a one-tailed paired t-test with α-level = 0.05.

Results

Here, we present the results obtained from the pre-registered analyses as explained above, which replicated the conditions of the seminal study by Callaway & Yeager (1960), followed by reality checks and a set of exploratory analyses.

Results of pre-registered analysis

Stage 1: Selection of the fast/slow phase bins along a-cycle

We collected an average of 1034 (SD = 219) responses per participant. An average of 77 (SD = 53; 7.41%) trials were excluded because the RTs fell out of the 50 – 300 ms range and 341 (SD = 190; 33%) trials were excluded because the amplitude threshold criterion was not met, leaving an average of 617 (SD = 36; 60%) valid trials per participant. Among the valid trials, 280 (SD = 35; 45.33%) trials hit the target phase bin of interest whereas 337 (SD = 61; 54.67%) trials had to be relocated to the intended phase bin offline (most of them fell on neighbouring bins, see Reality check 1: Accuracy of phase estimation during the real-time experiment, below). Therefore, we reached the intended 50 valid trials per bin for each participant (following the elimination of excess trials). RTs for valid trials were on average 206 ms (SD=9 ms). We calculated the mean RT for each phase bin along the α-cycle for each participant (see **Figure 10** and **Supplementary Table 1** in *Annex I*; see **Supplementary Table 2** in *Annex I* for information about the number of trials at the individual level) and selected the phase bins associated with the slowest and fastest mean RTs, to be used in Stage 2. Overall, the mean RT difference between slow and fast phase bins in Stage 1 was 12 ms (SD = 4; Max = 17 ms; Min = 8 ms). At this point, if the distribution of slow and fast RTs meets the expectations of the α-theory, the corresponding slow and fast phase bins should fall on roughly opposite angles (approximately 180°). However, what we observed is that for most of the participants, slow and fast phase bins were closer than 180°, being the mean difference 90° (SD = 51°).

Stage 2: Validation of the a-phase relation to RT speed

In Stage 2, we collected an average of 408 (SD = 103) trials per participant. Among these, 31 (SD = 14; 7.65%) trials were excluded because they fell outside the RT criterion, 144 (SD = 84; 35.30%) trials were excluded for not satisfying the amplitude threshold criterion, and 33 (SD = 24; 8.09%) trials for not falling in the bin acceptance zone. After trial exclusion, we were left with a total of 200 valid trials each participant (100 trials per bin), as intended. Among these, an average of 107 (SD = 24; 54%) trials hit the target phase bin of interest (± 1 bin), whereas 93 (SD = 24; 46%) trials were relocated. Note that from the valid trials, we discarded those trials that shared a common phase bin in the phase bin acceptance zone, leaving 79 (SD = 15) and 86 (SD = 13) trials on average for predicted slow and

predicted fast trials, respectively. For information on the number of trials in Stage 2 at individual-level (see **Supplementary Table 3** in *Annex I)*.

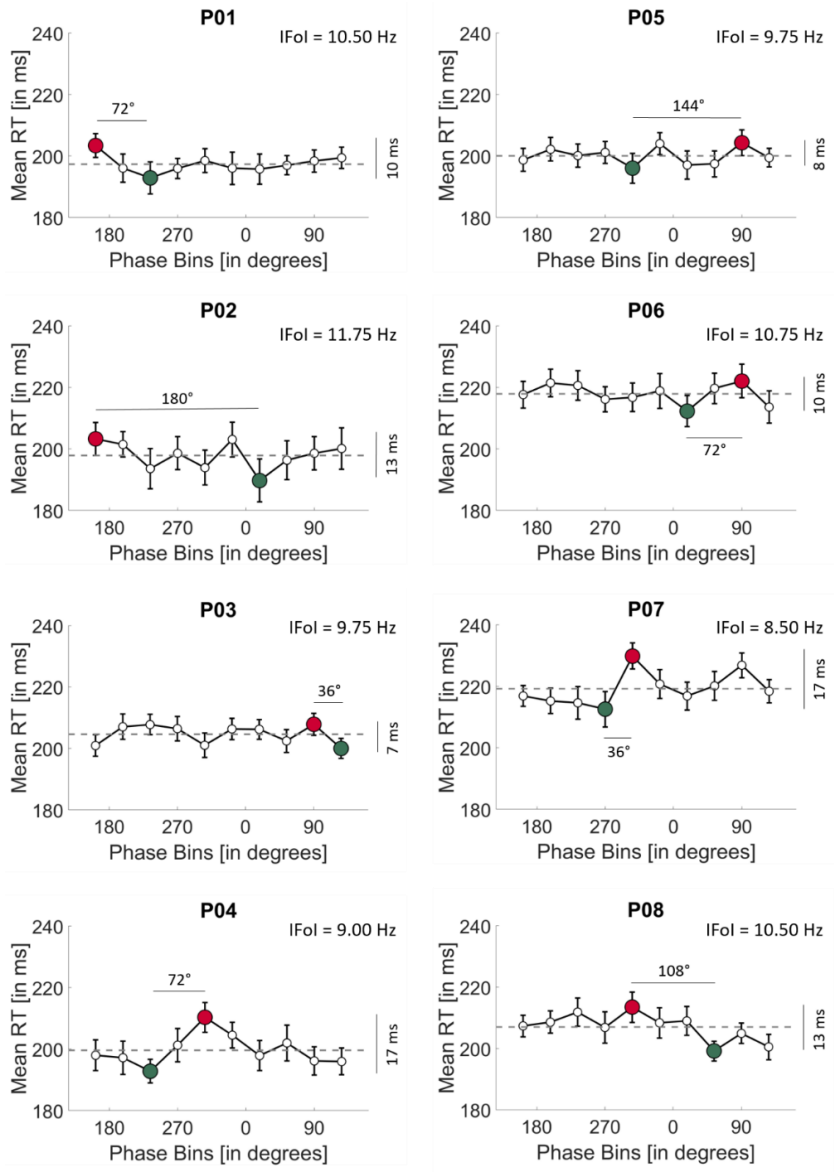

FIGURE 10. Individual mean RT (in ms, y-axis) plotted against the 10 phase bins (in degrees, x-axis) tested in Stage 1. The horizontal dashed line indicates the individual mean RT across all bins. For each participant, the graphs report the angular difference and the RT difference between the fast (green dot) and slow (red dot) phase bins. IFoI= Individual Frequency of Interest; Error bars = Standard Error of the Mean (SEM).

TABLE 1. Individual data for fast/slow phase bins including phase bin acceptance zone in Stage 2. For each participant, the number of trials (max=100), the tested angular points (degrees), and the mean RTs (ms) are reported for the fast and slow phase bins tested in Stage 2. Statistics indicate the results (t value, degrees of freedom, p-value, Cohen's dz and 95%-confidence intervals CI) of an unpaired t-test (right-tailed, $p<0.05$) comparing slow vs. fast RTs individually. Group level data and statistics are also reported.

	Slow phase bin			Fast phase bin								
Part.	**No. of trials**	**Phase bin**	**Mean (SD) RTs [in ms]**	**No. of trials**	**Phase bin**	**Mean (SD) RTs [in ms]**	**RT diff. phases [in ms]**	**Statistics**				
								t	**dof**	**p**	**dz**	**RT diff. 95% CI**
1	88	162°	198 (34)	85	234°	200 (37)	-3	-0.30	171	.62	-.05	[-10.43 7.24]
2	100	162°	196 (39)	100	18°	202 (30)	-9	-1.26	198	.90	-.18	[-14.24 1.90]
3	74	90°	203 (32)	59	126°	206 (39)	-3	-0.54	131	.71	-.10	[-11.70 5.88]
4	66	306°	202 (36)	86	234°	195 (39)	10	1.24	150	.11	.20	[-2.53 17.83]
5	100	54°	194 (29)	100	306°	191 (33)	-3	0.69	198	.24	.10	[-4.18 10.27]
6	62	54°	207 (34)	87	18°	207 (32)	8	-0.02	147	.51	-.00	[-9.05 8.85]
7	75	306°	200 (32)	78	270°	201 (40)	1	-0.21	151	.58	-.03	[-10.97 8.50]
8	68	306°	191 (39)	90	54°	193 (37)	-6	-0.36	156	.64	-.06	[-12.07 7.68]
Mean (SD)	**79 (15)**	**--**	**199 (5)**	**86 (13)**	**--**	**199 (6)**	**-1 (7)**	**--**	**--**	**--**	**--**	**--**
Group level	**633**	**--**	**199 (5)**	**685**	**--**	**199 (6)**	**-1**	**-0.30**	**7**	**.61**	**-.11**	**[-5.66 4.78]**

The mean RT difference across participants between slow and fast phase bins in Stage 2 was -0.439 ms (SD = 4), which was not significant according to a group t-test (t(7) = -0.2977, $p = 0.6127$, dz = -0.1052). Individually, none of the participants presented a significant difference in RTs between the visual targets presented in the predicted slow and fast phase bins of the α-cycle (all $ps > 0.1$; see **Table 1**).

Interim discussion and reality checks

The analyses according to the pre-registered pipeline adapted from Callaway & Yeager (1960) did not return a consistent relation between the phase of individual ongoing α-oscillations and the speed of responses to visual targets at the individual or group level. Compared to offline experimental approaches, where analyses can be adjusted retrospectively, real-time settings imply a priori parameter choices that

can affect the outcome. Therefore, we proceeded to exclude the possibility that the null results from the main analyses may have originated from a priori choices in the real-time setting. We focused on three aspects: First, we checked the accuracy of the closed-loop BCI system in sending the stimulus trigger at the intended phases along the α-cycle. Second, we questioned whether the choice of the IFoI based on resting EEG data was representative of the dominant α-frequency during the task. Finally, we checked that the electrode choice (O1) for the real-time α-phase estimation was representative of α-activity of interest in the occipito-parietal cluster of electrodes.

Reality check 1: Accuracy of phase estimation during the real-time experiment

The question here was how precisely the closed-loop BCI triggered visual stimuli at the desired phases along the α-cycle. We, therefore, selected all valid trials for each stage and extracted the phase at which the stimulus was presented from the empirical EEG offline, and computed the absolute difference between the desired and the actual phase using the Circular Statistics Toolbox (Berens, 2009). On average, across phase bins and participants, our BCI system hit +1.21° (SD = 33.70°) off the intended phase in Stage 1, and +3.79° (SD = 25.43°) in Stage 2 (see **Figure 11** and **Supplementary Figure 2** and **Supplementary Figure 3** in *Annex I* for individual results on phase accuracy in Stage 1 and Stage 2, respectively). The phase estimation accuracy of our real-time BCI setting seems comparable to previous attempts at phase-triggered events, like for example targeting the α-frequency in the motor cortex (Zrenner et al. 2018; Madsen et al. 2019) which typically achieved an accuracy within -12º to 5º off of the desired phase, with SDs between 48º and 55º.

We also decided to check the reasonable expectation of whether the accuracy of the phase estimation depended on the latencies from the reference point of the EEG signal (i.e., phase bins) and whether it was worse at increasing latencies. We rearranged phase accuracy values based on the phase bins and found, as expected, that both the mean and standard deviation of phase accuracy are worse at increasing latencies (see **Supplementary Figure 4** and **Supplementary Table 4** in *Annex I* for individual and group data). When subtracting the accuracy of the last-first latencies, the average mean varies -5.42º (SD = 9.38º) and the variability increases 32.20º (SD = 10.64º). Finally, we calculated the cumulative percentage of trials as a function of the phase bin difference between target and hit phases. **Supplementary Table 5** in *Annex I* shows the results at the individual and group level.

Overall, 45% of trials felt in the target phase bin, 88% of trials within ±1 bin, and nearly all trials within ±2 bins.

These overall results show a reliable alignment at each of the targeted phases of the α-cycle. Although extrapolating approximately over one α-cycle has led to more unreliable phase accuracy at increasing latencies, the accuracies are still within safe limits in terms of our purposes. Note that accuracy of phase estimation was checked against real data as part of the BCI setting, so that trials with erroneous estimations that satisfied the trial validity criteria (i.e., RT and amplitude) were eventually relocated if necessary to the hit phase bin in Stage 1 or discarded if did not fall within the acceptance zone in Stage 2. We, therefore, think that the possibility that null results in the α-phase – RTs relationship might be explained by an inaccurate triggering of targets is minimal.

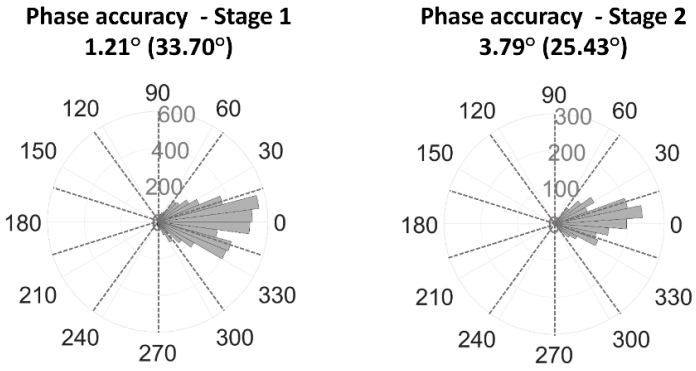

FIGURE 11. **Rose plot of phase accuracy for valid trials across participants in Stage 1** (total No. of trials = 4933) and **in Stage 2** (total No. of trials = 1600). For convenience, all phases have been realigned to 0**º**. Dotted lines denote boundaries between phase bins.

Reality check 2: Frequency of interest during the real-time experiment

The real-time stages of the experiment used the IFoI, which was estimated in a 5-min pre-experiment screening session from a cluster of occipito-parietal electrodes (see Screening and estimation of the IFoI for more details). This pre-screening is a common practice in order to customize the EEG analysis in terms of individual frequency, especially in the α-band. One potential problem, however, is that the frequency measured in the screening session was not representative of the relevant frequency during the task. Small deviations between the relevant α-frequency during task execution and the one actually used

might be mitigated in our protocol because we used a relatively large spectral window (IFoI ± 5 Hz). However, large deviations might affect the subsequent steps of the online protocol, such as filtering and forward prediction. To estimate if such deviations took place, we compared the IFoI used in the real-time experiment stages (that is, the one estimated from the screening stage) against the actual dominant α frequency recorded during task execution. IFoI during task execution was computed following the same procedure as for the IFoI in the screening stage. To avoid potential contamination from visual and motor evoked responses, we used EEG epochs from +500 ms after button press to stimulus onset of the next trial (duration about 2 s, depending on inter-trial jitter). We computed the power spectrum density (PSD) within the α-band (5-15 Hz) for O1-electrode (the electrode in the BCI setting) and for the OP-cluster (the same as used in the screening session for the selection of the IFoI: P7, P3, Pz, P4, P8, O1, Oz, O2) using the Welch method (window = 500 ms; overlap = 10%; resolution = 0.25 Hz). For each participant, the power spectrum was normalized by the mean power in the 1 to 40 Hz window. **Figure 12A** illustrates the single frequency peak within the α-band during task execution, plotted against the IFoI at rest used in the real-time experiment. Overall, the mean peak difference between rest (OP-cluster) and task (O1-electrode) IFoIs was 0.16 Hz (SD = 0.23), with a maximum absolute mean difference of 0.50 Hz in participant 8 (see **Supplementary Table 6** in *Annex I* for individual results). IFoI at rest in OP-cluster was very close to the dominant α-frequency during task execution from the same electrode, with deviations of the central frequency of less than 1 Hz. Moreover, we decided to check whether the instantaneous frequency differed from the IFoI on a trial-by-trial basis. We calculated the instantaneous frequency for each trial using the Hilbert transform. We band-pass filtered the data from O1 electrode within 5-15 Hz (Butterworth filter order 2, one-pass), epoched from –2 to 2 s (from stimulus onset), demeaned and detrended. We computed the instantaneous frequency using the MATLAB function 'instfreq'. We selected the prestimulus window of interest of -1 to 0 s from stimulus onset (same time window as the one-second buffer in the real-time experiment) to average the instantaneous frequency within the selected window. **Supplementary Figure 5** in *Annex I* shows a heatmap chart of the variation of the phase accuracy as a function of the frequency difference from IFoI for each participant, in which colour denotes the number of trials. All the participants show a mean frequency deviation from IFoI lower than 1

Hz. Participant P08 shows the smaller variability in frequency deviation (mean SD=0.32 Hz), whereas participants P03 and P05 show the larger variability (mean SD = 0.73 Hz) (see **Supplementary Table 5** in *Annex I*). At group-level, the average mean frequency across participants is 0.73 (SD = 0.24) Hz. Note that we were extrapolating approximately one α-cycle from a reference point at the peak of the EEG signal. Therefore, we would expect to see that if the error in the frequency estimation is negative (i.e., actual instantaneous frequency is slower than the estimated IFoI), then there will be a positive error in the phase estimation (i.e., the stimuli would reach an earlier hit phase and the target phase would happen afterwards in time). Hence, we expected the direction of the correlation to be negative. To check for this hypothesis, we decided to compute a linear correlation between the frequency difference from IFoI and the phase accuracy for each participant by adopting a directional one-tailed hypothesis testing. **Supplementary Table 6** in *Annex I* shows the results, including Pearson's coefficient with its p-value. Overall, we see that 5 out of 8 participants present a negative correlation, as expected, and only participants P01 ($p = .04$), P02 ($p = .001$) and P07 ($p < .001$) show a significant negative correlation.

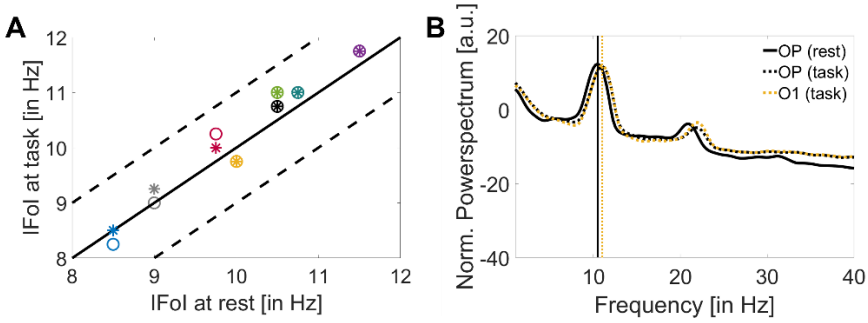

FIGURE 12. (A) IFoI [in Hz] at rest using OP-cluster (P7, P3, Pz, P4, P8, O1, Oz, O2) vs IFoI during the task [in Hz] for two different electrode set conditions: OP-cluster (circles) and O1-electrode (asterisks). Dashed lines denote ±1 Hz and each colour denotes a participant. **(B) Power spectrum of a representative participant (P08) showing the biggest mean difference (0.50 Hz) between IFoI at rest computed at OP-cluster (solid black line) and IFoI at task computed with O1-electrode (dotted yellow line).** Power spectrum computed at OP-cluster at task is also plotted (dotted black line).

We can, therefore, conclude that the BCI setting employed here was successful in centring the spectral analysis around the desired relevant frequency of interest and variation in frequency from the IFoI at a single-trial level might have influenced the phase accuracy of the BCI

setting. However, as stated in the previous section, if there was a deviation in the frequency from the IFoI in a given trial, we took that into account by checking the empirical phase at stimulus presentation and reallocate it if necessary to the hit phase bin in Stage 1 or discarded if did not fall within the acceptance zone in Stage 2.

Reality check 3: Electrode of interest used in the real-time experiment

As for the frequency of interest, we had to a priori decide about the electrode of interest to be used in the BCI system. Following Callaway & Yeager (1960), we chose O1-electrode. This choice appeared convenient to limit real-time computational delays due to clustering over a larger set of electrodes. However, it is perhaps important to check that the signal picked up from O1-electrode in the real-time stages was representative of the α-frequency dominant in a wider occipito-parietal cluster. Therefore, we compared the activity in O1-electrode to that of a cluster of occipito-parietal electrodes (OP cluster: P7, P3, Pz, P4, P8, O1, Oz, O2). The spectral comparison was analogous to the one described for the reality check 2 (IFoI rest vs IFoI task). The results, illustrated in **Figure 12B** (see **Supplementary Figure 6** and **Supplementary Table 6** in *Annex I* for individual data), show that the two α estimates were within 0.20 Hz. In five out of the eight participants, the relevant frequency peak using the occipito-parietal cluster was the same as in O1-electrode. We can, therefore, confirm that the α-fluctuations picked up from O1-electrode as our IFoI during the real-time experiment were closely representative of the occipito-parietal activity.

Exploratory analyses

In the present study, we aimed at employing a closed-loop BCI approach to show that the phase of ongoing α-oscillations measured with EEG can be harnessed to expedite RTs. This proof-of-concept can not only open avenues for neuro-devices but also help to test the relevance of the α-theories. To do so, we sought to achieve a conceptual replication of a seminal study where such effects had been reported in the past (Callaway and Yeager 1960). Although our setting included some corrective measures and online checks, we ensured that the system successfully phase-locked visual stimulation to ongoing occipital α-oscillations, the pre-registered analyses returned null results. We decided to explore the data further to find out if phase effects on RTs could be found using other approaches.

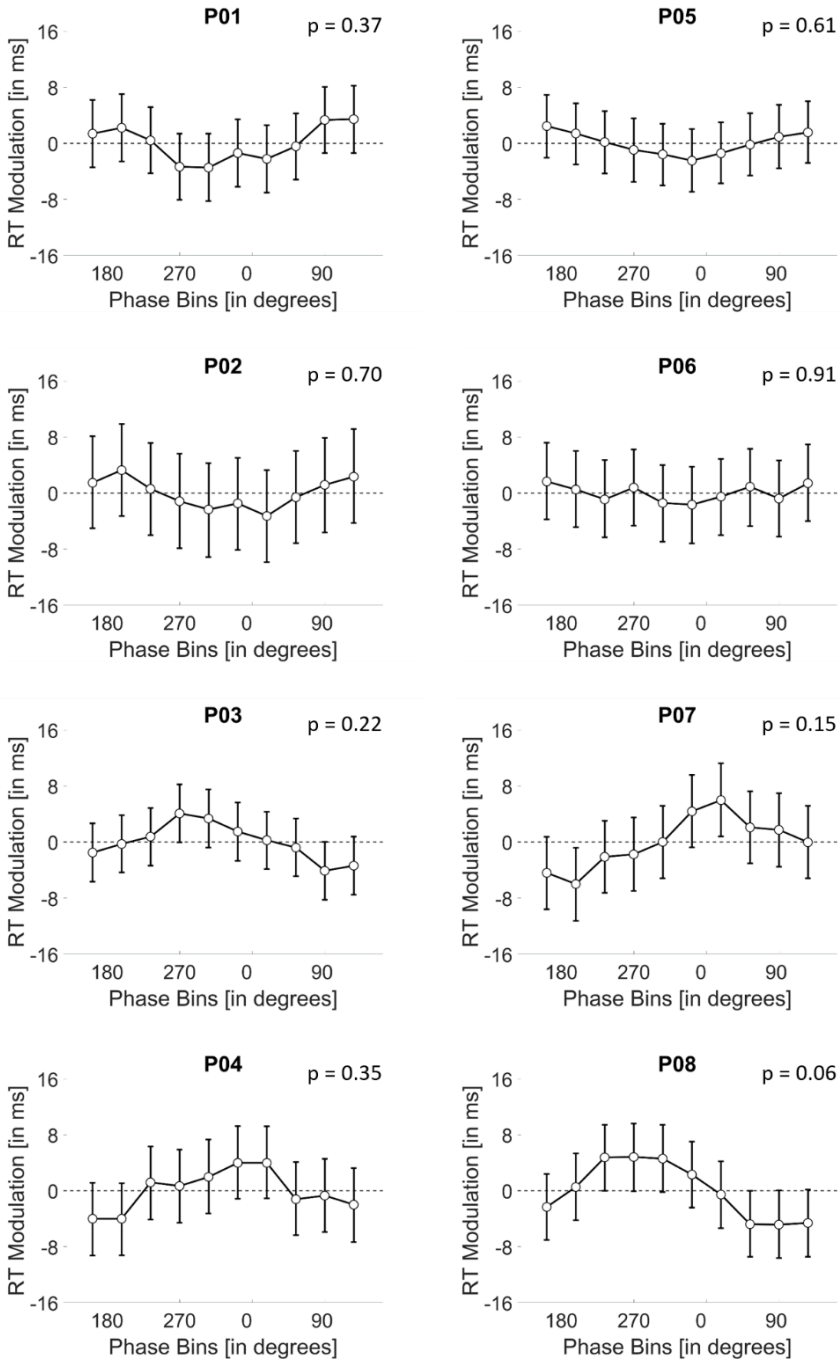

FIGURE 13. Phase-RT modulation for each phase bin (centred on the target phases) in Stage 1 for all participants. P-value of the modulation comes from using a Monte Carlo randomization procedure (N = 10,000 randomizations). Error bars denote the 95%-confidence intervals (CI) of the randomizations.

Re-analysis of Stage 2 data including only trials for fast/slow phases

In the main analysis of Stage 2, we decided to include trials in which our online phase estimation was ± 1 phase bins from the intended (fast/slow) phase. This decision was taken under the assumption that, by definition, phase effects fluctuate gradually, so that excitability in phase bins near the maximum peak (minimum peak) would still be relatively high (low). However, we decided to re-do the analysis in Stage 2 and select only those trials falling strictly in the slow and fast phase bins, while excluding those falling in ± 1 phase bin acceptance zone (as well as all the rest, as before). We re-calculated the mean RT between slow and fast phase bins and found a mean difference of -0.625 ms (SD = 7), which was not significant neither at individual nor at the group level ($t(7) = -0.2496$, $p = 0.5950$, $dz = -0.0883$). Note that the number of trials was much reduced, leaving 55 (SD=18) and 52 (SD = 9) trials on average for predicted slow and predicted fast trials, respectively. For information on the number of trials and statistics at individual-level, see **Supplementary Table 7** in *Annex I*. These findings are in line with those found in the pre-registered results.

Smoothing the RT-phase modulation

The main purpose of Stage 1 was to estimate the phase bins with fastest and slowest RTs for later use in Stage 2. However, given that we collected a minimum of 50 RTs for each of the 10 bins distributed throughout the α-cycle, one could search for a possible phase-ordered pattern in the RTs in that dataset. As described in the Results section, plotting the mean RTs for each phase bin (**Figure 10**) did not seem to highlight any discernible oscillatory pattern. However, we did not perform a formal statistical analysis at that stage. In this follow up analysis, we adapted an analytical approach used by Fiebelkorn et al. (2013) to test statistically for an oscillatory pattern in Stage 1 data. The logic behind this approach is that if a phase-dependent modulation of RTs exists, then RTs should vary significantly around opposite phases of α (as in the idealized example in **Figure 9**).

Therefore, we looked for pairs of phases 180° apart that could result in a larger difference between RTs. We calculated the average RT over the trials lumped within -90° and +90° around each phase bin to obtain 10 phase-centred RT averages. Then, we normalized each phase-centred RT average by the average RT across all trials. If RTs were modulated by phase, the normalized phase-centred RTs would resemble a sine wave. To test the statistical significance of possible

phase modulation, we transformed these phase-centred RT averages to the frequency domain through a fast Fourier Transform (FFT). We tested the significance (α-level = 0.05) of the peak in the FFT for one cycle using a Monte Carlo randomization procedure (10,000 randomizations). The statistical tests showed that none of the participants displayed a significant RT modulation (p-values ranged from 0.11 to 0.92; **Figure 13**). This outcome confirmed the results from the pre-registered analysis on phase effects, described above.

Searching for phase opposition at stimulus onset

If the response to a stimulus is related to the phase of the α-activity, we should expect a pattern of opposition within the α-frequency (the narrow band EEG) when comparing between slow and fast RT trials at stimulus onset (time = 0) (Mathewson et al. 2009). We checked for this possibility by offline band-pass filtering data from electrode O1 using a Butterworth filter (order 2, two-pass) around the IFoI ± 5 Hz band. No re-referencing was applied. All valid trials from Stage 1 were used for the analysis. EEG data were epoched from – 200 ms to 300 ms (t=0 being the stimulus onset time), and then demeaned and baseline corrected (- 200 ms to 0 ms). To average across subjects with different IFoI, the time dimension of the EEG was transformed into α-cycle units (the time vector multiplied by the IFoI; data resampled by linear interpolation). RTs were median-split into slow and fast categories. The inter-participants average RT was 231 ms (SD = 9) for slow trials and 182 ms (SD = 8) for fast trials. **Figure 14** shows the narrow-band activity for the slow and fast RTs, and for all trials pooled together (see, **Supplementary Figure 7** in *Annex I*, for individual plots). Although visual inspection suggests an opposition pattern in the narrow-band activity between slow and fast trials at stimulus onset, this pattern is not statistically significant. This can be appreciated by comparing the apparent difference with the large overlap in the confidence intervals (fast trials mean = -0.4454 μV, 95% CI = [-1.5599, 0.6691] μV; slow trials mean = 0.3901 μV, 95% CI = [-0.6210, 1.4012] μV). However, to test for phase opposition beyond visual inspection, we used the Phase Opposition Sum (POS) method (VanRullen 2016a). We forward-filtered the data from electrode O1 using a Butterworth filter (order 2, one-pass) around the IFoI ± 5 Hz band and computed the phase by means of the Hilbert transform. We applied the POS on phase values at stimulus onset for fast vs slow trials, both at individual and group-level. The statistical significance was assessed using non-parametric permutations tests (10,000 iterations) using random shuffles of trial assignment to

slow/fast bins to compute the distributions of POS values to be expected by chance for each subject. For the group, the distribution of POS values to be expected by chance corresponded to the average of individual POS values to be expected by chance. The p-value associated to measured POS at individual (group) level corresponded to the proportion of times that individual (group averaged) POS obtained in the permutation exceeded measured individual (group averaged) POS.

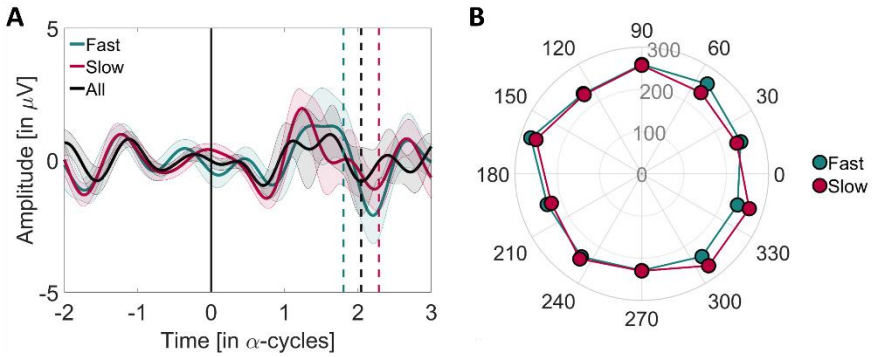

FIGURE 14. (A) Grand average of the narrow-band activity time-locked to visual stimulus presentation for fast (green), slow (red), and all (black) trials from O1-electrode in time of the α-cycles. Thin lines represent the standard error of the mean (SEM) interval. Vertical dashed lines denote the mean RTs for all slow (red), fast (green) and all trials (black). **(B) Polar plot of the representation of the overall number of trials across participants for each phase bin (dots) for fast and slow trials.**

In line with the results of the pre-registered analyses, we did not observe a significant group-level effect of POS between slow and fast RTs ($p = .932$) nor at individual-level.

Effect size equivalence test

The present study was a replication of a previous one testing a relationship between the α-phase and RT (Callaway and Yeager 1960). The results were at variance with that original study: we did not find evidence for such a relationship. We decided to perform an equivalence testing (Lakens et al. 2018) to compare the effect size in the original study with that reached in the present, even if we had already looked at the data. Callaway and Yeager (1960) reported data from 8 participants and achieved a mean difference between slow and fast RT of 8.13 ms (SD = 5.11; dz = 1.59). In a new study, it would then be reasonable to expect a minimum effect size equal to 33% of

the original effect size, assuming the effect in the original study were true (Simonsohn 2015). This means that we would expect a minimum theoretical effect size of 2.681 ms (or dz = 0.53). Incidentally, our aim before the study was to achieve RT differences that would also be relevant in terms of BCI application in real life, and therefore possibly larger than the meagre 2.7 ms effect size derived from the present estimation (admittedly, performed a posteriori). Nevertheless, if not useful at the practical level, one would hope to gather some information at the theoretical level. In the present study, we tested 8 participants and obtained a mean difference between slow and fast RTs of -0.439 ms (SD = 4.171 ms; dz = 0.105) (Stage 2). Given this sample size we cannot reject that the real difference between conditions is bigger than 0 ($t(7) = -0.298$, $p = 0.775$, α-level = 0.05, one-tailed) or that the effect size is between -.53 and .53 ($t(7) = 1.521$, $p = 0.09$, given equivalence bounds of – 2.68 and 2.68 ms and α-level = 0.05). The equivalence test was ran also at the individual level: None of the participants showed an RT difference in the expected direction over the 2.68 ms limit that it is a reasonable value to be anticipate based on Callaway and Yeager (1960). Note that the objective of this study was to find effects at participant level. Therefore, the group tests performed here and in previous sections are exploratory and must be interpreted with caution as they are very likely underpowered.

Discussion

The present study aimed at providing a proof of concept for harnessing on the phase of ongoing α-oscillations recorded non-invasively with EEG for real-time BCI, and to garner support for the role of such occipito-parietal α-oscillations in visual perception. Evidence of this kind is valuable because it can help achieve a better understanding of the relation between the occipito-parietal α-phase and behavioural outcome (i.e., speed of reaction times to visual events), and lay the groundwork for possible BCI applications. Our study was a modern replication of Callaway and Yeager's study (1960), where participants performed a speeded detection on visual targets triggered in real-time at different angles of a participant's α-cycle. First, we sampled RTs to visual targets presented at 10 different phase bins throughout the α-cycle (Stage 1) to select the phases associated with slowest/fastest RTs. Second, we measured RTs to visual targets presented at these two pre-selected phase bins (Stage 2). If a consistent phase-RT relation exists in the expected direction, it follows

that, in Stage 2, stimuli presented at the slow phase would have led to slower RTs compared to stimuli presented at the fast phase.

Contrary to what was expected, the analyses did not return a consistent relation between the phase of ongoing α-oscillations and RTs neither at the group nor at the individual level. Because this experiment was run in real-time, most analytical choices had been made a priori, based on previous literature (Callaway and Yeager 1960). Please note that obtaining the expected results using a priori set analytical pipeline would implicitly corroborate the brain-behaviour theory behind the decisions for the closed-loop. In this sense, closed-loop BCI can be considered a test bench for brain-behaviour theories. However, because some of the prior choices might have been decisive in producing a null result in the present study, we performed a few reality-checks a posteriori. First, we verified that the intended phase of visual stimulation and the actual one were in alignment by comparing the time of stimulus delivery with the empirical EEG measurements, offline. Real-time phase estimation was less than 5º off the intended phase (+1.21 ± 33.70° and +3.79 ± 25.43°, in Stages 1 and 2, respectively), which compares well with estimation accuracy in other modern phase-based closed-loop BCIs (Zrenner et al. 2018; Madsen et al. 2019). We also demonstrated that the accuracy of the phase estimation depended on the latencies along the α-cycle. We found an average mean variation of -5.42º (SD = 9.38º) and an increase of variability of 32.20º (SD = 10.64º) between the last and the first latencies. Second, we double-confirmed that the initial choice of the frequency of interest was representative of the predominant α-frequency during task execution by analysing the data both at single-trial and stage-dataset levels. Third, we validated our choice of the electrode (O1) for the real-time analysis as representative of the central frequency of interest in the occipito-parietal cluster, the most common for the α-rhythm in visual perception (Myers et al. 2014; Samaha et al. 2015; Benwell et al. 2017; Harris et al. 2018; Ruzzoli et al. 2019). Taking all the results together, we reckon that both the estimation over almost one α-cycle and the difference in frequency from IFoI on a trial-by-trials basis are probably the main reasons why phase accuracy varied over latencies along the α-cycle and why we had to reallocate trials in Stage 1 and enlarge Stage 2 acceptance zone to ± 1 phase bin. However, we would like to highlight that, in practical terms, nearly an average of 88% of the trials felt within ±1 bin, which we do not consider to be a poor phase estimation for a BCI setting given the resolution of our EEG system and the method we

implemented to estimate the phase by extending a sinus using the IFoI from a reference point in the EEG signal.

It is important to note that even if the data we obtained were variable across participants, the focus of our analysis was on the individual effects because one of the interests in this study was BCI application. The cross-validation protocol implemented in our design (selection and validation of phase bins from Stage 1 to Stage 2 within the same individual) also highlighted a substantial within-participant variability, in many cases leading to opposite trends from Stage 1 to Stage 2 (e.g., the expected fast phase bin returned, on average, the slowest RTs).

As we mentioned in the introduction, the relation between the posterior prestimulus α-phase and behaviour has been (and it still is) based on a popular hypothesis, leading to several sister theories (Ellingson 1956). For example, the α-phase has been interpreted as a sensory gateway (Bartley and Bishop 1932); a sensory gateway with a functional inhibitory role (Jensen and Mazaheri 2010); as a scanning mechanism (Walter 1950); as evidence for excitability cycles (Bishop 1932; Lindsley 1952; VanRullen 2016b). The main point in common between these theories is that reactions (accuracy or RTs) to visual stimuli correlate with (and can be predicted by) the oscillatory activity from the occipito-parietal cortex in the α-band. A critical analysis of the literature shows that this hypothesis has not been free of controversy: Early studies reported no (Walsh 1952; O'Hare 1954), or weakly significant effects (Lansing 1957; Callaway and Yeager 1960; Callaway 1961, 1962; Dustman and Beck 1965). Null evidence is also reported in modern times with respect to accuracy (Benwell et al. 2017; Ruzzoli et al. 2019). The present study adds to the previous literature showing that the α-phase/RTs relationship is variable and not reliable when targeted in real-time, at least using extra-cranial EEG.

Perhaps it is worth mentioning at this point that we focused on human non-invasive studies (i.e., EEG or MEG) on the role of the α-phase on perception because one our goals was to provide evidence for the possibility to capitalize on this well-studied relationship for BCI settings. We acknowledge, indeed, that prior studies have frequently found a reliable relationship between α-power and spatial attention (e.g., Worden et al. 2000; Kelly et al. 2006; Thut et al. 2006) or visual memory (Palva and Palva 2007), however, the main focus here was narrowed to visual detection performance (Walsh 1952; Lansing et al. 1959; Bompas et al. 2015; Benwell et al. 2017; Ruzzoli et

al. 2019). In this specific case, despite the α-power/behaviour correlation has been more solidly established in the literature, the present study was not optimized to reveal power/behaviour relationships. Indeed, we introduced measures to achieve a consistently high α-power to facilitate reliable phase estimations for stimulus presentation, resulting in a small variability in α-power[4].

Returning to the focus of the present study, which relates to the putative effect of α-phase on RTs to visual events, we should consider three critical aspects of our design that might have influenced the negative outcome. First, we asked the participants to perform the task with their eyes closed. The eyes closed strategy, also implemented in Callaway and Yeager's study (1960), induces higher α-power at occipito-parietal locations which is convenient for reliable phase estimation. However, whether and how performing a perceptual task with the eyes closed jeopardized the outcome is unknown. Excluding the possibility that an eyes-closed condition could also involve sub-cortical generators of the α-activity (Lopes da Silva et al. 1973; Bollimunta et al. 2011; Sokoliuk et al. 2019), we did not find any theoretical caveat against the eyes-closed strategy, which was instead technically convenient. Please note that others have successfully used eyes-closed preparations in the past (Lansing et al. 1959; Callaway and Yeager 1960) and more recently (Lim et al. 2013; Hwang et al. 2015). Based on this, we doubt that the eyes-closed condition may have been critical to producing a null result. The second aspect of our design was to use speeded detection, therefore adopting RTs instead of accuracy as the measure of interest. Even if the α-theories have been related to both (RTs: Walsh 1952; Lansing 1957; Lansing et al. 1959; Callaway and Yeager 1960; Accuracy: van Dijk et al. 2008; Busch et al. 2009), no explicit claims have been made on possible differences between the two measures regarding their sensitivity to prestimulus oscillations. One would believe that if the temporal structure of α-oscillations is important to parse sensory information into perception, then it should be relevant for both RTs and accuracy. Furthermore, unlike accuracy,

[4] An exploratory analysis, presented in the *Supplementary Materials (Annex I)*, confirms both the low power variability and the null power to RT correlation; see **Supplementary Table 8, Supplementary Figure 8, and Supplementary Figure 9.**

RT is a continuous measure potentially more sensitive to moment-to-moment variation in excitability than the dichotomic responses in a detection task. Another aspect of our design that merits discussion was that stimulus intensity was supra-threshold and fixed across participants. This is often the approach in experiments measuring RT. Yet, one could perhaps argue that the stimulus was so strong that possibly subtle phase-dependent variations in sensory responses were saturated, thereby having a negligible impact on behaviour. It is difficult to answer this question examining previous literature because luminance levels have been rarely reported in a precise fashion. Callaway (1962) published the results of a study examining the RT – α-phase relationship with dim and bright visual stimuli (although the actual luminance was not reported) and stated that the depth of such modulation did not vary consistently as a function of brightness. To the best of our knowledge, the only study measuring the RT – α-phase relationship where stimulus intensity was reported clearly is Dustman and Beck (1965). The authors found a consistent effect of RT to α-phase with stimuli of 0.7 lum/m^2 (that is, 0.128 cd/m^2) at 40 cm distance to the subject's (closed) eyes. This is brighter than our stimulus intensity (0.076 cd/m^2). In the absence of reliable information about the stimulus intensity in past studies, one can also look at the response latencies as a proxy. The average RT in our study was 206 ms (SD = 9) in Stage 1, and 199 ms (SD = 6) in Stage 2. Past studies where a significant RT – α-phase relationship was reported range from faster responses than ours (167 ± 22 ms, Dustman and Beck 1965) to slower (245 ± 15 ms and 236 ± 12 ms respectively for slow and fast RTs in Callaway and Yeager 1960; 295 ± 51ms and 348 ± 64ms for bright and dim stimuli, respectively in Callaway 1962). Therefore, even if one cannot be certain of a possible saturation in neural responses following our stimuli, the stimulus strength and the speed of ensuing latencies were within the range of past studies reporting positive effects.

Finally, a fair question to ask is whether the occipito-parietal α-phase is a critical parameter for perception, but difficult to be extracted from EEG-based closed-loop BCI, or whether it is not critical at all. Fluctuations in neuronal excitability giving way to the oscillatory patterns observable with EEG (and MEG) are ubiquitous in the brain, and the relationship between these fluctuations and neural responses to stimuli is well established in physiology (Bishop 1932; Buzsáki and Draguhn 2004). This makes oscillations seen in the EEG appealing candidates to explain and predict behaviour. However, the outcomes

of tests regarding the role of occipito-parietal α-phase in the organization of the visual flow of information have been positive (Lansing 1957; Lansing et al. 1959; Callaway and Yeager 1960; Mathewson et al. 2009) as well as negative (Walsh 1952; O'Hare 1954; Benwell et al. 2017; Ruzzoli et al. 2019). One could argue that a relationship between phase and visual detectability (and hence, response latencies) may exist, but it was obscured by the signal-to-noise variability when recoding from scalp electrodes in EEG. This is, in fact, likely given by the oscillatory patterns in neural excitability so frequently observed in intra-cranial recordings (Bishop 1932; Lopes da Silva and van Storm Leeuwen 1977; Lakatos et al. 2008) or animal studies (Haegens et al. 2011; Spaak et al. 2012; Fiebelkorn et al. 2018, 2019). Based on this, one would have to conclude that despite the results from the present study are far from significant, they are also not conclusive as to disproof an effect and challenge the α-theories meaningfully.

Apart from theoretical considerations, we also had a second main goal in mind running this experiment: To provide a proof-of-concept for the use of oscillatory phase as a real-time control signal in a BCI. We estimated that a minimum RT difference between slow/fast phases of 2.681 ms could be expected (33% of the effects in Callaway and Yeager 1960). However, from a more practical perspective, we wonder whether such a small (and variable) effect can be efficiently picked up by scalp EEG and, if so, whether it can be considered meaningful in a BCI application. Saving less than 3 ms in, for example, the efficiency of warning signals would seem close to nothing in most applied contexts.

Conclusions

Taken together, we must infer that our data do not support a relationship between the phase of α-fluctuations measured extra-cranially and response latencies to visual events. A prudent conclusion is that theoretical and empirical knowledge regarding this relationship may need to progress further to generate enough confidence to attempt the application of the α-theory to neuro-devices. Further research might investigate the influence of parameters such as the eyes-closed strategy, the different sensitivity of discrimination performance vs reaction times as the dependent variable, or the impact of stimulus intensity. We believe that, at present, the effort to implement a closed-loop BCI application based on the relationship of

occipito-parietal α-phase measured with EEG and reactions to visual events might not pay off. In addition, we encourage other scientists and BCI practitioners to use BCI settings for hypothesis-testing with a priori set methods in the cognitive neuroscience field as a test-bench for brain-behavioural theories and to explore the feasibility of EEG-based BCI applications.

CHAPTER 3

Using occipital α-bursts to modulate behaviour in real-time

"If you can't give me poetry,
can't you give me poetical science?".

ADA LOVELACE

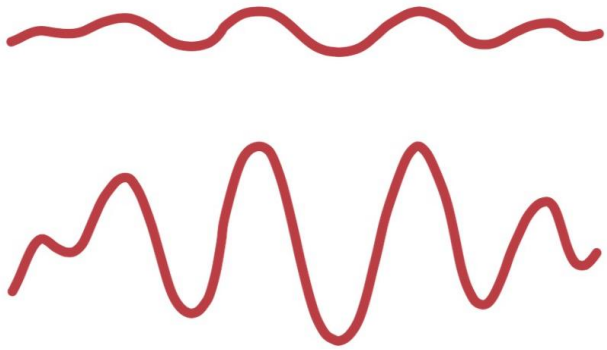

In this chapter I closely follow our study: I. Vigué-Guix & S. Soto-Faraco. *Using occipital α-bursts to modulate behaviour in real-time.* Submitted to *Nature Communications*, 2022.

Background

Fluctuations in neural excitability, reflected in ongoing brain oscillations, are thought to impact the visual processing of sensory inputs and behavioural outcomes (Iemi et al. 2022; Benwell et al. 2017; Benwell et al. 2019; Hanslmayr et al. 2007). Many studies have established a relationship between the amplitude of ongoing activity in the alpha band (α, 8-13 Hz) before stimulus presentation and perceptual performance (Ergenoglu et al. 2004; Hanslmayr et al. 2005a; Hanslmayr et al. 2007; van Dijk et al. 2008). Some of these studies have specifically linked response variability in visual tasks to changes in the amplitude of pre-stimulus α-oscillations in the posterior brain regions prior to stimulus presentation (Bompas et al. 2015; Foster et al. 2017; Huang et al. 2019; Lin et al. 2013; Linkenkaer-Hansen et al. 2004; Yang et al. 2014; van Dijk et al. 2008; Bays et al. 2015).

Although all of these findings are based on averaging pre-stimulus activity, a few recent studies have provided evidence that oscillatory activity may not only be sustained but also consists of burst-like events of high-power neural activity occurring stochastically at different rates, times, and durations (Jones 2016; Lundqvist et al. 2016; Feingold et al. 2015; Shin et al. 2017; Tinkhauser et al. 2017; van Ede et al. 2018; Zich et al. 2020). An illustrative example is hippocampal theta. Many studies have observed overall increases in average theta power related to navigation in the human hippocampus (Ekstrom et al. 2005; Watrous et al. 2013). However, when looking at single trials in intracranial EEG studies, theta appears in distinct bouts of activity and not (only) consistent power changes in the spectrum (Goyal et al. 2020). Similarly, α-occipital, one of the most well-known oscillatory characteristics of the human EEG, appears to be expressed in burst-like events (Kosciessa et al. 2020; van Ede et al. 2018; Sherman and Guillery 1998, 2001). Nevertheless, it is overwhelmingly studied by averaging many trials, perhaps overlooking important physiological relevant aspects of its temporal, spectral, and temporal structure (Zich et al. 2020). Sustained high power in the averaged spectrum can arise due to increased rates or durations of bursts, power changes of bursts, or an overall increase of power across the spectrum. Thus, with traditional trial-averaged analysis, bursts are challenging to capture, and a trial-by-trial approach can optimally help ascertain burst events (Stokes and Spaak 2016).

A promising investigation avenue is using new analysis strategies to study the functional role of bursts in dynamic aspects of cognition and behaviour. To this end, real-time analyses have the untapped potential to capture a more accurate representation of moment-to-moment variations of the cortical dynamics (Lundqvist and Wutz 2021) and brings the opportunity to trigger stimuli timed-locked to the occurrence or absence of bursts events in the ongoing signal. Thus, real-time analysis can provide a robust test of whether burst-like events are associated with particular behavioural outcomes and can naturally provide a crucial proof of concept for brain-computer interface (BCI) applications. However, to the best of our knowledge, real-time BCI targeting α-bursts from the human brain has not been addressed. The present study reports the outcome of such a novel test using scalp EEG measurements of an ongoing, posterior α-activity-based BCI system for real-time burst-triggered stimulus presentation in a visual perception task. So far, α-bursts in the EEG from the occipital cortex have been used as a physiological measure for assessing attentional state and related to errors in driving studies (Papadelis et al. 2007). In addition, EEG α-bursts have been demonstrated to be superior to the EEG α-band power measures in terms of sensitivity and specificity for assessing the driver fatigue under real traffic conditions (Simon et al. 2011; Borghini et al. 2014). Although these kinds of studies mainly use offline data analyses, findings like these have the potential to extrapolate to real-time monitoring/warning systems in real-world scenarios, for example, in activities in which sustained attention is crucial, such as driving vehicles, piloting aeroplanes, and operating heavy machinery.

Supposing that the accumulation of α-bursts over trials correlates with the behaviour observed in trial-averaged α-power (Lundqvist and Wutz 2021), then, by specifically targeting the α-burst events, we should see a similar behavioural performance as in trial-averaged studies, but on a much fine-grained scale of oscillatory dynamics of the EEG signal. Based on the empirical evidence and the well-known inhibitory hypothesis of α-activity over sensory cortices (Klimesch et al. 2007; Jensen and Mazaheri 2010; Iemi et al. 2022), we hypothesised that target presentation during the presence of α-bursts would impact subsequent reaction time (RT). In particular, targets presented during α-bursts would lead to slower RT (i.e., worst performance), whereas targets presented outside α-bursts resulted in faster RT (i.e., better performance). This hypothesis, if confirmed, would not only help

corroborate and extend α-theories currently based on findings from averaged trials (Klimesch et al. 1998; Makeig and Jung 1995; Wyart and Tallon-Baudry 2009; Kirschfeld 2008; Bompas et al. 2015; Yang et al. 2014; Lin et al. 2013; Makeig and Inlow 1993; Campagne et al. 2004; Makeig and Jung 1996; Jung et al. 1997; Hanslmayr et al. 2013; Lal and Craig 2002; Horne and Baulk 2004), but also provide evidence of the putative role of dynamic α-bursts in real-time perception and subsequent behaviour.

Here, we implemented a go/no-go visual detection task in which target presentation was determined in real-time based on the occurrence or the absence of α-bursts in the ongoing occipital EEG signal (**Figure 15**). We estimated bursts by adapting the eBOSC method (Kosciessa et al. 2020) to the real-time analysis pipeline of the BCI setting and used the last 45 s as the background window, as similarly done in previous applications of the method (Whitten et al. 2011). When a burst event (or its absence) for at least three cycles of the individual alpha frequency (here, Individual Frequency of Interest; IFoI) was detected, the visual stimulus was triggered. In go trials (80%), participants had to respond as fast as possible to the green light, whereas in no-go trials (20%), participants had to inhibit the response when seeing the red light. In both trials, stimuli were randomly and equally delivered during the occurrence/absence of α-bursts at the target onset. Each participant collected 240 trials: go/burst (N = 96), go/no-burst (N = 96), no-go/burst (N = 24), and no-go/no-burst (N = 24). Note that our task's stimulus intensity was weaker than regular go/no-go tasks since we wanted to induce a perceptual rather than decisional bias (Benwell et al. 2021) and increase false alarm rates (Chaumon and Busch 2014). To this end, our study aimed to provide (i) evidence for the functional relevance of oscillatory α-bursts in visual perception and (ii) a proof-of-concept for a real-time burst-triggered stimulus presentation BCI setting. The hypothesis, procedure, and analysis pipeline were pre-registered before data collection (https://osf.io/z98ms/). Deviations from the pre-registered procedure are clearly stated in the manuscript. Data and code used in this experiment will be shared upon publication.

To preview the results, stimulus presentation contingent upon the occurrence or absence of occipital α-bursts impacts behaviour. This study shows that it is possible to directly address the connection between oscillatory bursts and behaviour utilising an EEG-based BCI system, allowing for burst-triggered stimulus presentation in real-time.

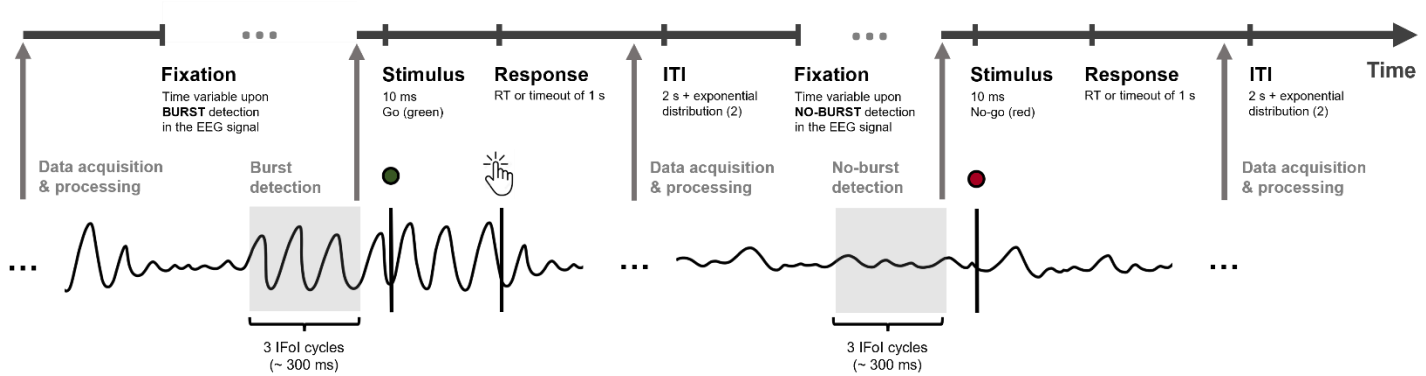

FIGURE 15. Schema of the dynamics of the sequence of trials in the go/no-go task. Participants had to fixate their gaze on the position of the LED while the BCI system acquired and processed new EEG data. When the pipeline found a (no-)burst – (non-)oscillatory activity for at least three cycles of the individual frequency of interest (IFoI), the stimulus was triggered. In go trials (green light), participants had to respond as fast as they could to the stimuli (with a timeout of 1 s), whereas in no-go trials (red light), participants had to inhibit the response. After the response (or the timeout), the BCI system acquired and processed new data while there was an inter-trial interval (ITI) of 2 s + an exponential distribution (mean = 2 s). Go-stimuli occurred in 80% of trials, with no-go stimuli occurring in 20%. In both types of trials, stimuli were delivered randomly and equally during the occurrence/absence of α-bursts (oscillatory activity) at the target onset. Overall, there are four conditions in our go/no-go task: go/burst (n=96), go/no-burst (n=96), no-go/burst (n=24), and no-go/no-burst (n=24). Here, only go/burst and no-go/no-burst are exemplified.

Methods

Participants

Sample size. We set to complete a dataset with N = 12 participants. As per the necessary exclusion requirements set a priori (see below), the attrition rate was high. Of the total 43 participants initially recruited, 16 were discarded for not satisfying the required α-peak criterion in the screening stages (seven did not show a peak at rest, three had double-peak, and six did not show a peak during the task), one was discarded for low discrimination performance, and 14 because of the duration criterion. The final dataset contained EEG and behavioural data from the remaining 12 participants (mean age of 24 years, eight females, all right-handed) without previous history of neurological or psychiatric diseases, with normal or corrected to normal vision, within 18-35 years of age. All participants took part in the study voluntarily after giving informed consent, and they were compensated for their time 10€ per hour. The duration of the experiment varied between 60 and 120 minutes. The study was designed in accordance with the Declaration of Helsinki and was approved by the Institutional Committee for Ethical Review of Projects (CIREP-UPF) (University Pompeu Fabra, Barcelona, Spain) before starting the recruitment. Data from excluded participants were not analysed.

Exclusion criteria. A participant was excluded if any of the following criteria were met: *(i) No amplitude peak within the a-band*: This criterion applied to both screening stages across the study and ensured that the individual's endogenous α-oscillation was registered with a sufficiently high signal-to-noise ratio (SNR) to enable the algorithm to classify the (non)occurrence of α-bursts from the ongoing EEG signal. This decision was based on two sub-criteria: strength and uniqueness (see Screening and estimation of the individual frequency of interest (IFoI) section for more details). *(ii) Time limit of total test duration:* This criterion was applied during the Training block and the Experimental session. Given that the duration of the study depends on the estimation of occurrence or absence of bursts in the ongoing EEG signal, we decided to establish an objective limit. Thus, we stopped the experiment if a participant spent more than 20 minutes in the Training block or any blocks of the Experimental stage. *(iii) False alarms in no-go trials*: This criterion was applied after data collection if a participant had responded in 60% or more trials in the no-go condition. *(iv) Low coefficient of variation (CV) in reaction time (RT):* This criterion was also applied after data collection and ensured that participants had

sufficient RT-variability with a minimum CV of 15% (Terentjeviene et al. 2018).

Experimental procedure and materials

Participants sat on a comfortable chair wearing an EEG cap in front of a green-red bi-colour LED (Manufacturer: Kingbright, Reference: L-59SURKCGKW) at a distance of 90 cm at eye level in a dark and acoustically and electrically attenuated chamber. The LED was attached to a parallel port (forward voltage = 3.84 V, forward current = 0.5 μA) and mounted in a serial circuit with different value resistances depending on the LED colour (one green light resistance = 217 kΩ, and two possible red-light resistances = 933 kΩ or 820 kΩ). The resistance of the green light was permanently fixed, whereas the resistance of the red light was adjusted for each participant to reach the most similar subjective brightness between colours. Note that using different red lights across participants for the no-go trials did not influence the RTs (see *Supplementary Materials in Annex II* for more details).

During the go/no-go task, visual stimuli were presented to participants via the illumination of the LED either in green or red (10 ms duration), at a time decided from the real-time analysis of the EEG-based BCI setting (see below; **Figure 15**). Participants were asked to respond with their right finger via a button press as fast as possible each time the LED was lit up in green (go condition) or withhold the response if the LED turned red (no-go condition). Once the response had been given or had reached the timeout with no response (of 1 second), an Inter-Trial-Interval of 2 seconds + exponential distribution (mean of 2 seconds) of time up to 20 seconds started to prevent fixed temporal expectation. Then, a new trial started with the search for a new (no-)burst event. RTs were measured from the onset of the visual target until a button press was detected. Trials were randomised across conditions in both the training and experimental blocks of the study.

The experimental protocol followed four phases. In the *(i) IFoI-rest screening test*, a 5-minutes of resting EEG with closed eyes was recorded to determine the individual frequency of interest (i.e., IFoI-rest) within the α-band (see Screening and estimation of the individual frequency of interest (IFoI) for more details). This value was further used in the *(ii) Training block of 40 trials* (identical to the Experimental blocks, see below) introduced to familiarise participants with the task and to

acquire new data to estimate the IFoI during the task. This procedure considered the potential changes in the individual α-peak (both in amplitude and frequency) between eyes-closed vs eyes-open and between resting-state and in-task mode (Benwell et al. 2019; Samaha and Postle 2015). The updated value was used in the *(iii) Experimental blocks*, where visual targets were triggered depending on the (non-)occurrence of bursts in the α-activity from the ongoing EEG signal (see Real-time stimulus presentation). The experimental session consisted of 6 blocks, each block ending after acquiring a total of 40 valid trials (lasting 14 minutes on average). Each participant completed a total of 240 valid trials, 192 for go-trials (80%) and 48 for no-go trials (20%). Out of these trials, half of the trials were triggered during a burst and half during a no-burst event. The primary measures were reaction times (RT), commission errors (i.e., false alarm responses to no-go stimuli), and omission errors (i.e., misses to go stimuli). After the collection of data for each participant, the *(iv) Post-hoc behavioural screening* was applied for False alarms in no-go trials and Low coefficient of variation (CV) in reaction time (RT) (see details in Participants section).

EEG recordings. Continuous EEG data was recorded from 16 passive electrodes (F3, Fz, F4, FC1, FC2, C3, Cz, C4, P7, P3, Pz, P4, P8, O1, Oz, O2) placed according to the 10-20 international system. Additional external electrodes were used for recording horizontal ocular movements (one electrode) and left and right mastoids (two electrodes), placed for offline re-referencing. The AFz electrode was used as the online reference and the right mastoid as the ground electrode. The data was recorded using an ENOBIO 20 5G system at a sampling rate of 500 Hz and a touch-proof medical adapter (all manufactured by Neuroelectrics, Barcelona, Spain).

Screenings and estimation of the individual frequency of interest (IFoI). The EEG data was filtered by applying a Notch filter at 50 Hz, a high-pass filter using a second-order Butterworth at 0.5 Hz, and a low-pass filter using an eighth order Butterworth filter, and data was linearly demeaned. We estimated the power spectrum density within the α-band (5-15 Hz) from the Oz-electrode using the Welch method (window = 500 ms; overlap = 10%; resolution = 0.25 Hz). Power spectrum was averaged across the electrodes of interest for each participant and normalised by the mean power spectrum from 0.5 to 45 Hz. We verified that the strength of the peak (power at the local maximum within the 5 to 15 Hz window) was greater than average power in the 0.5 to 45 Hz window. If a single frequency peak existed

within a ±5 Hz band from the IFoI peak, it was considered the individual frequency of interest (IFoI) and used later as a parameter for the real-time analyses. Otherwise, participants were excluded (see *Exclusion Criteria* above).

Real-time triggering of visual stimuli during α-bursts. We developed a real-time EEG-based BCI setting using custom-written code in MATLAB (The MathWorks Inc., Natick, MA, USA) and the Lab Streaming Layer (LSL) library (Swartz Center for Computational Neuroscience, UCSD, USA). We adapted the BCI setting from Vigué-Guix et al. (2020) and designed a new setting to trigger visual stimuli at the occurrence/absence of α-bursts in real-time estimated from electrode Oz. We also built a GUI in MATLAB to keep track of the experiment on a trial-by-trial basis. To trigger a visual target, the BCI setting iterated through the following steps (see *Supplementary Materials* in *Annex II* for the detailed algorithm): *(i) Data acquisition* of a 45-second sliding window of the most up-to-date data (Whitten et al. 2011); *(ii) Data reflection* of the beginning and end of the window; (*iii) Data filtering and demeaning* with a band-pass forward filter of 4th-order Butterworth between 0.5 and 45-Hz; *(iv) Time-frequency analysis* using 6-cycle Morlet wavelets within 2 to 38 Hz; *(v) Data trimming* with reflected edges were removed; *(vi) Log(frequency)-log(power) fitting* of the wavelet-derived power spectrum using a robust regression; *(vii) Threshold estimations* of artifact, burst power, no-burst power, and duration threshold; *(viii) Checking necessary conditions for triggering stimulus* in terms of power and duration criteria (if conditions were not met, loop went back to step (i)); *(iv) Stimulus presentation* of visual targets (go or no-go, depending on condition); *(x) Behavioural response* collection or timeout of 1-second; *(xi) Data acquisition update* of the 45-second window with the most up-to-date data, and repetition of the (i-v) steps. *(xii) RT criterion check* (RT within 50 and 1000 ms, only applied in the go condition), *burst criterion check* (90% of data points of the last three cycles had to be higher than the burst power threshold and lower than the *artefact power threshold*), or *no-burst criterion check* (90% of data points of the last three cycles had to be lower than the no-burst power threshold and lower than the *artefact threshold*); *(xiii) Trial counter* of the number of valid trials and continued with the next iteration until reaching the number of trials of a block (N = 40). Note that if a step/criterion was not satisfied at any point of the iteration, the BCI setting started a new iteration from step (i). Participants had a break between blocks, and a new block began with the BCI setting starting from step (i).

Statistical analyses

Only valid go trials of each α-burst condition were included in the analyses and for all tests α-level was 0.05, unless otherwise indicated. Given that reaction time data do not follow a normal distribution but a positive right-skewed distribution, the statistical significance was assessed using nonparametric permutations tests (Ernst 2004; Morís Fernández and Vadillo 2020) both at individual and group levels. For the *individual (single-participant) statistical tests*, we tested the difference of the mean-RT distributions between burst and no-burst using a Monte Carlo randomisation procedure (100,000 randomisations) individually for each participant (i.e., one-tailed permutation test) to obtain a p-value associated with the observed mean-RT difference. In the *group-level statistical tests*, we performed the same procedure and estimated the p-value of the inter-individual mean burst/no-burst difference of RTs for all participants.

Results

Results of the pre-registered analysis

According to the pre-registered pipeline, the analyses did return a consistent relation between the occurrence/absence of α-bursts in the ongoing occipital EEG signal and the speed of responses to visual targets, both at the individual and the group level. In all 12 participants but two, RTs for go stimuli were slower on average (486 ms; SD = 50 ms) when presented during burst events (as predicted) and faster (486 ms; SD = 50 ms) when presented in the absence of bursts (see **Supplementary Figure 10** in *Annex II* for RT histograms). In five out of those 10 participants, the difference was significant at the individual level (p-values ranged from *<.001* to *.03*; **Supplementary Table 9** in *Annex II*). In line with the individual results shown in **Figure 16**, the group-level difference between burst and no-burst RTs was highly significant (p = *<.001*; **Supplementary Table 9** in *Annex II*), reaching a mean difference of 19 ms (SD = 17; Max = 55 ms; Min = -6 ms).

Interim discussion and reality checks

Compared to offline experimental approaches where analysis parameters can be adjusted retrospectively, real-time settings imply a priori parameter choices to constrain the hypothesis and offer more explanatory power. As pre-registered, we performed some reality

checks offline to ensure that the a priori choices in the real-time setting conform to expectations. We focused on three critical aspects: first, we checked that we had triggered the stimuli during intended (no-)burst events in the real-time experiment, using the recorded data; second, we checked whether the choice of the IFoI based on training EEG data was representative of the dominant α-frequency during the task; and finally, we checked that the electrode choice (Oz) for the real-time α-burst estimation was representative of α-activity of interest in a larger occipito-parietal (OP) cluster of electrodes.

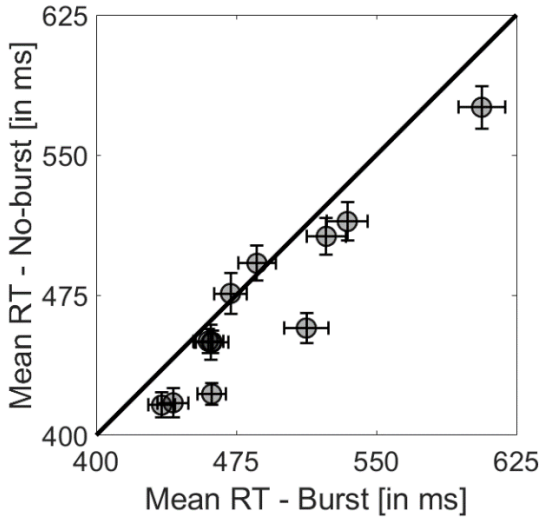

FIGURE 16. Individual mean reaction times (RT) for burst (x-axis) and no-burst (y-axis) trials for validated trials. Each circle denotes a participant. Horizontal error bars denote the SEM of burst trials, and vertical error bars denote the SEM of no-burst trials. Points below the diagonal line denote that no-burst mean RTs are faster than burst mean RTs. Symbol overlap is coded darker.

Reality check 1: True detection of burst events

We checked, retrospectively, whether real-time target presentation truly occurred during periods of occurrence or absence of α-burst events (see definition in *Methods*). We divided the estimated burst and no-burst trials from the dataset and epoched the data from -45 s to 2 s from stimulus onset (a larger window than the real-time analysis that included the post-stimulus interval). With these, we replicated offline the same analysis performed in real-time (see *Supplementary Materials* in *Annex II* for more details). Note that the analysis was applied at the single-trial level in the real-time study, whereas the offline analyses in this section also apply trial-averaged analysis (comparable with the existing traditional literature: e.g., van Dijk et al. 2008).

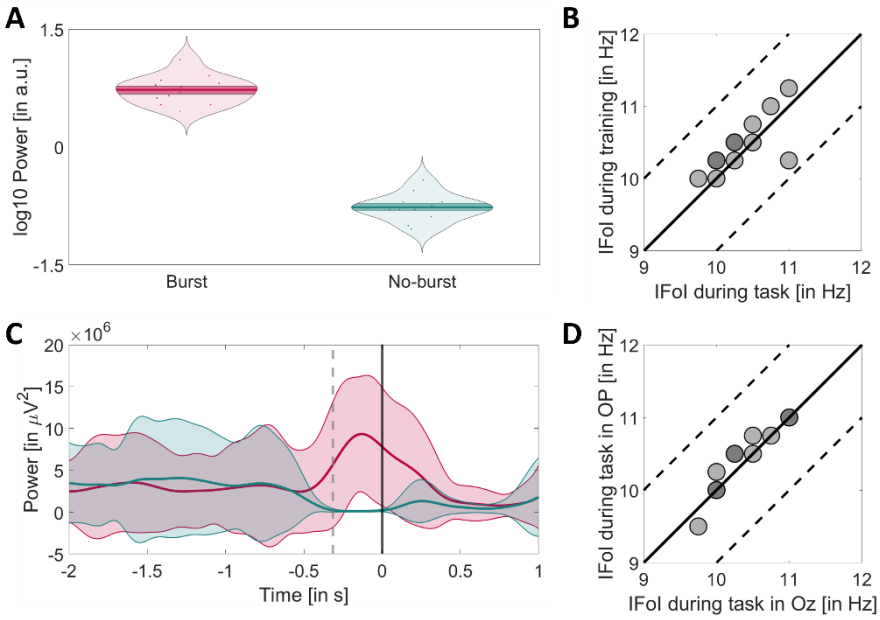

FIGURE 17. Reality checks of the study. (A) Group-level log-transform mean power at the time window of interest (TWoI) for burst (in red) and no-burst (in green) trials within -2 to 1s from stimulus onset. Solid lines denote the mean power of burst and no-burst trials. Dark shaded areas represent the standard error of the mean interval. Each dot denotes a participant. **(B) Individual mean power of burst (in red) and no-burst (in green) trials for participant (P09) within -2 to 1s from stimulus onset.** Solid lines denote the mean power of burst and no-burst trials. Shaded areas represent the standard deviation (SD) interval. Solid vertical line denotes the stimulus onset, and dotted vertical lines denote the window of interest (i.e., the last three cycles of IFoI) from stimulus onset. **(C) Comparison of individual IFoI during the task [in Hz] and IFoI during the training [in Hz] using Oz electrode.** Dashed lines denote ±1 Hz, and each dot denotes a participant**.** Dot overlap is coded darker. **(D) Comparison of individual IFoI during the task [in Hz] using Oz electrode and IFoI during the task [in Hz] using OP-cluster of electrodes**. Dashed lines denote ±1 Hz, and each dot denotes a participant. Dot overlap is coded darker.

For all participants, we calculated the mean power at the time-window of interest (i.e., three-cycles prior to stimulus; TWoI) for burst (Mean = 5.83 μV^2; SD = 2.75 μV^2) and no-burst (Mean = 0.18 μV^2; SD = 0.08 μV^2) trials (**Figure 17A**, **Supplementary Figure 11,** and **Supplementary Table 10** in *Annex II*). Overall, the mean power difference between burst and no-burst was 5.65 μV^2 (SD = 2.69; Max = 12.58 μV^2; Min = 2.73 μV^2). We applied a one-tailed t-test (independent samples) with α-level = 0.05 to the mean power values at the TWoI between burst and no-burst trials and found that the two distributions were significantly different from each other (all participants p = *<.001*; **Supplementary Table 10** in *Annex II*).

Although the statistical analysis was performed within the TWoI, we decided to plot the average of the trials on a wider time window around stimulus onset (-2 to 1 s) to visualise the difference in mean α-power between conditions. In **Figure 17C,** the individual representative plot from one participant (P09) shows a clear difference between the mean (SD) power across conditions (see **Supplementary Figure 12** in *Annex II* for all individual plots). As reflected by the shaded area, burst trials show larger variability (i.e., SD) than no-burst trials in power within the TWoI. In addition, we related the log-transformed mean power at the TWoI with the RT for no-/burst trials at the individual level and found that log-power distributions of both conditions were separated (see **Supplementary Figure 13** in *Annex II* for individual figures). Finally, we checked the amplitude thresholds and demonstrated that they were correctly adjudicated during the study according to the ongoing α-burst activity (see **Supplementary Figure 14** in *Annex II* for individual figures). These results confirm that our approach successfully identified and separated trials with and without α-bursts in ongoing EEG.

Reality check 2: Selection of the frequency of interest (IFoI)

Here, we checked for any potential deviations between IFoI used to estimate bursts in real-time during the task extracted from the training and the actual IFoI during the task execution for each participant. During the training, the mean IFoI peak was 10.60 Hz (SD = 0.41 Hz) with a mean amplitude of 5.12 dB (SD = 3.11 dB), whereas, during task execution, the mean IFoI peak was 10.35 Hz (SD = 0.41 Hz) with an amplitude of 5.72 dB (SD = 2.73 dB) (**Figure 17B**, see **Supplementary Table 11** in *Annex II* for individual results). Overall, the mean peak IFoI difference between task and training was -0.25 Hz (SD = 0.11; Max = -0.5 Hz; Min = 0 Hz), with a mean amplitude IFoI difference of 0.61 dB (SD = 1.63; Max = 3.47 dB; Min = 0.22 dB). The variation in frequency from the IFoI at the single-trial level seems negligible from a time-frequency analysis standpoint. Thus, we can conclude that the BCI setting employed in this study successfully centred the spectral analysis around the desired relevant frequency of interest.

Reality check 3: Representativity of the electrode of interest

Similarly, we had to decide a priori about the electrode/s of interest used in the BCI setting as for the frequency of interest. We chose the Oz electrode, which was convenient to curtail real-time computational delays. However, one potential concern is that the frequency estimated

by that single electrode could be unrepresentative of the α-frequency dominant in a wider cluster of occipito-parietal (OP) electrodes. Therefore, we compared the spectral peak activity in Oz-electrode to that of an OP-cluster of electrodes (P7, P3, Pz, P4, P8, O1, Oz, O2) retrospectively (**Figure 17D**). The comparison process was analogous to the one described for *Reality check 2*. For the OP-cluster, we computed the IFoI peak (Mean = 10.43 Hz; SD = 0.46 Hz) and IFoI amplitude (Mean = 4.65 dB; SD = 3.49 dB) during the task (see **Supplementary Table 11** in *Annex II* for individual results). This yielded that the IFoI of the α-bursts estimated from Oz during the real-time experiment were closely representative of the OP-activity.

Exploratory analyses

RT fits using the ex-Gaussian function

Here, we explored how the distributions differed between burst and no-burst to learn more about the origin of the RT differences seen in the main pre-registered analysis. We characterised the RT-distributions by fitting an ex-Gaussian function, a convolution of a Gaussian and an exponential distribution (Hockley 1984; Luce 1986; Ratcliff and Murdock 1976). Whereas the mean (μ) and standard deviation (σ) for the Gaussian part are thought to reflect, but not exclusively, stimulus- or response-related processes (Schmitz and Wilhelm 2016), the exponential component (τ, which reflects the skewness of the distribution) is sensitive to central attentional processes, especially those that require inhibitory control (McAuley et al. 2006; Shao et al. 2012; Spieler et al. 1996). We used the *exgauss* toolbox in MATLAB (Bram Zandbelt 2014) to perform the RT fits. For each participant, we performed a one-tailed permutation test (100,000 randomisations) for the μ parameter (the same statistical tests applied in the main analysis of the study under the same hypothesis, see Statistical analysis) and a two-tailed permutation test (100,000 randomisations) for σ and τ parameters (since we did not have any hypothesis about them).

Figure 18A illustrates the ex-Gaussian fit for a representative participant (P09), including the RT distribution fit and the psychometric curves for burst and no-burst trials (see **Supplementary Figure 15** in *Annex II* for individual figures). The average μ for burst and no-burst trials was 400 ms (SD = 38 ms) and 393 ms (SD = 41 ms), respectively. The mean RT difference between burst and no-burst was 7 ms (SD = 20 ms; Max = 32 ms; Min = -1 ms). Overall, 7 out of

twelve participants showed a difference in RTs in the expected direction (see **Supplementary Table 12** in *Annex II* for individual results), with 2 out of these showing a significant p-value ($p < .02$) in the μ parameter. However, we did not observe a significant group-level difference between burst and no-burst ($p = .13$). In terms of σ (burst was 39 ms, SD = 10 ms; no-burst was 37 ms, SD = 14 ms), the average difference was not significant at the group level, and only one participant (P07) showed a significant difference with more variability in burst trials compared to no-burst trials ($p = .01$). Finally, for parameter τ, burst was 86 ms (SD = 17 ms) and no-burst 74 ms (SD = 22 ms), leading to a significant group difference of 12 ms (SD = 17; Max = 41 ms; Min = -1 ms; $p = .01$). Three participants (P01, P03, P07) showed a significant p-value ($p < .05$) for the difference in τ (p-values ranged from .003 to .02), in the same direction as the group. Taking these results together seems that the difference we found in the main analysis between burst and no-burst RTs ($p = <.001$) was best captured by the skewness of the distribution reflected in the exponential component (τ). This finding could be related to the sensitivity to central attentional processes and the requirement of inhibitory control (McAuley et al. 2006; Shao et al. 2012; Spieler et al. 1996) for the go/no-go task. However, given the exploratory nature of this analysis and the fact that overall robust RT differences seemed to diffuse across the various parameters, the interpretation of this analysis should be treated with caution.

Omission and commission errors

Many previous studies optimised to investigate accuracy have found a consistent relationship between high alpha-power and missed targets in detection tasks (Busch et al. 2009; Ergenoglu et al. 2004; Mathewson et al. 2009). Although our study was optimised for RT measurements, we explored the relationship between misses (omission errors in go trials) and burst occurrence. What is more, despite the low number of no-go trials, we think exploring false alarms (commission errors in no-go trials) during periods with and without burst activity would be informative. If α-bursts indicate periods of lowered sensitivity, one might expect a higher error rate during these episodes (higher α-power) than during no-burst episodes (lower α-power reflecting higher sensitivity). This hypothesis was considered only for go trials (Chaumon and Busch 2014; Hanslmayr et al. 2007; Klimesch et al. 2007) since we did not have any expectations with no-go trials.

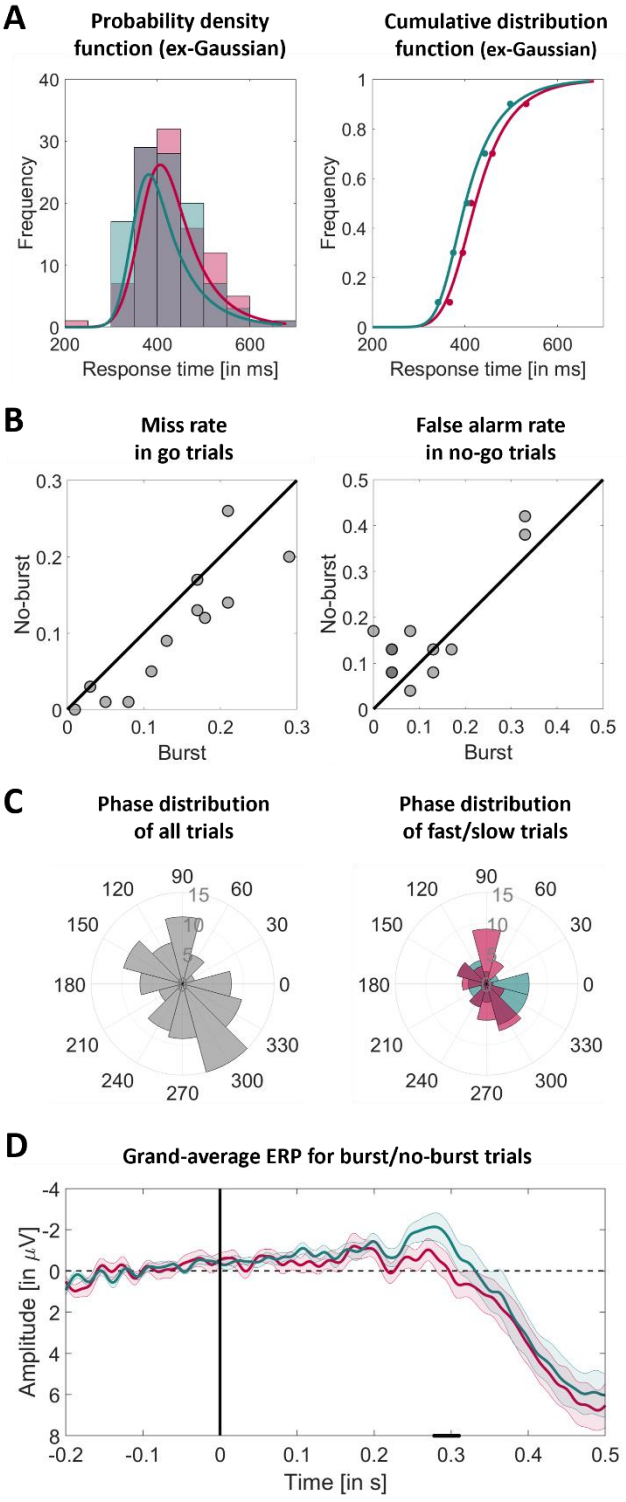
A
Probability density function (ex-Gaussian)
Cumulative distribution function (ex-Gaussian)
Frequency
Response time [in ms]
B
Miss rate in go trials
False alarm rate in no-go trials
No-burst
Burst
C
Phase distribution of all trials
Phase distribution of fast/slow trials
D
Grand-average ERP for burst/no-burst trials
Amplitude [in μV]
Time [in s]

FIGURE 18. Exploratory analyses of the study. (A) Individual ex-Gaussian fit for burst (in red) and no-burst (in green) trials. For participant P09, the probability density function (PDF) of burst and no-burst trials (on the left) and the cumulative distribution function (CDF) of each trial condition (on the right) are shown. **(B) Comparison of error rates for burst and no-burst trials.** Omission error rates (miss rate) in go trials (on the left) and false alarms or commission error rates in no-go trials (on the right) are shown. Each dot denotes a participant. Points below the diagonal line denote that burst trials contain higher error rates than no-burst trials. Dot overlap is coded darker. **(C) An individual rose plot of the phase distribution at stimulus onset for valid-burst trials (in degrees).** For participant P09, the rose plot of phases for all valid-burst trials (on the left) and the rose plot of fast/slow trials within valid-burst trials (on the right) are shown. Each bin corresponds to 30º**. (D) Grand average ERP of the broad-band activity time-locked to visual stimulus presentation for burst (in red) and no-burst (in green) of go trials from Oz-electrode across time (within -0.2 s to 0.5 s from stimulus onset).** Shaded areas represent the standard error of the mean (SEM) interval. Vertical solid line denotes stimulus onset presentation, and horizontal dashed line denotes zero amplitude. Solid dark line at the bottom of the x-axis denotes the significant cluster of p-values from a paired t-test (α-level = 0.05) for burst and no-burst ERPs over time (p-values were corrected for multiple comparisons via cluster-based permutation test; N = 100,000 randomisations).

In order to increase the number of total trials and capture errors, we decided to use all trials in which stimuli were correctly triggered according to the occurrence of an oscillatory burst event (or its absence) and relax the RT criterion. The resulting trials were divided into burst and no-burst conditions for go and no-go trials (**Supplementary Table 13** in *Annex II*). For these comparisons, we used a two-tailed paired t-test. The results revealed a significant difference in error rates between burst and no-burst conditions for both go (t (11) = 3.15, $p = .01$) and no-go trials (t (11) = -2.29, $p = .04$) at group-level. In particular, in go trials, omission errors (misses) were more prevalent during a burst episode than during a no-burst (**Figure 18B, left**). In no-go trials, commission errors (false alarms) were more prevalent during a no-burst episode than a burst episode (**Figure 18B, right**). As expected, bursts (high α-power) were related to higher miss rates in go trials; however, in no-go trials, false alarms were more prevalent during the absence of a burst (low α-power).

A key aspect when interpreting these results relies on the differences in cognitive processes between go (i.e., answering to stimuli) and no-go trials (i.e., inhibiting the response to stimuli) and on the assumption that the level of α-power reflects the sensory excitability needed to detect a stimulus (Hanslmayr et al. 2007; Klimesch et al. 2007). In go trials, lower oscillatory α-power (i.e., stronger excitability) may lead to higher detection accuracy and faster reaction times, whereas higher oscillatory α-power (i.e., lower excitability) would impair accuracy (e.g., slower RTs and more false alarms). However, the level of α-power is also thought to reflect the level of inhibition (Klimesch et al. 2007). To

this end, in no-go trials, where inhibition is needed to stop the response, higher oscillatory α-power (i.e., stronger inhibition) would help and lead to fewer false alarms. On the contrary, lower oscillatory α-power (i.e., weak inhibition) may lead to answering to visual stimuli producing thereby higher false alarms. We tentatively conclude that our results in the error rate difference are in line with the expected findings and those in the literature, using single-trial and group-averaged pre-stimulus α-power offline.

Phase-behaviour opposition

Some past and recent studies have addressed the relationship between α-phase and behavioural responses to visual stimuli in humans. Although several studies have related the α-phase of occipito-parietal areas to performance in visual perception (Jensen et al. 2011; Jensen and Mazaheri 2010; Samaha and Postle 2015; van Dijk et al. 2008; VanRullen 2016b), other studies have also reported no (O'Hare 1954; Walsh 1952) or weakly significant effects (Callaway 1962; Callaway and Alexander 1960; Dustman and Beck 1965; Lansing 1957), and even null evidence for accuracy (Benwell et al. 2017; Ruzzoli et al. 2019) and RTs (Vigué-Guix et al. 2020). Although this analysis was not pre-registered, we explored the potential α-phase/RT relationship at stimulus onset. If the response to a stimulus is related to the α-phase at its onset, we should expect a pattern of opposition within the α-oscillations when comparing slow and fast RT trials at stimulus onset (time = 0; Mathewson et al. 2009). We checked for this opposition pattern using the phase opposition sum (POS) method (VanRullen 2016a).

We selected only valid-burst trials (which contain oscillatory activity and a valid response) for this analysis, leading to N = 96 trials for each participant. Trials were half-split into slow (50% RTs) and fast (50% RTs) categories, resulting in N = 48 trials for each condition and participant. EEG data were epoched from −45 to 2 s and then demeaned. No re-referencing was applied. We forward-filtered the signal (electrode Oz) using a Butterworth filter (order 4, one-pass) around the IFoI ± 5 Hz band and computed the phase at stimulus onset using the Hilbert transform.

We plotted the distribution phases (**Figure 18C**; see **Supplementary Figure 16** and **17** in *Annex II* for the individual phase distribution of all trials and fast/slow trials, respectively) and calculated the averaged phase between fast and slow RTs and their difference in phase using the Circular Statistics Toolbox in MATLAB (Berens 2009). We

applied the POS on phase values for fast/slow trials at individual and group levels. The statistical significance was assessed using nonparametric permutations tests (10,000 iterations/surrogates). Comparing the empirical POS value to surrogate POS distributions dispense with the assumption that the distribution of phases across trials is random and uniform (McLelland et al. 2016). We did not observe any significant group-level effect of POS between slow and fast RTs ($p = .32$) nor at an individual level for any participant (all ps > .1; see **Supplementary Table 14** in *Annex II* for individual results). The average phase angle difference among participants between slow and fast trials was -43° (SD = 57°). Overall, the results did not return a consistent relationship between the phase of ongoing α at stimulus onset and the speed of responses.

ERP analysis time-locked to visual stimulus

Although the primary aim of this study was to investigate the influence of the ongoing pre-stimulus oscillatory activity on reaction time, we also analysed the event-related potentials (ERPs) to visual stimuli in go trials separately for the burst and no-burst conditions. Previous studies have linked pre-stimulus EEG α-power and the visual evoked potentials (Başar et al. 1998; Mazaheri and Jensen 2008) and produced mixed effects on different latencies (Başar et al. 1998; Brandt et al. 1991; Ergenoglu et al. 2004; Fellinger et al. 2011; Roberts et al. 2014). Therefore, our assessment here was utterly exploratory. In addition, we did not expect to find identifiable ERP components, given that our stimulus intensity was made weak for the purposes of the task. We selected only go trials due to the low trial number of no-go events and potential differences in task relevance and motor preparation between the two types of trials. We band-pass filtered the recorded EEG data from electrode Oz using a Butterworth filter (order 4, two-pass, zero-phase) between 0.5 and 40 Hz for each participant. EEG data were re-referenced offline to the left and right mastoids' average. EEG data were epoched from −200 to 400 ms and then demeaned. All epochs were baseline-corrected with respect to the mean voltage over the 200 ms preceding the onset of stimuli, followed by averaging for burst and no-burst conditions. Since this was an exploratory analysis, we targeted a broad time window, between 200 and 500 ms. For statistical assessment, we performed sample by sample paired t-tests between the mean visual-evoked ERPs at the Oz electrode between burst and no-burst. We used a cluster-based permutation test procedure (100,000 randomisations) to correct p-values (Maris and Oostenveld 2007; Meyer et al. 2021).

Figure 18D shows the (stimulus-locked) ERPs of valid-go trials for burst and no-burst conditions. We found a significant difference between burst and no-burst conditions ($p < .05$) in a 32 ms time window between 280–312 ms after stimulus presentation. Based on previous literature, this period would correspond to the putative N2 (255–360 ms) component (Koivisto and Revonsuo 2003, 2010; Sheldon and Mathewson 2021). We reckon that this difference in the ERP might reflect the RT-effect found between burst and no-burst trials at group-level in the main analysis. As suggested in the ERP studies addressing go/no-go tasks mentioned above, the larger the peak of the N2 component (here, larger ERP for no-burst), the faster the responses (here, shorter RTs for no-burst events).

Exclusion of trials due to power criterion

Although the present study succeeded at detecting α-bursts in the ongoing EEG activity through our custom-built BCI setting (see *Reality check 1*), the estimation accuracy of (no-)burst varied across participants and conditions, as reflected in the average number of trials of 344 (SD = 78; 52%) excluded for the power threshold criterion (see *Supplementary Materials* in *Annex II* and **Supplementary Table 15** for more details). For the estimation of burst episodes and the subsequent triggering of the stimuli in real-time, we sought oscillatory activity above a certain power threshold with respect to the overall spectrum for at least three cycles (~300 ms) of the IFoI of the participant (more details in the Methods section). Note that there was an unavoidable time gap between the decision to trigger a stimulus (based on the most updated EEG data) and the actual stimulus presentation due to computational time (~72 ± 5 ms). For this reason, we sent the stimulus around three-quarters of a cycle ahead of time, and then trials were checked for burst criteria after sending the stimulus for online sorting. We consider this is probably the main reason why an average of 52% of trials were excluded for not satisfying the power criterion at the time of stimulus delivery. We looked for any differences between burst and no-burst trials, and we found that an average of 116 trials were excluded in burst compared to 220 trials excluded in no-burst conditions (see *Supplementary Materials in Annex II* and **Supplementary Table 16** in *Annex II*). At the individual level, 10 out of twelve participants showed more trials excluded in no-burst trials than burst (see **Supplementary Figure 18** in *Annex II*). Thus, our criteria made it more difficult to pass a non-burst event during the task execution than to detect a burst of oscillatory α-activity in the ongoing EEG signal. Please note that the criterion for no-burst was not simply the absence

of a burst event, but power in the IFoI had to be within the lowest 5%. In addition, we found a significant correlation between the IFoI amplitude during task execution and the number of trials excluded for burst (ϱ = -.62; p = *.02*) and no-burst (ϱ = .51; p = <*.05*) trials at group-level (see *Supplementary Materials in Annex II*). During the task, participants with higher IFoI amplitude had fewer trials excluded for bursts than no-bursts. On a general note, we can say that we succeeded in achieving the second main goal of the study: detecting α-bursts in the ongoing EEG activity using a BCI setting for burst-triggered stimulus presentation in a go/no-go task.

Discussion and Conclusions

The present study aimed to provide supporting evidence that one can harness bursts in real-time to predictably modulate behavioural outcomes: the speed of reactions and the likelihood of omission and commission errors. We found that targets presented during α-burst episodes led to slower RTs than those presented outside, leaving an RT difference of 19 ms found between conditions. Regrading errors, targets presented during bursts were more likely to be missed in go trials, whereas in no-go trials, those presented in the absence of bursts led to false alarms more often. Together, we suggest that the behavioural differences found between burst and no-burst conditions appear to unfold over the processing of the target, perhaps at different stages. For example, the fact that the most apparent difference in the ex-Gaussian fit analysis affected the skewness of the distribution, together with the relatively late difference in the ERPs, suggests that at least a part of this effect would involve late processing stages of decision or response selection. We consider that these effects can relate to the sensitivity of central attentional processes and the requirement of inhibitory control in a go/no-go task, as suggested in previous studies (McAuley et al. 2006; Shao et al. 2012; Spieler et al. 1996). In addition, there is evidence that larger N2 peaks relate to faster RTs (Bahramali et al. 1998; Starr et al. 1995). In the same vein, we observed larger ERP amplitudes in the N2 time window for bursts condition than no-bursts, which relates to our main finding of burst generating faster responses. Overall, we reckon that burst episodes are periods of lowered sensitivity due to the high α-power, which inhibits the response to visual stimuli as reflected by slower RTs and more misses in go trials. On the other hand, no-burst episodes, as periods of higher sensitivity due to low α-power, may facilitate the answering and

produce more false alarms in no-go trials and faster RTs in go trials. In addition, when applying the phase opposition sum (POS) method to fast/slow RTs in burst trials, we did not see an effect of α-phase at stimulus onset, suggesting that the RT-effect (found in the primary analysis) is principally a result of the oscillatory power of α-bursts.

It is worth mentioning that the first goal of this study was to provide evidence for the intrinsic function of oscillatory α-bursts on reactions to visual events for the possibility to capitalise on this brain-behaviour relationship for an EEG-based BCI application. Prior studies on the α-theories have frequently found a reliable relationship between the pre-stimulus α-power and the behavioural outcome in visual perception using single-trial and within-subject averages (Bompas et al. 2015; Campagne et al. 2004; Horne and Baulk 2004; Jung et al. 1997; Kirschfeld 2008; Lal and Craig 2002; Lin et al. 2013; Makeig and Inlow 1993; Makeig and Jung 1995; Wyart and Tallon-Baudry 2009; Yang et al. 2014). However, a fair question and a key challenge are to understand whether the behaviour and the sustained oscillatory activity observed in trial-averaged power (Lundqvist and Wutz 2021) is actually due to the accumulation of transient high-power burst events that happen at different rates, times, and durations from trial-to-trial (Lundqvist and Wutz 2021; van Ede et al. 2018; Zich et al. 2020). One way to address this challenge is by using a BCI to target the oscillatory dynamics of the EEG signal (reflected in the α-burst events) at the single-trial level. The oscillatory burst event analysis can serve as a sensitive tool to capture single-trial differences, which would go unnoticed with a standard approach of trial-averaged power. Such an approach can answer whether a similar neural-behavioural relationship applies to the much more fine-grained scale of moment-to-moment dynamics of the EEG signal and which form it may take (Pernet et al. 2011). As far as we know, we are the first to use this novel approach in targeting, specifically, burst-like events of oscillatory α-activity from the occipito-parietal cortex of human brains in real-time using an EEG-based BCI setting in order to address its link, on a trial-by-trial basis, to reaction times in a go/no-go task. Similar findings are in line with recent studies of oscillatory burst-like events underlying cognitive and motor operations in other frequency bands (Feingold et al. 2015; Lundqvist et al. 2016; Sherman et al. 2016; Shin et al. 2017; Wutz et al. 2020).

Moreover, it would be ideal to make explicit in the current formulation of the α-theories whether and how transient events of rhythmic oscillatory activity (bursts) in the ongoing brain activity gate

sensory information and shape perception on a trial-by-trial basis. Although the functional inhibition account (e.g., Klimesch et al. 2007) is specific to the α-oscillatory activity, it does not distinguish between sustained oscillatory activity and burst events. On that note, Peterson and Voytek (2017) have recently proposed that α-oscillations control cortical gain by modulating the balance between excitatory and inhibitory background activity, and they make the novel prediction that α-activity plays two functional roles: a robust, sustained oscillation mode (>5-10 cycles) that suppresses cortical gain and a weak, bursting mode (of 1-3 cycles) for rapid, temporally-precise gain increases. This view would align with (Jensen and Mazaheri 2010) and (Mazaheri and Jensen 2010). Together, new models, theories, and analytical methods (see Lundqvist and Wutz 2021) are starting to consider different types of α-activity and assess their respective roles in cognitive processes.

Apart from the theoretical implications, another goal of this study was to provide a proof of concept for using oscillatory α-bursts as a control signal for a BCI. We found that harnessing the detection of neural burst events achieved RT differences of up to 55 ms (Mean = 19 ms; Max = 55 ms; Min = -6 ms). One should consider whether such a difference could be meaningful for an EEG-based BCI application from a practical perspective. Note that the potential relevance of such a system does not hinge so much on the average but single instances. One must consider that time savings can potentially be more considerable on some occasions (for example, looking at the most favourable case, participant P09, one could save as much as 250 ms on roughly 10% of the trials). These are substantial results if one considers this is the first proof of concept where many of the parameters and protocol features have been necessarily arbitrary, given the lack of precedent.

One of the major concerns of the study was the high exclusion rate of participants (31 out of 43). However, pre-screening is a common practice in hypothesis-driven real-time BCI studies (Callaway and Yeager 1960; Lansing 1957; Vigué-Guix et al. 2020). Note that oscillatory activity in the α-band should be present to establish the role of α-oscillations in subsequent perception. In our study, nearly half of the excluded participants were not either eligible because it was not possible to measure α-activity from their human scalp or because there was not a unique oscillatory activity within the α-band. The other half of the participants were excluded for not reaching enough α-activity variability to fully account for the two conditions of our study (i.e., low/high oscillatory α-activity). Note that this is also why nearly 50%

of trials in the real-time study were rejected because of α-power. Nonetheless, our exclusion rates are comparable with previous studies rejecting almost two-thirds of their participants (Callaway and Yeager 1960; Vigué-Guix et al. 2020) and even 92 out of 100 participants (Lansing 1957) for similar reasons. On a general account, it has been thought that individual differences in the measurement of activity with EEG may be partially due to physiological differences (e.g., the thickness of the skull), technical and methodological factors (e.g., type of EEG montage), or specific factors such age, arousal, or cognitive demands (Klimesch 1999).

Although our findings from the study are well in line with a host of older findings relating to α-power and behaviour, we went beyond those studies in two important ways. First, our study harnessed real-time data analysis trial by trial using an EEG-based BCI system. Second, we focused on bursts of α-activity. Evidence of this kind demonstrates the putative functional role of bursts of oscillatory neural α-activity in occipital areas (Hughes and Crunelli 2005; Hughes et al. 2011; Wutz et al. 2020). Moreover, the real-time trial-to-trial nature of this approach provides a potential basis for control signals in EEG-based BCI applications supported by brain-behaviour theories (here, α-theories). For instance, a passive BCI using brain-state dependent stimulation (BSDS; Jensen et al. 2011) could benefit from our findings and build a BCI application in which stimuli are triggered only in the absence of neural α-burst events. Such BCI would help prevent slower reactions and omission errors. Therefore, this study has shown that it is possible to directly address the connection between oscillatory bursts and behaviour utilising an EEG-based BCI system, allowing for burst-triggered stimulus presentation in real-time. Real-time studies using EEG-based BCI systems are promising research tools than can be used as a test bench for brain-behavioural theories in cognitive neuroscience.

CHAPTER 4

Using α-phase coupling to determine the locus of attention in space

"Where attention goes,
neural firing flows and neural connection grows."

DANIEL SIEGEL

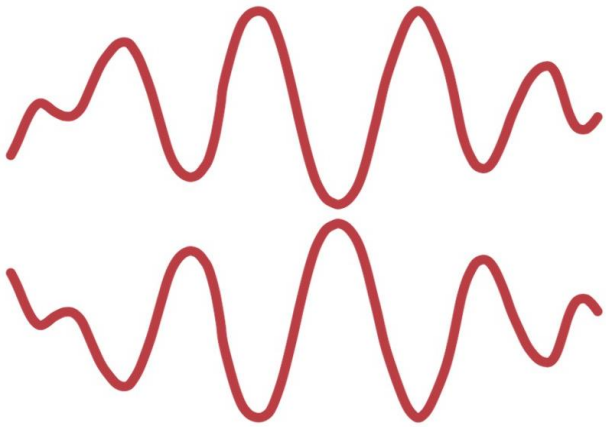

In this chapter, I closely follow our study: M. Esparza, I. Vigué-Guix, M. Torralba, & S. Soto-Faraco. *Long-range α-synchronization as control signal for BCI: A feasibility study.* Submitted to eNeuro, 2022.

Background

A few decades ago, imagining an interface between the human brain and a computer was closer to science fiction than to scientific achievement. Nowadays, brain-computer interfaces (BCIs) can read out brain activity, extract features from that activity, and convert those features into outputs used for monitoring, controlling devices, or even modifying cognitive states (Blankertz et al. 2016). One significant challenge of BCIs is finding reliable control signals from brain activity with sufficiently high signal-to-noise ratio (SNR) at a trial-by-trial level to allow successful classification. Ideally, the appearance of the target brain activity should depend on endogenous mental/brain states that the user can control at will. The use of non-invasive, cost-effective, and light-weight neuroimaging devices can, in turn, facilitate transfer to real applications. For now, EEG is the most viable candidate to achieve this.

Some EEG-based BCIs have used motor imagery as a control signal (e.g., imagined right/left-limb movement; Padfield et al. 2019), whereas others have used neural correlates of covert visuospatial attention (CVSA; van Gerven and Jensen 2009; Treder et al. 2011; Tonin et al. 2013). Here, we will concentrate on the latter. In human behaviour, CVSA is used to direct processing resources to relevant locations in the environment whilst disengaging from irrelevant locations (Pashler 1999; Foster and Awh 2019; Petersen and Posner 2012). CVSA can be manipulated with the Posner cueing protocol (Posner 1980), which induces a robust effect on behavioural performance: higher accuracy and faster reaction times for targets appearing at the cued (attended) location compared to targets appearing in un-cued, putatively unattended locations (Posner 1980; Posner et al. 1980).

Attention shifts in CVSA produce changes in oscillatory activity in the alpha-band (α, 8–14 Hz) at parieto-occipital regions (Klimesch 1999; Foster et al. 2017; van Diepen et al. 2019). Typically, α-power presents a direction-specific imbalance when attention is covertly oriented to either the left or right visual field, revealing its potential as a control signal for BCI implementations (Rihs et al. 2007; Thut et al. 2006; Astrand et al. 2014b). This neural correlate is thought to correspond to a late stage in the brain processes involved in CSVA shifts. First, cueing information is integrated through sensory pathways in a bottom-up fashion, reaching higher visual areas in the parietal cortex

(e.g., intraparietal sulcus) and eventually frontal regions (e.g., frontal eye fields) (Petersen and Posner 2012). From there on, top-down modulation shifts attention to the corresponding hemifield, where it is maintained during target anticipation (Simpson et al. 2011). The mechanism involved in this top-down modulation is thought to involve long-range α-synchronization between frontal and posterior cortex, which eventually leads to classical interhemispheric imbalances in α-power observed in the visual cortex (Sauseng et al. 2005; Doesburg et al. 2009; Lobier et al. 2018). This long-range synchronization is a potential mechanism to increase the fidelity and effectiveness of communication throughout the brain (Clayton et al. 2018) among occipital, parietal, and frontal regions (Sadaghiani and Kleinschmidt 2016). Synchronising excitability cycles between distant neural populations increases the likelihood of spikes from one region discharging post-synaptic potentials during a specific (excitable) phase of the other (Fries 2005, 2015). Despite the overwhelming evidence supporting these models of visual processing, there is still debate on their temporal dynamics, lateralisation patterns and individual-level variability. Further research on these aspects may provide deeper insight into the exact mechanisms of long-range α-synchronization within the frontoparietal network (FPN).

The present study addressed whether long-range α-synchronisation in the FPN presents direction-specific lateralised patterns (i.e., contralateral to ipsilateral differences) regarding the attended location, and if such patterns emerge in single-trial dynamics with sufficient signal strength to make for a reliable control signal in BCI. To the best of our knowledge, BCIs based on attention have only used α-power as a control signal, despite the evidence of links between long-range α-synchronisation and behavioural performance, using group-level analyses (Sauseng et al. 2005; Doesburg et al. 2009; Doesburg et al. 2016). We addressed this by measuring EEG during CVSA using a Posner task and examining the time course of long-range α-phase synchronisation between cue onset and target appearance. This time window is essential for BCI since it is the period during which participants lateralise their attention covertly. Our approach was to replicate the analysis pipeline of Sauseng et al. (2005), reproduce the group effect at the target-locked window, and extend our analysis to the cue-to-target window, more relevant for BCI. We finally assessed the classification of attentional loci at the single-trial level using long-range α-phase synchronisation as a proof of concept for BCI.

Methods

Participants

We used data from a previous, unrelated study (Torralba et al. 2016). The dataset consisted of 15 participants (mean age = 22; SD = 3; 7 female). All participants provided informed consent and had a normal or corrected-to-normal vision. The study was run in accordance with the Declaration of Helsinki and the experimental protocol approved by the local ethics committee CEIC Parc de Salut Mar (Barcelona, Spain). Five participants who presented equivalent detection and discrimination rates for stimuli appearing at cued and un-cued locations were discarded from the analysis, leaving a total of 10 participants.

Task

Before the experimental session, the participant's EEG activity was recorded during a five-minute recording at rest with eyes closed to extract the individual alpha frequency (IAF; see below) used in the analyses. In the experimental session, participants performed a modified version of the Posner cueing task (see **Figure 19A**). The trial started with the onset of a central fixation cross, placed between two placeholder squares located 20º of visual angle left and right off centre, vertically shifted 20º of visual angle below the fixation cross (see **Figure 19A**). After 200 ms fixation period, a central auditory cue (100 ms duration) indicated the likely target location through either high pitch (2000 Hz) or low pitch (500 Hz) tones, the mapping was randomized across subjects. Participants should covertly attend to the indicated side, without moving their eyes, during a jittered inter-stimulus interval (ISI; 2000 ± 500 ms). The use of a jittered ISI was employed in order to avoid participants falling into a constant rhythmic pattern. Next, the target (a Gabor grating tilted 45º left or right, 50 ms duration) appeared briefly inside one of the placeholders, with 75% validity regarding the cued location. The grating contrast was adjusted individually, as described below. A noise pattern of equal overall luminance as the target was presented at the alternative placeholder, with the exact timings as the target. Participants were asked first to indicate if they had detected the target (yes/no detection) and subsequently the target's tilt (left/right discrimination). Both answers were made by keypress, in an un-speeded fashion, and with response mapping (top-bottom) orthogonal to the attention manipulation and varied from trial to trial. An inter-trial interval of

1000 ms followed the response, and a new trial began. Unless otherwise noted, the EEG analyses were done on validly cued trials that responded correctly. On average, 289.9 ± 11.3 trials from each participant were employed for the EEG analysis.

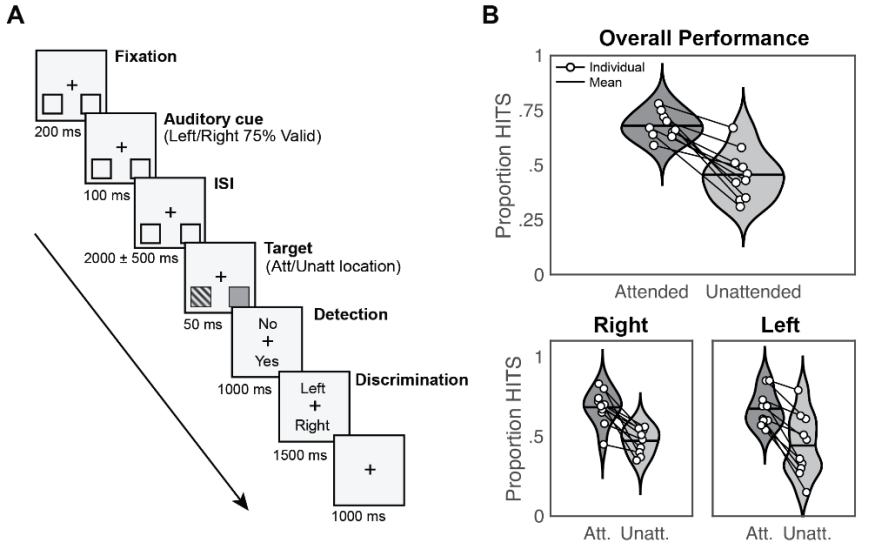

FIGURE 19. Experimental design and response rates. (A) Schematic trial representation. A black fixation cross in the middle of the screen and two squares (to-be-attended locations) at the bottom left, and bottom right positions were displayed continuously. At the beginning of each trial, participants were instructed to gaze at the fixation cross. After 200ms (fixation period), an auditory cue appeared for 100ms (cue period) indicating which hemifields participants must attend (75% validity). After a jittered interstimulus interval of 2000 ± 500 ms, a target appeared at the targeted location during 50ms (target period). Participants had to report first if they had seen the target (detection task), and after 1000 ms, the location of the target (left/right discrimination task) during 1500ms. An intertrial interval (ITI) of 1000ms followed, and a new trial began (Adapted from Torralba et al. 2016). (B) Response rates for detected and discriminated trials (HITS) related to attended and unattended trials. Black lines over violin plots represent the mean value. Both overall performance (top) and right/left hemifields (bottom) are shown. White dots indicate individual values (Adapted from Torralba et al. 2016).

The Gabor gratings used as stimuli were 0.002 cycles per degree, with a size of 3.35º, and were embedded in white noise. The contrast was adjusted individually using a preliminary threshold titration procedure in which thresholds for both sides (left and right) were independently adjusted to a 70% detection rate when cued (in the attended location). Stimuli were presented on a 21" CRT screen with a refresh rate of 100 Hz and a resolution of 1024 x 768 pixels. The experiment was

implemented in MATLAB R2015b (MATLAB, RRID: SCR_001622) using the Psychophysics Toolbox (Psychophysics Toolbox, RRID: SCR_002881).

EEG recording

EEG recordings were obtained from 64 Ag/AgCl electrodes positioned according to the 10-10 system with AFz as ground and nose tip as reference. Impedances were kept below 10 kΩ. The employed system was an active actiCHAmp EEG amplifier from Brain Products (Munich, Germany). The signal was sampled at 500 Hz and processed in MATLAB 2020 and 2015 (MATLAB, RRID: SCR_001622) using custom functions and the FieldTrip toolbox (FieldTrip, RRID: SCR_004849).

EEG pre-processing

In order to remove eye movements, blinks, and muscle artefacts, Independent Component Analysis (ICA) was carried out (Makeig et al. 1995). Additionally, manual artefact rejection was applied to discard trials where any EOG components had an amplitude higher than 50 μV. Defective channels were repaired using neighbours calculated by triangulation and splines for interpolating channel data. Following these steps, the data was demeaned and notch filtered at 50 Hz to exclude line noise. Next, fifth-order high-pass and sixteenth-order low-pass IIR Butterworth filters were employed to limit the signal between 16 and 45 Hz (Sauseng et al. 2005). The filtering was done forward and backwards (two-pass), which resulted in zero phase lag.

Determination of the individual alpha frequency (IAF)

The frequency of interest used in analyses of this study was adjusted for each participant depending on the individual alpha frequency (IAF) extracted from the five-minute recording (eyes closed) previous to the experiment (see above). The IAF was determined based on the presence of a single peak (i.e., a local maximum) within the considered frequency band of interest (5-15 Hz) on the power spectrum density (PSD). A spectrogram was extracted for each parieto-occipital electrode (P7, P5, P3, P1, Pz, P2, P4, P6, P8, PO3, PO4, POz, PO9, PO10, O1, Oz, O2) using the Welch method (segments of 1000 ms with a 10% overlap, a Hanning taper to avoid spectral leakage and 0.25 Hz frequency resolution). The power spectrum was averaged

across electrodes for each participant and normalised by the mean power from 1 to 40 Hz.

Time-frequency analysis

We performed long-range synchronisation analyses in two time windows. The first was time-locked to the target onset (target-locked) to replicate Sauseng et al.'s (2005) methods and validate our analysis pipeline. The second was time-locked to the cue onset (cue-locked) to estimate long-range α-phase synchronisation during covert visuospatial attention shifts.

Following Sauseng et al. (2005), for the target-locked analysis we used two windows of 200 ms: a pre-target (-200 to 0 ms) and a post-target window (200 ms to 400 ms). The latter excludes the interval 0 to 200 ms, most affected by the phase resetting effect of target presentation. For the cue-locked analysis, we used the cue-to-target time window between 500 ms and 1500 ms post-cue and divided it into five consecutive and non-overlapping 200 ms windows. By analysing from 500 ms onwards[5] we avoid the event related potential (ERP) caused by cue presentation and allow endogenous attention shift to build up, a process which takes a few hundreds of milliseconds (Foxe and Snyder 2011). All epoched data was mirror-reflected to avoid edge artefacts (Cohen 2014) when performing the time-frequency analysis. Afterwards, data were trimmed, and reflected edges were removed.

We computed the Fourier coefficients using 5-cycle Morlet wavelets (Grossmann and Morlet 1984) with 16 logarithmically spaced frequencies ranging from 2.6 to 42 Hz. For the analysis centred on the individual alpha frequency (IAF), we only used wavelets within the upper α-band (9.54 – 14.31 Hz) (Sauseng et al. 2005), whereas, for the exploratory analysis, we used the whole frequency range. This difference allowed us to conduct a hypothesis-driven analysis using the upper α-band to replicate Sauseng et al. (2005) and an exploratory analysis to explore further long-range α-phase synchronisation in other frequency bands beyond the IAF.

---

[5] The cue-locked analysis period ends at 1500 ms, which was the minimum possible duration of the cue-to-target interval (duration of 2000 ± 500 ms, see *Methods*).

Connectivity measures

Three regions of interest (ROI) were defined for the analyses: A fronto-medial (FM) ROI (Fz, FC1, FC2) and two symmetric posterior regions; the parietal left (PL) ROI (P5, P7, PO3, O1) and the parietal right (PR) ROI (P6, P8, PO4, O2). To infer connectivity between each of these parietal ROIs and the FM location, we used Phase Locking Value (Lachaux et al. 1999). This metric reports the consistency of phase differences between two locations across multiple trials and is not affected by power differences. Mathematically, the PLV is expressed as the absolute value of the average complex unit-length phase differences:

$$PLV(x,y) = \left|\frac{1}{n}\sum_{k=1}^{n} e^{i(\varphi_x(k)-\varphi_y(k))}\right| \quad (1)$$

where n corresponds to the total number of trials indexed by k and φ_x, φ_y correspond to the phases at electrodes x and y, respectively. PLV was calculated according to **equation (1)** using the phases for every combination of individual electrode pairs of the FM-PR and FM-PL networks. Then, these values were averaged, resulting in a time series of PLV FM-PR and FM-PL networks for each of the frequencies of interest and condition (attended left and attended right) trials. Subsequently, the PLV time series were collapsed as either ipsilateral (FM-PL network and attend left; FM-PR and attend right) or contralateral (FM-PR network and attend left; FM-PL and attend right). Therefore, for each participant and frequency of interest, two time series of PLV were obtained (contra- and ipsilateral PLV).

Classification

The trial classification was performed using Support-Vector Machines (SVM). We selected the FM-PR and FM-PL connectivity for the metric used as input to the SVM. Attended right and attended left labels of each trial were provided as ground truth for the algorithm. The main goal of the classifier was to infer where the participant was attending on each trial based on the long-range α-phase synchronisation in the left and right frontoparietal networks. Note that PLV is computed across trials, and SVM aims to classify on a single-trial basis, so PLV was also calculated across time points (Cohen 2015). As a validation step, we repeated the target-locked analysis

employing this metric (i.e., cross-time PLV) before proceeding with the cue-locked classification attempt.

We divided the cue-locked interval ranging from 500 to 1500 ms in bins of 200 ms, yielding five values for FM-PR connectivity and five for FM-PL connectivity. The resulting ten values were used for the SVM input to perform the optimisation and classification of the trials. Note that for the classification, we only used the data from the participants that achieved a significant difference in PLV values between parietal left and right ROIs in the pre-target window of the target-locked analyses. For each participant, trials were split into a training (80%) and testing (20%) set of trials to avoid overfitting. Then, the training set was subdivided into sub-training (80%) and validation sets (20%).

Our initial approach was to use a linear kernel for the classification. However, after evaluating the option through cross-validation of the validation set and obtaining a negative result (i.e., classification was not better than chance level), we decided to use instead of a Gaussian kernel (i.e., Radial Basis Function). In order to select the most suitable and efficient values for classifying attended left and attended right trials from the validation set, we optimised the parametric space of the SVM, comprised of margin and gamma (γ) parameters, and explored the parametric landscape ranging from 10^{-6} to 10^{3} in steps of 10 for both constants.

Inter-hemispheric power imbalance exploratory analysis

Besides calculating the long-range α-phase coupling, we also computed the inter-hemispheric α-power imbalance at parietal regions both at the individual and at group-level as a reality check. To extract the α-power during the task, we selected the epoch from -1.5 to 3 s in cue-locked trials by convolving the EEG signal with a set of complex Morlet wavelets (Grossmann and Morlet 1984) of 6-cycles. The frequencies of the wavelets ranged from IAF - 1 Hz to IAF + 1 Hz in 1 Hz steps. For instance, an IAF peak of 10 Hz would have a bandwidth ranging from 8.33 to 11.67 Hz. The power in each of the two symmetric ROIs at posterior regions (PL and PR ROIs; same used in the connectivity analysis) was averaged, and the power imbalance was computed in terms of the lateralisation index of α-power, according to the formula proposed by Thut et al. (2006):

$$Lateralization\ Index = \frac{\alpha(PR\ ROI) - \alpha(PL\ ROI)}{mean\ of\ \alpha(PL+PR\ ROI)} \quad (2)$$

where α(PL ROI) and α(PR ROI) are the average of α-power over left and right regions of interest, respectively. **Equation (2)** leads to smaller (negative) values in the case of α-activity was more prominent over the left hemisphere than the right (α(PL ROI) > α(PR ROI)) and to larger (positive) values for the opposite pattern (α(PL ROI) < α(PR ROI)). According to theory and previous findings, values of LI reflecting attention directed to the right visual field should be larger than LI values reflecting leftward directed attention.

Finally, we also checked whether there was any relationship between the α-power imbalance and the contra-ipsi difference of PLV for each attended location. We explored the correlations between α-lateralization indexes and the effect in PLV contra-ipsi differences at the pre-target (-200 to 0 ms) and post-target (200 to 400 ms) windows using Pearson correlations.

Statistical analyses

A one-tailed nonparametric Monte Carlo permutation test was computed to determine significant differences in PLV between networks for each attended location (Mostame et al. 2019). For each participant, the attended right or left labels were randomly assigned to trials, and surrogate PLVs were calculated from the resulting dataset. This process was repeated 10,000 times (iterations) to create a null distribution of PLV values. The obtained p-value corresponded to the proportion of surrogate iterations with a contra-ipsi difference larger than the actual measured value (one-tailed test). This process was performed on every time window defined in the previous section. For the group analysis, the procedure was equivalent, but surrogate PLV distributions were averaged across participants before the statistical test. For the statistical assessment of the α-power imbalance over time between attended left and attended right trials, we performed a cluster-based permutation test procedure (100,000 randomisations) for each participant and at the group-level (one-tailed permutation test; Maris and Oostenveld 2007; Meyer et al. 2021). We assessed that lateralisation indexes for attended-right and attended-left trials were significantly two different distributions by applying a one-tailed t-test (independent samples) with α-level = 0.05 for each participant. At

group-level, we performed a one-tailed paired t-test with the mean lateralisation indexes for attended right and attended left trials for each participant with α-level = 0.05. Correlations between α-power imbalance and the contra-ipsi difference of PLV were corrected for multiple comparisons by applying the False Discovery Rate (FDR) of Benjamini and Hochberg (Benjamini and Hochberg 1995).

Results

Behavioural results

As expected, behavioural results in see, **Figure 19B** show that the detection rate was superior for cued (attended) trials (mean = 0.68 ± SEM = 0.02) compared to un-cued (unattended) ones (0.46 ± 0.04). The pattern on each hemifield was equivalent to the overall pattern: on the left hemifield attended (0.68 ± 0.03) and unattended (0.47 ± 0.03); for the right hemifield attended (0.67 ± 0.03), and unattended (0.44 ± 0.06).

Target-locked long-range alpha synchrony

As described in the analyses section, long-range synchrony was estimated using PLV between a frontal ROI and each of two lateralized parietal ROIs. Here, we describe the target-locked analysis, mainly carried out to reproduce Sauseng et al. (2005). **Figure 20** shows the group-level connectivity analysis of the upper α-band (9.54 - 14.31 Hz). Phase coupling is depicted as the mean across the pre-target window (-200 to 0 s) and the post-target window (200 to 400 ms), as well the temporal course (from to -500 to 500 ms). Regarding the left frontoparietal network (**Figure 20A, left**), PLV was consistently higher when attention was directed right (contralateral) than left (ipsilateral) in both pre-target and post-target windows, although the PLV difference did not reach significance in the pre-target window. Regarding the right network (**Figure 20A, right**), PLV was stronger when attention was directed left (contralateral) than right (ipsilateral) in the post-target window, whereas the pre-target window does not show this difference. This pattern generally replicates Sauseng et al.'s (2005) results, as indicated by the dashed lines in **Figure 20A** representing the mean phase-coupling from their study. Lower panels in **Figure 20A** display the temporal course of phase coupling to provide a time resolved illustration of the phase-coupling effect.

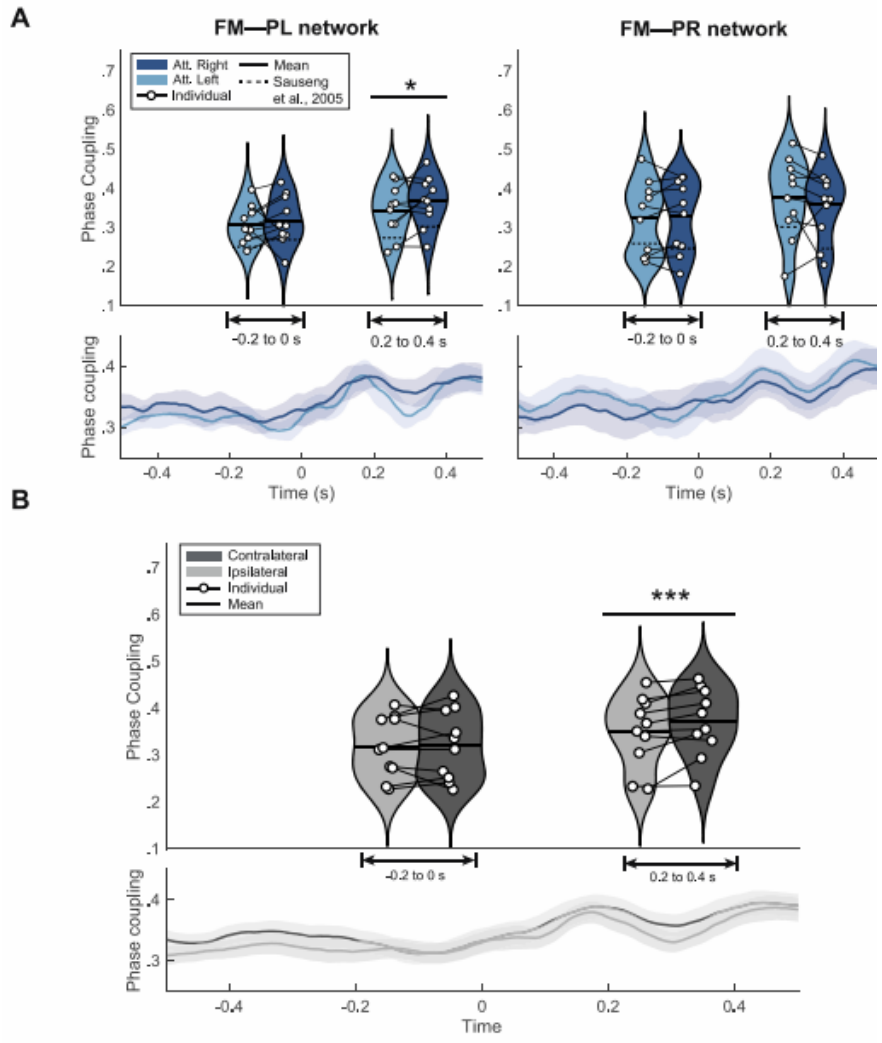

FIGURE 20. Target-locked results. (A) Target-locked results of the phase-coupling for attended left (light blue) and attended right (dark blue) in FM-PL and FM-PR networks. The lower panels depict the cross-trial average time course (± shaded SEM) of PLV in both conditions (attended left and attended right). Upper panels present the binned violin plots (mean and median) of the pre-target window (-200 to 0 ms) and the post-target window (200 to 400 ms); *$p < 0.05$. Dashed lines denote the results from Sauseng et al., (2005). (**B) Target-locked results collapsed as either ipsilateral (FM-PL network and attended left; FM-PR and attended right) or contralateral (FM-PR network and attended left; FM-PL and attended right).** The lower panel shows the cross-trial average time course (± shaded SEM) of PLV in ipsilateral (light grey) and contralateral (dark grey) conditions. The upper panel exhibits the distribution of individual PLV with a violin plot, superimposed by the mean and the contra- to ipsilateral differences between individual PLV; ****p < 0.001*.

For the attend right condition, PLV values in the left network should be higher than PLV values for the attended left. The inverse pattern should hold in the right network. Moreover, **Figure 20B** presents the PLV with side of attention collapsed as contra- and ipsilateral with respect to the corresponding network. Individual PLV values, marked as black dotted lines, exhibit a consistent contra- to ipsilateral increase in the post-target window. Group-level statistical analysis further showcased a significant difference limited to this time window (200 to 400 ms, $p < 0.001$).

In the single-subject analyses, 8 out of 10 participants showed contralateral PLV increases, in which 5 of them were significant (P04, $p < 0.001$; P05, $p < 0.001$; P06, $p < 0.05$; P07, $p < 0.001$; and P10, $p < 0.01$; see **Supplementary Figure 19** in *Annex III*). The lack of significant differences in the pre-target window is consistent with individual phase coupling, as no clear contra-ipsi trends emerged. Five participants had higher contralateral PLV values in this time window, 3 of which exhibited a significant behaviour (P04, $p < 0.05$; P05, $p < 0.001$; and P10, $p < 0.05$; see **Supplementary Figure 19** in *Annex III*).

Cue-locked long-range alpha synchrony

The primary aim of this study was to explore the cue-to-target interval before target presentation (500 ms to 1500 ms after cue onset) to ascertain whether attention-based long-range connectivity during the orienting period could be a reliable signal for BCI control. Considering that the cue indicates the hemifield to which participants should voluntarily lateralise their attention, differences in contralateral and ipsilateral connectivity may potentially emerge in this time window. So far, we have seen that this attention shift had significant consequences on behaviour and target processing (post-target connectivity). At the group level, however, no significant difference between contralateral and ipsilateral connectivity in the upper α-band was found in any of the five 200 ms time windows considered in the cue to target period (see **Figure 21A**). At the individual level, only one participant (P05) showed a significant increase in the contralateral PLV in four out of five-time windows (see **Supplementary Figure 20** in *Annex III*). This participant also showed a significantly higher contralateral connectivity in both the pre-target and post-target time windows of the target-locked analysis.

We chose the upper α-band a priori given prior findings of Sauseng et al. (2005) as well as the effects in the target-locked analyses of our own

data. However, we conducted additional analyses to explore other frequencies (between 2.4 and 42 Hz) in search of differences between contralateral and ipsilateral PLV (see, **Figure 21B**). Values were collapsed as the difference between both measures (contra-ipsi) and z-scored. Over time, neither clear trends across frequencies nor apparent increases are observed in either contralateral or ipsilateral connectivity. Individual results of the exploratory analysis show the same results and do not present relevant PLV patterns in any participant aside from upper α-band findings in P05 (see **Supplementary Figure 21** in *Annex III*).

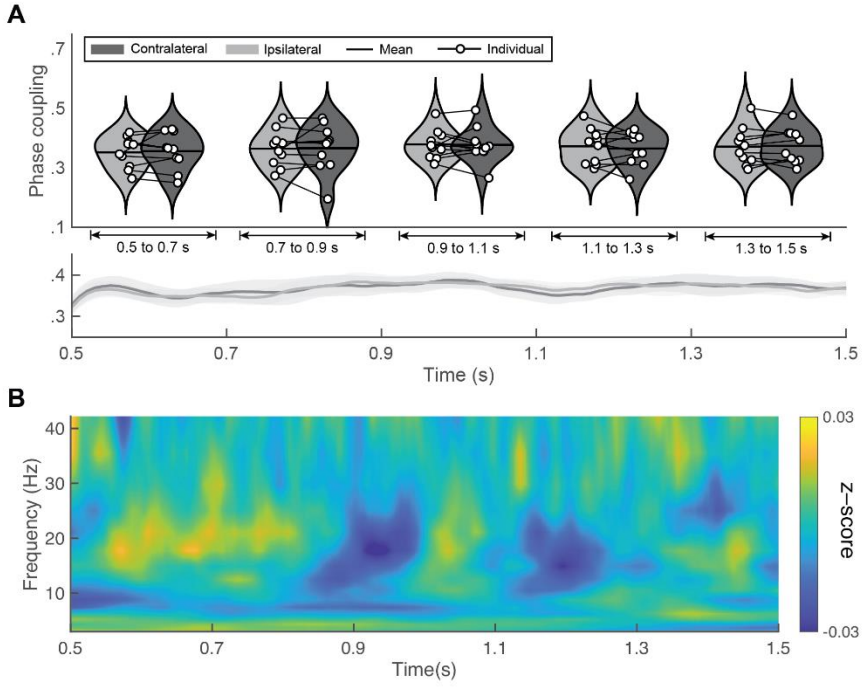

FIGURE 21. Cue-locked results. (A) Group-level results of upper-alpha PLV. Upper panel shows phase coupling for ipsilateral (light grey) and contralateral (dark grey) sides in time-windows of 200 ms from the cue-locked interval (500 ms to 1500 ms after cue presentation). Lower panel shows mean and standard error of the mean (SEM) of the PLV values. (**B) Exploratory analysis of PLV differences**. Group-level temporal evolution of the z-scored difference between contralateral and ipsilateral PLV for each frequency band (2.4 - 42 Hz with 16 logarithmic steps). Z-score values range from -0.03 to 0.03.

Classification

The results are hardly promising in generalising the use of long-range connectivity for BCI control. However, BCI protocols are often very

sensitive to individuals. Here, we intended to seek proof-of-concept evidence. With this goal in mind, we attempted single-trial classification from selected participants datasets, as either attended right or attended left, according to cue-locked connectivity patterns. To maintain statistical independence between dataset selection and test, participant selection was based on the target-locked data. We selected the 3 participants (P04, P05 and P10) for whom we found significant connectivity differences in the pre-target time window of the target-locked analysis, and their data were used for the classification. Please note that this participant selection of the pre-target window, from -200 to 0 ms from target onset, is aligned differently than the cue-locked analysis window, which considers times up until -500 ms from target presentation. The total number of trials for each participant was 272 (P04), 310 (P05), and 338 (P10).

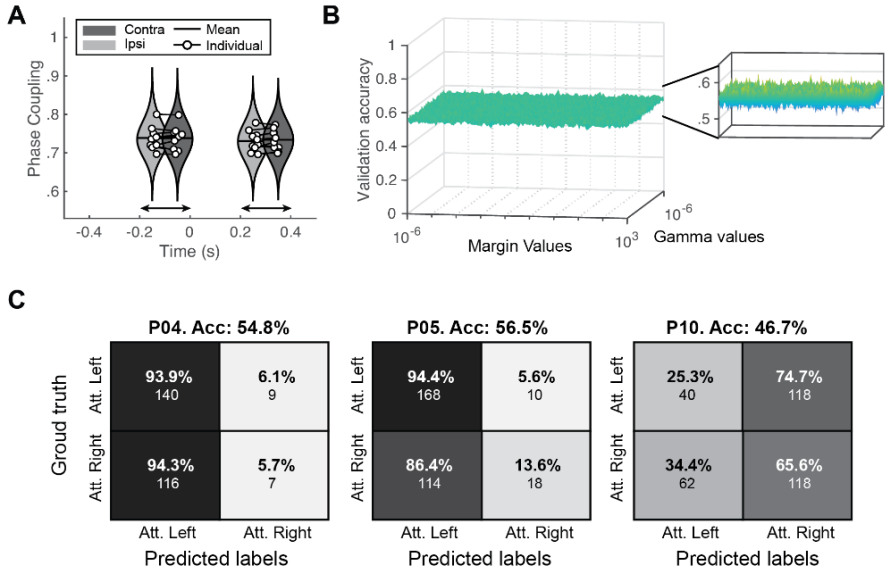

FIGURE 22. Classification outcomes. (A) Cross-time PLV reality check. Replication of results from **Figure 21** calculating PLV across time points rather than across trials. **(B) Optimisation results of gamma and margin parameters of the Gaussian kernel SVM.** Ten-fold validation accuracies with varying margin values (x-axis) and gamma values (y-axis). Inset shows a detailed view of the z-axis. **(C) Confusion matrices of the classification outcomes for each participant.** Y-axis represents ground truth labels (attended right or attended left) and x-axis represents the classifier's outcomes. Percentages represent the fraction of correctly classified trials of each condition (i.e., each row sums to 100%). Under the percentage is the gross number of classified

As described in the methods section, we carried out a validation of cross-time PLV in the target-locked window to understand whether this metric could replicate group-level differences between contra- and ipsilateral networks found through cross-trial PLV. These results can be seen in **Figure 22A**. Statistical analysis showed no significant differences between contra- and ipsilateral scenarios in either time window. Individual values also remained non-significant (see **Supplementary Figure 22** in *Annex III*). Considering the large parametric landscape of SVM implementations we optimized the gamma and margin parameters of a Gaussian kernel (see **Figure 22B**). From a qualitative perspective, no clear maximum validation accuracy values emerge from the landscape, although quantitative analysis identified a margin of 5.01×10^{-6} and a γ value of 2.51×10^{-2} to have the most optimal validation set of the outcome. The lack of a clear minimum suggests that the model may be unable to classify individual trials regardless of the parametric values.

Ten-fold cross-validation was carried out independently on all participants' trials to reduce the inter-individual variability and improve the classification accuracy. Single trials predicted as either attended right or attended left were contrasted with the actual cue direction in each trial. Classification outcomes of each participant are shown in **Figure 22C**, which resulted in virtually chance level sorting (0.548, 0.565, and 0.467, respectively). Confusion matrices display the distribution of each class, revealing the skewed distribution of values towards attended left labels, which is far from the ideal clustering along the diagonal of the matrix.

Inter-hemispheric power imbalance

As a reality check on the dataset, we addressed whether there was a difference in the α-power inter-hemispheric imbalance between attended left and attended right trials. We performed the cue-locked analysis at the group level, using the Lateralization Index (LI) described by Thut et al. (2006) (see **Figure 23A**). On average, the lateralisation index was significantly different between attended right and attended left in the expected direction ($p = .01$, Cohen's d = -0.8356). At the individual level, 7 out of the 10 participants showed a significant difference in lateralization index between the two attention conditions ($p = <.001$; see **Supplementary Figure 23** in *Annex III*). We also performed a time-resolved version of this analysis within the said window. The cluster-based permutation test (**Figure 23B**) showed significance within two time periods, from 0.66 to 0.82 s and

1.34 to 1.5 s. At the individual level, only for one participant (P01), the cluster-based permutation test revealed a significant cluster over time from 0.6 to 1 s (see **Figure 23**). Generally, these results are consistent with the results of previous studies (e.g., Tonin et al. 2012; Thut et al. 2006), at least at the group level. It is more challenging to compare single-subject data with other studies, as it usually is not reported or statistically analysed.

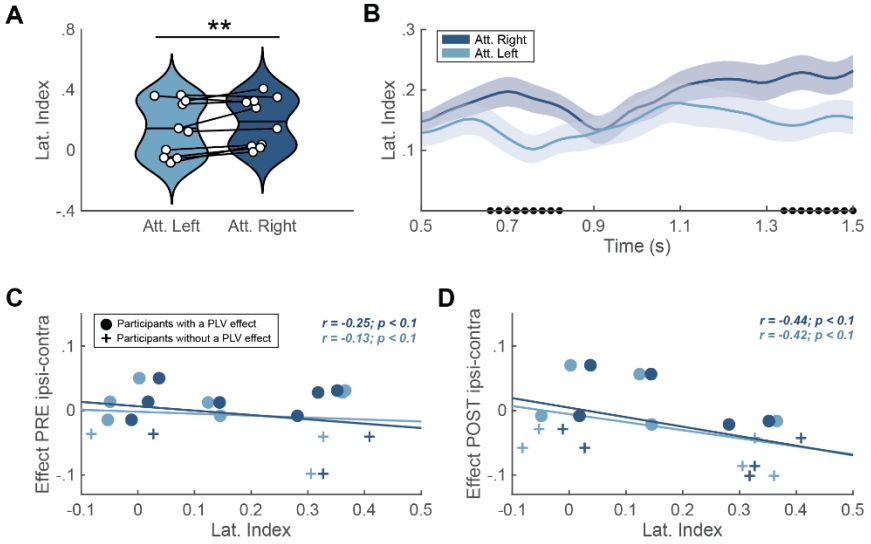

FIGURE 23. Lateralisation index reality check. (A) Averaged lateralization index for attended left (light blue) and attended right (dark blue; *p > 0.05). White dots denote individual scores, and horizontal line indicates the group mean. **(B) Lateralisation index (mean ± SEM) over time.** Solid lines and shaded areas represent mean and standard error of the mean (SEM) interval, respectively. Dots on in the x-axis denote the significant difference over time between attended left (light blue) and attended right (dark blue) via cluster-based permutation test. **(C-D) Lateralisation indexes and the difference of contra- to ipsilateral PLV for attended left (light blue) and attended right (dark blue) at the pre-target window (C) and the post-target window (D).** At the pre-target the correlations for attended right ($r = -0.25$, $p > 0.05$) and attended left ($r = -0.13$, $p > 0.05$) did not reach significance and neither did the correlations for attended right ($r = -0.44$, $p > 0.05$) and attended left $r = -0.42$, $p > 0.05$) at the post-target window. Crosses denote participants with a significant effect in PLV contra-ipsi differences at the pre-target window (-200 to 0 ms; P04, P05, and P10) and the post-target window (200 to 400 ms; P04, P05, P06, P07, and P10). Dots represent the rest of the participants.

Finally, we explored the potential correlation between α-power inter-hemispheric imbalance measured with the lateralization index and α-phase coupling for each attended location (see **Figure 23 C-D**). In the

pre-target window (**Figure 23C**), the correlations for attended-right ($r = -0.25$, $p > 0.05$) and attended-left $r = -0.13$, $p > 0.05$) did not reach significance. Neither did the correlations for attended-right ($r = -0.44$, $p > 0.05$) and attended-left $r = -0.42$, $p > 0.05$) at the post-target (**Figure 23D**) window. A visual inspection indicated that participants showing an effect in PLV contra-ipsi differences are below the correlation fit in pre-target and post-target windows, suggesting that those participants have a more negative effect in PLV contra-ipsi differences.

Discussion

The present study addressed the relationship between shifts in visuospatial attention and the lateralisation of α-band coherence between frontal and parietal sites, intending to assess their feasibility as a control signal in BCI. Previous studies, using group-averaged multi-trial analyses, found increased long-range α-synchronization in the hemisphere contralateral to the attended side of space, and suggested that it reflects top-down mechanisms of visual attention (Sauseng et al. 2005; Doesburg et al. 2009). We reasoned that if contra- to ipsilateral differences in synchronisation would emerge as a result of endogenous top-down mechanisms, they should be present following cue presentation as participants shift their attention. This hypothesis stems from instructing participants to shift their attention laterally in expectancy of target appearance engages frontoparietal visual processing pathways (Corbetta and Shulman 2002; Hopfinger et al. 2000; Asplund et al. 2010). Here, we sought proof of concept that long-range neural synchronisation engaged in this network could be used for BCI control on a trial-by-trial basis.

In attention orienting protocols, the cue-to-target period offers the possibility of implementing a BCI control harnessing covert attentional orienting in individual trials due to lateralisation of attention in anticipation of the target appearance. This would open the possibility of designing active BCI systems controlled by the user's voluntary decision to attend left or right covertly. Therefore, our study employed long-range α-synchronization in the frontoparietal network (FPN) to investigate whether this brain measure could potentially discriminate attended locations of the left/right visual field.

We found significant group-level differences in contra- to ipsilateral long-range α-synchronization around target onset time in direct

replication of Sauseng et al. (2005). These results help confirm the importance of lateralized long-range α-synchrony along the FPN during orienting and especially reveal the potential of EEG to grasp these effects, at least during target processing at the group level. However, similar differences in synchrony were not observed during the post cue time window, which was the time of interest for BCI purposes. We extended the cue-locked analysis to other frequencies outside the α-band, with equally negative results. Finally, given the high individual variability of single-trial analysis outcomes, we attempted to classify the individual trials of selected participants for whom significant synchronisation differences following cue presentation were found, a benchmarking process that nevertheless rendered chance-level classification. Below, we discuss how these results may be influenced by various methodological aspects (e.g., different time windows, classifier's input metric) and how they fit into state-of-the-art literature. Please note that because the focus of our study was on single-trial analysis, the sample size was relatively small for the group analyses (N = 10). Although this sample size was sufficient to confirm previous findings, the negative results of the group analyses should be interpreted with caution until a more extensive study is conducted.

Frontoparietal network synchronisation characterises visuospatial attention

A result to emerge from our study is that long-range α-synchronization within the FPN was associated with visuospatial attention orienting, in line with its putative role in this cognitive process (Jensen et al. 2015; Siegel et al. 2008; Doesburg et al. 2009; Sacchet et al. 2015). We observed a spatially distributed difference in upper α-coherence, with increased synchrony in the FPN pathway contralateral to the attended hemifield. According to current attention theories, the mechanism underlying this finding may relate to an initial attentional modulation stemming from frontal areas such as the frontal eye fields (FEF) and the intraparietal sulcus (IPS) (Corbetta and Shulman 2002; Kastner and Ungerleider 2000; Helfrich et al. 2018), leading to a state of α-band desynchronization in the relevant area of the visual cortex (i.e., contralateral to attended hemifield) in anticipation of relevant information (Capotosto et al. 2009; Marshall et al. 2015). This explanation aligns with the well-established evidence that contralateral α-power suppression (also reproduced in our results) enables visual stimuli processing in the attended location (Doesburg et

al. 2009; Thut et al. 2006; Yamagishi et al. 2003; Babiloni et al. 2006; Foxe and Snyder 2011; Klimesch et al. 2007; Lange et al. 2013), and that cyclic phase-dependent inhibition in low-level visual cortex dictates behavioural performance (i.e., reaction times; Haegens et al. 2011; Klimesch 2012; Jensen et al. 2014; Samaha et al. 2015; VanRullen 2016b). Both accounts align with the idea that local α-power and long-range α-synchronization may have separate roles in attention and perception (Bonnefond et al. 2017; Palva and Palva 2007, 2011; Palva and Palva 2018; Sadaghiani and Kleinschmidt 2016).

Our results of the increased contralateral synchronisation within the FPN replicate the work of Sauseng et al. (2005) and validate our methodology and analysis pipeline (e.g., time-frequency analysis, synchronisation metric), setting the ground for the intended proof of concept test regarding transference to BCI. However, lateralized frontoparietal connectivity patterns in attentional and perceptual disposition remain challenged in the literature and the role of α-power and α-phase algether (Ruzzoli et al. 2019; van Diepen et al. 2019; Antonov et al. 2020). Lobier et al. (2018) found α-synchronization associated with visuospatial attention but revealed distinct patterns of lateralization regarding the visual system and top-down attentional networks. They showed stronger ipsilateral synchronization within the visual system (in line with Doesburg et al. 2009; Siegel et al. 2008) but no consistent lateralisation in long-range networks, suggesting their different involvement in visuospatial attention. D'Andrea et al. (2019) found a modulation of frontoparietal alpha-beta cross-frequency synchronization during attention orienting, but not in alpha-synchronization alone. Further, this cross-frequency connectivity pattern was strongly associated with right hemisphere frontal dominance (in line with Heilman and van den Abell 1980; Zago et al. 2017). This finding agrees with previous evidence of the crucial role of the right FEF in top-down attentional modulation (Esterman et al. 2015; Hung et al. 2011; Silvanto et al. 2006), supported by evidence using TMS (e.g., Capotosto et al. 2009). In light of this evidence and our results, the exact relationship between contralateral frontoparietal α-synchronization and shifts in attention orienting is still unclear. Positive findings, however, such as the ones in the present study using a target-locked analysis, represent a basis for exploring earlier time windows capable of shedding light on the mechanism underlying FPN α-synchronization.

Correlations between long-range alpha-synchronisation and individual reaction times in visuospatial tasks suggest this neural correlate may be observable at a single-subject level (Lobier et al. 2018). Despite this, significant group-level target-locked dynamics of increased synchrony did not transfer to all individuals in our study. The observed variability may be partially explained by individual differences in anatomical tracts of attentional relevance (e.g., superior longitudinal fasciculus). Findings employing MRI suggest that volumetric differences in these structures impact local visual cortex oscillations, leading to variability in EEG traces (Marshall et al. 2015; D'Andrea et al. 2019). However, this variability of individual results is challenging to set in the perspective of previous research simply because published studies do not report single-subject statistics. Ultimately, the outcomes of this study leave an incomplete understanding as to whether there is a true group effect that does not extend to all individuals or, contrarily, whether individual effects of specific participants are large enough to induce a group-level finding in previous research.

Lateralized patterns of α-synchronization appear in target-locked but not cue-locked time windows

Long-range α-synchronization presented contralateral increases at the post-target (200 to 400 ms, with t = 0 as target appearance) and the pre-target window (-200 to 0 ms). However, only the former time window resulted significantly. This result is slightly different from Sauseng et al. (2005), who observed significant contralateral synchronisation increases within the FPN network at both time windows. However, the numerical differences were in the same line in both studies, and the different outcomes of some statistical significance tests may be due to a lack of statistical power. Another potential explanation for the absence of significant findings at the pre-target window may be the difference in experimental paradigms. The task employed here had a long post-cue interval ranging from 2000 to 2500 ms (jittered between trials). Sauseng et al. (2005), on the other hand, had a shorter delay between cue and target appearance of 600-800 ms, thereby perhaps leading to a more concentrated time window where the attention shift may have taken place. If participants shifted attention at varying times from cue onset up to target appearance, this might explain why we were unable to capture the effect in anticipatory visuospatial attention.

In cueing paradigms, bottom-up integration of cue information through sensory pathways precedes top-down modulation of

visuospatial attention (Simpson et al. 2011). The temporal course of this cognitive operation is thought to begin only after 150 ms of visual cueing in voluntary attention and includes frontal regions approximately after 350 ms. Furthermore, from 400-500 ms onwards, frontal and parietal regions are thought to be solely involved in attentional shifting and target discrimination (Simpson et al. 2011). Thus, if the FPN does present direction-specific synchronisation, we anticipated this would appear from 500 ms after cue onset onwards. Contrary to what we expected, we did not observe any significant contra- to ipsilateral differences in the cue-locked time windows (500 to 1500 ms after cue onset). Previous studies employing a similar time window showed lateralisation patterns in parietal regions in alpha and beta bands (Siegel et al. 2008; Pantazis et al. 2009) and frontoparietal lateralisation in the theta and gamma band (Green and McDonald 2008; Gregoriou et al. 2009). Therefore, we extended our cue-locked analysis to other frequencies, achieving no significant contra- to ipsilateral differences. Note that PLV values were averaged across 200 ms windows, and this excludes, to a certain extent, the confound of frontal and parietal regions having different activation over time. Altogether, despite the evidence across multiple frequencies of synchronisation in the cue-target time window, we did not find patterns of lateralised cue-locked connectivity within or outside the alpha-band.

Our negative results in the cue-locked analysis may align with the notion that late periods after cue onset are associated with direction-specific activity in parieto-occipital regions but not in frontal regions (e.g., FEF) (Doesburg et al. 2009; Simpson et al. 2011). Long-range α-synchronization may, therefore, initially shift attention (shortly after cue presentation) and later (close to target presentation) maintain it at the directed hemifield favouring perception and releasing lateralised patterns (Lobier et al. 2018; Kastner and Ungerleider 2000; Hopfinger et al. 2000; Grent-'t-Jong and Woldorff 2007). This idea resonates with the essential question formerly posed by Sauseng et al. (2005), debating whether frontal involvement in long-range α-synchronization is a causative or consequential correlate of posterior activation. Furthermore, it motivated the exploration of cue-locked intervals where bottom-up and top-down processing may have elicited stronger effects on α-band synchronisation.

Finally, to ensure participants correctly lateralised their attention during the cue-target interval, we carried out a reality check by

calculating the α-power imbalance using the lateralisation index during this period (Thut et al. 2006). There was a clear difference in the averaged lateralisation index during the time course between 500 and 1500 ms at group-level. We further employed this metric (i.e., lateralisation index) to perform an exploratory analysis of its relationship with the difference in synchronization between contra- and ipsilateral networks. Considering lateralised local alpha activity and lateralised long-range alpha-synchronization are both relevant in successful attention orienting, we hypothesised that these two mechanisms would have a significant positive correlation. Therefore, individuals with high lateralisation index values should also present lateralised synchronization within the FPN. In contrast to our expectations, there was no significant correlation between these two metrics, neither at the pre-target nor the post-target time windows.

Ultimately, we did not observe a significant increase in contralateral long-range α-synchronization in the five 200 ms bins following cue onset. This time frame offered potential as it occurs much before target appearance and could be robustly employed in a covert visuospatial BCI decoder. By expanding our analysis to several frequencies and carrying out the aforementioned reality checks, we conclude that PLV measured from EEG may not serve as a reliable metric in capturing direction-specific synchronisation from frontal to posterior regions, despite this evidence being present in parietal to occipital synchrony (Doesburg et al. 2009).

EEG estimates of long-range α-synchronization may not serve as a reliable control signal for BCI

The use of long-range α-synchronization to decode attentional direction yielded chance level results. We employed 200 ms time bins of contralateral and ipsilateral FPN connectivity as input in an SVM classifier. Non-linear SVMs are widely employed in decoding cognitive neural correlates of behavioural states. Furthermore, they outperform other classifiers such as artificial neural networks, non-linear Bayesian estimators, and recurrent reservoir networks (Astrand et al. 2014a). Prior work using SVMs, mainly centred around primate models and invasive recordings, successfully decoded the attentional spotlight from frontal sites (Gaillard et al. 2020; Tremblay et al. 2015; Esghaei and Daliri 2014). Although these modalities (i.e., LFP, intracranial-EEG) have a high signal-to-noise ratio (SNR), the objective of the present study is to perform a BCI proof of concept and, thus, a more

practical and suitable imaging method must be employed. This same principle can be utilized to discard other modalities such as fMRI, where the temporal resolution is too low for real-time implementations, or MEG, where the equipment is expensive and requires a magnetically shielded room limiting its potential transfer out-of-lab applications. Contrarily, EEG is an affordable imaging modality with a straightforward setup which provides high temporal resolution and portability. However, the inconvenience of using EEG is low spatial resolution and low SNR. Despite this, decoders have been commonly employed in BCI design, parieto-occipital changes in α-band activity to predict covert visuospatial attention tasks (Tonin et al. 2013; Treder et al. 2011). However, the integrated approach between frontal and parieto-occipital attentional decoding has not been attempted. Here, we found that cue-locked synchronisation enclosed in the FPN α-band is insufficient to determine the attentional location. This may be due to an inherent lack of connectivity in the cue-target interval or more likely the inability of EEG to register synchronization patterns due to the limitations mentioned above.

Another potential cause why cue-locked FPN connectivity was not sufficient for classifying single trials may be due to the change in PLV calculation from average to single-trial. Standard cognitive research employs multiple trials to estimate consistent findings on electrophysiological markers (M/EEG). BCIs, need by design to perform estimates robustly and accurately in a single-trial fashion and thus require a trade-off between spatial (i.e., single-channel decoding is preferred) and temporal resolution. PLV is a measure of consistency across multiple trials and cannot serve as a single-trial control signal. Therefore, we computed PLV across time points within the same realisation. This new measure is also referred to in the literature as the inter-site phase clustering (ISPC) and may represent a different underlying process than that captured by classic PLV (Cohen 2015). This prompts the question of whether long-range α-synchronization is incapable of decoding the attended location, or rather the single-trial nature of IPSC over time is responsible for this.

In sum, long-range α-synchronization within the FPN estimated with EEG may not serve as a control signal for BCI. This limitation may be due to incomplete information on neural correlates due to the lack of cross-frequency analysis or the computational techniques surrounding ISPC over time.

Conclusions

We found direction-specific contralateral patterns of upper α-synchronization (i.e., PLV) within the FPN following target appearance in a covert visuospatial task. This finding, however, did not extend to pre-target or cue-locked time windows. The modulatory role of α-synchronization in anticipatory attention through frontal, parietal and occipital regions suggests that PLV may not constitute a reliable metric for this top-down visual processing. Furthermore, chance-level classification resulting from using this metric in an SVM indicates that long-range α-synchronization may not be a suitable control signal for BCI.

CHAPTER 5

General Discussion

"The ability to perceive or think differently is more important than the knowledge gained."

DAVID BOHM

The main goals of the present dissertation were threefold: (i) to develop a custom-build EEG-based BCI system allowing for brain-state dependent stimulation (BSDS), (ii) to provide evidence of the role of α-oscillations in visual perception and spatial attention, and (iii) to provide proof-of-concept of BCI applications linking α-oscillations to behavioural responses adopting insights from brain-behavioural theories in order to modulate behavioural performance.

The general hypothesis was that if the fluctuations in the ongoing brain activity shape perception and subsequent behaviour, then, by identifying specific brain states beneficial or detrimental for processing (depending on the features of oscillations: phase, power, frequency), it should be possible to alter behavioural performance by presenting stimuli timed to those states. Although many previous studies have already addressed this question, the innovative approach here was to understand better the brain-behaviour relationship under the scope of an EEG-based BCI for brain-state dependent stimulation (BSDS).

The two first studies presented in this dissertation (**Chapters 2 & 3**) provided evidence of the role of α-phase and bursts in α-power, respectively, in visual detection. Both studies were performed in real-time using our custom-build EEG-based BCI for BSDS. The third study (**Chapter 4**) aimed at providing proof of concept for a potential control signal for a BCI using α-phase long-range synchronisation between frontoparietal areas to estimate the direction of the user's attention in a visuospatial attention task.

In this chapter, I will summarise the findings of this thesis and discuss the implications of the results concerning the relevant literature published in parallel to our studies. Finally, I will discuss the limitations and possible avenues for future research.

Summary of the results

Study 1: Occipital α-phase was not predictive of the speed of visual detection

The first study of the present dissertation (**Chapter 2**) was a modern replication of Callaway and Yeager's (1960) study. Participants (n=8) performed a visual speeded detection task on stimuli triggered in real-time at different latencies of a participant's α-cycle using an EEG-based BCI system. First, RTs were sampled to visual targets triggered at ten phase bins along the estimated pre-stimulus α-cycle (Stage 1) in the ongoing EEG. Based on this, we selected two phase bins associated with the slowest and fastest RTs. Second, RTs to visual targets were presented only at these pre-selected bins (Stage 2). In the case of a phase-RT link existence grounded by the α-theories, stimuli presented at the slow phase would have slower RTs than stimuli triggered at the fast phase. However, contrary to what we expected, our results did not return a consistent relation between the phase of ongoing α-oscillations and RTs neither at the group level nor at the individual level. In addition, we explored alternative methods of analysing our data to find a potential phase-behaviour relationship. First, we re-did the analysis in Stage 2 by selecting only those trials falling strictly in the slow- and fast-phase bins. Second, we adopted an approach used by Fiebelkorn et al. (2013) to test statistically for an oscillatory pattern in Stage 1 data and check for the existence of a phase-dependent modulation of RTs. Third, we checked for a phase opposition pattern when comparing slow/fast RT trials at stimulus onset. None of these exploratory analyses revealed any significant phase-behaviour link.

Study 2: The (non-)occurrence of α-bursts can be used to modulate behaviour in a go/no-go task

Our second study (**Chapter 3**) used a go/no-go visual detection task in which target presentation was determined in real-time contingent upon the occurrence or absence of α-bursts in the ongoing occipital EEG signal. We estimated (no-)burst activity in real-time by adapting the eBOSC method (Kosciessa et al. 2020) through a custom-built

BCI setting and captured the subsequent reaction time to visual targets. Confirming the hypothesis that a consistent relationship between burst activity and RT exists, stimuli presented during α-burst events led to slower RTs than those presented during the absence of α-bursts. This trend held for ten out of 12 participants, and five showed a statistically-significant difference. The average RT difference (19 ms) was overwhelmingly significant at the group level. In addition, we compared the differences in error rates in go trials (omission errors) and no-go trials (commission errors) for burst and no-burst trials. In general, omission errors in go trials were more prevalent during a burst episode, and commission errors in no-go trials were more prevalent during a no-burst episode.

Study 3: α-phase synchrony between frontoparietal areas cannot be used to estimate the direction of spatial attention

In our third and last study (**Chapter 4**) of this dissertation, we aimed to extend the current concept of BCI systems, which use real-time brain activity as a local phenomenon, to BCI systems that use long-rage connectivity between brain regions. This idea is based on the proposed communication-through-coherence (CTC) hypothesis (Fries 2005, 2015). With this aim in mind, we investigated the relationship between shifts in visuospatial attention and the lateralisation of long-range α-coupling to assess its feasibility as a control signal in BCI applications. We used existing EEG data previously collected from a cohort of participants (N = 10) while performing a covert visuospatial attention (CVSA) task. We found lateralised patterns of phase coupling in the α-band between frontoparietal regions after target presentation, replicating Sauseng et al.'s (2005) previous findings. This pattern, however, did not transfer to the cue-target interval, the ideal time window for BCI in which participants covertly lateralised their attention according to cue presentation. Furthermore, using cue-locked synchronisation measures as input for a support vector machine (SVM) decoder returned chance-level classification. The present findings suggest that long-range α-synchronization measured from EEG may not sufficiently reflect the direction-specific top-down attentional processing on a trial-by-trial basis and, thus, may not constitute a reliable signal for BCI control.

Evidence of the role of α-oscillations and their link to visual perception and spatial attention

The elusive relationship between α-phase and behaviour in visual detection

Our first study (**Chapter 2**) revealed no evidence that presenting visual stimuli to the phase of spontaneous α-oscillations bore any influence on subsequent reaction times. This link was also absent in offline exploratory data analyses at the group and the individual level. In our second study (**Chapter 3**), albeit it was mainly designed to measure bursts in alpha power, we also explored the potential relationship between the phase during α-bursts at stimulus onset. Consistent with the first study, we did not find a phase-behaviour relationship at the group or the individual level. However, because the second study was not optimised to address phase effects, it may have lacked statistical power (we only had N = 48 trials in each condition to assess the putative role of the α-phase and RTs in our go/no-go task).

According to Mathewson et al. (2011), moments of high α-power should be the ideal scenario for the emergence of the phase-behaviour relationship. This is based on the evidence that α-phase over posterior regions predicted the detection of the visual target and performance only when α-power was high (Mathewson et al. 2011). It is worth noting that the level of α-power was high when measuring phase effects on behaviour in both of our studies. The first study (**Chapter 2**) introduced measures, such as eyes closed, to achieve that α-power was consistently high to facilitate the phase estimation in real-time for stimulus presentation. In contrast, in the second study (**Chapter 3**), our protocol required variability in oscillatory α-activity (low and high α-power trials), and we chose to use only high-power trials for the exploratory tests of phase/behaviour correlation. Therefore, it would appear that using high power should enhance the perceptual fluctuations due to the oscillatory α-phase. However, we did not see it in any of the studies presented in this dissertation.

Overall, our findings join a growing body of studies casting doubt on the effect of α-phase prior to stimulus arrival in visual perception (Walsh 1952; O'Hare 1954; van Diepen et al. 2019; Benwell et al. 2017; Benwell et al. 2019; Ruzzoli et al. 2019; Michail et al. 2021). Although many other studies have found a positive phase/behaviour relationship (Lansing 1957; Lansing et al. 1959; Callaway and Yeager 1960; Nunn and Osselton 1974; van Dijk et al. 2008; Busch et al. 2009;

Mathewson et al. 2009; Busch and VanRullen 2010; Dugué et al. 2011; Hanslmayr et al. 2013; Milton and Pleydell-Pearce 2016; Ronconi and Melcher 2017; Samaha et al. 2015; Zazio et al. 2021), the evidence appears mixed for the pre-stimulus phase-behaviour link and thus, the role of α-oscillations in visual perception. Given the wide range of degrees of freedom in experimental choices and analytical pipelines, it would seem logical to think that some of these factors may be crucial for explaining the mixed results (Ruzzoli et al. 2019), and perhaps essential for the design of effective BCI control based on alpha-phase.

One aspect worth paying attention to is our choice of using a visual speeded detection task, thus adopting RTs instead of accuracy to designate behaviour performance. Even if the brain-behaviour α-theories have related α -phase to both RTs (Walsh 1952; Lansing et al. 1959; Callaway and Yeager 1960) and accuracy (van Dijk et al. 2008; Busch et al. 2009; Mathewson et al. 2009), no explicit claims have been made about possible differences between the two measures regarding their perceptual sensitivity to ongoing oscillations. Bringing back the points suggested in the discussion of **Chapter 2**, if fluctuations of α-oscillations gate sensory information into perception, then (i) both measures (RTs and accuracy) should be relevant, and (ii) RTs may be suited to measure moment-to-moment variations in excitability compared to detection responses. Another aspect of interest that merits mention in this discussion is that our study used a supra-threshold stimulus at fixed luminance levels across participants. Although this is often the standard approach in RT experiments, it is worth noting that some studies that found a positive phase-behaviour link used near-threshold stimuli (Mathewson et al. 2009; Busch et al. 2009; van Dijk et al. 2008). Thus, it may be possible that the stimulus produces a strong neural response that subtle phase-dependent variations in responses were saturated, and its impact on behaviour was negligible.

Finally, as suggested in the discussion of the first study (**Chapter 2**), a relationship between phase and visual detectability (and hence, response latencies) may exist, and perhaps it was obscured by the signal-to-noise variability when recoding from scalp electrodes in EEG. Based on this, we conclude that the results from our studies are not conclusive as to disproof an effect and challenge the α-theories meaningfully. However, we believe that they may pose a more serious limit to the usage of the posterior alpha phase for BCI control.

Oscillatory α-bursts influence behaviour in visual perception

In our first study (**Chapter 2**), we also explored a potential power/behaviour relationship and failed to see it. This might be surprising at first sight because the previous literature is relatively consistent on the significant relationship between ongoing α-power and behaviour. However, please note that the study was not optimised to reveal this precise relationship, given the consistent high α-power induced by the eyes closed situation. Our second study (**Chapter 3**), which was designed to estimate power variations in mind, provided evidence of an existing link between oscillatory α-power at stimulus onset and subsequent responses to that stimulus. Visual stimuli presented during the occurrence of α-burst events (i.e., brief moments of high-oscillatory α-power) led to slower RTs compared to those presented during the absence of α-bursts (i.e., low-oscillatory α-power). Our findings align with the inhibition hypothesis of α-activity (Klimesch et al. 2007; Jensen and Mazaheri 2010; Foxe and Snyder 2011), suggesting that the state of α-power in posterior regions predicts visual cortical excitability and the likelihood of perceiving the stimulus input. In particular, high α-power leads to an inhibitory state of visual processing that lowers the likelihood of stimulus perception, whereas an excitatory state produced by low α-power increases such likelihood. In line with this, several studies have suggested that fluctuations in pre-stimulus oscillatory α-power may contribute to trial-to-trial behavioural variability (Makeig and Jung 1996; Linkenkaer-Hansen et al. 2004; Ergenoglu et al. 2004; Hanslmayr et al. 2007; Lakatos et al. 2008; Bollimunta et al. 2008; Bompas et al. 2015). Other studies have further confirmed the link between pre-stimulus α-power and detection performance (Busch et al. 2009; Chaumon and Busch 2014; Ergenoglu et al. 2004; Iemi and Busch 2018; Limbach and Corballis 2016; Ruzzoli et al. 2019; Iemi et al. 2022). It has been recently suggested that the α-power/performance link may be due to a more a question of the criterion in the response bias rather than an increased perceptual sensitivity (Limbach and Corballis 2016; Iemi et al. 2017). Regarding RTs, previous studies have reported a positive α-power link (Min and Herrmann 2007; Bollimunta et al. 2008; Kelly and O'Connell 2013; Bompas et al. 2015; Michail et al. 2021), though not always (Gonzalez Andino et al. 2005; Del Percio et al. 2007; Bollimunta et al. 2008; van Dijk et al. 2008; Bays et al. 2015). Recent findings by Iemi et al. (2022) have shown that the relationship between pre-stimulus α-activity, behaviour (RT), and excitability is mediated by modulation of post-stimulus excitability (broadband high-

frequency activity in 70-150 Hz). In line with the functional inhibition hypothesis (Klimesch et al. 2007), they proposed that, by modulating neuronal excitability, ongoing α-oscillations influence behaviour and the strength (but not the precision) of neural stimulus representations.

Furthermore, in the second study (**Chapter 3**), we compared the differences in **error rates** in go trials (omission errors) and no-go trials (commission errors or false alarms) for burst and no-burst trials. We found higher error rates for no-go trials than go trials, as one would expect in this go/no-go task with 80% go and 20% no-go trials. More importantly, omission errors in go trials were more prevalent during a burst episode than during no-burst events; instead, commission errors in no-go trials were more prevalent during the absence of a burst episode than during a burst. As pointed out in **Chapter 3**, we consider it is important to disentangle the interpretation of the go/no-go results due to the cognitive differences in the processes between answering (i.e., go trials) and inhibiting the response (i.e., no-go trials) to a given stimulus. Our results align with the notion that the α-power level reflects the sensory excitability and the level of inhibition for stimulus detection (Hanslmayr et al. 2007; Klimesch et al. 2007).

Comparable results beyond bursts in the α-band have been found in studies linking beta bursts (β, ~20Hz) with reaction time and movement onset, in which the presence of β-bursts delayed the response in humans and animals (Leventhal et al. 2012; Khanna and Carmena 2017; Little et al. 2019). Recent findings by Diesburg et al. (2021) in β-bursts using invasive human recordings found increases in subcortical β-bursts in successful stop trials, suggesting that bursts act as inhibitory signals for the motor system. Together, the response would vary depending on α-bursts and might help optimise performance in an excited state and protect against false positives in a relatively disengaged state. Thus, when pre-stimulus α-power is low (or during the absence of an α-burst episode), there is a greater propensity to answer, thus producing false alarming. In contrast, when pre-stimulus α-power is high (or during the occurrence of α-bursts events), there is an inhibition towards answering visual stimuli, thus, producing more misses in go trials. Despite our putative interpretations of our findings, it would be of great interest to further investigate the relationship between α-bursts and errors, considering the detection and inhibition of responses towards a stimulus.

The implication of oscillatory α-bursts in the α-theories

Although our findings from the second study (**Chapter 3**) align with a host of older findings (discussed above) relating to α-power and behaviour, we went beyond these past studies in two important ways. First, our study harnessed real-time stimulus-triggering and data analysis on a trial-by-trial basis (this aspect will be later discussed). Second, we focused on burst events rather than rhythmically sustained oscillations. Many approaches to estimating oscillatory dynamics of brain signals contain the underlying assumption that brain oscillations are sustained oscillatory states for convenience. However, it is clear from looking at traces of EEG that the signal is far from stationary (Vidaurre et al. 2011; Krauledat 2008), even in short time scales. Recent studies have provided evidence of burst events underlying cognitive and motor operations in different frequency bands (Feingold et al. 2015; Lundqvist et al. 2016; Lundqvist and Wutz 2021; Lundqvist et al. 2018; Lundqvist et al. 2022; Khanna and Carmena 2017; Sherman et al. 2016; Shin et al. 2017; Little et al. 2019; Wutz et al. 2020). These findings started a debate about the roles of sustained oscillatory dynamics versus the transient nature of burst events (see van Ede et al. 2018 for discussion), and new methods for oscillatory analyses have recently emerged (Zich et al. 2020; Lundqvist and Wutz 2021). As we mentioned in the Introduction, in many cases, the appearance of sustained oscillatory activity can come from averaging across many trials. Instead, it may be better captured by transient high-signal burst events that happen at different rates, times, and durations from trial to trial.

Moreover, typical approaches for quantifying oscillations do not check for the presence of a peak within the frequency range of interest of the power spectrum to ascertain clear, distinct oscillatory activity. These approaches can be confounded by the mixture of oscillatory and aperiodic activity in the power spectrum (1/f background noise; Haegens et al. 2014; Donoghue et al. 2020; Iemi et al. 2022). Some researchers have recently started applying methods to differentiate these two types of activity (Peterson et al. 2017; Peterson and Voytek 2017; Donoghue et al. 2020; Iemi et al. 2022) since this distinction is critical for understanding the underlying dynamics of brain oscillations. Our study adopted a recent version of the eBOSC algorithm (Kosciessa et al. 2020) to systematically detect the occurrence or absence of oscillatory α-bursts in single-trial EEG activity. Thus, our BCI algorithm truly assessed oscillatory activity in the form of burst events. It is unclear, though, whether and how our

findings relate to the oscillatory burst events found with micro- (e.g., single-cell measurements) and mesoscale (e.g., local field potential, LFP) neural mechanisms since their contribution to M/EEG oscillatory activity and their link with behaviour are not well-established (Musall et al. 2014; Cohen 2017b). Several interpretations of this account have been recently explored. For instance, van Ede et al. (2018) explored four conceptual interpretations of frequency-specific burst patterns in LFP or M/EEG measurements and proposed that the generator of bursts may or may not be rhythmic (van Ede et al. 2018).

Lastly, in the light of the previous discussion, it would be necessary for the current formulation of the α-theories explicitly incorporate bursts: whether and how transient events of rhythmic oscillatory activity in ongoing brain dynamics gate sensory information and shape perception on a trial-by-trial basis. It is worth noticing that the functional inhibition account (e.g., Klimesch et al. 2007) is specific to the **α-oscillatory activity** and, thus, does not distinguish between sustained oscillatory activity and burst events. On that note, Peterson and Voytek (2017) have recently proposed that α-oscillations control cortical gain by modulating the balance between excitatory and inhibitory background activity. In their model, they make the novel prediction that α-activity plays two functional roles: a robust, sustained oscillation mode (>5-10 cycles) that suppresses cortical gain and a weak, bursting mode (of 1-3 cycles) for rapid, temporally-precise gain increases. This model would align with Jensen and Mazaheri (2010) and Mazaheri and Jensen (2010).

Moreover, the recent **oscillation-based probability of response (OPR)** model by Zazio et al. (2020), based on the functional inhibition hypothesis (Jensen and Mazaheri 2010; Klimesch et al. 2007; Schalk 2015), proposes that the probability of responding to incoming stimuli in visual perception can be associated with ongoing α-oscillations and coupling mechanisms of alpha-gamma interaction. Since the OPR model does not assume stationarity, its predictions are based on the moment in time of the stimulation and can thus be extended to burst-like activity. Together, new models and theories are starting to consider different types of α-activity and their respective roles in cognitive processes, highlighting the notion that the cortex's status may better represent the effects of ongoing oscillations at the time of stimulation.

Long-range α-phase synchronisation characterises visuospatial attention but may not serve to estimate covert orienting

In our third study (**Chapter 4**), we found significant group-level differences in contra- vs ipsilateral long-range α-coupling around target presentation as a function of attention direction. This result replicated the findings reported by Sauseng et al. (2005) and further supports the notion that attention shifts are reflected in the synchronisation between frontal and visual α-oscillations contralateral to the attended hemifield (Sauseng et al. 2005; Doesburg et al. 2009). In general lines, they are consistent with the communication-through-coherence theory (Fries 2005, 2015). However, the main goal of that study was to address the feasibility of using long-range α-coupling patterns as a control signal for a BCI. We reasoned that if contra- to ipsilateral differences in α-coupling have been found at the target-locked time window in a growing body of studies (Sauseng et al. 2005; Doesburg et al. 2009; Jensen et al. 2015; Siegel et al. 2008; Sacchet et al. 2015), they may also be present when the lateralisation of attention unfolds, after cue presentation. However, the results did not reveal any α-coupling differences in the cue-to-target period, and neither did our exploratory analysis of other frequencies outside the α-band. Note that the fundamental idea of this study relied on the use of fluctuations induced by the endogenous shifts in attention (instead of the use of mere consequence of exogenous activity evoked by the target). Hence, we thought that the Posner paradigm was an adequate task to elicit a robust brain-behavioural effect in α-coherence, given its substantial behavioural effect that has been extensively reviewed and replicated (Petersen and Posner 2012; Carrasco 2018). Nonetheless, group-level significant increases in contralateral frontoparietal connectivity in post-target time windows show the involvement of the frontoparietal network in visuospatial attention. Despite the exact mechanisms through which this occurs remains poorly understood, contralateral dominant synchronisation allows for differentiating attended locations within the visual field.

Different electrophysiological α-features related to different cognitive functions

Almost after a century of discovering the existence of α-oscillations, their specific roles in cognitive processes are still a matter of debate (Pavlov et al. 2021). In particular, it has been suggested that α-oscillations reflect more than one role aspect in cognition (Sadaghiani and Kleinschmidt 2016), and some of these roles have been unified in

a recent opinion article by Clayton et al. (2018), assigning five roles to α-oscillations (inhibitor, perceiver, predictor, communicator, and stabiliser of information). One possible explanation of the mixture of roles is the variety of ways in which α-oscillations can vary independently (e.g., power, phase, long-range phase synchronisation). Specifically, different electrophysiological α-features may relate to various cognitive functions. For example, α-power in the visual cortex is negatively associated with visual attention (**Chapter 3**), whereas contra-lateral α-phase-coupling between frontoparietal areas is positively associated with visual attention (**Chapter 4**; van Diepen et al. 2019). On this note, Zazio et al. (2021) have recently stated that the brain-behavioural effects of pre-stimulus α-power and α-phase on visual perception might have different cortical generators and might reflect different mechanisms of perceptual modulation. As Clayton et al. (2018) outlined, further research in this area is clearly needed.

A gap between α-theory and practice: mixed methods and results for brain-behaviour effects

Despite the confidence placed on the α-theories by a good number of authors, there is a large mixture of findings on the role of α-features in visual perception and attention and their link to behaviour. Perhaps this inconsistency leads to differences in experimental factors and methodological approaches across studies (Benwell et al. 2017; Benwell et al. 2018; Ruzzoli et al. 2019; Zazio et al. 2021). For instance, at least a portion of the variability in the literature in detecting pre-stimulus α-phase effects could be due to the features used in the behavioural protocol, such as the stimulus eccentricity in the visual field, temporal expectation (Ruzzoli et al. 2019), or stimulus duration/intensity (Benwell et al. 2017; Benwell et al. 2018).

Moreover, the mixed evidence regarding the detection of pre-stimulus α-power effects might be due to whether power is estimated in relevant or irrelevant brain areas for a given task (due to attention modulation, for example), which behavioural outcome is emphasised (accuracy or speed), or on spurious temporal dependencies and correlations in both α-power and RT estimates (Schaworonkow et al. 2015). Another explanation for the mixed evidence in the literature might be due to differences in methodological approaches used for EEG analysis across studies. Recent evidence by Alam et al. (2020) found that the parameter choices in the spectral analysis (e.g., time-frequency transformation, filtering) of EEG data and the time window

of interest can strongly affect the results in various ways, for example, by influencing phase estimation.

These findings raise the need for a consistent EEG processing pipeline to assess brain-behavioural links. Standardising analyses (when possible) could help find a reliable link between pre-stimulus α-oscillations and subsequent behaviour if it were to exist and help produce reproducible research. Finally, another possibility of the mixed positive and negative findings in the literature might be an overestimation of effect sizes of the α-features in visual perception and attention (Ruzzoli et al. 2019). For instance, the perceptual variability explained by pre-stimulus α-phase would be around 10-20% (VanRullen 2016b), whereas a modulation in hit rate and response variability explained by α-power would be ~12% (Busch et al. 2009; Bompas et al. 2015). These differences make it challenging to infer the precise variability explained by oscillatory α-features in visual perception and attention. One potential solution for this discrepancy might be to create multi-lab initiatives to replicate and reproduce the same experimental tasks, methodological approaches, and analysis pipelines across different research labs. One example of this is the ongoing project of #EEGManyLabs (Pavlov et al. 2021). Another potential solution might be to stop generalising the role of brain oscillations in distinct cognitive processes in broad terms based on unified studies with mixed procedures, analysis, and effects despite studying the same "cognitive process". Alternatively, we should unpack those studies by looking at the commonalities and differences across studies providing evidence (or lack thereof) about brain oscillations in a given cognitive process, using a given task with specific procedures, methods, and analyses. Those differences used in the studies can rely on the number of participants and trials, feature target of oscillations (e.g., power, phase, phase synchrony), task type (e.g., detection, discrimination), the stimulus eccentricity in the visual field (e.g., centred, lateralised), stimuli intensity (e.g., near-threshold, supra-threshold), differences across the data analysis pipeline in terms of preprocessing, filtering and time-frequency analysis, or behavioural outcome (e.g., reaction time, accuracy, subjective confidence of performance), among others. One example of this second approach is the public table (an online version of the table can be found here: https://osf.io/tyfwu/) provided by Ruzzoli et al. (2019), including the main parameters used in existing literature regarding phase-behavioural correlation in human visual studies. In this way, we can compare across studies and find the features of the behavioural

paradigm, methodological approaches and parameters of the analysis pipeline used, leading to positive evidence.

EEG-based BCI as a test bench for brain-behavioural theories

Optimal target of brain states using an EEG-based BCI system

The first two studies of this dissertation (**Chapters 2 & 3**) illustrated how BCI systems could be used for brain-state dependent stimulation targeting different features of oscillations to gain new insight into the functional role of ongoing brain activity and its link to behaviour. We built an EEG-based BCI system for BSDS, achieving one of the main aims of this dissertation. A critical methodological aspect of the brain-behaviour relation using a BCI system is the optimal target of brain states (i.e., features of oscillations). In our first study (**Chapter 2**), the BCI system targeted specific phase latencies along the α-cycle and achieved an overall accuracy of phase estimation within less than 5° error. This performance compares well with estimation accuracy in other modern phase-based BCIs (Madsen et al. 2019; Zrenner et al. 2018). Given the method used to estimate the phase (i.e., extending a sinus using the IFoI from a reference point in the EEG signal), the phase estimation accuracy varied along with the latencies of the α-cycle, achieving an increase in variability of 32° between the last and the first latencies. Thus, the longer the time gap between the reference point and the latency of interest, the more variability the estimation performance. In addition, 88% of the trials, on average, felt within the phase of interest (phase ±1 bin), which is not a poor phase estimation for a BCI setting given our EEG system resolution. Moreover, in our second study (**Chapter 3**) targeting (no-)bursts, nearly 50% of trials were discarded for not satisfying the conservative power criterion when detecting (non-)oscillatory signals in the ongoing EEG due to the variability of α-activity in each individual.

Outlook of EEG-based BCI systems for hypothesis-driven BSDS as research tools in cognitive neuroscience

Almost a decade ago, Jensen et al. (2011) stated that BCI-BSDS was likely to become a more frequently used tool in cognitive neuroscience given the growing interest in brain states for cognition. As mentioned in the Introduction, a very limiting number of studies have specifically employed BSDS to study sensory perception focused on real-time

stimulus triggering on the features of ongoing α-oscillations and correlated feature-specific stimulus presentation with participant's performance (e.g., Callaway and Yeager 1960; Dustman and Beck 1965). Note that this dissertation's research approach and literature focus were narrowed to sensory BSDS based on monitoring real-time EEG activity and stimulus triggered based on the feature of brain oscillations. However, beyond this scope, a few other studies have used a similar approach using non-invasive neuroimaging techniques for electrical and magnetic stimulation (e.g., tACS, TMS; see Bergmann 2018 for a review). For instance, some researchers have provided evidence of a brain-behavioural link using EEG-TMS between α-phase, neural excitability, and visual perception (Dugué et al. 2011), while others have recently used closed-loop BCI systems for EEG-TMS stimulation as a potential therapeutical tool in motor areas (Zrenner et al. 2016; Zrenner et al. 2018). The critical aspect of neuromodulation of brain oscillations (either sensory, electrical, or magnetic) relies on providing a more direct link between brain activity and behaviour, potentially on a single-trial basis. The capacity to decode brain states in real-time from an individual with the possibility of altering behaviour (given the ground on brain-behaviour theories) opens unprecedented opportunities in both BCI and cognitive neuroscience fields (see Horschig et al. 2014). The possibility of moving away from trial-averaged and group-level analysis toward single-trial and individual analysis opens the door to real-time BCI systems in different research labs worldwide and makes the quest to have EEG-based BCIs applied in real life more feasible than ever (Vansteensel et al. 2017).

First-pass proofs-of-concept for EEG-based BCI applications

Advances in the cognitive neuroscience field should go beyond research labs and have an impact in the real word, and BCI applications seem a robust candidate for this transition. That is why the final aim of this dissertation was to seek potential proof-of-concept of EEG-based BCI applications while adopting insights from a hypothesis-driven brain-behavioural relationship. The prospects that we had at the beginning of this PhD were to find a solid brain-behavioural link that could provide a proof of concept for using oscillatory features as a real-time control signal in a BCI. Based on the evidence, a potential BCI application could be used to predict, alter, or modulate behaviour (and augment human cognition) while engaging in visual perception or spatial attention tasks. For instance, we did not

find a phase-RT link in our first study (**Chapter 2**). However, we performed an effect size equivalence test based on 33% of the effects in Callaway and Yeager (1960) and estimated a minimum RT difference of almost 3 ms between slow and fast phases. We did not consider this difference meaningful in most applied contexts from a practical perspective toward a BCI application. However, the results in our second study (**Chapter 3**) could be further considered. We achieved an averaged RT difference of 19 ms between burst and no-burst conditions. In a similar line, Bompas et al. (2015) reported that pre-stimulus α-amplitude of MEG oscillations accounted for a variance in RT to the same extent as any robust behaviour effect introducing a latency difference of 15-20 ms. However, as highlighted in the study discussed in **Chapter 3**, the potential relevance relies on the time that the BCI application could save on some occasions, which is variable from trial to trial. For example, our most favourable participant could save as much as 250 ms on roughly 10% of the trials. These results could be interpreted as the first pass of a proof-of-concept that could be a starting point for prospective BCI applications. Lastly, our third study (**Chapter 4**) was the first attempt at synchrony-based BCI that, albeit unsuccessful, should help break new ground to map endogenous attention shifts to real-time control of brain-computer actuated systems via synchrony estimation. Further research could use new analysis and classification methods to provide such a proof of concept. Together, the studies presented in this dissertation account for the idea that developing proofs-of-concept under hypothesis-driven frameworks can lead to upcoming research lines involving BCI systems.

General assumptions and limitations

Reverse engineering and one-to-one mapping of the brain-behaviour relationship

This dissertation has used an EEG-based BCI system that capitalises on the ongoing brain oscillations to modulate behaviour. We have assumed a one-to-one mapping of a relationship between features of the pre-stimulus α-oscillations and subsequent responses (on a trial-by-trial basis). As pointed out in the Introduction, offline studies studying a potential brain-behaviour relationship usually sort trials post-hoc based on the behavioural outcome (e.g., RTs), average responses, and statistically compare (e.g., t-test) across fast and slow RTs to conclude a brain-behavioural relationship. Here, the approach

was quite the inverse, and we assumed that the brain-behaviour link from previous research evidence was valid and supported by the α-theories. In the same way, like many other previous studies (e.g., Walsh 1952; Lansing 1957; Callaway and Yeager 1960; Dustman and Beck 1965), we searched for specific features in the brain oscillations (phase angles in **Chapter 2**, and the occurrence/absence of oscillatory burst events in **Chapter 3**) systematically to induce the fastest or slowest RTs. Note that the post-hoc approach is challenging to determine whether α-oscillations are central to visual perception and attention engagement or if they are just typical by-products of unrelated neural processes. Thus, our reverse-engineering approach in real-time can address this issue using BSDS research since it is possible to target different features of α-oscillations (Thut et al. 2011; Helfrich et al. 2014).

Accounting for the actual waveform shape of brain oscillations

In this dissertation, we have assumed that brain oscillations can be fully characterised in a sinusoidal way to simplify the spectral analysis methods. However, there is evidence to support the view that brain oscillations are, for the most part, quasi sinusoidal (Bullock et al. 2003). Furthermore, α-oscillations may also be asymmetric or biased (Jensen and Mazaheri 2010; Hyafil et al. 2015; Schalk 2015), meaning an asymmetric distribution of peak and trough amplitudes and α-amplitudes are not zero-mean. Thus, limiting oscillations as perfect and symmetric sinusoids may partially constrain the rich information (Cole and Voytek 2017; Cole and Voytek 2019). Several recent studies have started to analyse brain oscillations according to their actual waveform shape (e.g., Cole and Voytek 2017; Jensen and Mazaheri 2010; Jones 2016; Gips et al. 2017). Indeed, future studies could use standard analysis techniques (e.g., sine waves in wavelet analysis) as a first step to then apply more physiologically inspired analysis based on the actual waveform shape of oscillations (Cohen 2017b). Further, the shape of an oscillation could be treated as another relevant feature of oscillations as its phase, frequency, and power (Mazaheri et al. 2018).

The unavoidable time gap for real-time computational analysis

A significant limitation of real-time BCI-BSDS studies is that there is always an unavoidable time gap between the last updated data fragment read-out from the sensors and the subsequent stimulus presentation contingent upon a particular brain state estimated from those data. The length of this time gap mainly depends on the

computational time of the BCI algorithm to analyse the data through the analysis pipeline to find a particular brain state (i.e., target feature of oscillations) in which to trigger stimuli. For instance, in our first and second studies (**Chapters 2 & 3**), the BCI system had a minimum computational time gap of 20 and 70 ms, respectively. This difference between studies reflects the variation in target features and the complexity of the analysis performed in each study. For instance, in Study 1 (**Chapter 2**), the analysis relied on estimating the phase (a very target feature since it targets an instant in time) using the Hilbert transform after filtering the signal. Whereas in Study 2 (**Chapter 3**), the BCI system iterated through a more complex pipeline of data analysis in order to detect (non-)oscillatory EEG α-activity. Power, by definition, needs to be integrated in time and, thus, cannot be so well pinpointed in time compared to phase. Note that due to the intrinsic tendency of non-linearity and non-stationarities in the EEG activity (Buzsáki and Draguhn 2004; Arvaneh et al. 2013), the estimated feature of oscillations might differ from the actual one. A potential solution to attenuate this unavoidable computational time gap in the future may rely on robustifying the BCI pipeline against changes in EEG signals (Vidaurre et al. 2011; Krauledat 2008) and writing cost-efficient code when building the analysis pipeline of the BCI system for BSDS. Another potential practice that can help is to check the feature-target accuracy on a trial-by-trial basis after stimulus presentation, such as done here (**Chapters 2 & 3**). Note that the very last part of the EEG signal will always have to be anticipated in real-time studies, and checking for the trials' validity can help achieve a total number of trials equal across individuals.

High rate of participants' exclusion because of α-activity

Our first two studies (**Chapters 2 & 3**) relied on an a priori selection of experimental participants as similarly done in previous real-time studies capitalising on α-oscillations (e.g., Callaway and Yeager 1960). We pre-screened participants from a five-minute recording with eyes closed at the beginning of each experimental session and included only participants showing a clear peak in the 5-15 Hz range at posterior electrodes at rest (individual frequency of interest, IFoI). This screening was done because an oscillation in the α-band should be present to facilitate the analysis of the real-time BCI system and establish the role of α-oscillations in subsequent perception. One of the major concerns in both studies was the high exclusion rate of participants. In our first study (**Chapter 2**), we discarded 19 out of 27

(70%) participants: six for not satisfying the required α-peak criterion in the screening stage and 13 because of the time duration criterion experiment. In our second study (**Chapter 3**), 31 out of 43 (72%) participants were excluded: almost half for the required α-peak criterion and a half for the duration criterion.

Nonetheless, comparing our exclusion rates with previous studies shows that Callaway and Yeager (1960) rejected almost two-thirds of their participants for similar reasons. Lansing (1957) did the most restrictive pre-screening rejecting 92 out of 100 participants. One reason why it is possible only to measure an α-activity with EEG in some individuals may be partially due to anatomical differences, such as source depth and orientation, skull thickness, scalp tissues, and geometry of the variation in skull and scalp thickness (Cuffin 1993; Hagemann et al. 2008). A second reason may comprise individual variations in the properties of volume conduction between the brain cortex and the scalp surface (Myslobodsky et al. 1989; Myslobodsky et al. 1991; Hagemann et al. 2008). Thus, participants showing a reduced measure of EEG amplitudes may have a higher electrical resistance because of the layers' conductivity and thickness (Cuffin 1993; Nunez and Srinivasan 2006). Lastly, selecting only individuals with measurable strong α-activity from EEG may raise potential concerns that discovered effects in research doing pre-screening might not generalise to a broader experimental population.

Future work

In the future, experiments employing real-time BSDS could benefit from using conjunctions of predictive ongoing brain activity for triggering target stimuli, similarly as approached in this dissertation. The ideas presented below point toward using real-time studies to understand better the trial-to-trial dynamics of brain oscillations and their link to behaviour. Note that before attempting any of the following suggested studies in real-time, further research should be done to collect more evidence of such brain-behavioural links at the group, individual and trial-level.

Real-time BSDS study relating frontal α-phase with subsequent performance in visual perception

The α-phase effects on behaviour in visual perception have mainly been attributed to occipito-parietal areas (Varela et al. 1981;

Mathewson et al. 2009; Hanslmayr et al. 2013; Myers et al. 2014; Sherman et al. 2016; Milton and Pleydell-Pearce 2016; Harris et al. 2018; Benwell et al. 2017). However, there is also evidence of such an effect in frontal areas (Busch et al. 2009; Dugué et al. 2011; Hanslmayr et al. 2013; Milton and Pleydell-Pearce 2016; VanRullen 2016b; VanRullen et al. 2011). Although the idea that the frontal α-phase may also play a role in visual perception was mainly based on EEG topographies (e.g., Busch et al. 2009; Zoefel and VanRullen 2017), recent findings by Zazio et al. (2021) have provided support to this hypothesis. Thus, one potential real-time study could be an adaption of our first (**Chapter 2**), in which visual presentation of stimuli is based on the α-phase of a frontal electrode for the subsequent link to behaviour. Positive findings would help corroborate the view of pulsed inhibition employed by α-band oscillations (Jensen and Mazaheri 2010; Mathewson et al. 2011).

Real-time BSDS study relating the subjective confidence and objective performance to α-power in visual perception

The view that low α-power improves performance in visual perception (e.g., Ergenoglu et al. 2004) has been recently challenged. It has recently been suggested that pre-stimulus α-power is linked to **subjective measures** (i.e., response bias; how likely the observer is to report a stimulus) rather than objective measures of task performance (i.e., perceptual sensitivity; the ability to detect/discriminate a stimulus). The foundations behind this idea rely on the notion that if the amount of α-power reflects enhancement levels in cortical excitability, then low α-power should lead to a more liberal decision criterion but not to a better sensitivity of the upcoming visual stimulus (Iemi et al. 2017). Recent evidence has supported this view (Iemi et al. 2017; Iemi and Busch 2018; Lange et al. 2013; Chaumon and Busch 2014; Limbach and Corballis 2016; Benwell et al. 2018; Samaha et al. 2020). To this end, a real-time follow-up study could directly manipulate attention or detectability of the visual stimulus and measure participants' subjective confidence and objective performance to test how differences in pre-stimulus α-activity affect visual perception and subsequent task performance.

Real-time BCI study relating β-bursts in sensorimotor areas to increase visual perception

Several studies have supported the notion that transient, high-power event bursts in the beta-band (β, 13–30 Hz) in sensorimotor areas

influence behaviour (Jones et al. 2007; Jones et al. 2010; Shin et al. 2017). In particular, spontaneous β-bursts have been attributed to play an inhibitory role (Jones et al. 2010; Engel and Fries 2010; Haegens et al. 2011; Linkenkaer-Hansen et al. 2004), making them potential predictors of perceptual success and shifts in attention (e.g., Jones et al. 2010). Little et al. (2019) related β-power and behaviour trial-by-trial in a recent MEG study and found that β-activity emerged as brief high-power transient bursts. Interestingly, if a single β-burst event occurred within 200 ms before target presentation, the stimulus was less likely to be perceived. These findings have direct implications for BSDS studies to modulate behaviour causally. As a follow-up, the EEG-based BCI system used in our second study (**Chapter 3**) could be adapted for BSDS contingent upon the occurrence or absence of β-bursts in sensorimotor areas. Based on the theory and the collection of evidence, we should expect to find that stimuli presented during oscillatory β-power impair perception, whereas during the absence of β-bursts may benefit perception.

Real-time BCI study relating the coupling of γ-power and α-phase in visual perception

Existing evidence (Osipova et al. 2008; Voytek et al. 2010; Bahramisharif et al. 2013; Fiebelkorn and Kastner 2019; van Es et al. 2020), current theories (Mazaheri and Jensen 2010; Bonnefond et al. 2017), and models (Zazio et al. 2020) have related the coupling between gamma-power (γ, 30-100 Hz) and α-phase to visual perception. This notion assumes that the α-amplitude is asymmetric (Mazaheri and Jensen 2010) and that bursts of γ-power are integrated (or nested) within the α-phase (Spaak et al. 2012). To this end, a direct functional link between α-phase and γ-power could be empirically determined using a BSDS study. By detecting low/high α-power (associated with lower/higher number of nested γ-bursts, respectively) and triggering stimuli, one could provide evidence of such a brain-behavioural effect in visual perception. Positive findings on the perceptual modulation using the α-phase/γ-power coupling would ground the rhythmic pulsing hypothesis (Mazaheri and Jensen 2010) and the oscillation-based probability of response model (Zazio et al. 2020).

CHAPTER 6

Conclusions

"Nothing in life is to be feared; it is only to be understood.
Now is the time to understand more so that we may fear less".

MARIE CURIE

The results of this dissertation extend our knowledge about the role of brain α-oscillations in visual perception and spatial attention and its link to behaviour (aim two in this thesis). Also, hopefully, they will help open new avenues, or understand old ones, to harness that knowledge to build efficient BCIs. Previous studies have provided evidence of the brain-behaviour link primarily from offline studies doing group-averaged analyses. In this dissertation, we went one step further and explored the brain-behavioural relationship from another perspective, capitalising on trial-by-trial fluctuations of individuals. We created an EEG-based BCI system from scratch (aim one in this thesis), allowing for brain-state dependent stimulation.

Firstly, we demonstrated that we could target different features (e.g., phase, power, bursts) of α-oscillations in real-time, achieving a high target accuracy with our custom-built EEG-based BCI system. Our findings revealed that triggering stimuli contingent upon α-bursts episodes of high-oscillatory α-power (and not upon α-phase) leads to lower performance (i.e., slower RTs, higher omission errors). These findings ground the inhibitory role of ongoing α-oscillations in shaping visual processing (Klimesch et al. 2007; Jensen and Mazaheri 2010) by modulation of neuronal excitability (Haegens et al. 2011; Haegens et al. 2015; Iemi et al. 2022).

Moreover, we also corroborated the existence of direction-specific contralateral patterns of α-coupling between frontal and visual areas after target appearance in a covert visuospatial task. However, the α-

coupling pattern was not present at the beginning of the attention lateralisation (after cue appearance), which led to a chance-level classification when attempting to determine the locus of attention in space based on the α-coupling pattern. With our study's paradigm, methods, and dataset, long-range α-coupling may not be a suitable control signal for a BCI for determining attention location.

Taken together, the work behind this dissertation exemplifies how EEG-based BCI-BSDS can be used as research tools for hypothesis-testing in visual perception to provide new insight into the role of the oscillatory brain activity. For instance, garnering evidence following a hypothesis-driven approach can help better understand the relation between brain oscillations and behavioural outcomes. However, in our case, we could not seek proof-of-concept cases of EEG-based BCI applications in real-time adopting insights from a hypothesis-driven framework (aim three in this thesis).

Lastly, the EEG-based BCI-BSDS approach has the potential to become a more frequently used tool in cognitive neuroscience since it allows for the following advantageous aspects:

- Targeting distinct features (e.g., power, phase, bursts, shape) of brain oscillations for feature-triggered stimulus presentation.
- Allowing for hypothesis testing for brain-behavioural effects to ground the theories of brain oscillations and their link to behaviour.
- Setting methods and analysis pipeline a priori can be easily preregistered before collecting any data.
- Complementing group-averaged analysis with single-trial analysis at the individual level.
- Exploring the feasibility of developing online EEG-based BCI applications in neurotechnology for modulating behaviour, thus augmenting human performance.

BIBLIOGRAPHY

Abiri, Reza; Borhani, Soheil; Sellers, Eric W.; Jiang, Yang; Zhao, Xiaopeng (2019): A comprehensive review of EEG-based brain-computer interface paradigms. In *Journal of neural engineering* 16 (1), p. 11001. DOI: 10.1088/1741-2552/aaf12e.

Adrian, E. D.; Matthews, B. H. (1934): The interpretation of potential waves in the cortex. In *The Journal of physiology* 81 (4), pp. 440–471. DOI: 10.1113/jphysiol.1934.sp003147.

Alam, Raquib-Ul; Zhao, Haifeng; Goodwin, Andrew; Kavehei, Omid; McEwan, Alistair (2020): Differences in Power Spectral Densities and Phase Quantities Due to Processing of EEG Signals. In *Sensors (Basel, Switzerland)* 20 (21). DOI: 10.3390/s20216285.

Andermann, M. L.; Kauramäki, J.; Palomäki, T.; Moore, C. I.; Hari, R.; Jääskeläinen, I. P.; Sams, M. (2012): Brain state-triggered stimulus delivery: An efficient tool for probing ongoing brain activity. In *Open journal of neuroscience* 2.

Antonov, Plamen A.; Chakravarthi, Ramakrishna; Andersen, Søren K. (2020): Too little, too late, and in the wrong place: Alpha band activity does not reflect an active mechanism of selective attention. In *NeuroImage* 219, p. 117006. DOI: 10.1016/j.neuroimage.2020.117006.

Aricò, P.; Borghini, G.; Di Flumeri, G.; Sciaraffa, N.; Babiloni, F. (2018): Passive BCI beyond the lab: current trends and future directions. In *Physiological measurement* 39 (8), 08TR02. DOI: 10.1088/1361-6579/aad57e.

Arieli, A.; Sterkin, A.; Grinvald, A.; Aertsen, A. (1996): Dynamics of ongoing activity: explanation of the large variability in evoked cortical responses. In *Science (New York, N.Y.)* 273 (5283), pp. 1868–1871. DOI: 10.1126/science.273.5283.1868.

Arvaneh, Mahnaz; Guan, Cuntai; Ang, Kai Keng; Quek, Chai (2013): EEG data space adaptation to reduce intersession nonstationarity in brain-computer interface. In *Neural computation* 25 (8), pp. 2146–2171. DOI: 10.1162/neco_a_00474.

Asplund, Christopher L.; Todd, J. Jay; Snyder, Andy P.; Marois, René (2010): A central role for the lateral prefrontal cortex in goal-directed

and stimulus-driven attention. In *Nature neuroscience* 13 (4), pp. 507–512. DOI: 10.1038/nn.2509.

Astrand, Elaine; Enel, Pierre; Ibos, Guilhem; Dominey, Peter Ford; Baraduc, Pierre; Ben Hamed, Suliann (2014a): Comparison of classifiers for decoding sensory and cognitive information from prefrontal neuronal populations. In *PloS one* 9 (1), e86314. DOI: 10.1371/journal.pone.0086314.

Astrand, Elaine; Wardak, Claire; Ben Hamed, Suliann (2014b): Selective visual attention to drive cognitive brain-machine interfaces: from concepts to neurofeedback and rehabilitation applications. In *Frontiers in systems neuroscience* 8, p. 144. DOI: 10.3389/fnsys.2014.00144.

Babiloni, Claudio; Vecchio, Fabrizio; Bultrini, Alessandro; Luca Romani, Gian; Rossini, Paolo Maria (2006): Pre- and poststimulus alpha rhythms are related to conscious visual perception: a high-resolution EEG study. In *Cerebral cortex (New York, N.Y. : 1991)* 16 (12), pp. 1690–1700. DOI: 10.1093/cercor/bhj104.

Bahramali, H.; Gordon, E.; Li, W. M.; Rennie, C.; Wright, J. (1998): Fast and slow reaction time changes reflected in ERP brain function. In *The International journal of neuroscience* 93 (1-2), pp. 75–85. DOI: 10.3109/00207459808986414.

Bahramisharif, A. (2012): Covert visual spatial attention. A robust paradigm for brain-computer interfacing. [S.l.: s.n.].

Bahramisharif, Ali; van Gerven, Marcel A. J.; Aarnoutse, Erik J.; Mercier, Manuel R.; Schwartz, Theodore H.; Foxe, John J. et al. (2013): Propagating neocortical gamma bursts are coordinated by traveling alpha waves. In *J. Neurosci.* 33 (48), pp. 18849–18854. DOI: 10.1523/JNEUROSCI.2455-13.2013.

Baldauf, Daniel; Desimone, Robert (2014): Neural mechanisms of object-based attention. In *Science (New York, N.Y.)* 344 (6182), pp. 424–427. DOI: 10.1126/science.1247003.

Bartley, S. Howard; Bishop, Geo. H. (1932): THE CORTICAL RESPONSE TO STIMULATION OF THE OPTIC NERVE IN THE RABBIT. In *American Journal of Physiology-Legacy Content* 103 (1), pp. 159–172. DOI: 10.1152/ajplegacy.1932.103.1.159.

Başar, E.; Rahn, E.; Demiralp, T.; Schürmann, M. (1998): Spontaneous EEG theta activity controls frontal visual evoked potential amplitudes.

In *Electroencephalography and Clinical Neurophysiology* 108 (2), pp. 101–109. DOI: 10.1016/s0168-5597(97)00039-7.

Bays, Brett C.; Visscher, Kristina M.; Le Dantec, Christophe C.; Seitz, Aaron R. (2015): Alpha-band EEG activity in perceptual learning. In *Journal of vision* 15 (10), p. 7. DOI: 10.1167/15.10.7.

Bechtel, William; Abrahamsen, Adele (2010): Dynamic mechanistic explanation: computational modeling of circadian rhythms as an exemplar for cognitive science. In *Studies in history and philosophy of science* 41 (3), pp. 321–333. DOI: 10.1016/j.shpsa.2010.07.003.

Belyusar, Daniel; Snyder, Adam C.; Frey, Hans-Peter; Harwood, Mark R.; Wallman, Josh; Foxe, John J. (2013): Oscillatory alpha-band suppression mechanisms during the rapid attentional shifts required to perform an anti-saccade task. In *NeuroImage* 65, pp. 395–407. DOI: 10.1016/j.neuroimage.2012.09.061.

Benjamini, Yoav; Hochberg, Yosef (1995): Controlling the False Discovery Rate: A Practical and Powerful Approach to Multiple Testing. In *Journal of the Royal Statistical Society: Series B (Methodological)* 57 (1), pp. 289–300. DOI: 10.1111/j.2517-6161.1995.tb02031.x.

Benwell, Christopher S. Y.; Coldea, Andra; Harvey, Monika; Thut, Gregor (2021): Low pre-stimulus EEG alpha power amplifies visual awareness but not visual sensitivity. In *The European journal of neuroscience*. DOI: 10.1111/ejn.15166.

Benwell, Christopher S. Y.; Keitel, Christian; Harvey, Monika; Gross, Joachim; Thut, Gregor (2018): Trial-by-trial co-variation of pre-stimulus EEG alpha power and visuospatial bias reflects a mixture of stochastic and deterministic effects. In *The European journal of neuroscience* 48 (7), pp. 2566–2584. DOI: 10.1111/ejn.13688.

Benwell, Christopher S. Y.; London, Raquel E.; Tagliabue, Chiara F.; Veniero, Domenica; Gross, Joachim; Keitel, Christian; Thut, Gregor (2019): Frequency and power of human alpha oscillations drift systematically with time-on-task. In *NeuroImage* 192, pp. 101–114. DOI: 10.1016/j.neuroimage.2019.02.067.

Benwell, Christopher S. Y.; Tagliabue, Chiara F.; Veniero, Domenica; Cecere, Roberto; Savazzi, Silvia; Thut, Gregor (2017): Prestimulus EEG Power Predicts Conscious Awareness But Not Objective Visual Performance. In *eNeuro* 4 (6). DOI: 10.1523/eneuro.0182-17.2017.

Berens, Philipp (2009): CircStat : A MATLAB Toolbox for Circular Statistics. In *J. Stat. Soft.* 31 (10). DOI: 10.18637/jss.v031.i10.

Berger, Hans (1929): Über das Elektrenkephalogramm des Menschen. In *Archiv f. Psychiatrie* 87 (1), pp. 527–570. DOI: 10.1007/BF01797193.

Bergmann, Til O. (2018): Brain State-Dependent Brain Stimulation. In *Frontiers in psychology* 9, p. 2108. DOI: 10.3389/fpsyg.2018.02108.

Bishop, Geo. H. (1932): CYCLIC CHANGES IN EXCITABILITY OF THE OPTIC PATHWAY OF THE RABBIT. In *American Journal of Physiology-Legacy Content* 103 (1), pp. 213–224. DOI: 10.1152/ajplegacy.1932.103.1.213.

Blankertz, Benjamin; Acqualagna, Laura; Dähne, Sven; Haufe, Stefan; Schultze-Kraft, Matthias; Sturm, Irene et al. (2016): The Berlin Brain-Computer Interface: Progress Beyond Communication and Control. In *Frontiers in neuroscience* 10, p. 530. DOI: 10.3389/fnins.2016.00530.

Blankertz, Benjamin; Sannelli, Claudia; Halder, Sebastian; Hammer, Eva M.; Kübler, Andrea; Müller, Klaus-Robert et al. (2010): Neurophysiological predictor of SMR-based BCI performance. In *NeuroImage* 51 (4), pp. 1303–1309. DOI: 10.1016/j.neuroimage.2010.03.022.

Blume, Christine; Garbazza, Corrado; Spitschan, Manuel (2019): Effects of light on human circadian rhythms, sleep and mood. In *Somnologie : Schlafforschung und Schlafmedizin = Somnology : sleep research and sleep medicine* 23 (3), pp. 147–156. DOI: 10.1007/s11818-019-00215-x.

Bollimunta, Anil; Chen, Yonghong; Schroeder, Charles E.; Ding, Mingzhou (2008): Neuronal mechanisms of cortical alpha oscillations in awake-behaving macaques. In *J. Neurosci.* 28 (40), pp. 9976–9988. DOI: 10.1523/JNEUROSCI.2699-08.2008.

Bollimunta, Anil; Mo, Jue; Schroeder, Charles E.; Ding, Mingzhou (2011): Neuronal mechanisms and attentional modulation of corticothalamic α oscillations. In *The Journal of neuroscience : the official journal of the Society for Neuroscience* 31 (13), pp. 4935–4943. DOI: 10.1523/JNEUROSCI.5580-10.2011.

Bompas, Aline; Sumner, Petroc; Muthumumaraswamy, Suresh D.; Singh, Krish D.; Gilchrist, Iain D. (2015): The contribution of pre-stimulus neural oscillatory activity to spontaneous response time variability. In *NeuroImage* 107, pp. 34–45. DOI: 10.1016/j.neuroimage.2014.11.057.

Bonnefond, Mathilde; Jensen, Ole (2012): Alpha oscillations serve to protect working memory maintenance against anticipated distracters. In *Current biology : CB* 22 (20), pp. 1969–1974. DOI: 10.1016/j.cub.2012.08.029.

Bonnefond, Mathilde; Kastner, Sabine; Jensen, Ole (2017): Communication between Brain Areas Based on Nested Oscillations. In *eNeuro* 4 (2). DOI: 10.1523/ENEURO.0153-16.2017.

Borghini, Gianluca; Astolfi, Laura; Vecchiato, Giovanni; Mattia, Donatella; Babiloni, Fabio (2014): Measuring neurophysiological signals in aircraft pilots and car drivers for the assessment of mental workload, fatigue and drowsiness. In *Neuroscience and biobehavioral reviews* 44, pp. 58–75. DOI: 10.1016/j.neubiorev.2012.10.003.

Braeutigam, Sven; Lee, Nick; Senior, Carl (2019): A Role for Endogenous Brain States in Organizational Research: Moving Toward a Dynamic View of Cognitive Processes. In *Organizational Research Methods* 22 (1), pp. 332–353. DOI: 10.1177/1094428117692104.

Bram Zandbelt (2014): exgauss: a MATLAB toolbox for fitting the ex-Gaussian distribution to response time data: figshare.

Brandt, M. E.; Jansen, B. H.; Carbonari, J. P. (1991): Pre-stimulus spectral EEG patterns and the visual evoked response. In *Electroencephalography and Clinical Neurophysiology* 80 (1), pp. 16–20. DOI: 10.1016/0168-5597(91)90037-x.

Bressler, Steven L. (1996): Interareal synchronization in the visual cortex. In *Behavioural Brain Research* 76 (1-2), pp. 37–49. DOI: 10.1016/0166-4328(95)00187-5.

Brunner, Clemens; Birbaumer, Niels; Blankertz, Benjamin; Guger, Christoph; Kübler, Andrea; Mattia, Donatella et al. (2015): BNCI Horizon 2020: towards a roadmap for the BCI community. In *Brain-Computer Interfaces* 2 (1), pp. 1–10. DOI: 10.1080/2326263X.2015.1008956.

Bullock, T.H; Mcclune, M.C; Enright, J.T (2003): Are the electroencephalograms mainly rhythmic? Assessment of periodicity in wide-band time series. In *Neuroscience* 121 (1), pp. 233–252. DOI: 10.1016/S0306-4522(03)00208-2.

Busch, Niko A.; Dubois, Julien; VanRullen, Rufin (2009): The phase of ongoing EEG oscillations predicts visual perception. In *J. Neurosci.* 29 (24), pp. 7869–7876. DOI: 10.1523/JNEUROSCI.0113-09.2009.

Busch, Niko A.; VanRullen, Rufin (2010): Spontaneous EEG oscillations reveal periodic sampling of visual attention. In *Proceedings of the National Academy of Sciences of the United States of America* 107 (37), pp. 16048–16053. DOI: 10.1073/pnas.1004801107.

Buschman, Timothy J.; Miller, Earl K. (2009): Serial, covert shifts of attention during visual search are reflected by the frontal eye fields and correlated with population oscillations. In *Neuron* 63 (3), pp. 386–396. DOI: 10.1016/j.neuron.2009.06.020.

Buzsáki, György (2006): Rhythms of the Brain: Oxford University Press.

Buzsáki, György; Draguhn, Andreas (2004): Neuronal oscillations in cortical networks. In *Science (New York, N.Y.)* 304 (5679), pp. 1926–1929. DOI: 10.1126/science.1099745.

Buzsáki, György; Mizuseki, Kenji (2014): The log-dynamic brain: how skewed distributions affect network operations. In *Nature reviews. Neuroscience* 15 (4), pp. 264–278. DOI: 10.1038/nrn3687.

Callaway, Enoch (1961): DAY-TO-DAY VARIABILITY IN RELATIONSHIP BETWEEN ELECTROENCEPHALOGRAPHIC ALPHA PHASE AND REACTION TIME TO VISUAL STIMULI*. In *Annals of the New York Academy of Sciences* 92 (3), pp. 1183–1186. DOI: 10.1111/j.1749-6632.1961.tb40985.x.

Callaway, Enoch (1962): Factors influencing the relationship between alpha activity and visual reaction time. In *Electroencephalography and Clinical Neurophysiology* 14 (5), pp. 674–682. DOI: 10.1016/0013-4694(62)90082-2.

Callaway, Enoch; Alexander, J. D. (1960): The temporal coding of sensory data: an investigation of two theories. In *The Journal of general psychology* 62, pp. 293–309. DOI: 10.1080/00221309.1960.9920419.

Callaway, Enoch; Layne, Robert S. (1964): Interaction between the visual evoked response and two spontaneous biological rhythms: The EEG alpha cycle and the cardiac arousal cycle. In *Annals of the New York Academy of Sciences* 112, pp. 421–431. DOI: 10.1111/j.1749-6632.1964.tb26762.x.

Callaway, Enoch; Yeager, Charles L. (1960): Relationship between reaction time and electroencephalographic alpha phase. In *Science (New*

York, N.Y.) 132 (3441), pp. 1765–1766. DOI: 10.1126/science.132.3441.1765.

Campagne, Aurelie; Pebayle, Thierry; Muzet, Alain (2004): Correlation between driving errors and vigilance level: influence of the driver's age. In *Physiology & behavior* 80 (4), pp. 515–524. DOI: 10.1016/j.physbeh.2003.10.004.

Capotosto, Paolo; Babiloni, Claudio; Romani, Gian Luca; Corbetta, Maurizio (2009): Frontoparietal cortex controls spatial attention through modulation of anticipatory alpha rhythms. In *J. Neurosci.* 29 (18), pp. 5863–5872. DOI: 10.1523/jneurosci.0539-09.2009.

Carrasco, Marisa (2018): How visual spatial attention alters perception. In *Cognitive processing* 19 (Suppl 1), pp. 77–88. DOI: 10.1007/s10339-018-0883-4.

Cecere, Roberto; Rees, Geraint; Romei, Vincenzo (2015): Individual differences in alpha frequency drive crossmodal illusory perception. In *Current biology : CB* 25 (2), pp. 231–235. DOI: 10.1016/j.cub.2014.11.034.

Chaumon, Maximilien; Busch, Niko A. (2014): Prestimulus neural oscillations inhibit visual perception via modulation of response gain. In *Journal of cognitive neuroscience* 26 (11), pp. 2514–2529. DOI: 10.1162/jocn_a_00653.

Chavarriaga, Ricardo; Del Millan, José R. (2010): Learning from EEG error-related potentials in noninvasive brain-computer interfaces. In *IEEE transactions on neural systems and rehabilitation engineering : a publication of the IEEE Engineering in Medicine and Biology Society* 18 (4), pp. 381–388. DOI: 10.1109/TNSRE.2010.2053387.

Clayton, Michael S.; Yeung, Nick; Cohen Kadosh, Roi (2015): The roles of cortical oscillations in sustained attention. In *Trends in cognitive sciences* 19 (4), pp. 188–195. DOI: 10.1016/j.tics.2015.02.004.

Clayton, Michael S.; Yeung, Nick; Cohen Kadosh, Roi (2018): The many characters of visual alpha oscillations. In *The European journal of neuroscience* 48 (7), pp. 2498–2508. DOI: 10.1111/ejn.13747.

Cohen, M. X. (2014): Analyzing neural time series data: theory and practice. Cambridge, Massachusetts, USA: The MIT Press.

Cohen, Michael X. (2015): Effects of time lag and frequency matching on phase-based connectivity. In *Journal of neuroscience methods* 250, pp. 137–146. DOI: 10.1016/j.jneumeth.2014.09.005.

Cohen, Michael X. (2017a): Rigor and replication in time-frequency analyses of cognitive electrophysiology data. In *International journal of psychophysiology : official journal of the International Organization of Psychophysiology* 111, pp. 80–87. DOI: 10.1016/j.ijpsycho.2016.02.001.

Cohen, Michael X. (2017b): Where Does EEG Come From and What Does It Mean? In *Trends in neurosciences* 40 (4), pp. 208–218. DOI: 10.1016/j.tins.2017.02.004.

Cohen, Michael X.; Cavanagh, James F. (2011): Single-trial regression elucidates the role of prefrontal theta oscillations in response conflict. In *Frontiers in psychology* 2, p. 30. DOI: 10.3389/fpsyg.2011.00030.

Cole, Scott; Voytek, Bradley (2019): Cycle-by-cycle analysis of neural oscillations. In *Journal of neurophysiology* 122 (2), pp. 849–861. DOI: 10.1152/jn.00273.2019.

Cole, Scott R.; Voytek, Bradley (2017): Brain Oscillations and the Importance of Waveform Shape. In *Trends in cognitive sciences* 21 (2), pp. 137–149. DOI: 10.1016/j.tics.2016.12.008.

Corbetta, Maurizio; Shulman, Gordon L. (2002): Control of goal-directed and stimulus-driven attention in the brain. In *Nature reviews. Neuroscience* 3 (3), pp. 201–215. DOI: 10.1038/nrn755.

Corcoran, Andrew W.; Alday, Phillip M.; Schlesewsky, Matthias; Bornkessel-Schlesewsky, Ina (2018): Toward a reliable, automated method of individual alpha frequency (IAF) quantification. In *Psychophysiology* 55 (7), e13064. DOI: 10.1111/psyp.13064.

Cruzat, Josephine; Torralba, Mireia; Ruzzoli, Manuela; Fernández, Alba; Deco, Gustavo; Soto-Faraco, Salvador (2021): The phase of Theta oscillations modulates successful memory formation at encoding. In *Neuropsychologia* 154, p. 107775. DOI: 10.1016/j.neuropsychologia.2021.107775.

Cuffin, B. N. (1993): Effects of local variations in skull and scalp thickness on EEG's and MEG's. In *IEEE transactions on bio-medical engineering* 40 (1), pp. 42–48. DOI: 10.1109/10.204770.

Czeisler, C. A.; Duffy, J. F.; Shanahan, T. L.; Brown, E. N.; Mitchell, J. F.; Rimmer, D. W. et al. (1999): Stability, precision, and near-24-hour period of the human circadian pacemaker. In *Science (New York, N.Y.)* 284 (5423), pp. 2177–2181. DOI: 10.1126/science.284.5423.2177.

Damoiseaux, J. S.; Rombouts, S. A. R. B.; Barkhof, F.; Scheltens, P.; Stam, C. J.; Smith, S. M.; Beckmann, C. F. (2006): Consistent resting-

state networks across healthy subjects. In *Proceedings of the National Academy of Sciences of the United States of America* 103 (37), pp. 13848–13853. DOI: 10.1073/pnas.0601417103.

D'Andrea, Antea; Chella, Federico; Marshall, Tom R.; Pizzella, Vittorio; Romani, Gian Luca; Jensen, Ole; Marzetti, Laura (2019): Alpha and alpha-beta phase synchronization mediate the recruitment of the visuospatial attention network through the Superior Longitudinal Fasciculus. In *NeuroImage* 188, pp. 722–732. DOI: 10.1016/j.neuroimage.2018.12.056.

Del Percio, Claudio; Marzano, Nicola; Tilgher, Stefania; Fiore, Antonio; Di Ciolo, Enrico; Aschieri, Pierluigi et al. (2007): Pre-stimulus alpha rhythms are correlated with post-stimulus sensorimotor performance in athletes and non-athletes: a high-resolution EEG study. In *Clinical Neurophysiology* 118 (8), pp. 1711–1720. DOI: 10.1016/j.clinph.2007.04.029.

Delorme, Arnaud; Kothe, Christian; Vankov, Andrey; Bigdely-Shamlo, Nima; Oostenveld, Robert; Zander, Thorsten O.; Makeig, Scott (2010): MATLAB-Based Tools for BCI Research. In Desney S. Tan, Anton Nijholt (Eds.): Brain-Computer Interfaces. London: Springer London (Human-Computer Interaction Series), pp. 241–259.

Dias, N. S.; Mendes, P. M.; Correia, J. H. (2009): Feature Selection for Brain-Computer Interface. In R. Magjarevic, J. H. Nagel, Jos Vander Sloten, Pascal Verdonck, Marc Nyssen, Jens Haueisen (Eds.): 4th European Conference of the International Federation for Medical and Biological Engineering, vol. 22. Berlin, Heidelberg: Springer Berlin Heidelberg (IFMBE Proceedings), pp. 318–321.

Diesburg, Darcy A.; Greenlee, Jeremy Dw; Wessel, Jan R. (2021): Cortico-subcortical β burst dynamics underlying movement cancellation in humans. In *eLife* 10. DOI: 10.7554/eLife.70270.

Doesburg, Sam M.; Bedo, Nicolas; Ward, Lawrence M. (2016): Top-down alpha oscillatory network interactions during visuospatial attention orienting. In *NeuroImage* 132, pp. 512–519. DOI: 10.1016/j.neuroimage.2016.02.076.

Doesburg, Sam M.; Green, Jessica J.; McDonald, John J.; Ward, Lawrence M. (2009): From local inhibition to long-range integration: a functional dissociation of alpha-band synchronization across cortical scales in visuospatial attention. In *Brain research* 1303, pp. 97–110. DOI: 10.1016/j.brainres.2009.09.069.

Donoghue, Thomas; Haller, Matar; Peterson, Erik J.; Varma, Paroma; Sebastian, Priyadarshini; Gao, Richard et al. (2020): Parameterizing neural power spectra into periodic and aperiodic components. In *Nature neuroscience* 23 (12), pp. 1655–1665. DOI: 10.1038/s41593-020-00744-x.

Drewes, Jan; VanRullen, Rufin (2011): This is the rhythm of your eyes: the phase of ongoing electroencephalogram oscillations modulates saccadic reaction time. In *The Journal of neuroscience : the official journal of the Society for Neuroscience* 31 (12), pp. 4698–4708. DOI: 10.1523/JNEUROSCI.4795-10.2011.

Dugué, Laura; Marque, Philippe; VanRullen, Rufin (2011): The phase of ongoing oscillations mediates the causal relation between brain excitation and visual perception. In *The Journal of neuroscience : the official journal of the Society for Neuroscience* 31 (33), pp. 11889–11893. DOI: 10.1523/JNEUROSCI.1161-11.2011.

Dugué, Laura; McLelland, Douglas; Lajous, Mathilde; VanRullen, Rufin (2015): Attention searches nonuniformly in space and in time. In *Proceedings of the National Academy of Sciences of the United States of America* 112 (49), pp. 15214–15219. DOI: 10.1073/pnas.1511331112.

Dustman, Robert E.; Beck, Edward C. (1965): Phase of alpha brain waves, reaction time and visually evoked potentials. In *Electroencephalography and Clinical Neurophysiology* 18 (5), pp. 433–440. DOI: 10.1016/0013-4694(65)90123-9.

Eichele, Heike; Juvodden, Hilde T.; Ullsperger, Markus; Eichele, Tom (2010): Mal-adaptation of event-related EEG responses preceding performance errors. In *Frontiers in human neuroscience* 4. DOI: 10.3389/fnhum.2010.00065.

Ekstrom, Arne D.; Caplan, Jeremy B.; Ho, Emily; Shattuck, Kirk; Fried, Itzhak; Kahana, Michael J. (2005): Human hippocampal theta activity during virtual navigation. In *Hippocampus* 15 (7), pp. 881–889. DOI: 10.1002/hipo.20109.

ELLINGSON, R. J. (1956): Brain waves and problems of psychology. In *Psychological Bulletin* 53 (1), pp. 1–34. DOI: 10.1037/h0042562.

Engel, Andreas K.; Fries, Pascal (2010): Beta-band oscillations--signalling the status quo? In *Current opinion in neurobiology* 20 (2), pp. 156–165. DOI: 10.1016/j.conb.2010.02.015.

Enriquez-Geppert, Stefanie; Huster, René J.; Herrmann, Christoph S. (2017): EEG-Neurofeedback as a Tool to Modulate Cognition and Behavior: A Review Tutorial. In *Frontiers in human neuroscience* 11, p. 51. DOI: 10.3389/fnhum.2017.00051.

Ergenoglu, Tolgay; Demiralp, Tamer; Bayraktaroglu, Zubeyir; Ergen, Mehmet; Beydagi, Huseyin; Uresin, Yagiz (2004): Alpha rhythm of the EEG modulates visual detection performance in humans. In *Brain research. Cognitive brain research* 20 (3), pp. 376–383. DOI: 10.1016/j.cogbrainres.2004.03.009.

Ernst, Michael D. (2004): Permutation Methods: A Basis for Exact Inference. In *Statist. Sci.* 19 (4). DOI: 10.1214/088342304000000396.

Esghaei, Moein; Daliri, Mohammad Reza (2014): Decoding of visual attention from LFP signals of macaque MT. In *PloS one* 9 (6), e100381. DOI: 10.1371/journal.pone.0100381.

Esterman, Michael; Liu, Guanyu; Okabe, Hidefusa; Reagan, Andrew; Thai, Michelle; DeGutis, Joe (2015): Frontal eye field involvement in sustaining visual attention: evidence from transcranial magnetic stimulation. In *NeuroImage* 111, pp. 542–548. DOI: 10.1016/j.neuroimage.2015.01.044.

Feingold, Joseph; Gibson, Daniel J.; DePasquale, Brian; Graybiel, Ann M. (2015): Bursts of beta oscillation differentiate postperformance activity in the striatum and motor cortex of monkeys performing movement tasks. In *Proceedings of the National Academy of Sciences of the United States of America* 112 (44), pp. 13687–13692. DOI: 10.1073/pnas.1517629112.

Fellinger, R.; Klimesch, W.; Gruber, W.; Freunberger, R.; Doppelmayr, M. (2011): Pre-stimulus alpha phase-alignment predicts P1-amplitude. In *Brain research bulletin* 85 (6), pp. 417–423. DOI: 10.1016/j.brainresbull.2011.03.025.

Fiebelkorn, I. C.; Snyder, A. C.; Mercier, M. R.; Butler, J. S.; Molholm, S.; Foxe, J. J. (2013): Cortical cross-frequency coupling predicts perceptual outcomes. In *NeuroImage* 69, pp. 126–137. DOI: 10.1016/j.neuroimage.2012.11.021.

Fiebelkorn, Ian C.; Kastner, Sabine (2019): A Rhythmic Theory of Attention. In *Trends in cognitive sciences* 23 (2), pp. 87–101. DOI: 10.1016/j.tics.2018.11.009.

Fiebelkorn, Ian C.; Pinsk, Mark A.; Kastner, Sabine (2018): A Dynamic Interplay within the Frontoparietal Network Underlies Rhythmic Spatial Attention. In *Neuron* 99 (4), 842-853.e8. DOI: 10.1016/j.neuron.2018.07.038.

Fiebelkorn, Ian C.; Pinsk, Mark A.; Kastner, Sabine (2019): The mediodorsal pulvinar coordinates the macaque fronto-parietal network during rhythmic spatial attention. In *Nature communications* 10 (1), p. 215. DOI: 10.1038/s41467-018-08151-4.

Foster, Joshua J.; Awh, Edward (2019): The role of alpha oscillations in spatial attention: limited evidence for a suppression account. In *Current opinion in psychology* 29, pp. 34–40. DOI: 10.1016/j.copsyc.2018.11.001.

Foster, Joshua J.; Sutterer, David W.; Serences, John T.; Vogel, Edward K.; Awh, Edward (2017): Alpha-Band Oscillations Enable Spatially and Temporally Resolved Tracking of Covert Spatial Attention. In *Psychological science* 28 (7), pp. 929–941. DOI: 10.1177/0956797617699167.

Fox, Michael D.; Snyder, Abraham Z.; Zacks, Jeffrey M.; Raichle, Marcus E. (2006): Coherent spontaneous activity accounts for trial-to-trial variability in human evoked brain responses. In *Nature neuroscience* 9 (1), pp. 23–25. DOI: 10.1038/nn1616.

Foxe, John J.; Snyder, Adam C. (2011): The Role of Alpha-Band Brain Oscillations as a Sensory Suppression Mechanism during Selective Attention. In *Frontiers in psychology* 2, p. 154. DOI: 10.3389/fpsyg.2011.00154.

Freeman, Frederick G.; Mikulka, Peter J.; Scerbo, Mark W.; Scott, Lorissa (2004): An evaluation of an adaptive automation system using a cognitive vigilance task. In *Biological psychology* 67 (3), pp. 283–297. DOI: 10.1016/j.biopsycho.2004.01.002.

Freunberger, Roman; Fellinger, Robert; Sauseng, Paul; Gruber, Walter; Klimesch, Wolfgang (2009): Dissociation between phase-locked and nonphase-locked alpha oscillations in a working memory task. In *Hum. Brain Mapp.* 30 (10), pp. 3417–3425. DOI: 10.1002/hbm.20766.

Freunberger, Roman; Höller, Yvonne; Griesmayr, Birgit; Gruber, Walter; Sauseng, Paul; Klimesch, Wolfgang (2008): Functional similarities between the P1 component and alpha oscillations. In *The European journal of neuroscience* 27 (9), pp. 2330–2340. DOI: 10.1111/j.1460-9568.2008.06190.x.

Fries, Pascal (2005): A mechanism for cognitive dynamics: neuronal communication through neuronal coherence. In *Trends in cognitive sciences* 9 (10), pp. 474–480. DOI: 10.1016/j.tics.2005.08.011.

Fries, Pascal (2015): Rhythms for Cognition: Communication through Coherence. In *Neuron* 88 (1), pp. 220–235. DOI: 10.1016/j.neuron.2015.09.034.

Fries, Pascal; Womelsdorf, Thilo; Oostenveld, Robert; Desimone, Robert (2008): The effects of visual stimulation and selective visual attention on rhythmic neuronal synchronization in macaque area V4. In *J. Neurosci.* 28 (18), pp. 4823–4835. DOI: 10.1523/JNEUROSCI.4499-07.2008.

Friston, Karl (2002): Beyond phrenology: what can neuroimaging tell us about distributed circuitry? In *Annual review of neuroscience* 25, pp. 221–250. DOI: 10.1146/annurev.neuro.25.112701.142846.

Gaillard, Corentin; Ben Hadj Hassen, Sameh; Di Bello, Fabio; Bihan-Poudec, Yann; VanRullen, Rufin; Ben Hamed, Suliann (2020): Prefrontal attentional saccades explore space rhythmically. In *Nature communications* 11 (1), p. 925. DOI: 10.1038/s41467-020-14649-7.

Gallotto, Stefano; Sack, Alexander T.; Schuhmann, Teresa; Graaf, Tom A. de (2017): Oscillatory Correlates of Visual Consciousness. In *Frontiers in psychology* 8, p. 1147. DOI: 10.3389/fpsyg.2017.01147.

Gangadhar, Garipelli; Chavarriaga, Ricardo; Del Millan, Jose R. (2009): Anticipation based Brain-Computer Interfacing (aBCI). In : 2009 4th International IEEE/EMBS Conference on Neural Engineering. 2009 4th International IEEE/EMBS Conference on Neural Engineering (NER). Antalya, Turkey, 29/4/2009 - 2/5/2009: IEEE, pp. 459–462.

Gazzaniga, Michael; Ivry, Richard B.; Mangun, G. R. (2002): The cognitive neurosciences. 2nd ed. London: W.W. Norton & Co.

Gho, M.; Varela, F. J. (1988): A quantitative assessment of the dependency of the visual temporal frame upon the cortical rhythm. In *Journal de physiologie* 83 (2), pp. 95–101.

Gips, Bart; Bahramisharif, Ali; Lowet, Eric; Roberts, Mark J.; Weerd, Peter de; Jensen, Ole; van der Eerden, Jan (2017): Discovering recurring patterns in electrophysiological recordings. In *Journal of neuroscience methods* 275, pp. 66–79. DOI: 10.1016/j.jneumeth.2016.11.001.

Glass, L. (2001): Synchronization and rhythmic processes in physiology. In *Nature* 410 (6825), pp. 277–284. DOI: 10.1038/35065745.

Gonzalez Andino, Sara L.; Michel, Cristoph M.; Thut, Gregor; Landis, Theodor; Grave de Peralta, Rolando (2005): Prediction of response speed by anticipatory high-frequency (gamma band) oscillations in the human brain. In *Hum. Brain Mapp.* 24 (1), pp. 50–58. DOI: 10.1002/hbm.20056.

Gould, Ian C.; Rushworth, Matthew F.; Nobre, Anna C. (2011): Indexing the graded allocation of visuospatial attention using anticipatory alpha oscillations. In *Journal of neurophysiology* 105 (3), pp. 1318–1326. DOI: 10.1152/jn.00653.2010.

Goyal, Abhinav; Miller, Jonathan; Qasim, Salman E.; Watrous, Andrew J.; Zhang, Honghui; Stein, Joel M. et al. (2020): Functionally distinct high and low theta oscillations in the human hippocampus. In *Nature communications* 11 (1), p. 2469. DOI: 10.1038/s41467-020-15670-6.

Grandy, Thomas H.; Werkle-Bergner, Markus; Chicherio, Christian; Schmiedek, Florian; Lövdén, Martin; Lindenberger, Ulman (2013): Peak individual alpha frequency qualifies as a stable neurophysiological trait marker in healthy younger and older adults. In *Psychophysiology* 50 (6), pp. 570–582. DOI: 10.1111/psyp.12043.

Green, Jessica J.; McDonald, John J. (2008): Electrical Neuroimaging Reveals Timing of Attentional Control Activity in Human Brain. In *PLoS Biol* 6 (4), e81. DOI: 10.1371/journal.pbio.0060081.

Gregoriou, Georgia G.; Gotts, Stephen J.; Zhou, Huihui; Desimone, Robert (2009): High-frequency, long-range coupling between prefrontal and visual cortex during attention. In *Science (New York, N.Y.)* 324 (5931), pp. 1207–1210. DOI: 10.1126/science.1171402.

Grent-'t-Jong, Tineke; Woldorff, Marty G. (2007): Timing and sequence of brain activity in top-down control of visual-spatial attention. In *PLoS Biol* 5 (1), e12. DOI: 10.1371/journal.pbio.0050012.

Grossmann, A.; Morlet, J. (1984): Decomposition of Hardy Functions into Square Integrable Wavelets of Constant Shape. In *SIAM J. Math. Anal.* 15 (4), pp. 723–736. DOI: 10.1137/0515056.

Haegens, Saskia; Barczak, Annamaria; Musacchia, Gabriella; Lipton, Michael L.; Mehta, Ashesh D.; Lakatos, Peter; Schroeder, Charles E.

(2015): Laminar Profile and Physiology of the α Rhythm in Primary Visual, Auditory, and Somatosensory Regions of Neocortex. In *J. Neurosci.* 35 (42), pp. 14341–14352. DOI: 10.1523/JNEUROSCI.0600-15.2015.

Haegens, Saskia; Cousijn, Helena; Wallis, George; Harrison, Paul J.; Nobre, Anna C. (2014): Inter- and intra-individual variability in alpha peak frequency. In *NeuroImage* 92, pp. 46–55. DOI: 10.1016/j.neuroimage.2014.01.049.

Haegens, Saskia; Nácher, Verónica; Luna, Rogelio; Romo, Ranulfo; Jensen, Ole (2011): α-Oscillations in the monkey sensorimotor network influence discrimination performance by rhythmical inhibition of neuronal spiking. In *Proceedings of the National Academy of Sciences of the United States of America* 108 (48), pp. 19377–19382. DOI: 10.1073/pnas.1117190108.

Haegens, Saskia; Osipova, Daria; Oostenveld, Robert; Jensen, Ole (2010): Somatosensory working memory performance in humans depends on both engagement and disengagement of regions in a distributed network. In *Hum. Brain Mapp.* 31 (1), pp. 26–35. DOI: 10.1002/hbm.20842.

Hagemann, Dirk; Hewig, Johannes; Walter, Christof; Naumann, Ewald (2008): Skull thickness and magnitude of EEG alpha activity. In *Clinical Neurophysiology* 119 (6), pp. 1271–1280. DOI: 10.1016/j.clinph.2008.02.010.

Hanslmayr, Simon; Aslan, Alp; Staudigl, Tobias; Klimesch, Wolfgang; Herrmann, Christoph S.; Bäuml, Karl-Heinz (2007): Prestimulus oscillations predict visual perception performance between and within subjects. In *NeuroImage* 37 (4), pp. 1465–1473. DOI: 10.1016/j.neuroimage.2007.07.011.

Hanslmayr, Simon; Klimesch, Wolfgang; Sauseng, Paul; Gruber, Walter; Doppelmayr, Michael; Freunberger, Roman; Pecherstorfer, Thomas (2005a): Visual discrimination performance is related to decreased alpha amplitude but increased phase locking. In *Neuroscience letters* 375 (1), pp. 64–68. DOI: 10.1016/j.neulet.2004.10.092.

Hanslmayr, Simon; Sauseng, Paul; Doppelmayr, Michael; Schabus, Manuel; Klimesch, Wolfgang (2005b): Increasing individual upper alpha power by neurofeedback improves cognitive performance in human subjects. In *Applied psychophysiology and biofeedback* 30 (1), pp. 1–10. DOI: 10.1007/s10484-005-2169-8.

Hanslmayr, Simon; Volberg, Gregor; Wimber, Maria; Dalal, Sarang S.; Greenlee, Mark W. (2013): Prestimulus oscillatory phase at 7 Hz gates cortical information flow and visual perception. In *Current biology : CB* 23 (22), pp. 2273–2278. DOI: 10.1016/j.cub.2013.09.020.

Hari, R. (1997): Human cortical oscillations: a neuromagnetic view through the skull. In *Trends in neurosciences* 20 (1), pp. 44–49. DOI: 10.1016/S0166-2236(96)10065-5.

Harris, Anthony M.; Dux, Paul E.; Mattingley, Jason B. (2018): Detecting Unattended Stimuli Depends on the Phase of Prestimulus Neural Oscillations. In *The Journal of neuroscience : the official journal of the Society for Neuroscience* 38 (12), pp. 3092–3101. DOI: 10.1523/JNEUROSCI.3006-17.2018.

Hartmann, Thomas; Schulz, Hannah; Weisz, Nathan (2011): Probing of Brain States in Real-Time: Introducing the ConSole Environment. In *Frontiers in psychology* 2, p. 36. DOI: 10.3389/fpsyg.2011.00036.

Hassan, U.; Pillen, S.; Zrenner, C.; Bergmann, T. O. (2020): P170 BEST Toolbox: Brain Electrophysiological recording & STimulation Toolbox. In *Clinical Neurophysiology* 131 (4), e109-e110. DOI: 10.1016/j.clinph.2019.12.281.

He, Biyu J.; Zempel, John M.; Snyder, Abraham Z.; Raichle, Marcus E. (2010): The temporal structures and functional significance of scale-free brain activity. In *Neuron* 66 (3), pp. 353–369. DOI: 10.1016/j.neuron.2010.04.020.

Hebb, D. O. (1949): The Organisation of Behaviour. A neuropsychological theory. New York, NY: John Wiley & Sons.

Heilman, K. M.; van den Abell, T. (1980): Right hemisphere dominance for attention: the mechanism underlying hemispheric asymmetries of inattention (neglect). In *Neurology* 30 (3), pp. 327–330. DOI: 10.1212/wnl.30.3.327.

Helfrich, Randolph F.; Fiebelkorn, Ian C.; Szczepanski, Sara M.; Lin, Jack J.; Parvizi, Josef; Knight, Robert T.; Kastner, Sabine (2018): Neural Mechanisms of Sustained Attention Are Rhythmic. In *Neuron* 99 (4), 854-865.e5. DOI: 10.1016/j.neuron.2018.07.032.

Helfrich, Randolph F.; Schneider, Till R.; Rach, Stefan; Trautmann-Lengsfeld, Sina A.; Engel, Andreas K.; Herrmann, Christoph S. (2014): Entrainment of brain oscillations by transcranial alternating current

stimulation. In *Current biology : CB* 24 (3), pp. 333–339. DOI: 10.1016/j.cub.2013.12.041.

Hockley, William E. (1984): Analysis of response time distributions in the study of cognitive processes. In *Journal of Experimental Psychology: Learning, Memory, and Cognition* 10 (4), pp. 598–615. DOI: 10.1037/0278-7393.10.4.598.

Holland, Paul W.; Welsch, Roy E. (1977): Robust regression using iteratively reweighted least-squares. In *Communications in Statistics - Theory and Methods* 6 (9), pp. 813–827. DOI: 10.1080/03610927708827533.

Hopfinger, J. B.; Buonocore, M. H.; Mangun, G. R. (2000): The neural mechanisms of top-down attentional control. In *Nature neuroscience* 3 (3), pp. 284–291. DOI: 10.1038/72999.

Horne, James A.; Baulk, Stuart D. (2004): Awareness of sleepiness when driving. In *Psychophysiology* 41 (1), pp. 161–165. DOI: 10.1046/j.1469-8986.2003.00130.x.

Horschig, Jörn M.; Zumer, Johanna M.; Bahramisharif, Ali (2014): Hypothesis-driven methods to augment human cognition by optimizing cortical oscillations. In *Frontiers in systems neuroscience* 8, p. 119. DOI: 10.3389/fnsys.2014.00119.

Huang, Kuan-Chih; Chuang, Chun-Hsiang; Wang, Yu-Kai; Hsieh, Chi-Yuan; King, Jung-Tai; Lin, Chin-Teng (2019): The effects of different fatigue levels on brain-behavior relationships in driving. In *Brain and behavior* 9 (12), e01379. DOI: 10.1002/brb3.1379.

Huang, Zirui; Zhang, Jianfeng; Longtin, André; Dumont, Grégory; Duncan, Niall W.; Pokorny, Johanna et al. (2017): Is There a Nonadditive Interaction Between Spontaneous and Evoked Activity? Phase-Dependence and Its Relation to the Temporal Structure of Scale-Free Brain Activity. In *Cerebral cortex (New York, N.Y. : 1991)* 27 (2), pp. 1037–1059. DOI: 10.1093/cercor/bhv288.

Hughes, Stuart W.; Crunelli, Vincenzo (2005): Thalamic mechanisms of EEG alpha rhythms and their pathological implications. In *The Neuroscientist : a review journal bringing neurobiology, neurology and psychiatry* 11 (4), pp. 357–372. DOI: 10.1177/1073858405277450.

Hughes, Stuart W.; Lőrincz, Magor L.; Blethyn, Kate; Kékesi, Katalin A.; Juhász, Gábor; Turmaine, Mark et al. (2011): Thalamic Gap Junctions Control Local Neuronal Synchrony and Influence

Macroscopic Oscillation Amplitude during EEG Alpha Rhythms. In *Frontiers in psychology* 2, p. 193. DOI: 10.3389/fpsyg.2011.00193.

Hung, June; Driver, Jon; Walsh, Vincent (2011): Visual selection and the human frontal eye fields: effects of frontal transcranial magnetic stimulation on partial report analyzed by Bundesen's theory of visual attention. In *J. Neurosci.* 31 (44), pp. 15904–15913. DOI: 10.1523/jneurosci.2626-11.2011.

Hwang, Han-Jeong; Ferreria, Valeria Y.; Ulrich, Daniel; Kilic, Tayfun; Chatziliadis, Xenofon; Blankertz, Benjamin; Treder, Matthias (2015): A Gaze Independent Brain-Computer Interface Based on Visual Stimulation through Closed Eyelids. In *Scientific reports* 5, p. 15890. DOI: 10.1038/srep15890.

Hyafil, Alexandre; Giraud, Anne-Lise; Fontolan, Lorenzo; Gutkin, Boris (2015): Neural Cross-Frequency Coupling: Connecting Architectures, Mechanisms, and Functions. In *Trends in neurosciences* 38 (11), pp. 725–740. DOI: 10.1016/j.tins.2015.09.001.

Iemi, Luca; Busch, Niko A. (2018): Moment-to-Moment Fluctuations in Neuronal Excitability Bias Subjective Perception Rather than Strategic Decision-Making. In *eNeuro* 5 (3). DOI: 10.1523/ENEURO.0430-17.2018.

Iemi, Luca; Chaumon, Maximilien; Crouzet, Sébastien M.; Busch, Niko A. (2017): Spontaneous Neural Oscillations Bias Perception by Modulating Baseline Excitability. In *The Journal of neuroscience : the official journal of the Society for Neuroscience* 37 (4), pp. 807–819. DOI: 10.1523/JNEUROSCI.1432-16.2016.

Iemi, Luca; Gwilliams, Laura; Samaha, Jason; Auksztulewicz, Ryszard; Cycowicz, Yael M.; King, Jean-Remi et al. (2022): Ongoing neural oscillations influence behavior and sensory representations by suppressing neuronal excitability. In *NeuroImage* 247, p. 118746. DOI: 10.1016/j.neuroimage.2021.118746.

Jensen, Ole; Bahramisharif, Ali; Oostenveld, Robert; Klanke, Stefan; Hadjipapas, Avgis; Okazaki, Yuka O.; van Gerven, Marcel A. J. (2011): Using brain-computer interfaces and brain-state dependent stimulation as tools in cognitive neuroscience. In *Frontiers in psychology* 2, p. 100. DOI: 10.3389/fpsyg.2011.00100.

Jensen, Ole; Bonnefond, Mathilde; Marshall, Tom R.; Tiesinga, Paul (2015): Oscillatory mechanisms of feedforward and feedback visual

processing. In *Trends in neurosciences* 38 (4), pp. 192–194. DOI: 10.1016/j.tins.2015.02.006.

Jensen, Ole; Gips, Bart; Bergmann, Til Ole; Bonnefond, Mathilde (2014): Temporal coding organized by coupled alpha and gamma oscillations prioritize visual processing. In *Trends in neurosciences* 37 (7), pp. 357–369. DOI: 10.1016/j.tins.2014.04.001.

Jensen, Ole; Mazaheri, Ali (2010): Shaping functional architecture by oscillatory alpha activity: gating by inhibition. In *Frontiers in human neuroscience* 4, p. 186. DOI: 10.3389/fnhum.2010.00186.

Jones, Stephanie R. (2016): When brain rhythms aren't 'rhythmic': implication for their mechanisms and meaning. In *Current opinion in neurobiology* 40, pp. 72–80. DOI: 10.1016/j.conb.2016.06.010.

Jones, Stephanie R.; Kerr, Catherine E.; Wan, Qian; Pritchett, Dominique L.; Hämäläinen, Matti; Moore, Christopher I. (2010): Cued spatial attention drives functionally relevant modulation of the mu rhythm in primary somatosensory cortex. In *The Journal of neuroscience : the official journal of the Society for Neuroscience* 30 (41), pp. 13760–13765. DOI: 10.1523/JNEUROSCI.2969-10.2010.

Jones, Stephanie R.; Pritchett, Dominique L.; Stufflebeam, Steven M.; Hämäläinen, Matti; Moore, Christopher I. (2007): Neural correlates of tactile detection: a combined magnetoencephalography and biophysically based computational modeling study. In *The Journal of neuroscience : the official journal of the Society for Neuroscience* 27 (40), pp. 10751–10764. DOI: 10.1523/JNEUROSCI.0482-07.2007.

Jung, T. P.; Makeig, S.; Stensmo, M.; Sejnowski, T. J. (1997): Estimating alertness from the EEG power spectrum. In *IEEE transactions on bio-medical engineering* 44 (1), pp. 60–69. DOI: 10.1109/10.553713.

Kastner, S.; Ungerleider, L. G. (2000): Mechanisms of visual attention in the human cortex. In *Annual review of neuroscience* 23, pp. 315–341. DOI: 10.1146/annurev.neuro.23.1.315.

Kelly, S. P.; Lalor, E.; Reilly, R. B.; Foxe, J. J. (2005a): Independent Brain Computer Interface Control using Visual Spatial Attention-Dependent Modulations of Parieto-occipital Alpha. In : Conference Proceedings. 2nd International IEEE EMBS Conference on Neural Engineering, 2005. 2nd International IEEE EMBS Conference on Neural Engineering, 2005. Arlington, Virginia, USA, March 16-19, 2005: IEEE, pp. 667–670.

Kelly, Simon P.; Lalor, Edmund C.; Finucane, Ciarán; McDarby, Gary; Reilly, Richard B. (2005b): Visual spatial attention control in an independent brain-computer interface. In *IEEE transactions on biomedical engineering* 52 (9), pp. 1588–1596. DOI: 10.1109/TBME.2005.851510.

Kelly, Simon P.; Lalor, Edmund C.; Reilly, Richard B.; Foxe, John J. (2005c): Visual spatial attention tracking using high-density SSVEP data for independent brain-computer communication. In *IEEE transactions on neural systems and rehabilitation engineering : a publication of the IEEE Engineering in Medicine and Biology Society* 13 (2), pp. 172–178. DOI: 10.1109/TNSRE.2005.847369.

Kelly, Simon P.; Lalor, Edmund C.; Reilly, Richard B.; Foxe, John J. (2006): Increases in alpha oscillatory power reflect an active retinotopic mechanism for distracter suppression during sustained visuospatial attention. In *Journal of neurophysiology* 95 (6), pp. 3844–3851. DOI: 10.1152/jn.01234.2005.

Kelly, Simon P.; O'Connell, Redmond G. (2013): Internal and external influences on the rate of sensory evidence accumulation in the human brain. In *J. Neurosci.* 33 (50), pp. 19434–19441. DOI: 10.1523/JNEUROSCI.3355-13.2013.

Khanna, Preeya; Carmena, Jose M. (2017): Beta band oscillations in motor cortex reflect neural population signals that delay movement onset. In *eLife* 6. DOI: 10.7554/eLife.24573.

Kirschfeld, Kuno (2008): Relationship between the amplitude of alpha waves and reaction time. In *Neuroreport* 19 (9), pp. 907–910. DOI: 10.1097/WNR.0b013e328302c545.

Klimesch, W.; Doppelmayr, M.; Russegger, H.; Pachinger, T.; Schwaiger, J. (1998): Induced alpha band power changes in the human EEG and attention. In *Neuroscience letters* 244 (2), pp. 73–76. DOI: 10.1016/S0304-3940(98)00122-0.

Klimesch, Wolfgang (1999): EEG alpha and theta oscillations reflect cognitive and memory performance: a review and analysis. In *Brain research reviews* 29 (2-3), pp. 169–195. DOI: 10.1016/s0165-0173(98)00056-3.

Klimesch, Wolfgang (2012): α-band oscillations, attention, and controlled access to stored information. In *Trends in cognitive sciences* 16 (12), pp. 606–617. DOI: 10.1016/j.tics.2012.10.007.

Klimesch, Wolfgang; Sauseng, Paul; Hanslmayr, Simon (2007): EEG alpha oscillations: the inhibition-timing hypothesis. In *Brain research reviews* 53 (1), pp. 63–88. DOI: 10.1016/j.brainresrev.2006.06.003.

Koivisto, Mika; Revonsuo, Antti (2003): An ERP study of change detection, change blindness, and visual awareness. In *Psychophysiology* 40 (3), pp. 423–429. DOI: 10.1111/1469-8986.00044.

Koivisto, Mika; Revonsuo, Antti (2010): Event-related brain potential correlates of visual awareness. In *Neuroscience and biobehavioral reviews* 34 (6), pp. 922–934. DOI: 10.1016/j.neubiorev.2009.12.002.

Kosciessa, Julian Q.; Grandy, Thomas H.; Garrett, Douglas D.; Werkle-Bergner, Markus (2020): Single-trial characterization of neural rhythms: Potential and challenges. In *NeuroImage* 206, p. 116331. DOI: 10.1016/j.neuroimage.2019.116331.

Krauledat, Johannes Matthias (2008): Analysis of Nonstationarities in EEG Signals for Improving Brain-Computer Interface Performance. With assistance of Technische Universität Berlin, Klaus-Robert Müller.

Kuc, Alexander K.; Kurkin, Semen A.; Maksimenko, Vladimir A.; Pisarchik, Alexander N.; Hramov, Alexander E. (2021): Monitoring Brain State and Behavioral Performance during Repetitive Visual Stimulation. In *Applied Sciences* 11 (23), p. 11544. DOI: 10.3390/app112311544.

Lachaux, Jean-Philippe; Rodriguez, Eugenio; Martinerie, Jacques; Varela, Francisco J. (1999): Measuring phase synchrony in brain signals. In *Hum. Brain Mapp.* 8 (4), pp. 194–208. DOI: 10.1002/(sici)1097-0193(1999)8:4%3C194::aid-hbm4%3E3.0.co;2-c.

Lakatos, Peter; Karmos, George; Mehta, Ashesh D.; Ulbert, Istvan; Schroeder, Charles E. (2008): Entrainment of neuronal oscillations as a mechanism of attentional selection. In *Science (New York, N.Y.)* 320 (5872), pp. 110–113. DOI: 10.1126/science.1154735.

Lakatos, Peter; Shah, Ankoor S.; Knuth, Kevin H.; Ulbert, Istvan; Karmos, George; Schroeder, Charles E. (2005): An oscillatory hierarchy controlling neuronal excitability and stimulus processing in the auditory cortex. In *Journal of neurophysiology* 94 (3), pp. 1904–1911. DOI: 10.1152/jn.00263.2005.

Lakens, Daniël; Scheel, Anne M.; Isager, Peder M. (2018): Equivalence Testing for Psychological Research: A Tutorial. In *Advances in Methods*

and Practices in Psychological Science 1 (2), pp. 259–269. DOI: 10.1177/2515245918770963.

Lal, Saroj K. L.; Craig, Ashley (2002): Driver fatigue: electroencephalography and psychological assessment. In *Psychophysiology* 39 (3), pp. 313–321. DOI: 10.1017/s0048577201393095.

Landau, Ayelet Nina; Fries, Pascal (2012): Attention samples stimuli rhythmically. In *Current biology : CB* 22 (11), pp. 1000–1004. DOI: 10.1016/j.cub.2012.03.054.

Lange, Joachim; Oostenveld, Robert; Fries, Pascal (2013): Reduced occipital alpha power indexes enhanced excitability rather than improved visual perception. In *J. Neurosci.* 33 (7), pp. 3212–3220. DOI: 10.1523/jneurosci.3755-12.2013.

Lansing, Robert W. (1957): Relation of brain and tremor rhythms to visual reaction time. In *Electroencephalography and Clinical Neurophysiology* 9 (3), pp. 497–504. DOI: 10.1016/0013-4694(57)90037-8.

Lansing, Robert W.; Schwartz, Eric L.; Lindsley, Donald B. (1959): Reaction time and EEG activation under alerted and nonalerted conditions. In *Journal of experimental psychology* 58 (1), pp. 1–7. DOI: 10.1037/h0041016.

Leventhal, Daniel K.; Gage, Gregory J.; Schmidt, Robert; Pettibone, Jeffrey R.; Case, Alaina C.; Berke, Joshua D. (2012): Basal ganglia beta oscillations accompany cue utilization. In *Neuron* 73 (3), pp. 523–536. DOI: 10.1016/j.neuron.2011.11.032.

Lim, Jeong-Hwan; Hwang, Han-Jeong; Han, Chang-Hee; Jung, Ki-Young; Im, Chang-Hwan (2013): Classification of binary intentions for individuals with impaired oculomotor function: 'eyes-closed' SSVEP-based brain-computer interface (BCI). In *Journal of neural engineering* 10 (2), p. 26021. DOI: 10.1088/1741-2560/10/2/026021.

Limbach, Katharina; Corballis, Paul M. (2016): Prestimulus alpha power influences response criterion in a detection task. In *Psychophysiology* 53 (8), pp. 1154–1164. DOI: 10.1111/psyp.12666.

Lin, Chin-Teng; Huang, Kuan-Chih; Chuang, Chun-Hsiang; Ko, Li-Wei; Jung, Tzyy-Ping (2013): Can arousing feedback rectify lapses in driving? Prediction from EEG power spectra. In *Journal of neural engineering* 10 (5), p. 56024. DOI: 10.1088/1741-2560/10/5/056024.

Lindsley, Donald B. (1952): Psychological phenomena and the electroencephalogram. In *Electroencephalography and Clinical Neurophysiology* 4 (4), pp. 443–456. DOI: 10.1016/0013-4694(52)90075-8.

Linkenkaer-Hansen, Klaus; Nikouline, Vadim V.; Palva, J. Matias; Ilmoniemi, Risto J. (2001): Long-Range Temporal Correlations and Scaling Behavior in Human Brain Oscillations. In *J. Neurosci.* 21 (4), pp. 1370–1377. DOI: 10.1523/JNEUROSCI.21-04-01370.2001.

Linkenkaer-Hansen, Klaus; Nikulin, Vadim V.; Palva, Satu; Ilmoniemi, Risto J.; Palva, J. Matias (2004): Prestimulus oscillations enhance psychophysical performance in humans. In *The Journal of neuroscience : the official journal of the Society for Neuroscience* 24 (45), pp. 10186–10190. DOI: 10.1523/JNEUROSCI.2584-04.2004.

Little, Simon; Bonaiuto, James; Barnes, Gareth; Bestmann, Sven (2019): Human motor cortical beta bursts relate to movement planning and response errors. In *PLoS biology* 17 (10), e3000479. DOI: 10.1371/journal.pbio.3000479.

Lobier, Muriel; Palva, J. Matias; Palva, Satu (2018): High-alpha band synchronization across frontal, parietal and visual cortex mediates behavioral and neuronal effects of visuospatial attention. In *NeuroImage* 165, pp. 222–237. DOI: 10.1016/j.neuroimage.2017.10.044.

Lopes da Silva (1991): Neural mechanisms underlying brain waves: from neural membranes to networks. In *Electroencephalography and Clinical Neurophysiology* 79 (2), pp. 81–93. DOI: 10.1016/0013-4694(91)90044-5.

Lopes da Silva; van Lierop, T.H.M.T; Schrijer, C.F; van Storm Leeuwen, W. (1973): Organization of thalamic and cortical alpha rhythms: Spectra and coherences. In *Electroencephalography and Clinical Neurophysiology* 35 (6), pp. 627–639. DOI: 10.1016/0013-4694(73)90216-2.

Lopes da Silva; van Storm Leeuwen, W. (1977): The cortical source of the alpha rhythm. In *Neuroscience letters* 6 (2-3), pp. 237–241. DOI: 10.1016/0304-3940(77)90024-6.

Lopes da Silva; Vos, J.E; Mooibroek, J.; van Rotterdam, A. (1980): Relative contributions of intracortical and thalamo-cortical processes in the generation of alpha rhythms, revealed by partial coherence analysis. In *Electroencephalography and Clinical Neurophysiology* 50 (5-6), pp. 449–456. DOI: 10.1016/0013-4694(80)90011-5.

Lou, Hans C.; Joensson, Morten; Biermann-Ruben, Katja; Schnitzler, Alfons; Østergaard, Leif; Kjaer, Troels W.; Gross, Joachim (2011): Recurrent activity in higher order, modality non-specific brain regions: a Granger causality analysis of autobiographic memory retrieval. In *PloS one* 6 (7), e22286. DOI: 10.1371/journal.pone.0022286.

Lowet, E.; Roberts, M. J.; Bosman, C. A.; Fries, P.; Weerd, P. de (2016): Areas V1 and V2 show microsaccade-related 3-4-Hz covariation in gamma power and frequency. In *The European journal of neuroscience* 43 (10), pp. 1286–1296. DOI: 10.1111/ejn.13126.

Luce, R. Duncan (1986): Response Times. Their Role in Inferring Elementary Mental Organization: OUP USA.

Lundqvist, Mikael; Herman, Pawel; Warden, Melissa R.; Brincat, Scott L.; Miller, Earl K. (2018): Gamma and beta bursts during working memory readout suggest roles in its volitional control. In *Nature communications* 9 (1), p. 394. DOI: 10.1038/s41467-017-02791-8.

Lundqvist, Mikael; Rose, Jonas; Herman, Pawel; Brincat, Scott L.; Buschman, Timothy J.; Miller, Earl K. (2016): Gamma and Beta Bursts Underlie Working Memory. In *Neuron* 90 (1), pp. 152–164. DOI: 10.1016/j.neuron.2016.02.028.

Lundqvist, Mikael; Rose, Jonas; Warden, Melissa; Buschman, Tim; Herman, Pawel; Miller, Earl (2022): Reduced variability of bursting activity during working memory.

Lundqvist, Mikael; Wutz, Andreas (2021): New methods for oscillation analyses push new theories of discrete cognition. In *Psychophysiology*, e13827. DOI: 10.1111/psyp.13827.

Madsen, Kristoffer Hougaard; Karabanov, Anke Ninija; Krohne, Lærke Gebser; Safeldt, Mads Gylling; Tomasevic, Leo; Siebner, Hartwig Roman (2019): No trace of phase: Corticomotor excitability is not tuned by phase of pericentral mu-rhythm. In *Brain stimulation* 12 (5), pp. 1261–1270. DOI: 10.1016/j.brs.2019.05.005.

Makeig, Scott; Bell, Anthony J.; Jung, Tzyy-Ping; Sejnowski, Terrence J. (1995): Independent Component Analysis of Electroencephalographic Data. In : Proceedings of the 8th International Conference on Neural Information Processing Systems. Cambridge, MA, USA: MIT Press (NIPS'95), pp. 145–151.

Makeig, Scott; Inlow, Mark (1993): Lapse in alertness: coherence of fluctuations in performance and EEG spectrum. In

Electroencephalography and Clinical Neurophysiology 86 (1), pp. 23–35. DOI: 10.1016/0013-4694(93)90064-3.

Makeig, Scott; Jung, Tzyy-Ping (1995): Changes in alertness are a principal component of variance in the EEG spectrum. In *Neuroreport* 7 (1), pp. 213–216. DOI: 10.1097/00001756-199512000-00051.

Makeig, Scott; Jung, Tzyy-Ping (1996): Tonic, phasic, and transient EEG correlates of auditory awareness in drowsiness. In *Brain research. Cognitive brain research* 4 (1), pp. 15–25. DOI: 10.1016/0926-6410(95)00042-9.

Mansouri, Farrokh; Dunlop, Katharine; Giacobbe, Peter; Downar, Jonathan; Zariffa, José (2017): A Fast EEG Forecasting Algorithm for Phase-Locked Transcranial Electrical Stimulation of the Human Brain. In *Frontiers in neuroscience* 11, p. 401. DOI: 10.3389/fnins.2017.00401.

Maris, Eric; Oostenveld, Robert (2007): Nonparametric statistical testing of EEG- and MEG-data. In *Journal of neuroscience methods* 164 (1), pp. 177–190. DOI: 10.1016/j.jneumeth.2007.03.024.

Marshall, Tom R.; O'Shea, Jacinta; Jensen, Ole; Bergmann, Til O. (2015): Frontal eye fields control attentional modulation of alpha and gamma oscillations in contralateral occipitoparietal cortex. In *J. Neurosci.* 35 (4), pp. 1638–1647. DOI: 10.1523/jneurosci.3116-14.2015.

Martel, Adrien; Dähne, Sven; Blankertz, Benjamin (2014): EEG predictors of covert vigilant attention. In *Journal of neural engineering* 11 (3), p. 35009. DOI: 10.1088/1741-2560/11/3/035009.

Mathewson, Kyle E.; Gratton, Gabriele; Fabiani, Monica; Beck, Diane M.; Ro, Tony (2009): To see or not to see: prestimulus alpha phase predicts visual awareness. In *J. Neurosci.* 29 (9), pp. 2725–2732. DOI: 10.1523/JNEUROSCI.3963-08.2009.

Mathewson, Kyle E.; Lleras, Alejandro; Beck, Diane M.; Fabiani, Monica; Ro, Tony; Gratton, Gabriele (2011): Pulsed out of awareness: EEG alpha oscillations represent a pulsed-inhibition of ongoing cortical processing. In *Frontiers in psychology* 2, p. 99. DOI: 10.3389/fpsyg.2011.00099.

Mazaheri, Ali; Jensen, Ole (2008): Asymmetric amplitude modulations of brain oscillations generate slow evoked responses. In *J. Neurosci.* 28 (31), pp. 7781–7787. DOI: 10.1523/JNEUROSCI.1631-08.2008.

Mazaheri, Ali; Jensen, Ole (2010): Rhythmic pulsing: linking ongoing brain activity with evoked responses. In *Frontiers in human neuroscience* 4, p. 177. DOI: 10.3389/fnhum.2010.00177.

Mazaheri, Ali; Nieuwenhuis, Ingrid L. C.; van Dijk, Hanneke; Jensen, Ole (2009): Prestimulus alpha and mu activity predicts failure to inhibit motor responses. In *Hum. Brain Mapp.* 30 (6), pp. 1791–1800. DOI: 10.1002/hbm.20763.

Mazaheri, Ali; Slagter, Heleen A.; Thut, Gregor; Foxe, John J. (2018): Orchestration of brain oscillations: principles and functions. In *The European journal of neuroscience* 48 (7), pp. 2385–2388. DOI: 10.1111/ejn.14189.

McAuley, Tara; Yap, Melvin; Christ, Shawn E.; White, Desirée A. (2006): Revisiting inhibitory control across the life span: insights from the ex-Gaussian distribution. In *Developmental neuropsychology* 29 (3), pp. 447–458. DOI: 10.1207/s15326942dn2903_4.

McLelland, Douglas; Lavergne, Louisa; VanRullen, Rufin (2016): The phase of ongoing EEG oscillations predicts the amplitude of peri-saccadic mislocalization. In *Scientific reports* 6, p. 29335. DOI: 10.1038/srep29335.

Meyer, Marlene; Lamers, Didi; Kayhan, Ezgi; Hunnius, Sabine; Oostenveld, Robert (2021): Enhancing reproducibility in developmental EEG research: BIDS, cluster-based permutation tests, and effect sizes. In *Developmental cognitive neuroscience* 52, p. 101036. DOI: 10.1016/j.dcn.2021.101036.

Michail, Georgios; Toran Jenner, Lino; Keil, Julian (2021): Prestimulus alpha power but not phase influences visual discrimination of long-duration visual stimuli. In *The European journal of neuroscience*. DOI: 10.1111/ejn.15169.

Mierau, Andreas; Klimesch, Wolfgang; Lefebvre, Jérémie (2017): State-dependent alpha peak frequency shifts: Experimental evidence, potential mechanisms and functional implications. In *Neuroscience* 360, pp. 146–154. DOI: 10.1016/j.neuroscience.2017.07.037.

Milton, Alex; Pleydell-Pearce, Christopher W. (2016): The phase of pre-stimulus alpha oscillations influences the visual perception of stimulus timing. In *NeuroImage* 133, pp. 53–61. DOI: 10.1016/j.neuroimage.2016.02.065.

Min, Byoung-Kyong; Herrmann, Christoph S. (2007): Prestimulus EEG alpha activity reflects prestimulus top-down processing. In *Neuroscience letters* 422 (2), pp. 131–135. DOI: 10.1016/j.neulet.2007.06.013.

Mora-Sánchez, Aldo; Pulini, Alfredo-Aram; Gaume, Antoine; Dreyfus, Gérard; Vialatte, François-Benoît (2020): A brain-computer interface for the continuous, real-time monitoring of working memory load in real-world environments. In *Cognitive neurodynamics* 14 (3), pp. 301–321. DOI: 10.1007/s11571-020-09573-x.

Morís Fernández, Luis; Vadillo, Miguel A. (2020): Flexibility in reaction time analysis: many roads to a false positive? In *Royal Society open science* 7 (2), p. 190831. DOI: 10.1098/rsos.190831.

Mostame, Parham; Moharramipour, Ali; Hossein-Zadeh, Gholam-Ali; Babajani-Feremi, Abbas (2019): Statistical Significance Assessment of Phase Synchrony in the Presence of Background Couplings: An ECoG Study. In *Brain topography* 32 (5), pp. 882–896. DOI: 10.1007/s10548-019-00718-8.

Mountcastle, V. B. (1976): The world around us: neural command function for selective attention. In *Neurosciences Research Program bulletin* 14 suppl, pp. 1–47.

Musall, Simon; Pföstl, Veronika von; Rauch, Alexander; Logothetis, Nikos K.; Whittingstall, Kevin (2014): Effects of neural synchrony on surface EEG. In *Cerebral cortex (New York, N.Y. : 1991)* 24 (4), pp. 1045–1053. DOI: 10.1093/cercor/bhs389.

Muthukumaraswamy, Suresh D. (2013): High-frequency brain activity and muscle artifacts in MEG/EEG: a review and recommendations. In *Frontiers in human neuroscience* 7, p. 138. DOI: 10.3389/fnhum.2013.00138.

Myers, Nicholas E.; Stokes, Mark G.; Walther, Lena; Nobre, Anna C. (2014): Oscillatory brain state predicts variability in working memory. In *J. Neurosci.* 34 (23), pp. 7735–7743. DOI: 10.1523/jneurosci.4741-13.2014.

Myslobodsky, M. S.; Bar-Ziv, J.; van Praag, H.; Glicksohn, J. (1989): Bilateral alpha distribution and anatomic brain asymmetries. In *Brain topography* 1 (4), pp. 229–235. DOI: 10.1007/BF01129600.

Myslobodsky, M. S.; Coppola, R.; Weinberger, D. R. (1991): EEG laterality in the era of structural brain imaging. In *Brain topography* 3 (3), pp. 381–390. DOI: 10.1007/BF01129641.

Ngo, Hong-Viet V.; Martinetz, Thomas; Born, Jan; Mölle, Matthias (2013): Auditory closed-loop stimulation of the sleep slow oscillation enhances memory. In *Neuron* 78 (3), pp. 545–553. DOI: 10.1016/j.neuron.2013.03.006.

Nicolas-Alonso, Luis Fernando; Gomez-Gil, Jaime (2012): Brain computer interfaces, a review. In *Sensors (Basel, Switzerland)* 12 (2), pp. 1211–1279. DOI: 10.3390/s120201211.

Northoff, Georg (2018): The Spontaneous Brain: The MIT Press.

Nunez, Paul L.; Srinivasan, Ramesh (2006): Electric fields of the brain. The neurophysics of EEG. 2nd ed. / Paul L. Nunez, Ramesh Srinivasan. Oxford: Oxford University Press.

Nunn, C. M. H.; Osselton, J. W. (1974): The Influence of the EEG Alpha Rhythm on the Perception of Visual Stimuli. In *Psychophysiology* 11 (3), pp. 294–303. DOI: 10.1111/j.1469-8986.1974.tb00547.x.

O'Hare, J. J. (1954): The variability of auditory and visual reaction time with change in amplitude and phase of alpha rhythm. In *American Psychologist* 9, p. 444.

Oostenveld, Robert; Fries, Pascal; Maris, Eric; Schoffelen, Jan-Mathijs (2011): FieldTrip: Open source software for advanced analysis of MEG, EEG, and invasive electrophysiological data. In *Computational intelligence and neuroscience* 2011, p. 156869. DOI: 10.1155/2011/156869.

Osipova, Daria; Hermes, Dora; Jensen, Ole (2008): Gamma power is phase-locked to posterior alpha activity. In *PloS one* 3 (12), e3990. DOI: 10.1371/journal.pone.0003990.

Padfield, Natasha; Zabalza, Jaime; Zhao, Huimin; Masero, Valentin; Ren, Jinchang (2019): EEG-Based Brain-Computer Interfaces Using Motor-Imagery: Techniques and Challenges. In *Sensors (Basel, Switzerland)* 19 (6). DOI: 10.3390/s19061423.

Palva, J. Matias; Palva, Satu (2018): Functional integration across oscillation frequencies by cross-frequency phase synchronization. In *The European journal of neuroscience* 48 (7), pp. 2399–2406. DOI: 10.1111/ejn.13767.

Palva, J. Matias; Palva, Satu; Kaila, Kai (2005): Phase synchrony among neuronal oscillations in the human cortex. In *The Journal of*

neuroscience : the official journal of the Society for Neuroscience 25 (15), pp. 3962–3972. DOI: 10.1523/JNEUROSCI.4250-04.2005.

Palva, Satu; Palva, J. Matias (2007): New vistas for alpha-frequency band oscillations. In *Trends in neurosciences* 30 (4), pp. 150–158. DOI: 10.1016/j.tins.2007.02.001.

Palva, Satu; Palva, J. Matias (2011): Functional roles of alpha-band phase synchronization in local and large-scale cortical networks. In *Frontiers in psychology* 2, p. 204. DOI: 10.3389/fpsyg.2011.00204.

Pantazis, Dimitrios; Simpson, Gregory V.; Weber, Darren L.; Dale, Corby L.; Nichols, Thomas E.; Leahy, Richard M. (2009): A novel ANCOVA design for analysis of MEG data with application to a visual attention study. In *NeuroImage* 44 (1), pp. 164–174. DOI: 10.1016/j.neuroimage.2008.07.012.

Papadelis, Christos; Chen, Zhe; Kourtidou-Papadeli, Chrysoula; Bamidis, Panagiotis D.; Chouvarda, Ioanna; Bekiaris, Evangelos; Maglaveras, Nikos (2007): Monitoring sleepiness with on-board electrophysiological recordings for preventing sleep-deprived traffic accidents. In *Clinical neurophysiology : official journal of the International Federation of Clinical Neurophysiology* 118 (9), pp. 1906–1922. DOI: 10.1016/j.clinph.2007.04.031.

Pashler, H. (1999): The Psychology of Attention: MIT Press (A Bradford book). Available online at https://books.google.es/books?id=w_4MyczgUEcC.

Pavlov, Yuri G.; Adamian, Nika; Appelhoff, Stefan; Arvaneh, Mahnaz; Benwell, Christopher S. Y.; Beste, Christian et al. (2021): #EEGManyLabs: Investigating the replicability of influential EEG experiments. In *Cortex; a journal devoted to the study of the nervous system and behavior* 144, pp. 213–229. DOI: 10.1016/j.cortex.2021.03.013.

Pernet, Cyril R.; Sajda, Paul; Rousselet, Guillaume A. (2011): Single-trial analyses: why bother? In *Frontiers in psychology* 2, p. 322. DOI: 10.3389/fpsyg.2011.00322.

Petersen, Steven E.; Posner, Michael I. (2012): The attention system of the human brain: 20 years after. In *Annual review of neuroscience* 35, pp. 73–89. DOI: 10.1146/annurev-neuro-062111-150525.

Peterson, Erik J.; Rosen, Burke Q.; Belger, Aysenil; Voytek, Bradley; Campbell, Alana M. (2017): Aperiodic neural activity is a better

predictor of schizophrenia than neural oscillations. DOI: 10.1101/113449.

Peterson, Erik J.; Voytek, Bradley (2017): Alpha oscillations control cortical gain by modulating excitatory-inhibitory background activity. DOI: 10.1101/185074.

Pfurtscheller, G.; Stancák, A.; Neuper, Ch. (1996): Event-related synchronization (ERS) in the alpha band — an electrophysiological correlate of cortical idling: A review. In *International Journal of Psychophysiology* 24 (1-2), pp. 39–46. DOI: 10.1016/s0167-8760(96)00066-9.

Posner, M. I. (1980): Orienting of attention. In *The Quarterly journal of experimental psychology* 32 (1), pp. 3–25. DOI: 10.1080/00335558008248231.

Posner, Michael I. (1986): Chronometric explorations of mind. New York u.a.: Oxford Univ. Pr (+The Paul M. Fitts lectures, 3).

Posner, Michael I.; Snyder, Charles R.; Davidson, Brian J. (1980): Attention and the detection of signals. In *Journal of Experimental Psychology: General* 109 (2), pp. 160–174. DOI: 10.1037/0096-3445.109.2.160.

Raichle, Marcus E. (2015): The restless brain: how intrinsic activity organizes brain function. In *Philosophical transactions of the Royal Society of London. Series B, Biological sciences* 370 (1668). DOI: 10.1098/rstb.2014.0172.

Raichle, Marcus E.; Snyder, Abraham Z. (2007): A default mode of brain function: a brief history of an evolving idea. In *NeuroImage* 37 (4), 1083-90; discussion 1097-9. DOI: 10.1016/j.neuroimage.2007.02.041.

Ratcliff, Roger; Murdock, Bennet B. (1976): Retrieval processes in recognition memory. In *Psychological Review* 83 (3), pp. 190–214. DOI: 10.1037/0033-295X.83.3.190.

Ratcliff, Roger; Philiastides, Marios G.; Sajda, Paul (2009): Quality of evidence for perceptual decision making is indexed by trial-to-trial variability of the EEG. In *Proceedings of the National Academy of Sciences of the United States of America* 106 (16), pp. 6539–6544. DOI: 10.1073/pnas.0812589106.

Renard, Yann; Lotte, Fabien; Gibert, Guillaume; Congedo, Marco; Maby, Emmanuel; Delannoy, Vincent et al. (2010): OpenViBE: An Open-Source Software Platform to Design, Test, and Use Brain–

Computer Interfaces in Real and Virtual Environments. In *Presence: Teleoperators and Virtual Environments* 19 (1), pp. 35–53. DOI: 10.1162/pres.19.1.35.

Rihs, Tonia A.; Michel, Christoph M.; Thut, Gregor (2007): Mechanisms of selective inhibition in visual spatial attention are indexed by alpha-band EEG synchronization. In *The European journal of neuroscience* 25 (2), pp. 603–610. DOI: 10.1111/j.1460-9568.2007.05278.x.

Rizzolatti, Giacomo; Riggio, Lucia; Dascola, Isabella; Umiltá, Carlo (1987): Reorienting attention across the horizontal and vertical meridians: Evidence in favor of a premotor theory of attention. In *Neuropsychologia* 25 (1), pp. 31–40. DOI: 10.1016/0028-3932(87)90041-8.

Roberts, Daniel M.; Fedota, John R.; Buzzell, George A.; Parasuraman, Raja; McDonald, Craig G. (2014): Prestimulus oscillations in the alpha band of the EEG are modulated by the difficulty of feature discrimination and predict activation of a sensory discrimination process. In *Journal of cognitive neuroscience* 26 (8), pp. 1615–1628. DOI: 10.1162/jocn_a_00569.

Romei, Vincenzo; Gross, Joachim; Thut, Gregor (2010): On the role of prestimulus alpha rhythms over occipito-parietal areas in visual input regulation: correlation or causation? In *J. Neurosci.* 30 (25), pp. 8692–8697. DOI: 10.1523/jneurosci.0160-10.2010.

Romei, Vincenzo; Gross, Joachim; Thut, Gregor (2012): Sounds reset rhythms of visual cortex and corresponding human visual perception. In *Current biology : CB* 22 (9), pp. 807–813. DOI: 10.1016/j.cub.2012.03.025.

Ronconi, Luca; Melcher, David (2017): The Role of Oscillatory Phase in Determining the Temporal Organization of Perception: Evidence from Sensory Entrainment. In *The Journal of neuroscience : the official journal of the Society for Neuroscience* 37 (44), pp. 10636–10644. DOI: 10.1523/JNEUROSCI.1704-17.2017.

Ruzzoli, Manuela; Torralba, Mireia; Morís Fernández, Luis; Soto-Faraco, Salvador (2019): The relevance of alpha phase in human perception. In *Cortex; a journal devoted to the study of the nervous system and behavior* 120, pp. 249–268. DOI: 10.1016/j.cortex.2019.05.012.

Saalmann, Yuri B.; Pinsk, Mark A.; Wang, Liang; Li, Xin; Kastner, Sabine (2012): The pulvinar regulates information transmission

between cortical areas based on attention demands. In *Science (New York, N.Y.)* 337 (6095), pp. 753–756. DOI: 10.1126/science.1223082.

Sacchet, Matthew D.; LaPlante, Roan A.; Wan, Qian; Pritchett, Dominique L.; Lee, Adrian K. C.; Hämäläinen, Matti et al. (2015): Attention drives synchronization of alpha and beta rhythms between right inferior frontal and primary sensory neocortex. In *J. Neurosci.* 35 (5), pp. 2074–2082. DOI: 10.1523/jneurosci.1292-14.2015.

Sack, Robert L. (2009): The pathophysiology of jet lag. In *Travel medicine and infectious disease* 7 (2), pp. 102–110. DOI: 10.1016/j.tmaid.2009.01.006.

Sadaghiani, Sepideh; Kleinschmidt, Andreas (2016): Brain Networks and α-Oscillations: Structural and Functional Foundations of Cognitive Control. In *Trends in cognitive sciences* 20 (11), pp. 805–817. DOI: 10.1016/j.tics.2016.09.004.

Saha, Simanto; Mamun, Khondaker A.; Ahmed, Khawza; Mostafa, Raqibul; Naik, Ganesh R.; Darvishi, Sam et al. (2021): Progress in Brain Computer Interface: Challenges and Opportunities. In *Frontiers in systems neuroscience* 15, p. 578875. DOI: 10.3389/fnsys.2021.578875.

Samaha, Jason; Bauer, Phoebe; Cimaroli, Sawyer; Postle, Bradley R. (2015): Top-down control of the phase of alpha-band oscillations as a mechanism for temporal prediction. In *Proceedings of the National Academy of Sciences of the United States of America* 112 (27), pp. 8439–8444. DOI: 10.1073/pnas.1503686112.

Samaha, Jason; Iemi, Luca; Haegens, Saskia; Busch, Niko A. (2020): Spontaneous Brain Oscillations and Perceptual Decision-Making. In *Trends in cognitive sciences* 24 (8), pp. 639–653. DOI: 10.1016/j.tics.2020.05.004.

Samaha, Jason; Postle, Bradley R. (2015): The Speed of Alpha-Band Oscillations Predicts the Temporal Resolution of Visual Perception. In *Current biology : CB* 25 (22), pp. 2985–2990. DOI: 10.1016/j.cub.2015.10.007.

Sauseng, P.; Klimesch, W.; Stadler, W.; Schabus, M.; Doppelmayr, M.; Hanslmayr, S. et al. (2005): A shift of visual spatial attention is selectively associated with human EEG alpha activity. In *The European journal of neuroscience* 22 (11), pp. 2917–2926. DOI: 10.1111/j.1460-9568.2005.04482.x.

Sauseng, Paul; Klimesch, Wolfgang; Heise, Kirstin F.; Gruber, Walter R.; Holz, Elisa; Karim, Ahmed A. et al. (2009): Brain oscillatory substrates of visual short-term memory capacity. In *Current biology : CB* 19 (21), pp. 1846–1852. DOI: 10.1016/j.cub.2009.08.062.

Schalk, Gerwin (2015): A general framework for dynamic cortical function: the function-through-biased-oscillations (FBO) hypothesis. In *Frontiers in human neuroscience* 9, p. 352. DOI: 10.3389/fnhum.2015.00352.

Schalk, Gerwin; McFarland, Dennis J.; Hinterberger, Thilo; Birbaumer, Niels; Wolpaw, Jonathan R. (2004): BCI2000: a general-purpose brain-computer interface (BCI) system. In *IEEE transactions on bio-medical engineering* 51 (6), pp. 1034–1043. DOI: 10.1109/tbme.2004.827072.

Schatza, Mark J.; Blackwood, Ethan B.; Nagrale, Sumedh S.; Widge, Alik S. (2022): Toolkit for Oscillatory Real-time Tracking and Estimation (TORTE). In *Journal of neuroscience methods* 366, p. 109409. DOI: 10.1016/j.jneumeth.2021.109409.

Schaworonkow, Natalie; Blythe, Duncan A. J.; Kegeles, Jewgeni; Curio, Gabriel; Nikulin, Vadim V. (2015): Power-law dynamics in neuronal and behavioral data introduce spurious correlations. In *Hum. Brain Mapp.* 36 (8), pp. 2901–2914. DOI: 10.1002/hbm.22816.

Schmitz, Florian; Wilhelm, Oliver (2016): Modeling Mental Speed: Decomposing Response Time Distributions in Elementary Cognitive Tasks and Correlations with Working Memory Capacity and Fluid Intelligence. In *J. Intell.* 4 (4), p. 13. DOI: 10.3390/jintelligence4040013.

Sergeeva, Elena G.; Henrich-Noack, Petra; Bola, Michał; Sabel, Bernhard A. (2014): Brain-state-dependent non-invasive brain stimulation and functional priming: a hypothesis. In *Frontiers in human neuroscience* 8, p. 899. DOI: 10.3389/fnhum.2014.00899.

Shahid, Shahjahan; Prasad, Girijesh (2011): Bispectrum-based feature extraction technique for devising a practical brain-computer interface. In *Journal of neural engineering* 8 (2), p. 25014. DOI: 10.1088/1741-2560/8/2/025014.

Shao, Zeshu; Roelofs, Ardi; Meyer, Antje S. (2012): Sources of individual differences in the speed of naming objects and actions: the contribution of executive control. In *Quarterly journal of experimental*

psychology (2006) 65 (10), pp. 1927–1944. DOI: 10.1080/17470218.2012.670252.

Sheldon, Sarah S.; Mathewson, Kyle E. (2021): To see, not to see or to see poorly: Perceptual quality and guess rate as a function of electroencephalography (EEG) brain activity in an orientation perception task. In *The European journal of neuroscience*. DOI: 10.1111/ejn.15445.

Sherman, Maxwell A.; Lee, Shane; Law, Robert; Haegens, Saskia; Thorn, Catherine A.; Hämäläinen, Matti S. et al. (2016): Neural mechanisms of transient neocortical beta rhythms: Converging evidence from humans, computational modeling, monkeys, and mice. In *Proceedings of the National Academy of Sciences of the United States of America* 113 (33), E4885-94. DOI: 10.1073/pnas.1604135113.

Sherman, S. M.; Guillery, R. W. (1998): On the actions that one nerve cell can have on another: distinguishing "drivers" from "modulators". In *Proceedings of the National Academy of Sciences of the United States of America* 95 (12), pp. 7121–7126. DOI: 10.1073/pnas.95.12.7121.

Sherman, S. M.; Guillery, R. W. (2001): Exploring the thalamus: Academic Press.

Sherrington, C. (1906): The integrative action of the nervous system. New Haven, CT: Yale University Press.

Shin, Hyeyoung; Law, Robert; Tsutsui, Shawn; Moore, Christopher I.; Jones, Stephanie R. (2017): The rate of transient beta frequency events predicts behavior across tasks and species. In *eLife* 6. DOI: 10.7554/eLife.29086.

Siegel, Markus; Donner, Tobias H.; Oostenveld, Robert; Fries, Pascal; Engel, Andreas K. (2008): Neuronal synchronization along the dorsal visual pathway reflects the focus of spatial attention. In *Neuron* 60 (4), pp. 709–719. DOI: 10.1016/j.neuron.2008.09.010.

Silvanto, Juha; Lavie, Nilli; Walsh, Vincent (2006): Stimulation of the human frontal eye fields modulates sensitivity of extrastriate visual cortex. In *Journal of neurophysiology* 96 (2), pp. 941–945. DOI: 10.1152/jn.00015.2006.

Simon, Michael; Schmidt, Eike A.; Kincses, Wilhelm E.; Fritzsche, Martin; Bruns, Andreas; Aufmuth, Claus et al. (2011): EEG alpha spindle measures as indicators of driver fatigue under real traffic conditions. In *Clinical neurophysiology : official journal of the International*

Federation of Clinical Neurophysiology 122 (6), pp. 1168–1178. DOI: 10.1016/j.clinph.2010.10.044.

Simonsohn, Uri (2015): Small telescopes: detectability and the evaluation of replication results. In *Psychological science* 26 (5), pp. 559–569. DOI: 10.1177/0956797614567341.

Simpson, Gregory V.; Weber, Darren L.; Dale, Corby L.; Pantazis, Dimitrios; Bressler, Steven L.; Leahy, Richard M.; Luks, Tracy L. (2011): Dynamic activation of frontal, parietal, and sensory regions underlying anticipatory visual spatial attention. In *J. Neurosci.* 31 (39), pp. 13880–13889. DOI: 10.1523/jneurosci.1519-10.2011.

Sokoliuk, Rodika; Mayhew, Stephen D.; Aquino, Kevin M.; Wilson, Ross; Brookes, Matthew J.; Francis, Susan T. et al. (2019): Two Spatially Distinct Posterior Alpha Sources Fulfill Different Functional Roles in Attention. In *J. Neurosci.* 39 (36), pp. 7183–7194. DOI: 10.1523/jneurosci.1993-18.2019.

Spaak, Eelke; Bonnefond, Mathilde; Maier, Alexander; Leopold, David A.; Jensen, Ole (2012): Layer-specific entrainment of γ-band neural activity by the α rhythm in monkey visual cortex. In *Current biology : CB* 22 (24), pp. 2313–2318. DOI: 10.1016/j.cub.2012.10.020.

Spieler, D. H.; Balota, D. A.; Faust, M. E. (1996): Stroop performance in healthy younger and older adults and in individuals with dementia of the Alzheimer's type. In *Journal of experimental psychology. Human perception and performance* 22 (2), pp. 461–479. DOI: 10.1037//0096-1523.22.2.461.

Sporns, Olaf (2011): Networks of the brain. Cambridge, Mass., London: MIT Press.

Squires, K. C.; Wickens, C.; Squires, N. K.; Donchin, E. (1976): The effect of stimulus sequence on the waveform of the cortical event-related potential. In *Science (New York, N.Y.)* 193 (4258), pp. 1142–1146. DOI: 10.1126/science.959831.

Starr, A.; Sandroni, P.; Michalewski, H. J. (1995): Readiness to respond in a target detection task: pre- and post-stimulus event-related potentials in normal subjects. In *Electroencephalography and Clinical Neurophysiology/Evoked Potentials Section* 96 (1), pp. 76–92. DOI: 10.1016/0013-4694(94)00162-e.

Stokes, Mark; Spaak, Eelke (2016): The Importance of Single-Trial Analyses in Cognitive Neuroscience. In *Trends in cognitive sciences* 20 (7), pp. 483–486. DOI: 10.1016/j.tics.2016.05.008.

Terentjeviene, Asta; Maciuleviciene, Edita; Vadopalas, Kazys; Mickeviciene, Dalia; Karanauskiene, Diana; Valanciene, Dovile et al. (2018): Prefrontal Cortex Activity Predicts Mental Fatigue in Young and Elderly Men During a 2 h "Go/NoGo" Task. In *Frontiers in neuroscience* 12, p. 620. DOI: 10.3389/fnins.2018.00620.

Thut, Gregor; Miniussi, Carlo (2009): New insights into rhythmic brain activity from TMS-EEG studies. In *Trends in cognitive sciences* 13 (4), pp. 182–189. DOI: 10.1016/j.tics.2009.01.004.

Thut, Gregor; Nietzel, Annika; Brandt, Stephan A.; Pascual-Leone, Alvaro (2006): Alpha-band electroencephalographic activity over occipital cortex indexes visuospatial attention bias and predicts visual target detection. In *The Journal of neuroscience : the official journal of the Society for Neuroscience* 26 (37), pp. 9494–9502. DOI: 10.1523/JNEUROSCI.0875-06.2006.

Thut, Gregor; Schyns, Philippe G.; Gross, Joachim (2011): Entrainment of perceptually relevant brain oscillations by non-invasive rhythmic stimulation of the human brain. In *Frontiers in psychology* 2, p. 170. DOI: 10.3389/fpsyg.2011.00170.

Tinkhauser, Gerd; Pogosyan, Alek; Little, Simon; Beudel, Martijn; Herz, Damian M.; Tan, Huiling; Brown, Peter (2017): The modulatory effect of adaptive deep brain stimulation on beta bursts in Parkinson's disease. In *Brain : a journal of neurology* 140 (4), pp. 1053–1067. DOI: 10.1093/brain/awx010.

Tonin, L.; Leeb, R.; Del R Millán, J. (2012): Time-dependent approach for single trial classification of covert visuospatial attention. In *Journal of neural engineering* 9 (4), p. 45011. DOI: 10.1088/1741-2560/9/4/045011.

Tonin, L.; Leeb, R.; Sobolewski, A.; Del Millán, J. R. (2013): An online EEG BCI based on covert visuospatial attention in absence of exogenous stimulation. In *Journal of neural engineering* 10 (5), p. 56007. DOI: 10.1088/1741-2560/10/5/056007.

Tonin, Luca; Pitteri, Marco; Leeb, Robert; Zhang, Huaijian; Menegatti, Emanuele; Piccione, Francesco; Del Millán, José R. (2017): Behavioral and Cortical Effects during Attention Driven Brain-Computer Interface Operations in Spatial Neglect: A Feasibility Case Study. In

Frontiers in human neuroscience 11, p. 336. DOI: 10.3389/fnhum.2017.00336.

Torralba, Mireia; Soto-Faraco, Salvador; Ruzzoli, Manuela (2016): From brain oscillations to new technological applications: Proof of concept. In : PERCEPTION, vol. 45. SAGE PUBLICATIONS LTD 1 OLIVERS YARD, 55 CITY ROAD, LONDON EC1Y 1SP, ENGLAND, p. 289.

Torralba Cuello, Mireia; Drew, Alice; Sabaté San José, Alba; Morís Fernández, Luis; Soto-Faraco, Salvador (2022): Alpha fluctuations regulate the accrual of visual information to awareness. In *Cortex; a journal devoted to the study of the nervous system and behavior* 147, pp. 58–71. DOI: 10.1016/j.cortex.2021.11.017.

Trachel, R. E.; Brochier, T. G.; Clerc, M. (2018): Brain-computer interaction for online enhancement of visuospatial attention performance. In *Journal of neural engineering* 15 (4), p. 46017. DOI: 10.1088/1741-2552/aabf16.

Treder, Matthias S.; Bahramisharif, Ali; Schmidt, Nico M.; van Gerven, Marcel A. J.; Blankertz, Benjamin (2011): Brain-computer interfacing using modulations of alpha activity induced by covert shifts of attention. In *Journal of neuroengineering and rehabilitation* 8, p. 24. DOI: 10.1186/1743-0003-8-24.

Tremblay, Sébastien; Doucet, Guillaume; Pieper, Florian; Sachs, Adam; Martinez-Trujillo, Julio (2015): Single-Trial Decoding of Visual Attention from Local Field Potentials in the Primate Lateral Prefrontal Cortex Is Frequency-Dependent. In *J. Neurosci.* 35 (24), pp. 9038–9049. DOI: 10.1523/jneurosci.1041-15.2015.

Truccolo, Wilson A.; Ding, Mingzhou; Knuth, Kevin H.; Nakamura, Richard; Bressler, Steven L. (2002): Trial-to-trial variability of cortical evoked responses: implications for the analysis of functional connectivity. In *Clinical Neurophysiology* 113 (2), pp. 206–226. DOI: 10.1016/s1388-2457(01)00739-8.

Uddin, Lucina Q.; Menon, Vinod (2010): Introduction to special topic - resting-state brain activity: implications for systems neuroscience. In *Frontiers in systems neuroscience* 4. DOI: 10.3389/fnsys.2010.00037.

Uhlhaas, Peter J.; Singer, Wolf (2006): Neural synchrony in brain disorders: relevance for cognitive dysfunctions and pathophysiology. In *Neuron* 52 (1), pp. 155–168. DOI: 10.1016/j.neuron.2006.09.020.

van Diepen, Rosanne M.; Foxe, John J.; Mazaheri, Ali (2019): The functional role of alpha-band activity in attentional processing: the current zeitgeist and future outlook. In *Current opinion in psychology* 29, pp. 229–238. DOI: 10.1016/j.copsyc.2019.03.015.

van Dijk, Hanneke; Schoffelen, Jan-Mathijs; Oostenveld, Robert; Jensen, Ole (2008): Prestimulus oscillatory activity in the alpha band predicts visual discrimination ability. In *The Journal of neuroscience : the official journal of the Society for Neuroscience* 28 (8), pp. 1816–1823. DOI: 10.1523/JNEUROSCI.1853-07.2008.

van Ede, Freek; Quinn, Andrew J.; Woolrich, Mark W.; Nobre, Anna C. (2018): Neural Oscillations: Sustained Rhythms or Transient Burst-Events? In *Trends in neurosciences* 41 (7), pp. 415–417. DOI: 10.1016/j.tins.2018.04.004.

van Es, Mats W. J.; Gross, Joachim; Schoffelen, Jan-Mathijs (2020): Investigating the effects of pre-stimulus cortical oscillatory activity on behavior. In *NeuroImage* 223, p. 117351. DOI: 10.1016/j.neuroimage.2020.117351.

van Gerven, Marcel; Jensen, Ole (2009): Attention modulations of posterior alpha as a control signal for two-dimensional brain-computer interfaces. In *Journal of neuroscience methods* 179 (1), pp. 78–84. DOI: 10.1016/j.jneumeth.2009.01.016.

VanRullen, Rufin (2016a): How to Evaluate Phase Differences between Trial Groups in Ongoing Electrophysiological Signals. In *Frontiers in neuroscience* 10, p. 426. DOI: 10.3389/fnins.2016.00426.

VanRullen, Rufin (2016b): Perceptual Cycles. In *Trends in cognitive sciences* 20 (10), pp. 723–735. DOI: 10.1016/j.tics.2016.07.006.

VanRullen, Rufin; Busch, N. A.; Drewes, J.; Dubois, Julien (2011): Ongoing EEG Phase as a Trial-by-Trial Predictor of Perceptual and Attentional Variability. In *Frontiers in psychology* 2, p. 60. DOI: 10.3389/fpsyg.2011.00060.

VanRullen, Rufin; Carlson, Thomas; Cavanagh, Patrick (2007): The blinking spotlight of attention. In *Proceedings of the National Academy of Sciences of the United States of America* 104 (49), pp. 19204–19209. DOI: 10.1073/pnas.0707316104.

Vansteensel, M. J.; Kristo, G.; Aarnoutse, E. J.; Ramsey, N. F. (2017): The brain-computer interface researcher's questionnaire: from

research to application. In *Brain-Computer Interfaces* 4 (4), pp. 236–247. DOI: 10.1080/2326263X.2017.1366237.

Varela, F.; Lachaux, J. P.; Rodriguez, E.; Martinerie, J. (2001): The brainweb: phase synchronization and large-scale integration. In *Nature reviews. Neuroscience* 2 (4), pp. 229–239. DOI: 10.1038/35067550.

Varela, F. J.; Toro, Alfredo; Roy John, E.; Schwartz, Eric L. (1981): Perceptual framing and cortical alpha rhythm. In *Neuropsychologia* 19 (5), pp. 675–686. DOI: 10.1016/0028-3932(81)90005-1.

Vidaurre, C.; Kawanabe, M.; Bünau, P. von; Blankertz, B.; Müller, K. R. (2011): Toward unsupervised adaptation of LDA for brain-computer interfaces. In *IEEE transactions on bio-medical engineering* 58 (3), pp. 587–597. DOI: 10.1109/TBME.2010.2093133.

Vigué-Guix, Irene; Morís Fernández, Luis; Torralba Cuello, Mireia; Ruzzoli, Manuela; Soto-Faraco, Salvador (2020): Can the occipital alpha-phase speed up visual detection through a real-time EEG-based brain-computer interface (BCI)? In *The European journal of neuroscience*. DOI: 10.1111/ejn.14931.

Voytek, Bradley; Canolty, Ryan T.; Shestyuk, Avgusta; Crone, Nathan E.; Parvizi, Josef; Knight, Robert T. (2010): Shifts in gamma phase-amplitude coupling frequency from theta to alpha over posterior cortex during visual tasks. In *Frontiers in human neuroscience* 4, p. 191. DOI: 10.3389/fnhum.2010.00191.

Walsh, E. G. (1952): Visual reaction time and the alpha-rhythm, an investigation of a scanning hypothesis. In *The Journal of physiology* 118 (4), pp. 500–508. DOI: 10.1113/jphysiol.1952.sp004811.

Walter, W. Grey (1950): The Twenty-Fourth Maudsley Lecture: The Functions of Electrical Rhythms in the Brain. In *J. ment. sci* 96 (402), pp. 1–31. DOI: 10.1192/bjp.96.402.1.

Watrous, Andrew J.; Lee, Darrin J.; Izadi, Ali; Gurkoff, Gene G.; Shahlaie, Kiarash; Ekstrom, Arne D. (2013): A comparative study of human and rat hippocampal low frequency oscillations during spatial navigation. In *Hippocampus* 23 (8), pp. 656–661. DOI: 10.1002/hipo.22124.

Whitten, Tara A.; Hughes, Adam M.; Dickson, Clayton T.; Caplan, Jeremy B. (2011): A better oscillation detection method robustly extracts EEG rhythms across brain state changes: the human alpha

rhythm as a test case. In *NeuroImage* 54 (2), pp. 860–874. DOI: 10.1016/j.neuroimage.2010.08.064.

Wolpaw, Jonathan R.; Birbaumer, Niels; McFarland, Dennis J.; Pfurtscheller, Gert; Vaughan, Theresa M. (2002): Brain–computer interfaces for communication and control. In *Clinical Neurophysiology* 113 (6), pp. 767–791. DOI: 10.1016/s1388-2457(02)00057-3.

Worden, Michael S.; Foxe, John J.; Wang, Norman; Simpson, Gregory V. (2000): Anticipatory Biasing of Visuospatial Attention Indexed by Retinotopically Specific α-Bank Electroencephalography Increases over Occipital Cortex. In *J. Neurosci.* 20 (6), RC63-RC63. DOI: 10.1523/jneurosci.20-06-j0002.2000.

Wutz, Andreas; Zazio, Agnese; Weisz, Nathan (2020): Oscillatory Bursts in Parietal Cortex Reflect Dynamic Attention between Multiple Objects and Ensembles. In *J. Neurosci.* 40 (36), pp. 6927–6937. DOI: 10.1523/JNEUROSCI.0231-20.2020.

Wyart, Valentin; Tallon-Baudry, Catherine (2009): How ongoing fluctuations in human visual cortex predict perceptual awareness: baseline shift versus decision bias. In *The Journal of neuroscience : the official journal of the Society for Neuroscience* 29 (27), pp. 8715–8725. DOI: 10.1523/JNEUROSCI.0962-09.2009.

Yamagishi, Noriko; Callan, Daniel E.; Goda, Naokazu; Anderson, Stephen J.; Yoshida, Yoshikazu; Kawato, Mitsuo (2003): Attentional modulation of oscillatory activity in human visual cortex. In *NeuroImage* 20 (1), pp. 98–113. DOI: 10.1016/s1053-8119(03)00341-0.

Yang, Lingling; Leung, Howard; Plank, Markus; Snider, Joe; Poizner, Howard (2014): Alpha and beta band power changes predict reaction time and endpoint error during planning reaching movements. In : 2014 7th International Conference on Biomedical Engineering and Informatics. 2014 7th International Conference on Biomedical Engineering and Informatics (BMEI). Dalian, China, 14/10/2014 - 16/10/2014: IEEE, pp. 264–268.

Zago, Laure; Petit, Laurent; Jobard, Gael; Hay, Julien; Mazoyer, Bernard; Tzourio-Mazoyer, Nathalie et al. (2017): Pseudoneglect in line bisection judgement is associated with a modulation of right hemispheric spatial attention dominance in right-handers. In *Neuropsychologia* 94, pp. 75–83. DOI: 10.1016/j.neuropsychologia.2016.11.024.

Zander, Thorsten O.; Kothe, Christian (2011): Towards passive brain-computer interfaces: applying brain-computer interface technology to human-machine systems in general. In *Journal of neural engineering* 8 (2), p. 25005. DOI: 10.1088/1741-2560/8/2/025005.

Zazio, Agnese; Ruhnau, Philipp; Weisz, Nathan; Wutz, Andreas (2021): Pre-stimulus alpha-band power and phase fluctuations originate from different neural sources and exert distinct impact on stimulus-evoked responses. In *The European journal of neuroscience*. DOI: 10.1111/ejn.15138.

Zazio, Agnese; Schreiber, Marco; Miniussi, Carlo; Bortoletto, Marta (2020): Modelling the effects of ongoing alpha activity on visual perception: The oscillation-based probability of response. In *Neuroscience and biobehavioral reviews* 112, pp. 242–253. DOI: 10.1016/j.neubiorev.2020.01.037.

Zich, Catharina; Quinn, Andrew J.; Mardell, Lydia C.; Ward, Nick S.; Bestmann, Sven (2020): Dissecting Transient Burst Events. In *Trends in cognitive sciences* 24 (10), pp. 784–788. DOI: 10.1016/j.tics.2020.07.004.

Zoefel, Benedikt; VanRullen, Rufin (2017): Oscillatory Mechanisms of Stimulus Processing and Selection in the Visual and Auditory Systems: State-of-the-Art, Speculations and Suggestions. In *Frontiers in neuroscience* 11, p. 296. DOI: 10.3389/fnins.2017.00296.

Zrenner, Christoph; Belardinelli, Paolo; Müller-Dahlhaus, Florian; Ziemann, Ulf (2016): Closed-Loop Neuroscience and Non-Invasive Brain Stimulation: A Tale of Two Loops. In *Frontiers in cellular neuroscience* 10, p. 92. DOI: 10.3389/fncel.2016.00092.

Zrenner, Christoph; Desideri, Debora; Belardinelli, Paolo; Ziemann, Ulf (2018): Real-time EEG-defined excitability states determine efficacy of TMS-induced plasticity in human motor cortex. In *Brain stimulation* 11 (2), pp. 374–389. DOI: 10.1016/j.brs.2017.11.016.

ANNEX I -
Using α-phase to speed up visual detection

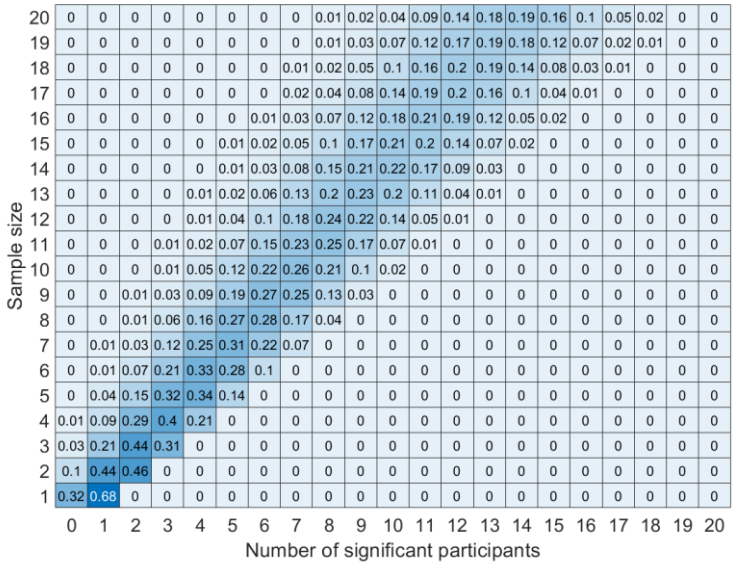

SUPPLEMENTARY FIGURE 1. Sample size estimation. Based on the results from Callaway and Yeager's (1960), we used a Monte Carlo simulation to estimate the probability to find a significant outcome (between RTs at fast and slow phase bins) in a given number of participants (x-axis), depending on the total sample size (y-axis) of our study. The question that our simulation wants to answer was: "*If Callaway's study is representative of the effect in the general population, how probable is to find a significant effect (at participant level) in X participants (x-axis) out of a sample of N participants (y-axis)?*". Each of the cells in the graph estimates the probability of finding X participants with a significant effect when running N participants. According to this simulation, we decided that if less than 3 participants (X<3) out of N=8 showed a significant difference in RTs between fast and slow phase bins, then the size of the effect in this experiment would have to be considered null or negligible compared to the original study (Callaway and Yeager 1960), assuming an error of 5%.

SUPPLEMENTARY TABLE 1. Individual results from Stage 1, showing the mean (SD) RT for each phase bin [in ms]. Red and green text represent the slower and the faster RTs for each participant, respectively.

Part.	Phase bins along α-cycle [in degrees]										Mean (SD) RT combined phases
	162°	**198°**	**234°**	**270°**	**306°**	**342°**	**18°**	**54°**	**90°**	**126°**	
1	**203 (27)**	196 (32)	**193 (37)**	196 (23)	199 (28)	196 (37)	196 (35)	197 (22)	198 (26)	199 (24)	**197 (3)**
2	**203 (38)**	202 (29)	194 (46)	199 (37)	194 (40)	203 (40)	**190 (49)**	196 (45)	199 (38)	200 (47)	**198 (4)**
3	201 (25)	207 (29)	208 (23)	206 (28)	201 (28)	206 (24)	206 (23)	202 (26)	**208 (25)**	**200 (23)**	**205 (3)**
4	198 (35)	197 (38)	**193 (27)**	201 (38)	**210 (35)**	205 (30)	198 (34)	202 (41)	196 (32)	196 (30)	**200 (5)**
5	199 (26)	202 (27)	200 (27)	201 (25)	**196 (34)**	204 (25)	197 (32)	197 (30)	**204 (30)**	199 (21)	**200 (3)**
6	218 (30)	221 (32)	221 (34)	216 (29)	217 (33)	219 (40)	**212 (35)**	220 (35)	**222 (39)**	214 (37)	**218 (3)**
7	217 (24)	215 (29)	215 (38)	**213 (41)**	**230 (30)**	221 (33)	217 (32)	220 (33)	227 (29)	218 (27)	**219 (5)**
8	207 (25)	209 (26)	212 (33)	207 (36)	**213 (35)**	208 (35)	209 (33)	**199 (23)**	205 (23)	200 (29)	**207 (5)**
Mean (SD)	**206 (8)**	**206 (9)**	**205 (11)**	**205 (7)**	**208 (12)**	**208 (8)**	**203 (9)**	**204 (10)**	**207 (11)**	**203 (8)**	**206 (9)**

SUPPLEMENTARY TABLE 2. Number of trials in Stage 1. For each participant, it is reported the total number of trials delivered, the number of trials excluded for reaction time (RTs), the number of trials excluded for not satisfying the amplitude threshold criterion, the number of valid trials, the number of hit trials, and the number of trials relocated.

Part.	No. all trials	No. trials excluded for RTs	No. trials excluded for amplitude	No. valid trials	No. hit trials	No. trials relocated
1	**929**	**35** / 927 4%	**306** / 927 33%	**588** / 927 63%	**346** / 588 59%	**242** / 588 41%
2	**1259**	**174** / 1259 14%	**527** / 1259 42%	**558** / 1259 44%	**257** / 558 46%	**301** / 558 54%
3	**827**	**47** / 827 6%	**151** / 827 18%	**629** / 827 76%	**256** / 629 41%	**373** / 629 59%
4	**911**	**76** / 911 8%	**183** / 911 20%	**652** / 911 72%	**244** / 652 37%	**408** / 652 63%
5	**1238**	**36** / 1238 3%	**542** / 1238 44%	**660** / 1238 53%	**253** / 660 38%	**407** / 660 62%
6	**1194**	**101** / 1194 8%	**503** / 1194 42%	**590** / 1194 50%	**313** / 590 53%	**277** / 590 47%
7	**1221**	**122** / 1221 10%	**453** / 1221 37%	**646** / 1221 53%	**277** / 646 43%	**369** / 646 57%
8	**695**	**22** / 695 3%	**63** / 695 9%	**610** / 695 88%	**290** / 610 48%	**320** / 610 52%
Mean (SD)	**1034 (219)**	**77 (53)** 7%	**341 (190)** 33%	**617 (36)** 60%	**280 (35)** 45%	**337 (61)** 55%

SUPPLEMENTARY TABLE 3. Number of trials in Stage 2. For each participant, it is reported the total number of trials delivered, the number of trials excluded for reaction time (RTs), the number of trials excluded for not satisfying the amplitude threshold criterion, the number of trials excluded for not hitting the phase bin acceptance zone, the number of valid trials, the number of hit trials, and the number of trials relocated.

Part.	No. all trials	No. trials excluded for RTs	No. trials excluded for amplitude	No. trials excluded for phase accuracy	No. valid trials	No. hit trials	No. trials relocated	No. trials post-hoc excluded
1	**317**	**14** / 317 4%	**96** / 317 30%	**7** / 317 2%	**200** / 317 63%	**156** / 200 78%	**44** / 200 22%	**27** / 200 14%
2	**476**	**58** / 476 12%	**196** / 476 41%	**22** / 476 5%	**200** / 476 42%	**116** / 200 58%	**84** / 200 42%	**0** / 200 0%
3	**440**	**27** / 440 6%	**166** / 440 38%	**47** / 440 11%	**200** / 440 45%	**104** / 200 52%	**96** / 200 48%	**67** / 200 34%
4	**328**	**28** / 328 9%	**60** / 328 18%	**40** / 328 12%	**200** / 328 61%	**96** / 200 48%	**104** / 200 52%	**48** / 200 24%
5	**571**	**33** / 571 6%	**267** / 571 47%	**71** / 571 12%	**200** / 571 35%	**73** / 200 37%	**127** / 200 63%	**0** / 200 0%
6	**494**	**17** / 494 3%	**223** / 494 45%	**54** / 494 11%	**200** / 494 40%	**94** / 200 47%	**106** / 200 53%	**51** / 200 26%
7	**368**	**38** / 368 10%	**123** / 368 33%	**7** / 368 2%	**200** / 368 54%	**104** / 200 52%	**96** / 200 48%	**47** / 200 24%
8	**272**	**35** / 272 13%	**22** / 272 8%	**15** / 272 6%	**200** / 272 74%	**115** / 200 57%	**85** / 200 43%	**42** / 200 21%
Mean (SD)	**408 (103)**	**31 (14)** 8%	**144 (84)** 35%	**33 (24)** 8%	**200 (0)** 49%	**107 (24)** 54%	**93 (24)** 46%	**35 (24)** 18%

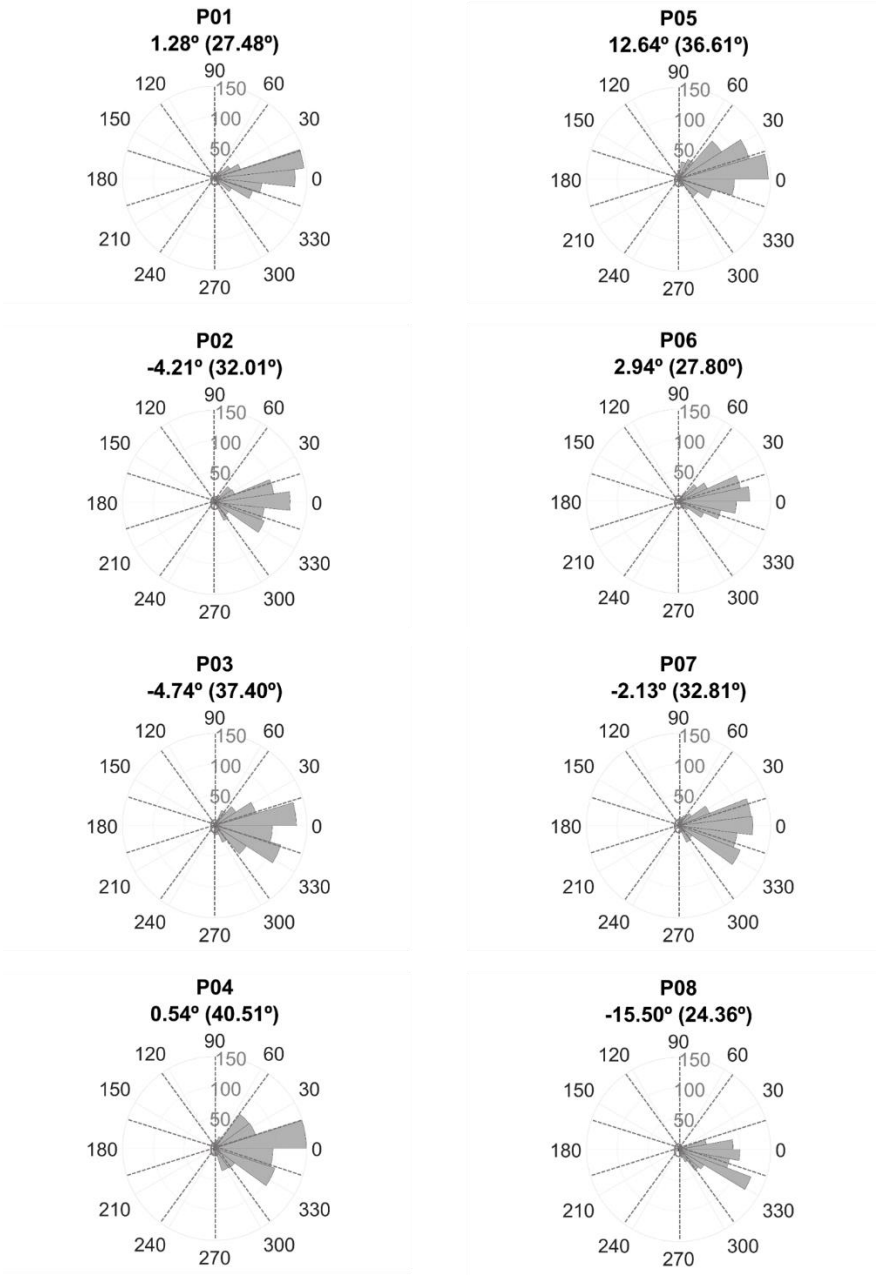

SUPPLEMENTARY FIGURE 2. Individual Rose plot of mean (SD) phase accuracy of hit phases for all validated trials in Stage 1 [in degrees]. Dotted lines denote boundaries between phase bins.

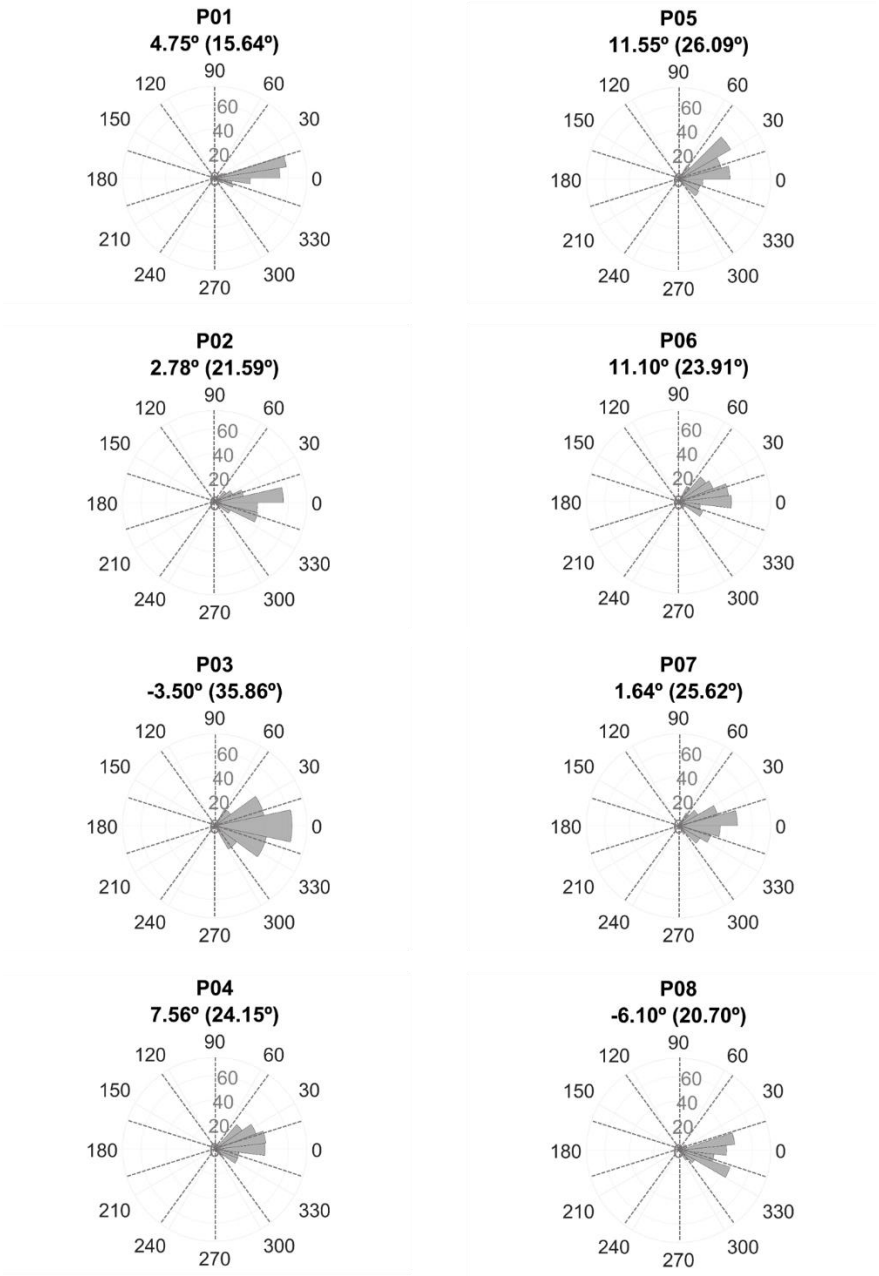

SUPPLEMENTARY FIGURE 3. Individual Rose plot of mean (SD) phase accuracy of hit phases for all validated trials in Stage 2 [in degrees]. Dotted lines denote boundaries between phase bins.

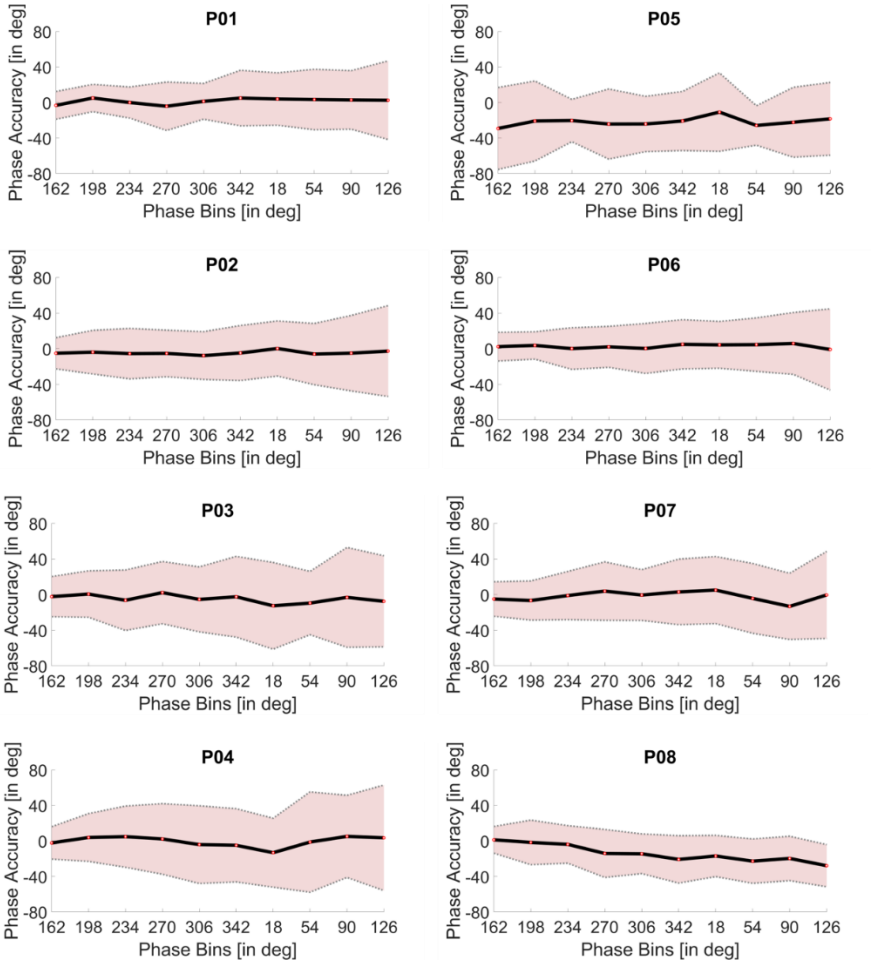

SUPPLEMENTARY FIGURE 4. Phase accuracy [in degrees] as a function of the phase bins at individual-level. The dark line corresponds to the mean phase accuracy and the shaded area denotes the standard deviation for each phase bin along the α-cycle.

SUPPLEMENTARY TABLE 4. Difference in mean and standard deviation accuracy computed between the last (i.e., phase bin 126º) and first (i.e., phase bin 162º) phase bins along the α-cycle at individual and group level in Stage 1.

Part.	Δ Mean last-first bins [in deg]	Δ SD last-first bins [in deg]
1	5.81	28.64
2	2.51	33.51
3	-5.25	28.57
4	5.74	41.15
5	10.91	-5.20
6	-3.16	29.52
7	4.54	29.43
8	-29.10	8.71
Mean (SD)	**-5.42 (9.38)**	**32.20 (10.64)**

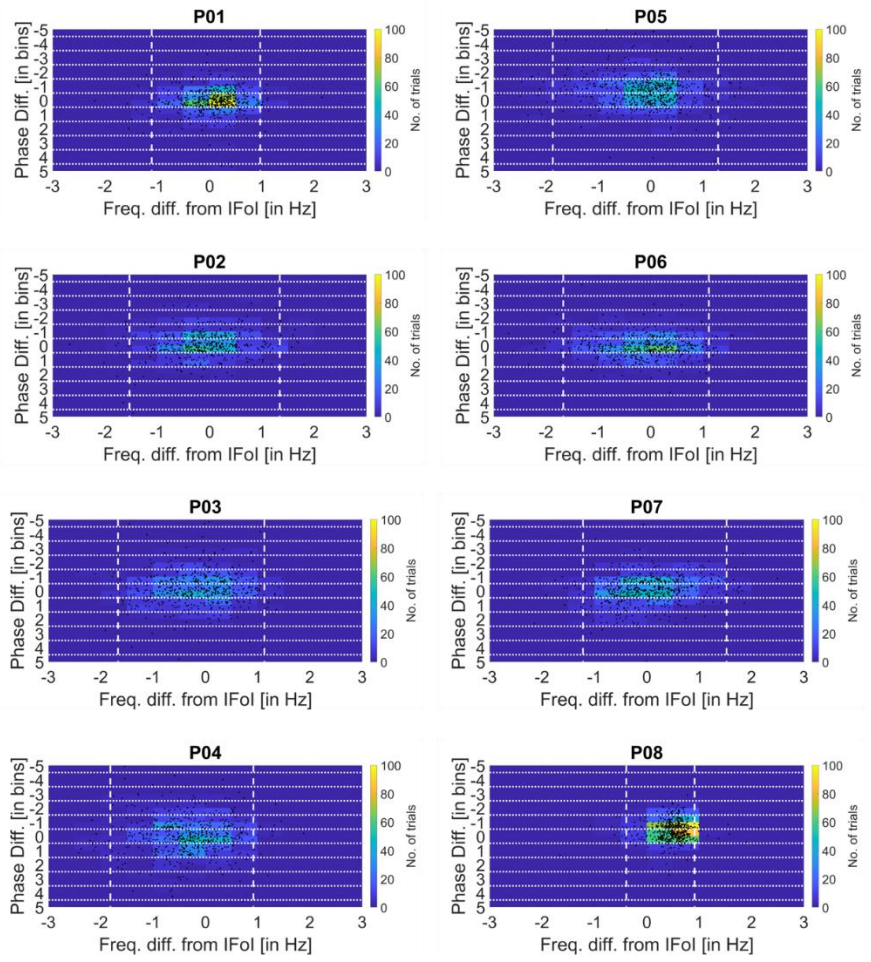

SUPPLEMENTARY FIGURE 5. Heatmap chart of phase difference [in bins] as a function of the frequency difference of valid trials compared to IFoI at individual-level. Vertical dashed lines denote the interval comprising 95% of the trials, and horizontal dotted lines correspond to phase bin boundaries. The colorbar counts the number of trials and black dots correspond to trials.

SUPPLEMENTARY TABLE 5. Comparison of the cumulative percentage of trials for phase bin difference between target and hit phase bins. Mean and standard deviation of the frequency difference between Individual Frequency of Interest (IFoI) peak [in Hz] and mean instantaneous frequency [in Hz] during task for Stage 1. Correlation (negative direction, one-tailed) between phase accuracy and frequency difference from IFoI peak and mean instantaneous frequency for Stage 1, including Pearson's coefficient (r) and p-value (p).

Part.	Cumulative percentage of trials for phase bin difference (target/hit)						Mean (SD) freq. diff. from IFoI [in Hz]	Correlation between phase acc. and freq. diff. from IFoI	
	0	±1	±2	±3	±4	±5		r	p
1	59%	93%	98%	99%	100%	100%	0.07 (0.50)	-0.07	.043
2	47%	88%	97%	99%	100%	100%	-0.11 (0.70)	-0.13	.001
3	40%	84%	95%	98%	99%	100%	-0.19 (0.73)	-0.01	.37
4	37%	81%	94%	98%	100%	100%	-0.31 (0.70)	0.00	.52
5	35%	83%	96%	98%	100%	100%	-0.13 (0.73)	0.09	.99
6	53%	93%	99%	100%	100%	100%	-0.14 (0.71)	0.03	.79
7	44%	87%	98%	99%	100%	100%	0.03 (0.70)	-0.24	<.001
8	47%	92%	100%	100%	100%	100%	0.48 (0.32)	-0.04	.15
Mean (SD)	**45 (8)**	**88 (5)**	**97 (2)**	**99 (1)**	**100 (0)**	**100 (0)**	**-0.04 (0.24)**	**--**	**--**

SUPPLEMENTARY TABLE 6. Comparison among the Individual Frequency of Interest (IFoI) peak [in Hz] and amplitude [in dB] at rest and during task execution for each participant using the occipital-parietal cluster (OP-cluster) and O1-electrode. The IFoI difference is computed between rest (OP-cluster) and task (O1-electrode).

Part.	IFoI (rest)		IFoI (task)				ΔIFoI rest-task [in Hz]
	OP-cluster		OP-cluster		O1-electrode		
	Peak [in Hz]	Amplitude [in dB]	Peak [in Hz]	Amplitude [in dB]	Peak [in Hz]	Amplitude [in dB]	
1	10.50	10.50	10.75	5.19	10.75	10.93	-0.25
2	11.75	6.54	11.75	-8.37	11.75	7.25	0
3	9.75	8.00	10.25	5.28	10.00	8.24	-0.25
4	9.00	9.99	9.00	1.19	9.25	9.12	-0.25
5	9.75	8.06	9.75	0.80	9.75	3.02	0
6	10.75	5.23	11.00	6.76	11.00	8.38	-0.25
7	8.50	9.06	8.25	-2.16	8.50	8.78	0
8	10.50	12.33	11.00	11.68	11.00	11.92	-0.50
Mean (SD)	**10.06 (1.03)**	**8.71 (2.26)**	**10.22 (1.16)**	**2.55 (6.12)**	**10.25 (1.07)**	**8.46 (2.67)**	**-0.19 (0.18)**

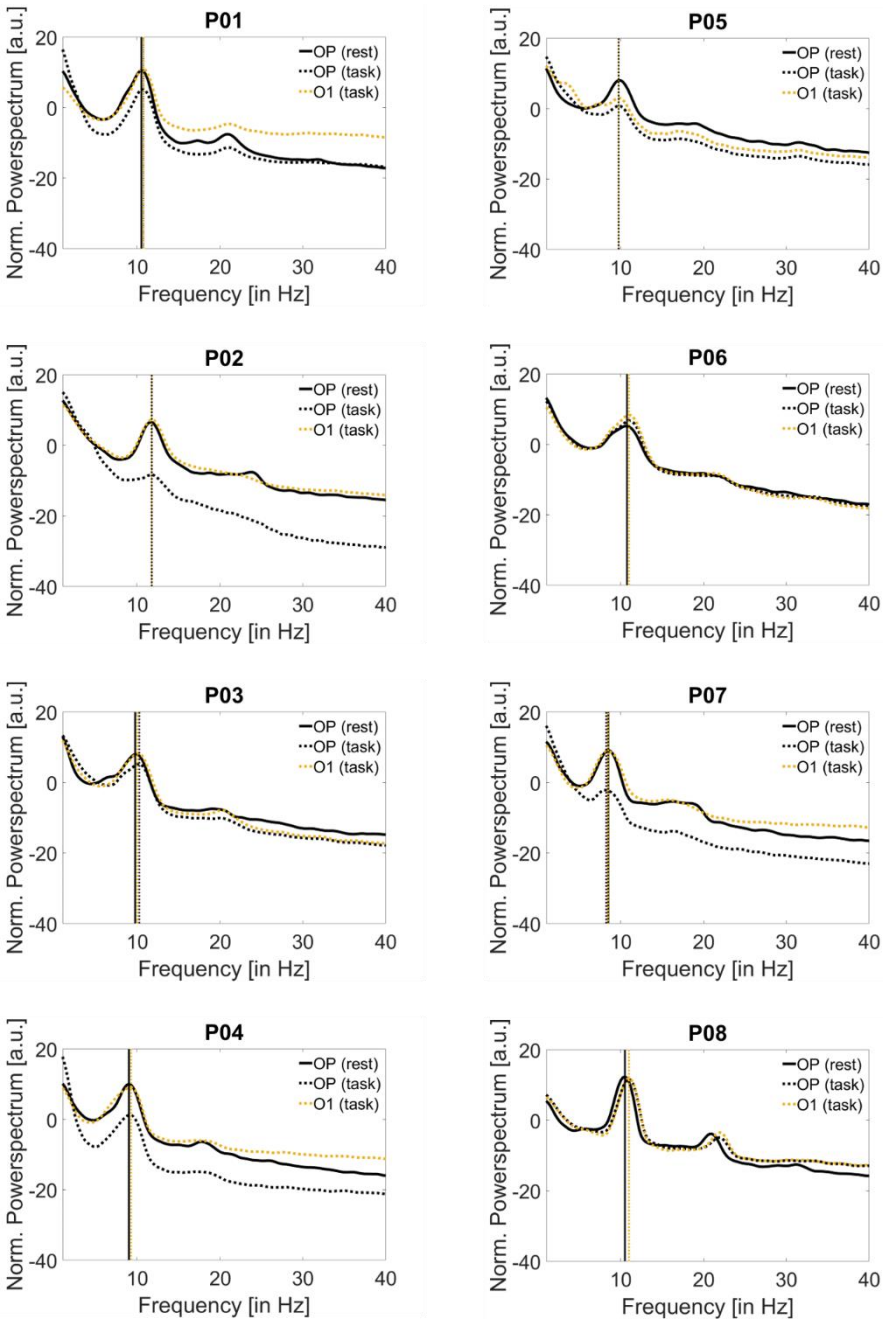

SUPPLEMENTARY FIGURE 6. Normalized power spectrum for each participant at rest (5-min eyes-closed recording) and during the task (Stage 1 dataset) from 1 to 40 Hz computed with OP-cluster and O1-electrode.

SUPPLEMENTARY TABLE 7. Individual data for fast/slow phase bins in Stage 2 including only trials that hit the fast/slow phases. For each participant, the number of trials (max=100), the tested angular points (degrees), and the mean RTs (ms) are reported for the fast and slow phase bins tested in Stage 2. Statistics indicate the results (t value, degrees of freedom, p-value, Cohen's d_z and 95%-confidence intervals CI) of an unpaired t-test (right-tailed, $p<0.05$) comparing slow vs. fast RTs individually. Group level data and statistics are also reported.

	Slow phase bin			Fast phase bin								
Part.	**No. of trials**	**Phase bin**	**Mean (SD) RTs [in ms]**	**No. of trials**	**Phase bin**	**Mean (SD) RTs [in ms]**	**RT diff. phases [in ms]**	**Statistics**				
								t	**dof**	**p**	**dz**	**RT diff. 95% CI**
1	85	162°	198 (34)	71	234°	201 (37)	-3	-0.51	154	.69	-.08	[-12.22 6.44]
2	68	162°	201 (39)	48	18°	210 (31)	-9	-1.25	114	.89	-.24	[-19.77 2.75]
3	60	90°	199 (31)	44	126°	203 (27)	-3	-0.53	102	.70	-.11	[-12.76 6.54]
4	47	306°	204 (37)	49	234°	194 (42)	10	1.28	94	.10	.26	[-3.04 23.68]
5	29	54°	189 (35)	44	306°	201 (27)	-3	-0.46	71	.68	-.11	[-15.24 8.53]
6	40	54°	209 (36)	54	18°	201 (27)	8	1.30	92	.10	.26	[-2.29 19.07]
7	48	306°	202 (30)	56	270°	201 (43)	1	0.07	102	.47	.01	[-11.60 12.66]
8	64	306°	190 (39)	51	54°	196 (32)	-6	-0.90	113	.81	-.17	[-17.28 5.07]
Mean (SD)	**55 (18)**	**--**	**199 (7)**	**52 (9)**	**--**	**200 (5)**	**-1 (7)**	**--**	**--**	**--**	**--**	**--**
Group level	**441**	**--**	**199 (7)**	**417**	**--**	**200 (5)**	**-1**	**-0.25**	**7**	**.60**	**-.09**	**[-6.38 5.20]**

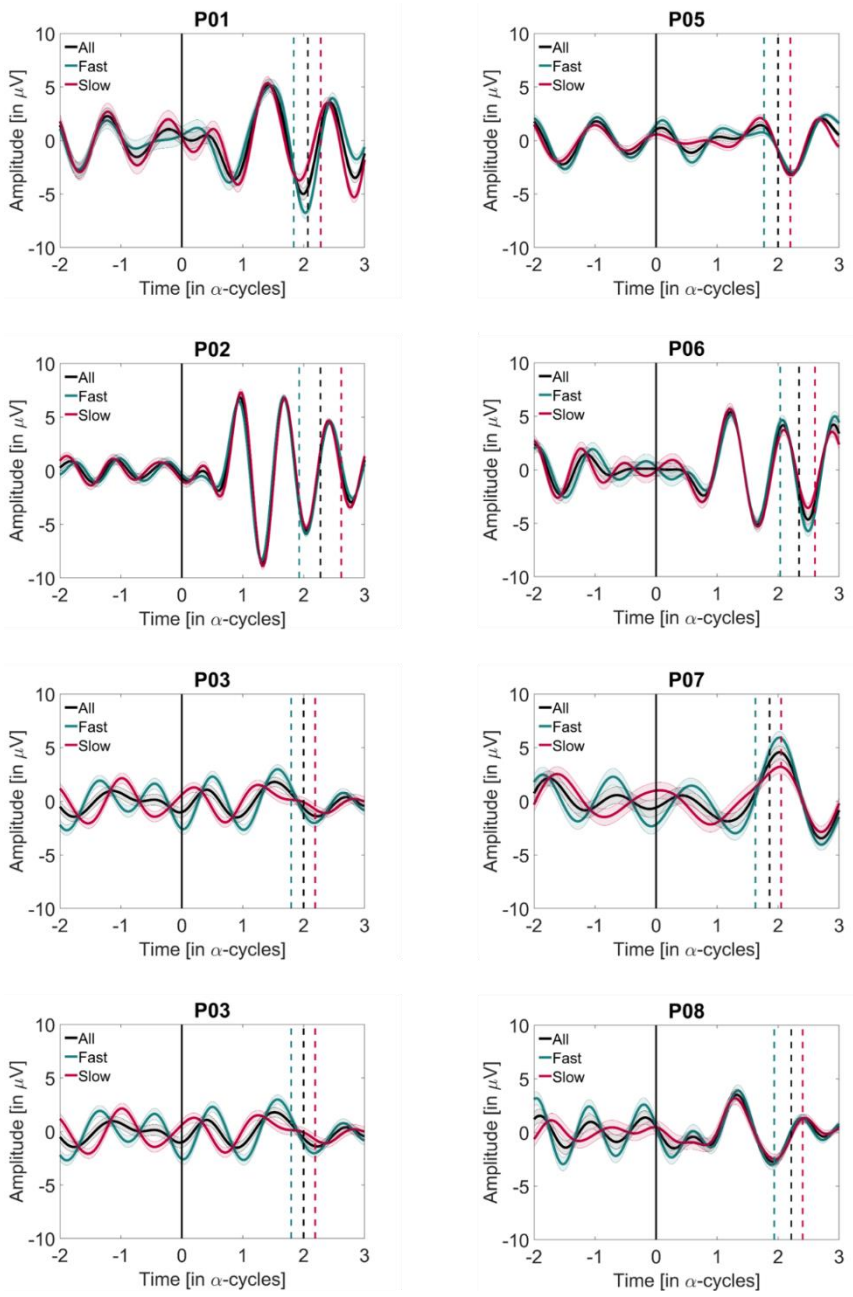

SUPPLEMENTARY FIGURE 7. Individual narrow-band ERPs for subjects from Stage 1 dataset time-locked to visual stimulus presentation denoting valid trials (black), fast trials (green), and slow trials (red). All plots include SEM interval shading. Dashed vertical lines are plotted to show the mean RT of the trials belonging to each subject (Table S1).

Correlation between RTs and prestimulus a-power

According to α-theories, in addition to phase dependency, the power of spontaneous pre-stimulus oscillations in the α-band has relevance for perception (Lindsley 1952; Lansing et al. 1959; Klimesch et al. 2007; Mathewson et al. 2011; Jensen et al. 2014). Despite the fact that our approach was not optimized to find behavioural differences as a function of power, we decided to explore a possible effect of pre-stimulus α-power in relation to slow/fast RTs, as suggested by previous evidence (Walsh 1952; Lansing et al. 1959; Bompas et al. 2015; Ruzzoli et al. 2019). Specifically, we anticipated that low pre-stimulus α-power would be associated with faster RTs. To this aim, we selected trials from Stage 1 (excluding the RT criterion 50 - 300 ms, in order to increase RT variability). To maximize potential differences in RTs as a function of the α-power, for each participant, we calculated the pre-stimulus power associated with the lower and the higher terciles of the RTs distribution. Data were band-pass filtered 5-15 Hz (Butterworth filter order 2, two-pass), epoched from –1000 ms to 0 ms (i.e., stimulus onset), demeaned and detrended. We computed power by means of the Hilbert transform and averaged within the epoch and across the occipito-parietal cluster used to calculate the IFoI. Please note that this cluster of electrodes has been previously associated to power-behavioural modulation (Myers et al. 2014; Bompas et al. 2015; Samaha et al. 2015; Benwell et al. 2017; Harris et al. 2018; Ruzzoli et al. 2019). Power was normalized with respect to the mean power of each participant and transformed to decibels. Group-level data (see **Supplementary Figure 8** and **Supplementary Table 8** for individual results, and **Supplementary Figure 9** for group results) were analysed using a t-test (left-tailed, $\alpha = 0.05$). No relationship was detected between pre-stimulus α-power and RTs at group ($t(7)= -0.0059$, $p = 0.4977$, $d_z = -0.0021$) nor at the individual level (all ps > 0.1) for all but one single participant ($t(584)= -4.1441$, $p = 0.00002$, $d_z= -0.3424$).

We speculate that the null relation between α-power and RTs in these data is caused by a lack of variability. Please note that despite this relationship has been reliably established in the literature (Ruzzoli et al. 2019; Lansing et al. 1959; Bompas et al. 2015; Walsh 1952), the present study was not optimized to reveal it. In particular, there was little variability in α-power during the experiment, because we introduced measures to achieve a consistently high α-power throughout the task (e.g., eyes closed) to facilitate reliable phase estimations. To ascertain this possibility, we compared the variability

in α-power in the present data with the data of another experiment where an effect of power has been found on a visual unspeeded detection task (Ruzzoli et al. 2019, data can be found here: https://osf.io/adrwv/). We found that α-power variability was about 4.5 times lower in the present study compared to the previous one (SD = 2dB vs. SD = 9 dB, respectively).

SUPPLEMENTARY TABLE 8. Number of trials, mean (SD) RT, and mean (SD) log-transformed and normalized pre-stimulus α-power (dB) for slow and fast trials. Individual t-tests assess statistical difference in the α-power ($p<0.05$). Only P01 showed a significance difference in the α-power between slow and fast trials.

	Slow trials			Fast trials			Statistics	
Part.	**No. of trials**	**Mean (SD) RTs [in ms]**	**Mean (SD) ΔPower [in dB]**	**No. of trials**	**Mean (SD) RTs [in ms]**	**Mean (SD) ΔPower [in dB]**	**t**	**p =**
1*	293	226 (20)	0.04 (0.94)	293	167 (20)	-0.35 (1.30)	-4.14	**<.001**
2	336	238 (24)	-0.16 (1.25)	336	156 (28)	-0.16 (1.27)	-0.02	.49
3	257	234 (20)	-0.15 (1.02)	257	179 (11)	-0.08 (1.06)	0.83	.80
4	273	239 (25)	-0.13 (0.92)	273	167 (16)	-0.06 (0.95)	0.87	.81
5	392	228 (21)	-0.40 (1.47)	392	170 (17)	-0.25 (1.45)	1.38	.92
6	341	256 (19)	-0.21 (1.14)	341	182 (16)	-0.06 (1.08)	1.75	.96
7	346	251 (19)	-0.24 (1.29)	346	181 (28)	-0.14 (1.23)	0.97	.83
8	225	238 (20)	-0.06 (1.23)	225	175 (21)	-0.20 (1.16)	-1.28	.10
Mean (SD)	***308 (55)***	***239 (22)***	**-0.12 (1.16)**	***308 (55)***	**172 (20)**	**-0.16 (1.19)**	--	--

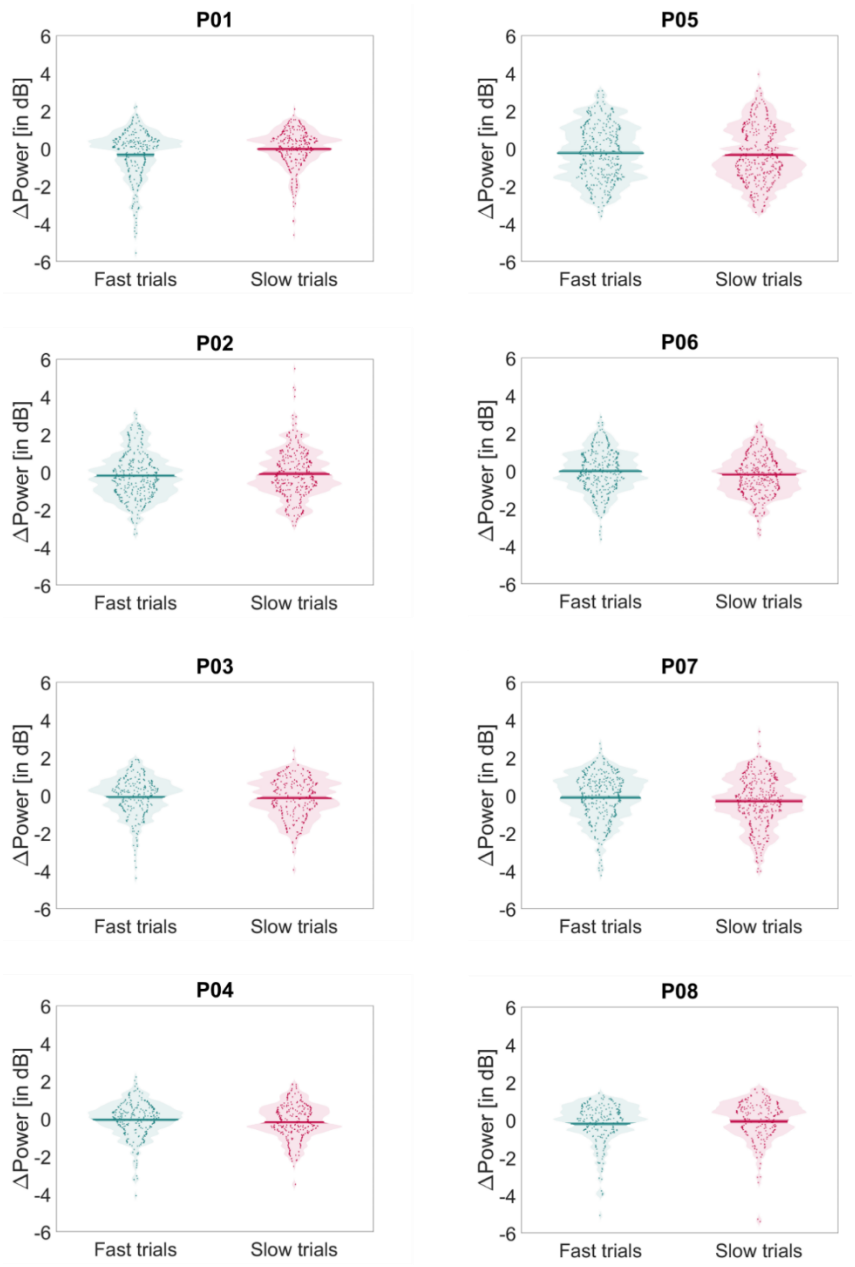

SUPPLEMENTARY FIGURE 8. Individual pre-stimulus α-power log-transformed and normalized by the mean power [in dB] over all trials in Stage 1 for fast (green) and slow (red) trials. Dots denote the power for each trial at individual level. Violin plots include the mean ± SEM power at individual level.

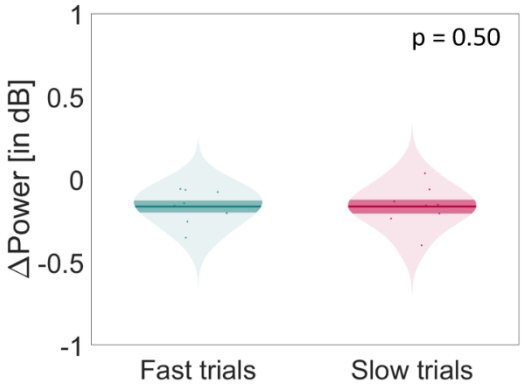

SUPPLEMENTARY FIGURE 9. Mean (dark line) ± SEM (shaded area) pre-stimulus α-power at group-level. Dots denote normalized mean power at individual-level, y-axis represents normalized power [in dB] for the fast and slow trials (x-axis). P-value of the result of the paired-test of the mean power from fast/slow trials.

ANNEX II - Using occipital α-bursts to modulate behaviour in real-time

METHODS: Algorithm for real-time burst-triggering of stimuli

To trigger a visual flash (target), the BCI setting iterated through the following steps:

1. *Data acquisition.* A 45-second sliding window (containing 22500 data points) was used to update an EEG data buffer with the most recent available data from the Oz-electrode and used for the estimate of background power (as in Whitten et al. 2011).
2. *Data reflection.* The first and last 2 s of data from the 45-s window were reversed in time and concatenated to the beginning and end (respectively) of the data buffer, leading to a 49-second window. This procedure attenuated edge artifacts from filtering and computing time-frequency analysis (Cohen 2014).
3. *Data filtering.* Data in the 49-second window was band-pass forward filtered between 0.5 and 45-Hz with a 4th-order Butterworth filter, and data was demeaned using MATLAB built-in functions.
4. *Time-frequency analysis.* Time-frequency transformation of the 49-second window was performed using 6-cycle Morlet wavelets (Grossmann and Morlet 1984) with 18 logarithmically spaced centre frequencies (as in Whitten et al. 2011), the IFoI was the 10th frequency and the approximate frequency-band ranged from 2 to 38 Hz.
5. *Data trimming.* EEG data and wavelet-derived power from the 49-second window was trimmed and reflected edges were removed, leading to the original 45-second window of the data buffer (Cohen 2014).
6. *Log(frequency)-log(power) fitting.* The wavelet-derived power spectrum was linearly fit in log(frequency)-log(power) coordinates using a robust regression with bisquare weighting (Holland and Welsch 1977; Kosciessa et al. 2020) to improve the linear fit of the background spectrum (Donoghue et al.

2020), with the underlying assumption that the EEG background spectrum is characterized by coloured noise of the form *A*f(-a)* (Buzsáki and Mizuseki 2014; He et al. 2010; Linkenkaer-Hansen et al. 2001). To further improve the linear fit of the background spectrum with the robust regression (Donoghue et al. 2020), power estimates within a wavelet passband around the IFoI (i.e., IFoI ± 1) were removed prior to fitting.

7. *Threshold estimations.* Power thresholds for rhythmicity (i.e., the occurrence of α-bursts) and non-rhythmicity (i.e., non-oscillatory signal) at each frequency was set at different percentiles of $\chi^2(2)$-distribution of power values, centred on the linearly fitted estimate of background power at the relevant frequency (for details see Whitten et al. 2011):
    - *Artifact threshold:* The power value was set at the 95th percentile of a $\chi^2(2)$-distribution of power values centred at the slowest frequency (around ~2 Hz) to discern between the true α-bursts and high-amplitude in the EEG signal due to eye blinks and muscle artifacts.
    - *Burst power threshold:* The power value was set at the 95th percentile of a $\chi^2(2)$-distribution of power values centred at the IFoI-task frequency.
    - *No-burst power threshold:* The power value was set at the 50th percentile of a $\chi^2(2)$-distribution of power values centred at the IFoI-task frequency.
    - *Duration threshold:* A theoretical duration threshold of a minimum duration of 2.5 cycles (i.e., ~200 ms prestimulus threshold-window containing 100 data points) of the IFoI was used and set at the end of the 49-second window.
8. *Checking necessary conditions for triggering stimulus.* Both power and duration criteria had to satisfy the necessary conditions for triggering stimulus depending on the trial EEG activity-type (i.e., burst/no-burst):
    - *Burst trials:* All data points from the prestimulus threshold-window had to be higher than *Burst power threshold* and lower than *Artifact threshold*.
    - *No-burst trials:* All data points from the prestimulus threshold-window had to be lower than *No-burst power threshold* and lower than *Artifact threshold*.

If in a given trial these criteria were met, the BCI setting continued and triggered the corresponding visual stimuli for the trial-type; otherwise, the BCI setting algorithm returned to step (1) and updated the initial EEG data buffer.

9. *Stimulus presentation.* Visual targets (go or no-go, depending on condition) were delivered after the validation depending on the trial-type.
10. *Button response.* Reaction time was collected from a button press via a response box connected to the parallel port. If no response was given by the participant (because of a no-go trial or a missed go trial), then the time-out of 1-second was reached and the BCI setting iterated towards the next step.
11. *Data acquisition update.* After the response, we updated the 45-second window with the most recent available data, as in step (1), and re-did the following steps until reaching again step (5).
12. *Trial validity criterion*. Check of trial validity with the updated data. This criterion was set in order to exclude trials in real-time and ensure that (no-)burst activity conditions were met during the computational time of the pipeline (~72 ± 5 ms) between acquisition of data in step (1) and stimulus presentation in step (9). Only trials that satisfied the following criteria were accepted as valid:
    - *(No-)burst criterion:*
        - *True detection of burst event:* 90% of data points of the last 3 cycles (~300 ms) of the IFoI before stimulus onset had to be higher than the *Burst power threshold* and lower than the *Artifact threshold*, both thresholds determined at step (7).
        - *True-detection of no-burst event:* 90% of data points of the last 3 cycles (~300 ms) of the IFoI before stimulus onset had to be lower than the *No-burst power threshold* and lower than the *Artifact threshold*, both thresholds determined at step (7).

- *Reaction time criterion*: RT within 50 and 1000 ms (only applied in the go condition)[6].

13. *Trial counter*. If the intended number of trials was reached in a given block (N=40), the algorithm of the BCI setting stopped; otherwise, another iteration started until the desired number of trials per condition was collected. In between blocks, participants had a break and a new block begun with the BCI setting starting from step (1).

Note that if at any point of the iteration a step/criterion was not satisfied, the BCI setting started a new iteration from step (1).

[6] Since the *Reaction time criterion* only applied to go trials, some no-go trials with actual responses were accepted as valid trials in this section (*see Exploratory Analysis* for further details).

METHODS: Different red lights in no-go trials across participants

Given that participants had two types of red-lights to adjust the intensity similarly to the green-light, we wanted to assess whether there was any relationship between the red-light used for the participants and their average reaction time (RT) in the task (**Supplementary Table 2**). We computed a t-test (independent samples) with α-level = 0.05 to compare the mean RTs between the first six participants (P01-P06; red light with 933 kΩ) and from the last six participants (P07-P012; red light with 820 kΩ). The result was not significant (*t (10) = 0.34, p = .74, dz = .20*). Thus, we can conclude that using different red lights across participants for the no-go trials did not influence the RTs.

SUPPLEMENTARY TABLE 9. Individual data of reaction time (RT) for burst and no-burst trials. For each participant, the mean (SD) RT of all trials, the Coefficient of Variation (CV), the mean (SD) RT for burst trials, the mean (SD) RT for no-burst trials, and the difference in mean RT between burst and no-burst. Individuals assess of statistical difference in the RT from the one-tailed permutation test ($p<0.05$). P-values in bold denote the significance difference in the RT between burst and no-burst trials for 5 participants (P07, P09, P10, P11, P12). RT difference in bold highlight the results that go in line with our hypothesis.

Part.	Mean (SD) RT (all trials) [in ms]	CV RT	Mean (SD) RT burst [in ms]	Mean (SD) RT no-burst [in ms]	RT diff. [in ms]	Statistics	
						p	d
1	457 (74)	0.16	462 (84)	450 (59)	**12**	.12	0.17
2	525 (104)	0.20	534 (107)	514 (101)	**20**	.09	0.19
3	456 (73)	0.16	460 (80)	450 (64)	**10**	.18	0.13
4	514 (99)	0.19	523 (104)	506 (95)	**17**	.12	0.17
5	490 (97)	0.20	486 (99)	492 (91)	-6	.67	-0.06
6	458 (92)	0.20	461 (90)	450 (91)	**12**	.18	0.13
7	592 (118)	0.20	606 (123)	576 (111)	**31**	**.03**	0.26
8	453 (99)	0.22	451 (95)	454 (103)	-2	.61	-0.04
9	428 (69)	0.16	435 (70)	416 (66)	**19**	**.03**	0.28
10	486 (101)	0.21	513 (115)	457 (79)	**55**	**<.001**	0.56
11	450 (81)	0.18	462 (76)	422 (56)	**40**	**<.001**	0.60
12	433 (84)	0.19	441 (82)	417 (75)	**24**	**.02**	0.30
Mean (SD)	**479 (91)**	**0.19 (0.02)**	**486 (94)**	**467 (83)**	**19 (17)**	**<.001**	**0.22 (0.20)**

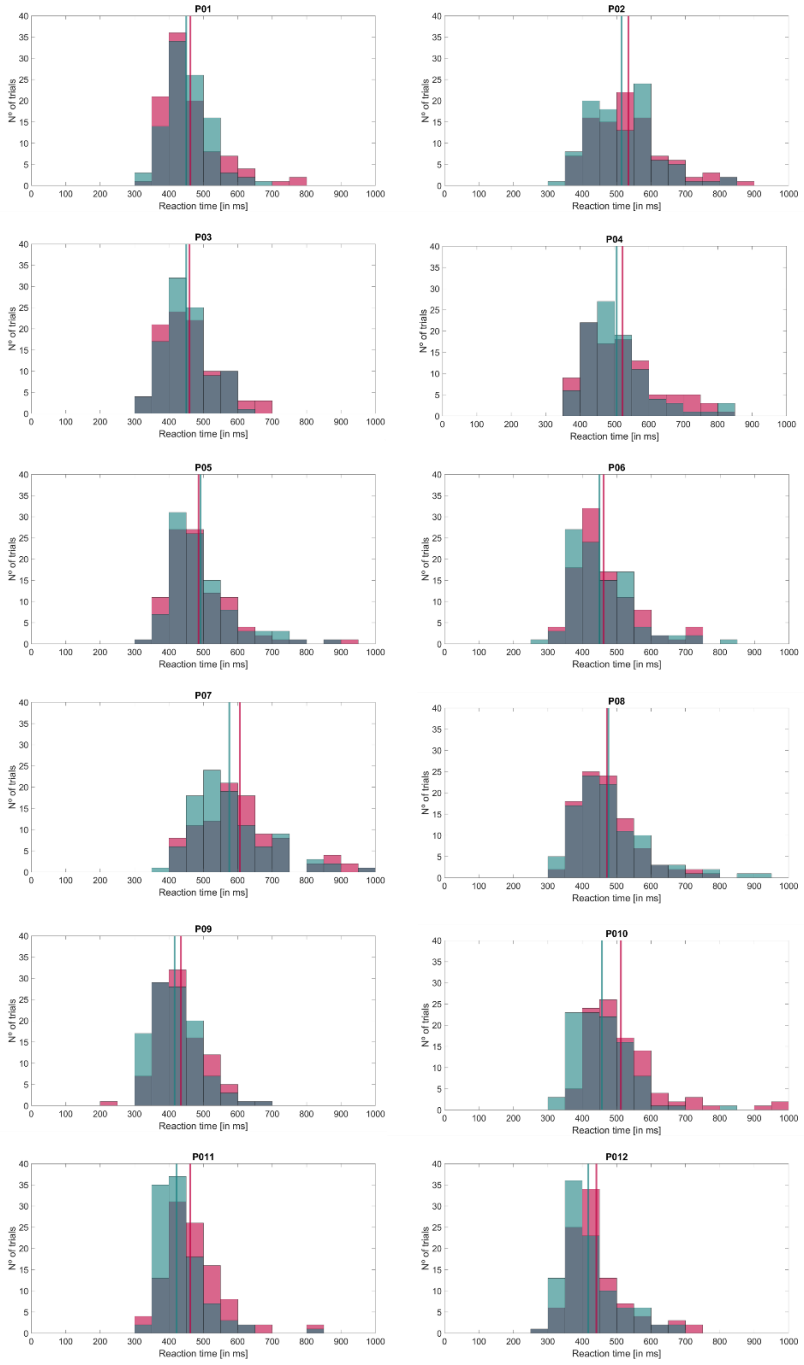

SUPPLEMENTARY FIGURE 10. Individual histogram of reaction times (RT) for burst (in red) and no-burst (in green) for all validated trials [in ms]. Vertical solid lines denote the mean RT of burst (in red) and no-burst trials (in green).

SUPPLEMENTARY TABLE 10. Individual power at the time-window of interest (TWoI) and amplitude thresholds data for burst and no-burst trials. For each participant, the mean (SD) pre-stimulus α-power [in μV^2] for burst and no-burst trials. Individual t-tests assess statistical difference in the α-power and amplitude thresholds ($p<.05$) and the effect size (Cohen's d; d) is also provided. All participants showed a significant difference ($p<.001$) in both the α-power and the amplitude thresholds between burst and no-burst.

	POWER TWoI					**AMPLITUDE THRESHOLDS**				
Part.	**Mean (SD) burst [in μV^2]**	**Mean (SD) no-burst [in μV^2]**	**Diff. power [in μV^2]**	**d**	**p**	**Mean (SD) burst [in μV]**	**Mean (SD) no-burst [in μV]**	**Diff. amp. Th. [in μV]**	**d**	**p**
1	3.46 (1.77)	0.16 (0.09)	3.30	2.63	**<.001**	1.23 (0.23)	0.28 (0.05)	0.94	5.66	**<.001**
2	6.14 (2.71)	0.28 (0.15)	5.86	3.05	**<.001**	2.75 (0.89)	0.64 (0.21)	2.11	3.27	**<.001**
3	7.08 (5.02)	0.13 (0.07)	6.96	1.96	**<.001**	1.26 (0.42)	0.29 (0.10)	0.97	3.19	**<.001**
4	4.93 (2.93)	0.09 (0.04)	4.84	2.34	**<.001**	0.80 (0.15)	0.20 (0.04)	0.68	6.02	**<.001**
5	4.52 (1.91)	0.18 (0.11)	4.34	3.21	**<.001**	1.70 (0.25)	0.39 (0.06)	1.31	7.13	**<.001**
6	6.45 (3.71)	0.20 (0.13)	6.25	2.38	**<.001**	2.13 (0.62)	0.49 (0.14)	1.64	3.66	**<.001**
7	2.83 (1.33)	0.10 (0.07)	2.73	2.91	**<.001**	1.08 (0.36)	0.25 (0.08)	0.83	3.20	**<.001**
8	4.21 (2.39)	0.16 (0.09)	4.05	2.40	**<.001**	1.36 (0.27)	0.32 (0.06)	1.05	5.29	**<.001**
9	8.08 (5.55)	0.20 (0.14)	7.89	2.01	**<.001**	1.78 (0.22)	0.41 (0.05)	1.37	8.45	**<.001**
10	3.45 (1.27)	0.17 (0.08)	3.27	3.63	**<.001**	1.86 (0.46)	0.43 (0.11)	1.43	4.23	**<.001**
11	5.84 (2.65)	0.16 (0.10)	5.68	3.03	**<.001**	1.57 (0.37)	0.36 (0.09)	1.21	4.46	**<.001**
12	12.96 (7.17)	0.38 (0.24)	12.58	2.48	**<.001**	3.13 (0.84)	0.72 (0.19)	2.41	3.97	**<.001**
Mean (SD)	**5.83 (2.75)**	**0.18 (0.08)**	**5.65 (2.69)**	**2.10**	**-**	**1.72 (0.68)**	**0.40 (0.16)**	**1.33 (0.52)**	**2.52**	**-**

Supplementary Fig. 3 shows the violin plots of the overall mean of power within the time-window of interest (TWoI) for burst and no-burst trials individually for each participant. We also plotted the average of the trials around stimulus onset (-2 to 1s) to visualize the difference in mean power between burst and no-burst conditions. In **Supplementary Fig. 4,** all the individual plots show a clearly a visual difference between the mean (SD) power across conditions. In particular, burst trials show a larger variability (i.e., SD) in power reflected in the shaded area compared to no-burst trials within the TWoI.

Furthermore, we decided to see the relationship between the log-transformed mean power of the TWoI and the reaction time (RT) for burst (in red) and no-burst (in green) trials at individual level. **Supplementary Fig. 5** shows that there is a clear distinction between our independent variable (i.e., the log-transformed mean power) for burst and no-burst trials, whereas the difference between the dependent variable (i.e., RTs) varies across participants.

Finally, we checked that amplitude thresholds were correctly adjudicated according to the ongoing α-burst activity. We calculated the amplitude thresholds across participants for burst (Mean = 1.72 μV; SD = 0.68 μV) and no-burst (Mean = 0.40 μV; SD = 0.16 μV) trials and also for each participant (see **Supplementary Table 4**). Overall, the mean amplitude difference between burst and no-burst thresholds was 1.33 μV (SD = 0.52; Max = 2.41 μV; Min = 0.68 μV). We assessed the difference between burst and no-burst amplitude thresholds by applying a one-tailed t-test (independent samples) with α-level = .05. All participants showed a significant p-value ($p = <.001$; **Supplementary Table 4**, **Supplementary Fig. 6**).

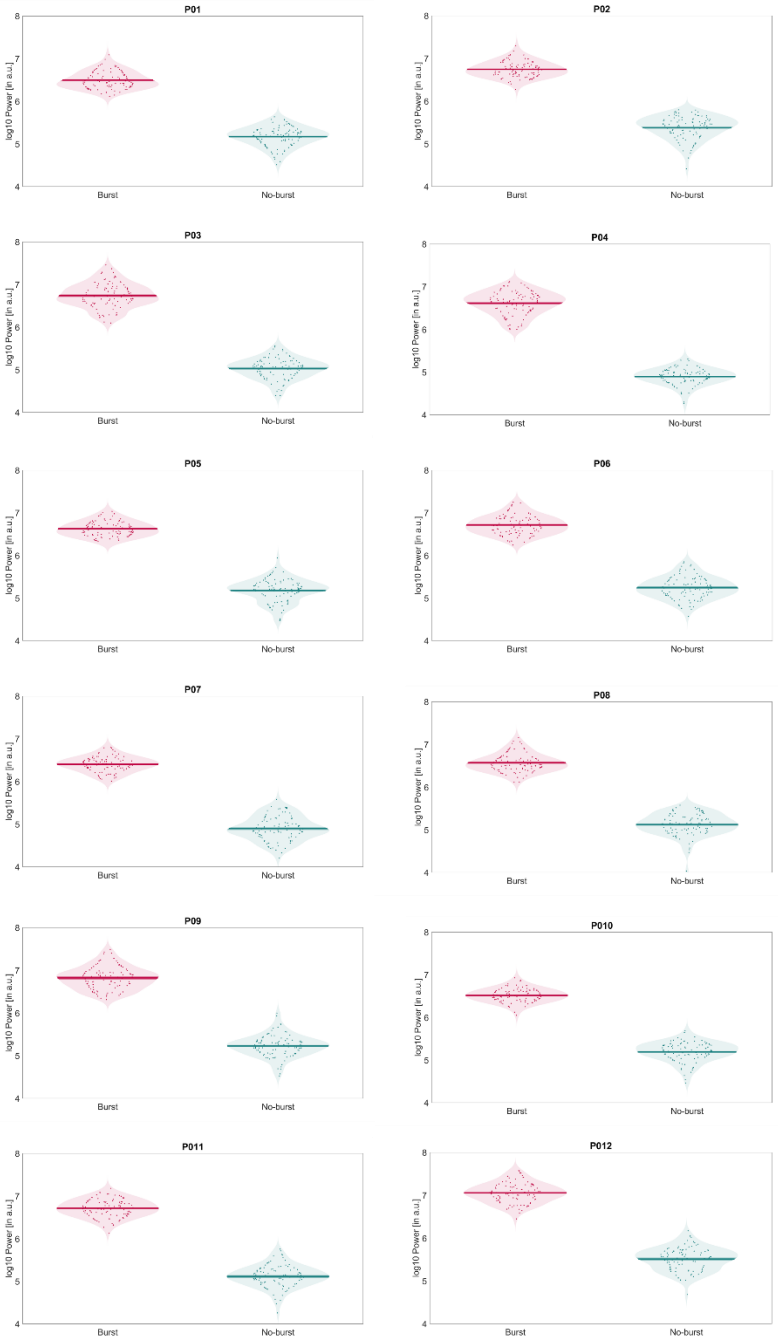

SUPPLEMENTARY FIGURE 11. Individual violin plots of the mean power for burst (in red) and no-burst (in green) for validated trials. Violin plots include the mean ± SEM power at individual level. Dots denote the mean power at the time-window of interest (TWoI, i.e., the last 3 cycles of IFoI) for each trial.

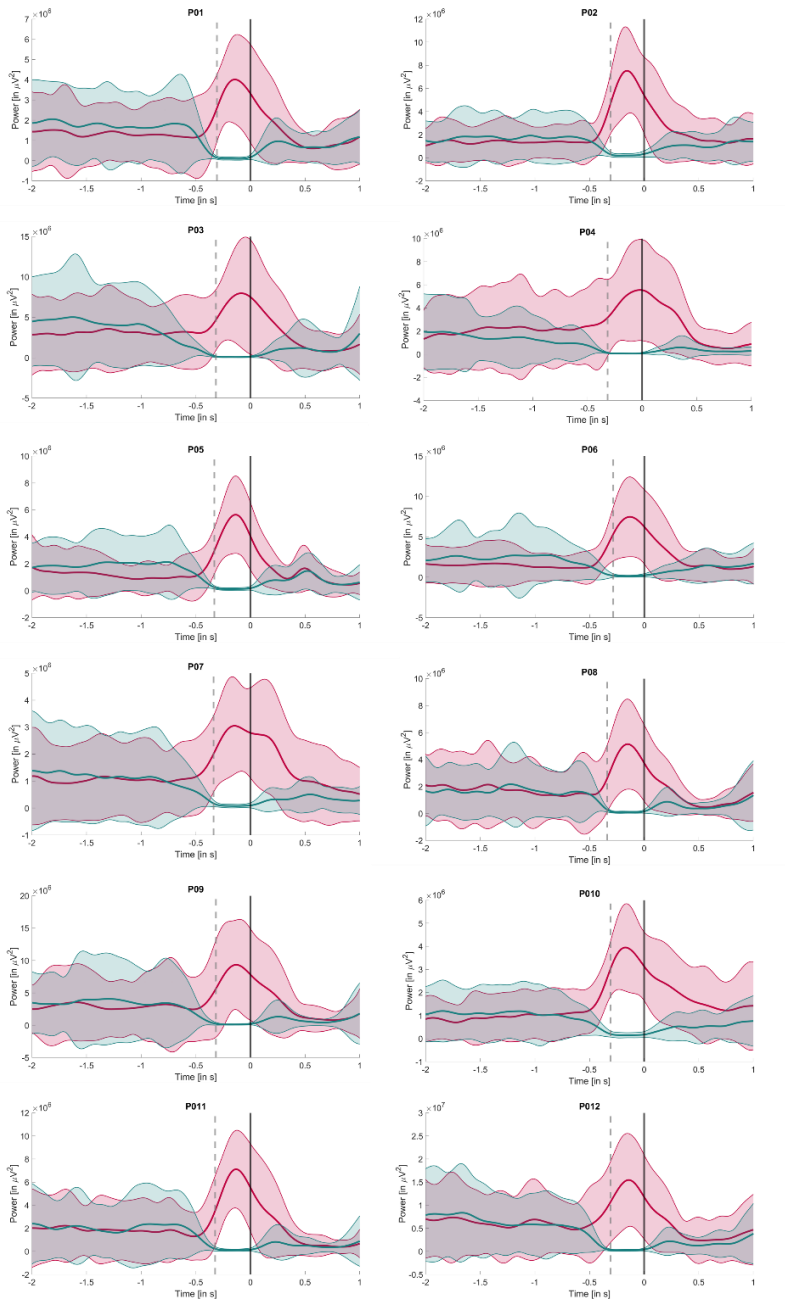

SUPPLEMENTARY FIGURE 12. Individual mean power of burst (in red) and no-burst (in green) trials at individual level within -2 to 1s from stimulus onset. Solid lines denote the mean power of burst and no-burst trials. Shaded areas represent the standard error of the mean (SEM) interval. Solid vertical line denotes the stimulus onset and dotted vertical lines denotes the time-window of interest (TWoI).

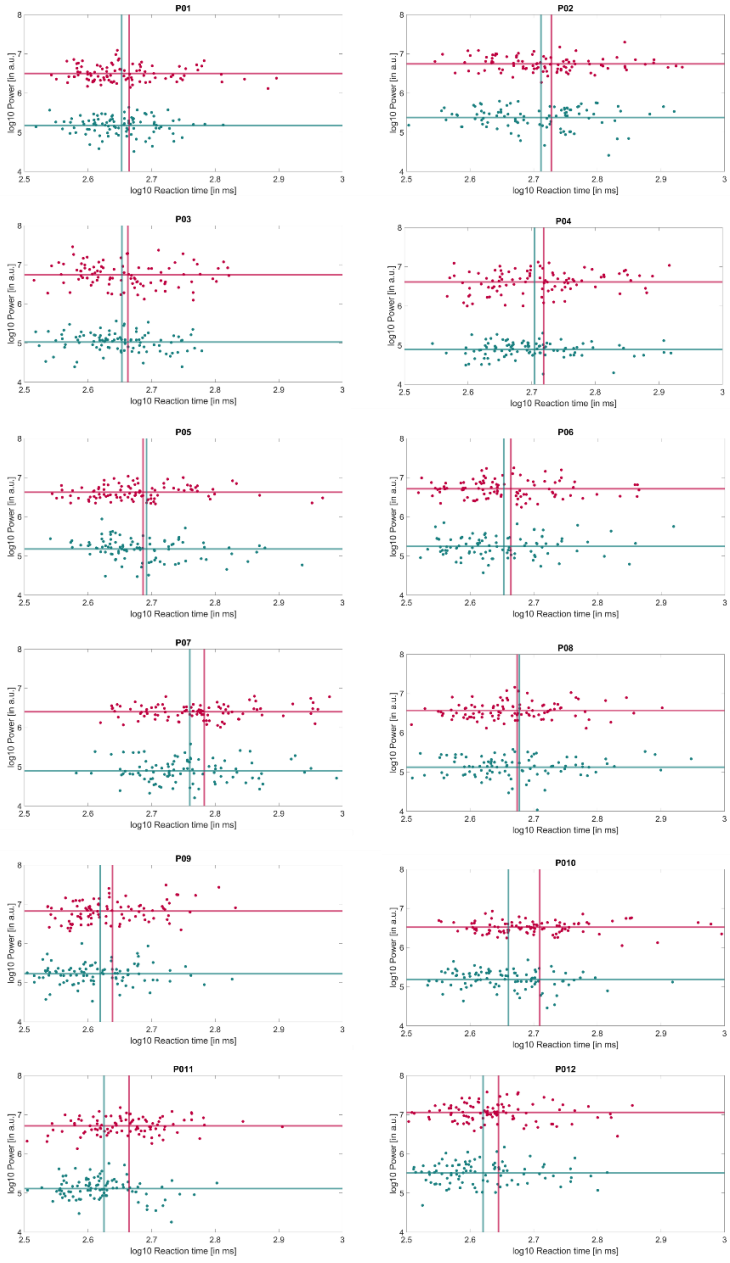

SUPPLEMENTARY FIGURE 13. Individual relationship between the log-transformed mean power at the time-window of interest (TWoI) and the reaction time (RT) for burst (in red) and no-burst (in green) for validated trials. Horizontal solid lines denote the mean power of burst (in red) and no-burst trials (in green), and vertical solid lines denote the mean RT of burst (in red) and no-burst trials (in green). Dots denote the mean power at the TWoI for each trial at individual level.

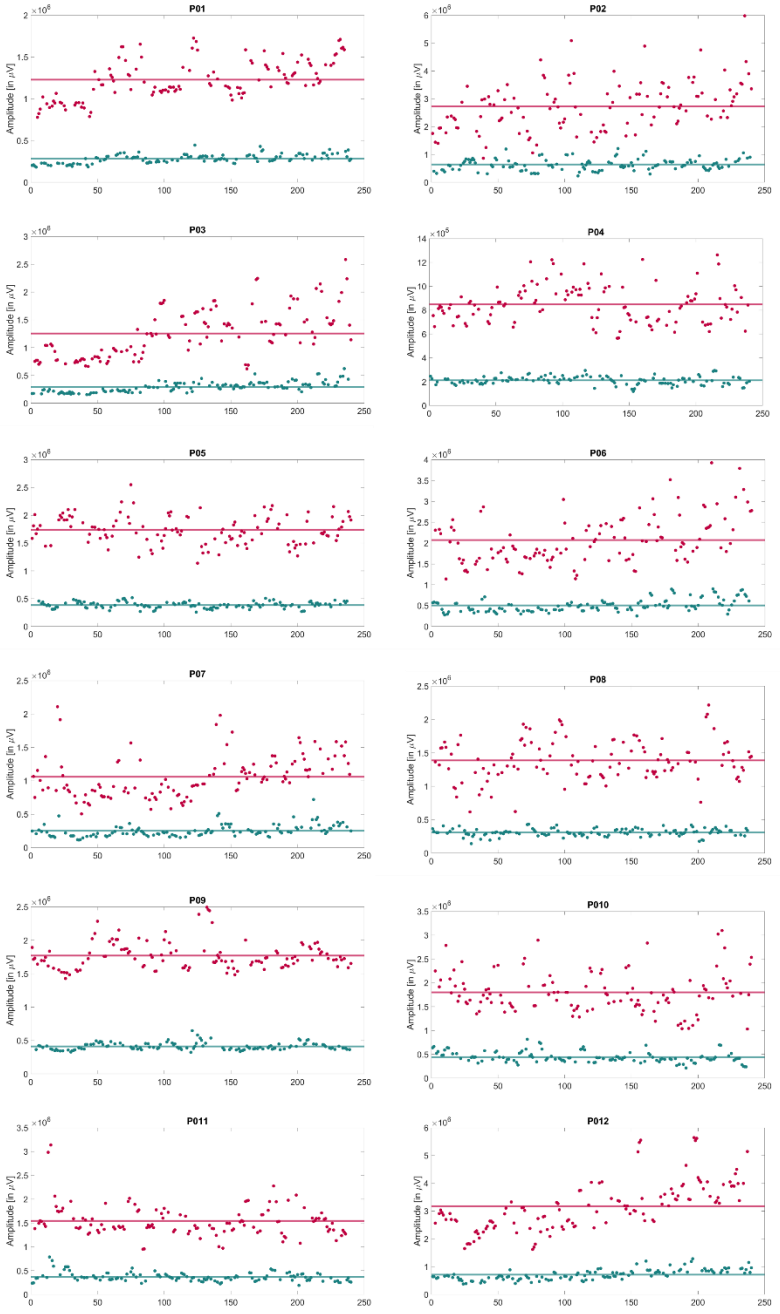

SUPPLEMENTARY FIGURE 14. Individual power thresholds for burst (in red) and no-burst (in green) for validated trials. Dots denote the amplitude thresholds for each trial at individual level for burst (in red) and no-burst trials (in green). Horizontal solid lines denote the mean power threshold for the cloud of dots of burst (in red) and no-burst trials (in green).

SUPPLEMENTARY TABLE 11. Individual difference between amplitude [in dB] and frequency peak [in Hz] of the Individual Frequency of Interest (IFoI) during the task and during the training using Oz-electrode and OP-cluster of electrodes. For each participant, the amplitude and frequency peak of the IFoI during the task and during the training for Oz-electrode and OP-cluster are provided, together with the difference in amplitude and frequency peak between task and training for Oz-electrode, and the difference in frequency peak between OP-cluster and Oz-electrode during the task and the training. NaN denotes that a peak was not found in the power spectrum (P02).

Part.	Oz-electrode				OP-cluster				ΔIFoI Oz task – training		ΔIFoI OP – Oz	
	IFoI (training)		IFoI (task)		IFoI (training)		IFoI (task)				Training	Task
	Peak [in Hz]	Amp. [in dB]	Peak [in Hz]	Amp. [in dB]	Peak [in Hz]	Amp. [in dB]	Peak [in Hz]	Amp. [in dB]	Peak [in Hz]	Amp. [in dB]	Peak [in Hz]	Peak [in Hz]
1	10.25	5.70	10.00	6.87	10.25	3.75	10.00	2.22	**0.25**	-1.17	**0.00**	**0.00**
2	10.75	2.97	10.25	2.19	10.50	-10.50	NaN	NaN	**-0.50**	-0.78	**-0.25**	**NaN**
3	10.50	9.91	10.50	9.11	10.50	8.55	10.50	7.91	**0.00**	-0.80	**0.00**	**0.00**
4	10.50	11.26	10.25	10.85	10.50	11.24	10.50	10.82	**-0.25**	-0.41	**0.00**	**0.25**
5	11.00	2.23	10.75	3.89	11.00	-0.25	10.75	-0.91	**-0.25**	1.65	**0.00**	**0.00**
6	10.00	2.00	9.75	4.29	9.50	1.54	9.50	2.62	**-0.25**	2.29	**-0.50**	**-0.25**
7	11.25	3.73	11.00	5.06	11.25	2.16	11.00	3.86	**-0.25**	1.33	**0.00**	**0.00**
8	11.25	5.36	11.00	2.68	11.25	3.90	11.00	3.16	**-0.25**	-2.69	**0.00**	**0.00**
9	10.50	6.72	10.25	6.94	10.50	5.01	10.50	6.20	**-0.25**	0.22	**0.00**	**0.25**
10	10.25	2.18	10.00	2.79	10.25	0.55	10.00	1.11	**-0.25**	0.61	**0.00**	**0.00**
11	10.75	2.57	10.50	6.04	10.75	0.25	10.75	6.00	**-0.25**	3.47	**0.00**	**0.25**
12	10.25	6.78	10.00	7.97	10.25	6.90	10.25	8.21	**-0.25**	1.19	**0.00**	**0.25**
Mean	**10.60**	**5.12**	**10.35**	**5.72**	**10.54**	**2.76**	**10.43**	**4.65**	**-0.25**	**0.61**	**-0.06**	**0.07**
(SD)	**(0.41)**	**(3.11)**	**(0.41)**	**(2.73)**	**(0.49)**	**(5.46)**	**(0.46)**	**(3.49)**	**(0.11)**	**(1.63)**	**(0.16)**	**(0.16)**

EXPLORATORY ANALYSIS: RT fits using the ex-Gaussian function

SUPPLEMENTARY TABLE 12. Individual ex-Gaussian fit parameters for burst and no-burst trials. The mean (μ), standard deviation (σ), the exponential parameters (τ), and the log-likelihood (fVal) are provided for burst and no-burst trials. Individuals assess of statistical difference in the RT from the one-tailed permutation test ($p<.05$). 2 participants (P11, P12) showed a significance difference in the μ RT between burst and no-burst trials, 1 participant (P11) showed a significant difference in σ RT between burst and no-bursts, and 2 other participants (P01, P03) showed a significance difference in the τ RT between burst and no-burst trials.

	Burst			**No-burst**			**Diff.**		**Diff.**		**Diff.**	
Part.	**μ RT [in ms]**	**σ RT [in ms]**	**τ RT [in ms]**	**μ RT [in ms]**	**σ RT [in ms]**	**τ RT [in ms]**	**μ RT [in ms]**	**p**	**σ RT [in ms]**	**p**	**τ RT [in ms]**	**p**
1	381	20	82	409	43	41	-28	.99	-23	**.01**	41	**.007**
2	438	53	97	439	68	76	-1	.52	-15	.35	21	.40
3	382	36	78	410	50	41	-28	.94	-15	.25	38	**.02**
4	417	42	106	419	35	88	-1	.52	7	.68	18	.39
5	399	36	87	407	28	85	-8	.73	7	.37	2	.93
6	376	34	86	364	34	86	12	.24	0	.99	-1	.98
7	496	61	110	474	48	101	22	.17	13	**.01**	9	**.01**
8	355	37	96	344	19	110	11	.17	17	.80	-14	.32
9	372	36	63	351	28	65	21	.08	8	.73	-2	.89
10	409	34	103	384	37	73	25	.11	-3	.90	30	.22
11	402	44	60	370	24	52	32	**.02**	20	.08	8	.63
12	370	37	71	344	28	73	26	**.01**	10	.31	-2	.90
Mean (SD)	**400 (38)**	**39 (10)**	**86 (17)**	**393 (41)**	**37 (14)**	**74 (22)**	**7 (20)**	**.13**	**2 (14)**	**.27**	**12 (17)**	**.01**

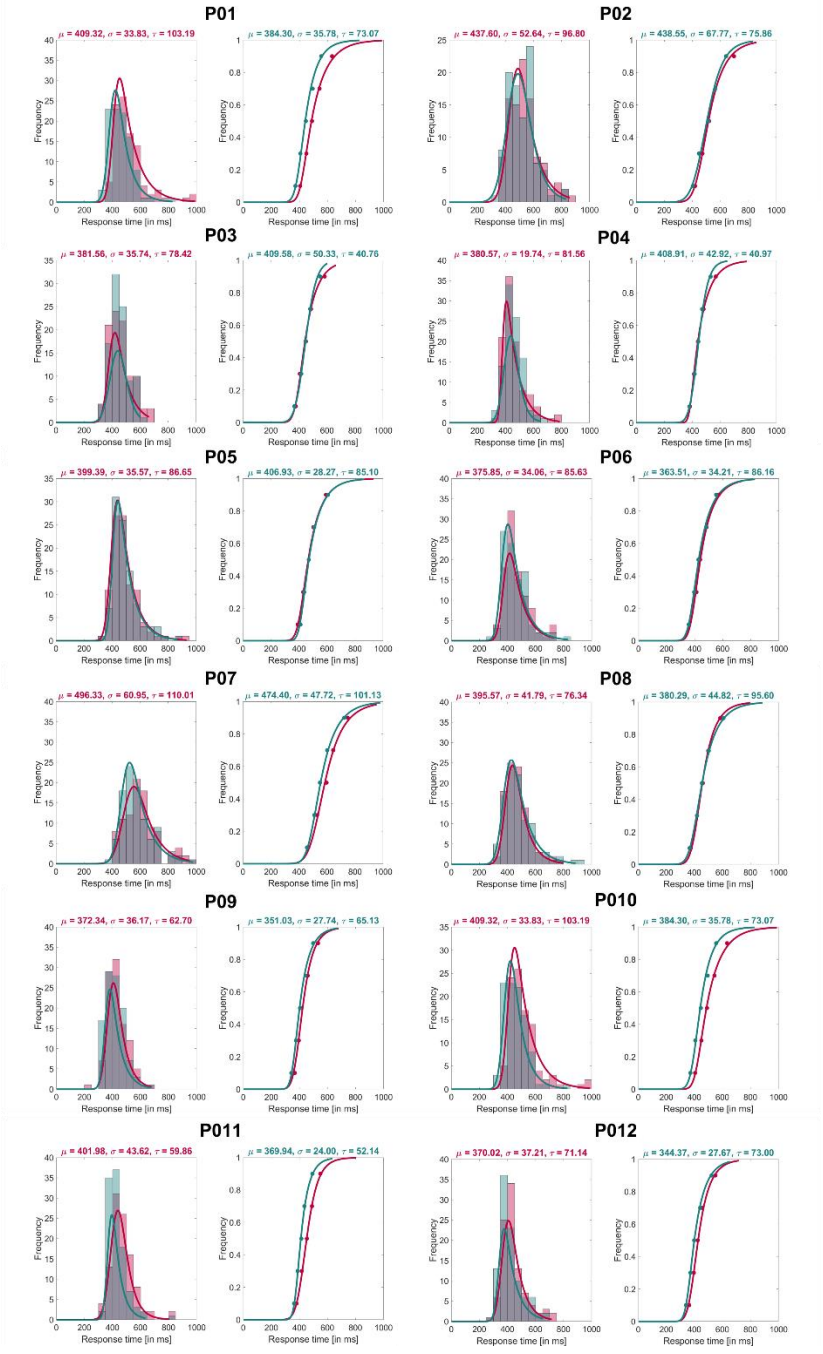

SUPPLEMENTARY FIGURE 15. Individual ex-Gaussian fits for burst (in red) and no-burst (in green) trials. For each participant, the histogram of burst and no-burst trials (on the left) is shown together with the probability density function curve of each trial condition (on the right).

EXPLORATORY ANALYSIS: Commission and omission error rates for burst and no-burst trials

SUPPLEMENTARY TABLE 13. Individual error rates for go and no-go trials. For each participant, the number of trials, the number of errors, and the error rate in each condition (go/burst, go/no-burst, no-go/burst, no-go/no-burst) are reported. Group-level t-tests assess statistical difference in error rates for burst and no-burst conditions for go and no-go trials.

Part.	Go				No-go			
	Burst		No-burst		Burst		No-burst	
	No. of trials	Omission error rate	No. of trials	Omission error rate	No. of trials	Commission error rate	No. of trials	Commission error rate
1	116	**0.17**	110	0.13	24	**0.17**	24	0.13
2	121	**0.21**	111	0.14	24	0.04	24	**0.13**
3	97	**0.01**	96	0.00	24	0.04	24	**0.08**
4	116	0.17	115	0.17	24	**0.08**	24	0.04
5	110	**0.13**	105	0.09	24	0.13	24	0.13
6	99	0.03	99	0.03	24	0.04	24	**0.08**
7	121	0.21	130	**0.26**	24	0.00	24	**0.17**
8	104	**0.08**	97	0.01	24	0.08	24	**0.17**
9	135	**0.29**	120	0.20	24	0.33	24	**0.42**
10	117	**0.18**	109	0.12	24	**0.13**	24	0.08
11	101	**0.05**	97	0.01	24	0.33	24	**0.38**
12	108	**0.11**	101	0.05	24	0.04	24	**0.13**
Mean (SD)	**112 (11)**	**0.14 (0.08)**	**108 (10)**	**0.10 (0.08)**	**24 (0)**	**0.12 (0.11)**	**24 (0)**	**0.16 (0.12)**

SUPPLEMENTARY TABLE 14. Individual phase opposition sum (POS) at stimulus onset for valid-burst trials between fast and slow RT. For each participant, the mean (SD) RT [in ms] and phase [in degrees] of the overall trials, the number of trials, mean (SD) RT [in ms] and mean (SD) phases [in degrees] for fast and slow trials, the difference in RT [in ms] and in phases [in degrees] between fast and slow trials are provided. Individuals and group-level assess of statistical difference in phases from the phase opposition sum (POS) method.

Part.	FAST RT			SLOW RT			Diff. RT [in ms]	Diff. phases [in º]	POS		
	No. trials	Mean (SD) RT [in ms]	Mean (SD) phase [in º]	No. trials	Mean (SD) RT [in ms]	Mean (SD) phase [in º]			POS value	Mean (SD) surrogate POS value	p
1	48	404 (23)	-180 (79)	48	521 (82)	169 (75)	**117**	**-11**	<.001	0.061 (0.064)	.94
2	48	454 (43)	-165 (78)	48	615 (91)	176 (75)	**161**	**-18**	0.002	0.052 (0.059)	.86
3	48	397 (30)	56 (74)	48	522 (63)	128 (75)	**125**	**72**	0.056	0.055 (0.062)	.36
4	48	442 (39)	-20 (78)	48	604 (82)	16 (77)	**162**	**35**	0.007	0.076 (0.074)	.85
5	48	420 (33)	-172 (75)	48	552 (99)	25 (77)	**133**	**-157**	0.192	0.125 (0.092)	.22
6	48	396 (31)	143 (71)	48	527 (80)	-169 (78)	**131**	**48**	0.020	0.035 (0.043)	.48
7	48	516 (52)	-147 (71)	48	697 (105)	138 (78)	**182**	**-75**	0.042	0.038 (0.048)	.32
8	48	408 (34)	-108 (75)	48	536 (74)	-179 (76)	**128**	**-71**	0.047	0.055 (0.061)	.41
9	48	382 (28)	172 (72)	48	488 (59)	86 (77)	**106**	**-86**	0.066	0.046 (0.055)	.26
10	48	435 (34)	-83 (74)	48	589 (116)	17 (71)	**154**	**-67**	0.064	0.035 (0.046)	.18
11	48	406	-27	48	518	-122	**112**	**-95**	0.106	0.060	.20

		(32)	(74)		(65)	(74)				(0.067)	
12	48	384 (32)	-150 (77)	48	499 (76)	163 (72)	**115**	**-47**	0.022	0.031 (0.041)	.42
Mean (SD)	**48**	**420 (38)**	**-**	**48**	**556 (60)**	**-**	**135 (24)**	**-43 (57)**	**0.052**	**0.056 (0.066)**	**.37**

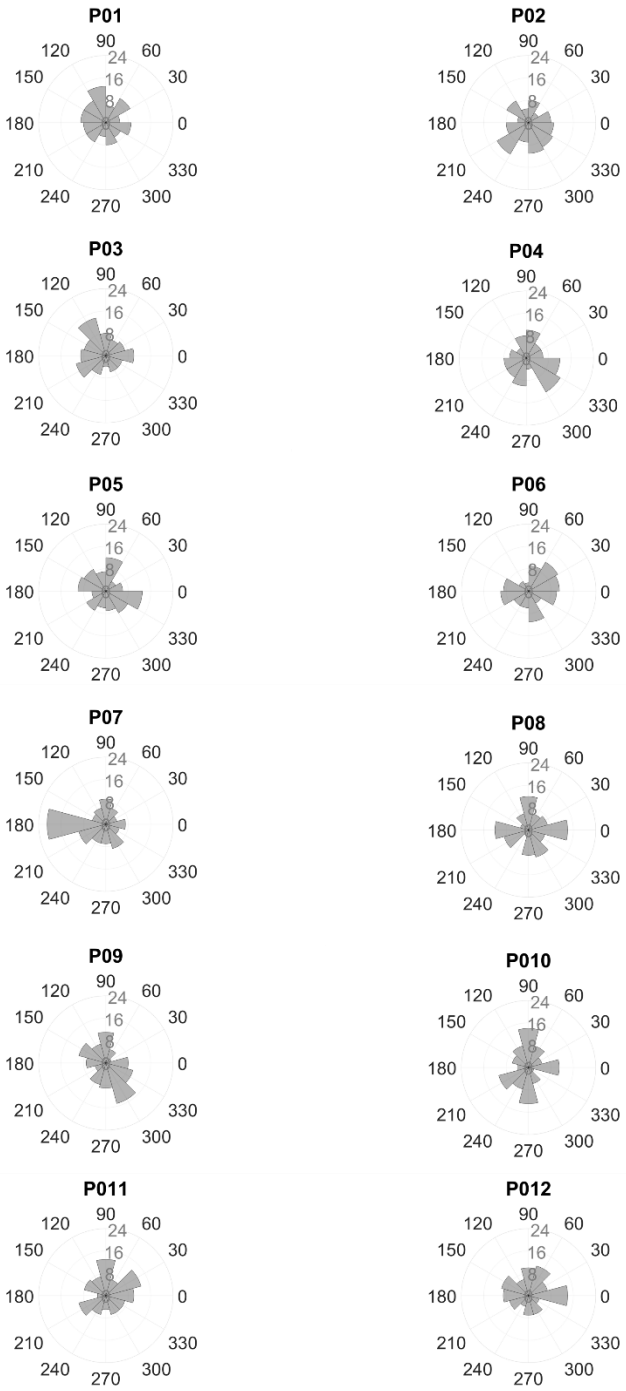

SUPPLEMENTARY FIGURE 16. Individual rose plot of the phase distribution at stimulus onset for valid-burst trials [in degrees]. Individual rose plot of phases for all trials for each participant. Each bin corresponds to 30º.

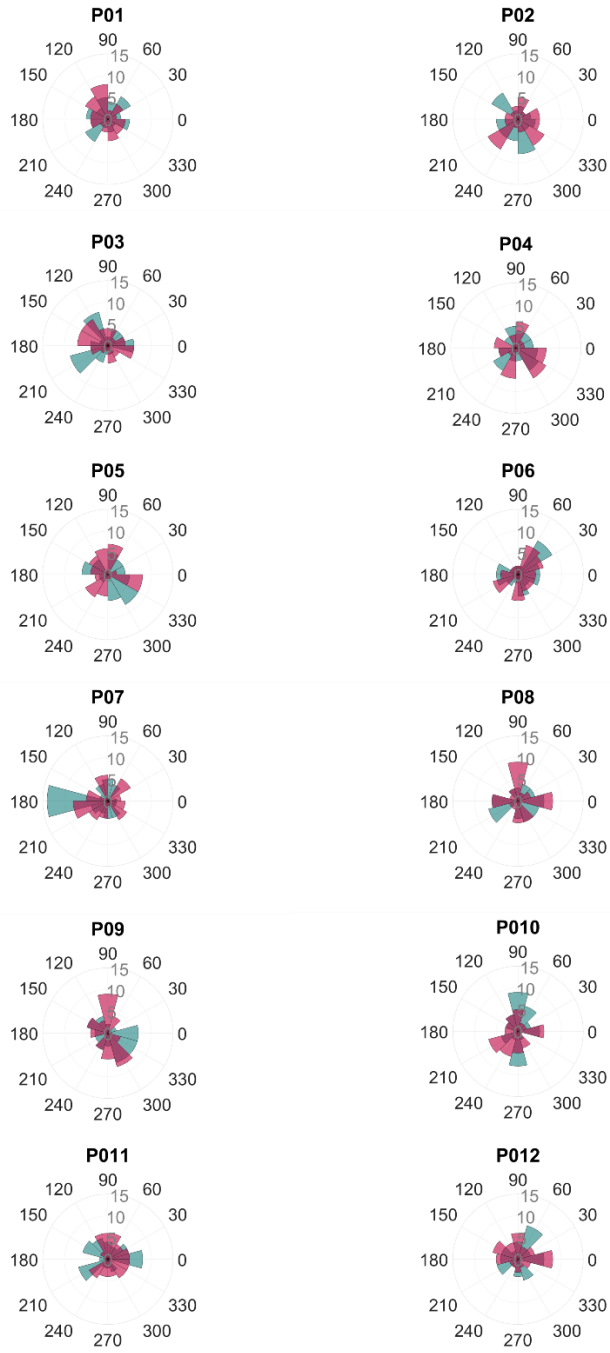

SUPPLEMENTARY FIGURE 17. Individual rose plot of the phase distribution at stimulus onset for valid-burst trials [in degrees]. Individual rose plot of phases for fast (in green) and slow (in red) trials for each participant. Each bin denotes 30º.

SUPPLEMENTARY TABLE 15. Individual number of excluded trials. For each participant, it is reported the total number of trials delivered, the sum of all the trials excluded for not satisfying the criteria of the stud (including the percentage; %), the number of trials excluded for reaction time (RTs), the number of trials excluded for not satisfying the power threshold criterion, and the number of trials excluded for not satisfying the artifact threshold criterion. The difference between the number of all trials and the number of excluded trials is the number of valid trials (N = 240).

Part.	No. all trials	All		RT		Power		Artifact	
		No. excl. trials	% excl. trials	No. excl. trials	% excl. trials	No. excl. trials	% excl. trials	No. excl. trials	% excl. trials
1	**760**	**520**	68%	**34**	4%	**462**	61%	**24**	3%
2	**738**	**498**	67%	**40**	5%	**361**	49%	**97**	13%
3	**580**	**340**	59%	**1**	0%	**308**	53%	**31**	5%
4	**574**	**334**	58%	**39**	7%	**272**	47%	**23**	4%
5	**616**	**376**	61%	**23**	4%	**318**	52%	**35**	6%
6	**588**	**348**	59%	**6**	1%	**298**	51%	**44**	7%
7	**571**	**331**	58%	**59**	10%	**227**	40%	**45**	8%
8	**669**	**429**	64%	**9**	1%	**404**	60%	**16**	2%
9	**725**	**485**	67%	**63**	9%	**372**	51%	**50**	7%
10	**724**	**484**	67%	**34**	5%	**375**	52%	**75**	10%
11	**565**	**325**	58%	**6**	1%	**259**	46%	**60**	11%
12	**741**	**501**	68%	**17**	2%	**473**	64%	**11**	1%
Mean (SD)	**654 (79)**	**414 (79)**	***63%* (4%)**	**28 (21)**	**4% (3%)**	**344 (78)**	**52% (7%)**	**43 (25)**	**7% (4%)**

SUPPLEMENTARY TABLE 16. Individual IFoI amplitude, the number of excluded trials for burst and no-burst trials, and the mean (SD) percentage of data points above/below the threshold for burst and no-burst trials, respectively. For each participant, the amplitude [in dB] of the Individual Frequency of Interest (IFoI) at task using Oz-electrode is given with the number of trials excluded for power, and for burst and no-burst trials separately.

Part.	IFoI (task) amp. [in dB]	No. excl. trials for power	No. burst trials	No. no-burst trials
1	5.70	462	97	**365**
2	2.97	361	**204**	157
3	9.91	308	46	**262**
4	11.26	272	61	**211**
5	2.23	318	130	**188**
6	2.00	298	140	**158**
7	3.73	227	72	**155**
8	5.36	404	155	**249**
9	6.72	372	92	**280**
10	2.18	375	**251**	124
11	2.57	259	72	**187**
12	6.78	473	69	**404**
Mean (SD)	**5.12 (3.11)**	**344 (78)**	**116 (63)**	**220 (77)**

In order to achieve the intended number of valid trials (n=240), we collected an average of 654 (SD = 79) responses per participant before filtering online according to preregistered values (see *Methods* section). On average per participant, 28 (SD = 21; 4%) trials were excluded for not satisfying the *reaction time criterion*, 344 (SD = 78; 52%) for not meeting the *power threshold* criterion, and 43 (SD = 25; 7%) because of the *artefact* criterion (see **Supplementary Table 7** for more details). Note that the exclusion of trials proceeded in the sequential order artefact, then power, then RT criterion, and once a trial was dropped, no further checks were done on the remaining criteria.

We decided to pay a closer look to the average of 52% (SD = 7%) of trials (**Supplementary Table 7**) excluded for not satisfying the *(no-)burst power threshold* criterion (see *Trial validity criteria*). To further explore the data, we selected the trials excluded for power criteria (which satisfied RT and artifact power criteria) and divided them into burst and no-burst categories. The mean number of trials excluded for power in burst trials was 116 (SD = 63; Max = 251; Min = 46), whereas in no-burst trials the mean number was 220 (SD = 77; Max = 404; Min = 124) (**Supplementary Table 8**). Overall, 10 out of twelve participants excluded more trials in no-burst trials compared to burst trials. These results show that it was more difficult to detect non-oscillatory activity during the task execution in comparison of detecting oscillatory burst activity in the EEG signal for most of the participants.

We also checked for a putative relationship between the IFoI peak amplitude during task execution and the number of trials excluded for power in each condition. We thought that participants who had higher IFoI amplitude during the task would have a smaller number of trials excluded for finding bursts compared to no-bursts. On the other way around, participants who had lower IFoI amplitude would have less trials excluded for no-burst compared to burst trials. **Supplementary Fig. 9** shows the individual IFoI amplitude during the task for burst (in red) and no-burst (in green) trials as a function of the number of trials excluded for power in each condition. With our hypothesis in mind, we performed a one-tailed Pearson correlation for burst (left-tailed) and no-burst (right-tail) trials and found a significant correlation at group-level for both burst ($\varrho = -.62; p = .02$) and no-burst ($\varrho = .51; p = <.05$) trials.

Overall, we can conclude that there was a difference in trial exclusion for power criteria depending on burst and no-burst trials for each participant, and the number of trials excluded for each condition was correlated with the IFoI amplitude during the task.

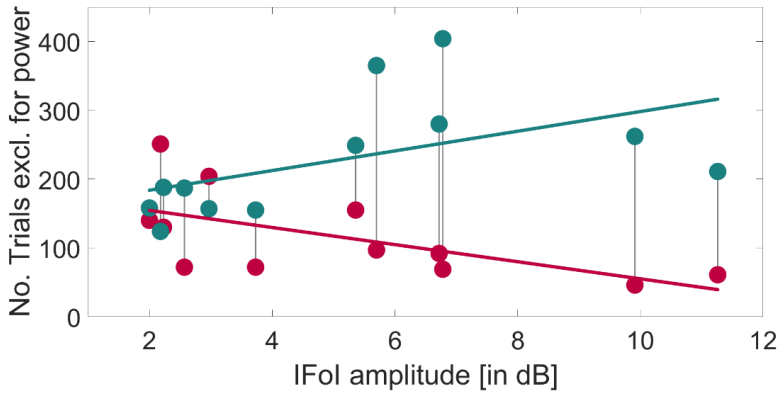

SUPPLEMENTARY FIGURE 18. Individual IFoI amplitude during the task for burst (in red) and no-burst (in green) trials as a function of the number of trials excluded for power in each condition. For each participant, the IFoI amplitude during the task (x-axis) presents two related values: number of excluded trials for not satisfying the burst-power condition (dots in red) and the no-burst condition (dots in green). Vertical lines between dots denote the pair of values for each participant. Solid lines denote the linear fit across participants for burst (in red) and no-burst (in green) trials. Group assess of Pearson correlation between IFoI amplitude and number of trials excluded for each participant for burst (left-tailed) and no-burst (right-tail). P-values denote significance in the Pearson correlation at group-level for burst (ϱ = -.66; p = .01) and no-burst (ϱ = .53; p = .04) trials.

ANNEX III -
Using long-range α-phase coupling to determine the locus of spatial attention

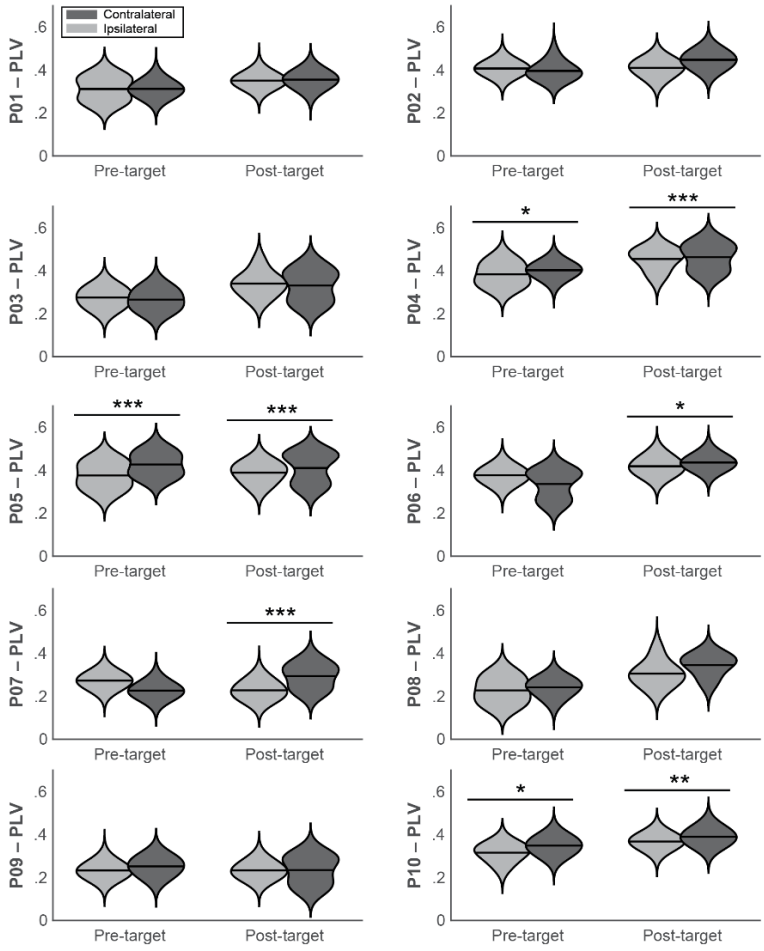

SUPPLEMENTARY FIGURE 19. Individual results of target-locked PLV index. Violin plots represent the phase-locking values (PLV) averaged over the pre-target (-200 to 0 ms, t = 0 as target appearance) and post-target time window (200 to 400 ms). Ipsilateral (FM-PL network and attended left; FM-PR and attended right) or contralateral (FM-PR network and attended left; FM-PL and attended right) scenarios are exhibited as either light grey or dark grey, respectively. *$p < 0.05$, **$p < 0.01$, ***$p < 0.001$.

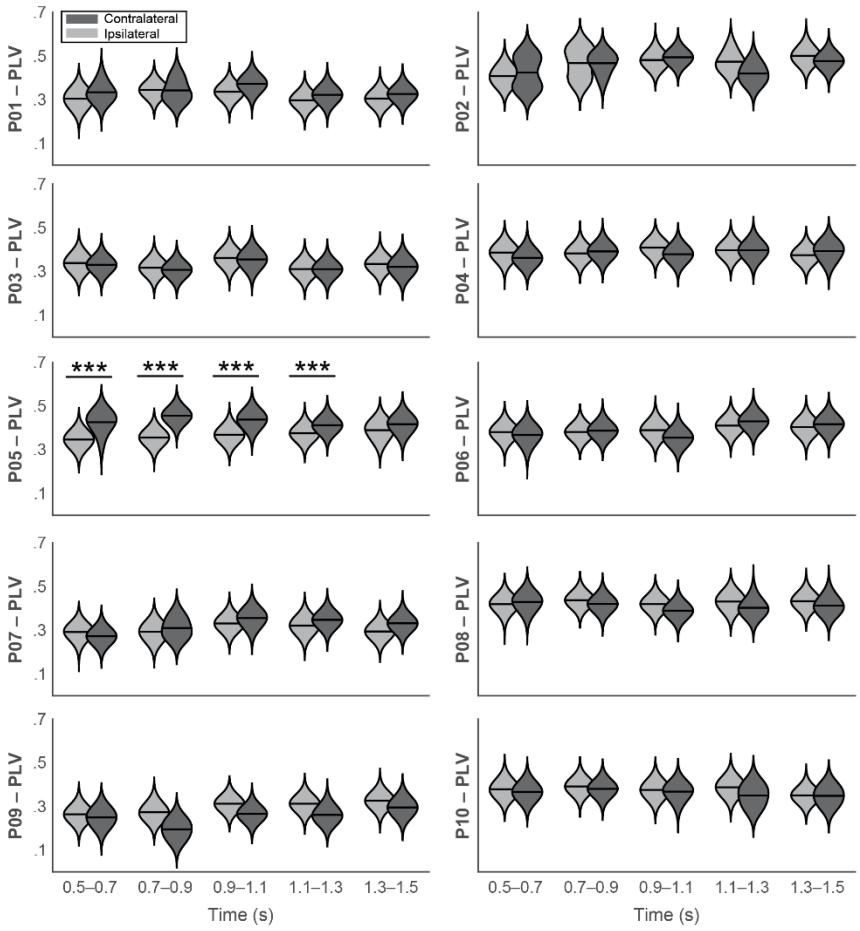

SUPPLEMENTARY FIGURE 20. Individual results of upper-alpha cue-locked PLV analysis. Violin plots represent the phase-locking values (PLV) averaged over the five time windows (500 to 700, 700 to 900, 1100 to 1300, and 1300 to 1500 ms; t = 0 as cue appearance). Ipsilateral or contralateral scenarios are exhibited as either light grey or dark grey, respectively. *p < 0.05.

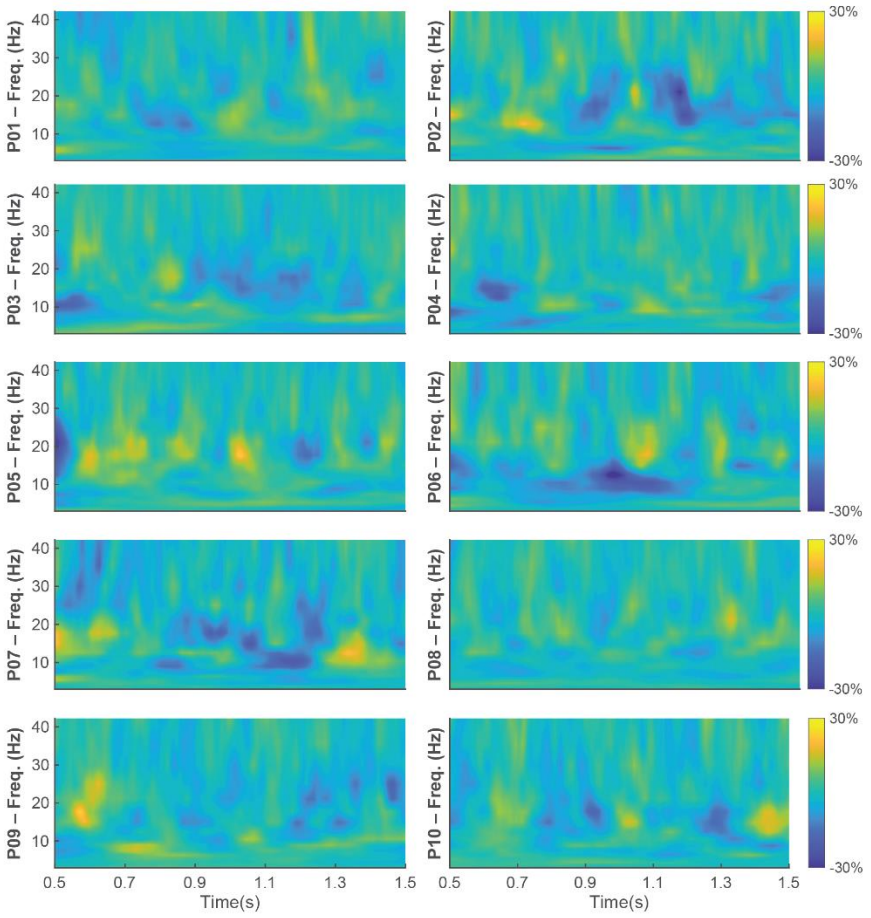

SUPPLEMENTARY FIGURE 21. Individual results of cue-locked exploratory PLV analysis. Differences in contra- to ipsilateral PLV are represented over frequencies (2.4 – 42 Hz in 16 logarithmic steps) as a percentage of change regarding the cross-frequency mean of each individual.

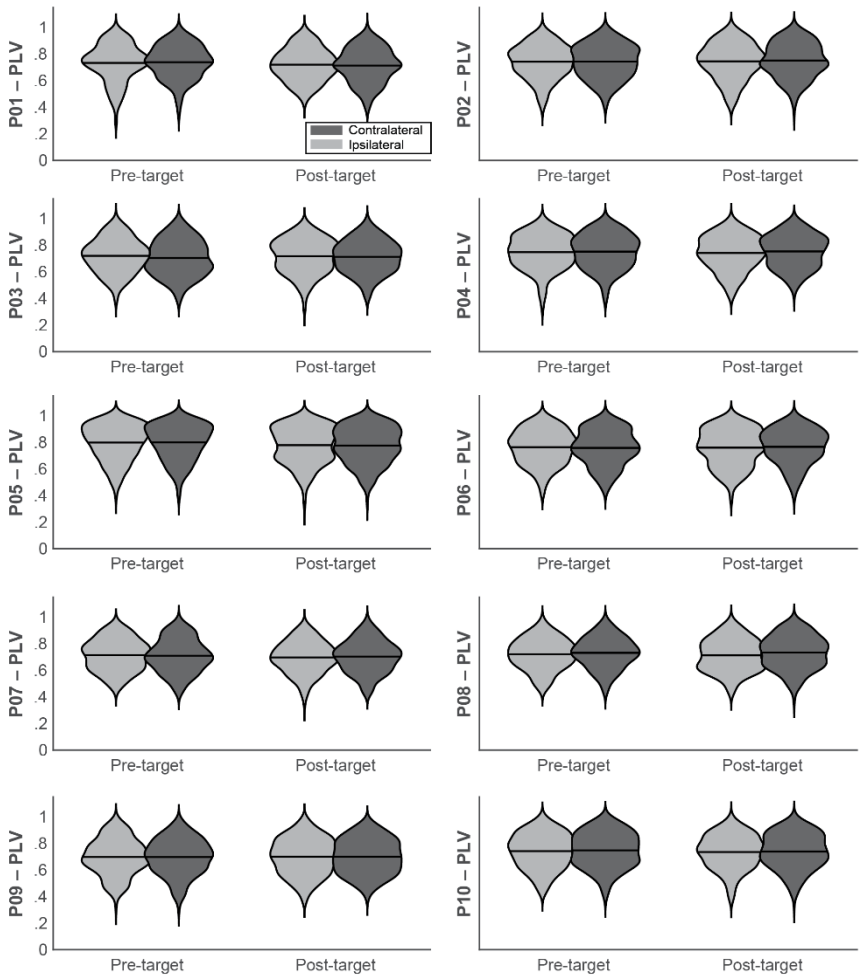

SUPPLEMENTARY FIGURE 22. Individual results of target-locked cross-time PLV. Violin plots represent the phase-locking values (PLV) obtained by calculating PLV as consistency throughout the pre-target (-200 to 0 ms) and post-target (200 to 400 ms) time windows. Ipsilateral or contralateral scenarios are exhibited as either light grey or dark grey, respectively.

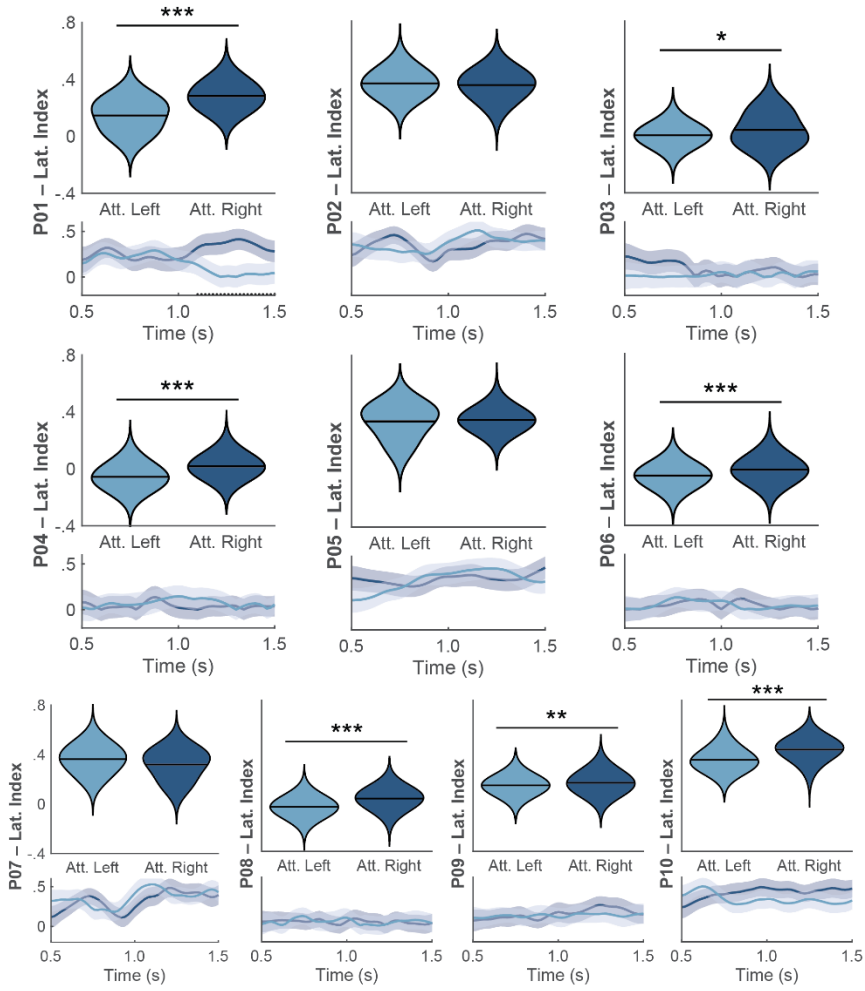

SUPPLEMENTARY FIGURE 23. Individual results of lateralisation index. Violin plots represent the averaged lateralised index for attended left (light blue) and attended right trials (dark blue) over the cue-locked time window. Shaded plots represent lateralisation over time (mean ± SEM). Dots in the x-axis denoted the significant differences over time between attended left and right via a cluster-based permutation test. *p < 0.05, **p < 0.01, ***p < 0.001.